UNIVERSITY OF LIVERPOOL

LAKE SEDIMENT RECORDS OF FLOOD FREQUENCY AND MAGNITUDE

Thesis submitted in accordance with the requirements of the University of Liverpool for the degree of Doctor in Philosophy

by

Daniel Neame Schillereff

February 2015

ABSTRACT

The recent spate of floods in many parts of Britain has stimulated substantial interest among scientists, policy makers and the public concerning contemporary trends in flood frequency and magnitude, in particular questioning whether these events exceed historical extremes. However, detecting a clear signal of recent intensification in the flood regime is hampered by the relatively short timescales covered by meteorological and river flow data. Lake sediment sequences have proven a valuable archive of historical flooding over centennial and millennial timescales elsewhere in Europe and globally, but this thesis presents one of the first attempts to extract flood histories from the sediments of lakes in Britain. It adapts a detailed field and lab-based approach to test the hypothesis that discrete layers can be distinguished from long sediment cores (1 – 3.5 m) that were probably deposited by high-magnitude floods based on their particle size and geochemical signatures.

The programme of research was developed and applied at Brotherswater (River Eden catchment), northwest England, and then further tested at the Loch of the Lowes (River Tweed catchment), southern Scotland. A detailed literature review led to the creation of a conceptual model to guide field site selection, based on the catchment-lake configuration and hydrological regime of individual sites. Characteristics deemed critical include a high catchment:lake area ratio to maximise sediment availability, limited pre-lake sediment storage and an effective sediment conveyor, as well as simple lake bathymetry.

The viability of μXRF scanning to characterise flood laminations within wet sediment cores was assessed in detail. A new method of calibrating geochemical concentrations where the water content varies substantially (50%) down-core based on x-ray scattering is described, and the first inter-comparison between different core scanners is performed. The analytical resolution of the ITRAX can reveal laminations too thin to manually sub-sample but the dataset can be noiser, especially after correction to the dry-mass basis. Caution should be used when interpreting ITRAX data at the sub-mm scale to ensure peaks and troughs represent real changes in sediment composition.

Inspection of multiple sediment cores extracted along a delta-proximal to distal transect in Brotherswater, coupled with high-resolution (0.5 cm) particle size measurements revealed silt-dominated (90^{th} percentile grain size (P90) ~ 16 μm)

sediment matrices frequently punctuated by coarser-grained sand layers (P90 >100 μm) that are lighter in colour. These layers cannot be easily characterised geochemically, most likely due to the volcanic bedrock in the catchment, but constitute the stratigraphical signature diagnostic of repeated high-magnitude floods for the River Eden catchment. Sediment supply varied substantially through the late-Holocene at Brotherswater, complicating the particle size record. A normalisation approach was tested to remove the background trend and identify notable particle size peaks (>1 standard deviation from the longer-term moving window) and the similar profiles produced for three cores from Brotherswater suggests the technique has been able to produce a record of major floods in the Patterdale Valley spanning the last 1500 years. Geochemical profiles at Brotherswater are dominated by enhanced metal deposition during the last 300 years, especially Pb, which mimics and could be used as a surrogate for production data for the nearby Hartsop Hall Lead Mine. The down-core pattern of Pb deposition is strongly reproducible in twelve cores extracted from different parts of the lake and reveals reveals the pattern, rate and controls over sediment deposition, with post-1860 accumulation rates four times greater near the inflow. A coherent chronology that integrates short-lived radionuclide dating (^{137}Cs, ^{241}Am, ^{210}Pb), ^{14}C ages and the geochemical contaminant markers for Brotherswater reveals that the last millennium was characterised by flood-rich and flood-poor phases generally 50 – 100 years in duration. The timing of these phases is significantly correlated with annual precipitation reconstructions, indicating a link between rainfall and flood generation. Some temporal correspondence between flood occurrence and phases of the North Atlantic Oscillation is observed but the relationship frequently breaks down. At Brotherswater, flood deposits have been most frequent during the 20th Century but isolating the influence of human activity on the sediment record is challenging.

Sixteen months of process monitoring at Brotherswater using sediment traps confirms the mechanics of sediment delivery and shows a strong continuity of current process to the late-Holocene sediment record. Particle size signatures were identified for a major winter flood, low-flow conditions and the regular flushing of the sediment system by successive low magnitude flood flows. Scaling the sediment trap data to an equivalent annual accumulation show how event delivery of coarse material may be masked by more regular fine-grained sedimentation through the year. The revealed anatomy of the annual sediment accumulation cycle has significant implications for palaeoflood

research with process understanding at each site clearly a critical precursor to any sediment-based flood investigation.

Laminations interpreted as palaeoflood deposits in the Loch of the Lowes sequence also exhibit prominent peaks in particle size but differ in colour and geochemical composition from Brotherswater, which highlights the importance of developing site-specific protocols for interpreting the sediment record. The coarse bands are much darker in colour and the Zr/Rb ratio appears to be an effective proxy of particle size in this case, with higher values reflecting coarser material. Preliminary chronological information suggest a finely-resolved palaeoflood record has been recovered extending approximately 350 years at the delta-proximal zone and perhaps twice as long in the central basin.

The thesis demonstrates that particle size data, supported by appropriately calibrated geochemical analyses, can generate high-resolution flood stratigraphies from upland UK lakes and these span millennia, extending our understanding of regional flood frequency.

ACKNOWLEDGEMENTS

The wholly positive experience I have had whilst producing this thesis is in no small part due to the advice and friendship of many colleagues and friends. I am indebted to my supervisor Richard Chiverrell for ceaseless enthusiasm, guidance and knowledge throughout my PhD (and MSc), as well as financial support for field work and conference attendance. If I successfully forge an academic career, his influence and support will have been essential. Neil Macdonald has been an invaluable supervisor, offering numerous suggestions and ideas that had not previously occurred to me, a never-ending willingness to read drafts, as well as setting up and assisting with the COST application that allowed me to visit IRSTEA (Lyon). I also owe a huge thank you to Janet Hooke for providing an alternative perspective on this research and providing helpful suggestions and feedback at all times.

John Boyle has been an invaluable source of advice through the years, always willing to jump up from his desk when Richard shouts down the corridor. Andreas Lang has probably attended more of my academic talks than any other person on earth; I am extremely grateful for his detailed feedback and encouragement! Thank you to Richard Bradshaw and Ian Snowball for setting up the DYNAMITE project and kindly inviting me along on four expeditions to Sweden, Ireland and the Lake District.; to Liz Whitfield for the opportunity to be involved with two really interesting dissertations and also to Frank Oldfield for providing the opportunity to work with him establishing *The Anthropocene Review* and taking a keen interest in my progress. I'd also like to thank John and Richard for the opportunity to co-author two really interesting book chapters with them.

Richard and Neil (as well as many other Liverpool colleagues) have provided excellent company on many entertaining field classes too. In fact, I must thank the School of Environmental Science Undergraduate cohorts as well; while my teaching responsibilities often surpassed my initial expections and took up significant portions of my time, the vast majority of my teaching experiences were wonderfully fulfilling .

The enthusiasm among my fellow members of the British Society for Geomorphology Postgraduate Forum was inspirational and I walked away with great feelings of satisfaction for our achievements. BSG members at all stages of their careers were supportive, interested and friendly, making my attendance at the annual conference a consistently positive experience.

A special thank you to Mike O'Connor for numerous ingenious practical suggestions in the lab and on field work as well as the other laboratory staff: Chris, Alan, Irene, Sandra and Josh and Suzanne in Cartographics.

Outside of the University of Liverpool, I am grateful to Pauline, Callum and Philippa for making my visit to the NERC Radiocarbon Facility both fascinating and enjoyable, Ian Croudace for the opportunity to visit the NOC-Southampton, assistance running cores on the ITRAX and the invitation to contribute a book chapter, and Michel Lang for amiably facilitating my stay at IRSTEA.

My time at Liverpool has been a joyous one, in no small part due to my fellow students. I was fortunate enough to be part of an exceptional BSc cohort, our MSc class were brilliant, especially Sarah and Charlotte, but, more importantly, the support and entertainment value of past and present PhD students and Post-docs in the Roxby throughout my PhD cannot be overstated – (in office order, as far as I can recall) Rafa, Onema, Bev, Jen, Tim, Fiona, Rachel, Karen Halsall, Hayley, Claire, John, Lee, Matt B, Madeleine, Kush, Josh, Amy, Matt W, Chris, Ai, Cai (haha), Raymond, Cyril, and Ian and Katharine although I cannot recall what office they were in... Special thanks to Lee, John and Andy D for days out in the fresh air and Jen, Tim and Bev for sharing the journey almost every step of the way. I was fortunate to forge bonds with wonderful PhD students elsewhere, especially Laura and Megan and Sarah and Emma. Finally, to my sister for exceptional coffee, a smiley face and inviting me to be a very willing test case for her massage diploma, Kirstie for perfectly-timed relaxing walks in the countryside and tasty, wholesome meals, my father, Scott, for taking the time out from his stressful life in Costa Rica to make invaluable comments on many of my draft chapters (as well as offering a rather convenient place to write up!) and my mother, Bridget, for on-going support and general loveliness; the knowledge you are always there if I need to pick up the phone is wonderful.

Thank you to Kayla Friedman and Malcolm Morgan of the Centre for Sustainable Development, University of Cambridge, UK for producing the Microsoft Word thesis template used to produce this document.

I am grateful to Drs Jeff Warburton (External Examiner) and John Boyle (Internal Examiner) for their thorough assessment, engaging discussion and many constructive comments offered during the *viva voce* of this thesis on November 5th, 2014.

CONTENTS

LIST OF TABLES

List of Figures

1 INTRODUCTION

1.1 RATIONALE AND BACKGROUND

The recent spate of floods in the UK, most recently during the winter of 2013/14 (Huntingford *et al.,* 2014) and high magnitude events in November 2009 in northwest England (Miller, J. *et al.,* 2013), summer 2007 (Marsh & Hannaford, 2007) and autumn/winter 2000/01 (Marsh, 2001) has led national policy makers, the media and the public to debate whether anthropogenic climate change is leading to more frequent and more severe floods (Wilby *et al.,* 2008). Some analyses indicate the frequency and severity of extreme floods has increased during the 20th century (e.g., Gorman and Schneider, 2009; Milly *et al.,* 2002), and physical mechanisms capable of triggering an intensification of the hydrological cycle in a warming world have been identified (Huntington, 2006). In addition, model scenarios from the IPCC Fifth Assessment Report (IPCC, 2013) project increased winter precipitation through the 21st century in the UK. Statistical algorithms (e.g., Coumou and Rahmstorf, 2012) and ensemble climate modelling (e.g., Pall *et al.,* 2011) have been used to assess whether the probability of extreme events have already or are shifting. That said, drawing a link between climate change and individual extremes remains hampered by a lack of long-term datasets to provide the necessary benchmark conditions (Macdonald, 2014). Developing new long-term records of flood recurrence and magnitude is required, and proxy data from sedimentary archives have the significant additional benefit of extending the historical context back in time before the trends visible in systematically recorded hydroclimate series.

Palaeoflood information has been extracted from instrumental (e.g., Robson, 2002) and historical sources in the UK (e.g., Lamb, 1977) and evidence of past floods preserved in geomorphic landforms and deposits has also been examined (e.g., Macklin and Rumsby, 2007), but reconstructions from sedimentary settings are sparse (e.g., Jones *et al.,* 2012; Werritty, Paine, Macdonald, Rowan, and McEwen, 2006). On a global scale, palaeoflood hydrology applied in alluvial environments has a long history (Baker, 2008 and references therein).

Lacustrine sediments have been more recently examined to recover flood information on all continents bar Antarctica. Lakes function as flood archives because they operate as sediment traps collecting materials eroded in catchments and transported through the fluvial system to the lake (e.g., Noren *et al.,* 2002; Chapron *et al.,* 2007; Page *et al.,* 2010; Schiefer *et al.,* 2011; Reinwarth *et al.,* 2013; Kämpf *et al.,* 2014a; Schlolaut *et al.,* 2014). The timespan and the temporal resolution of these records vary considerably, from single events (e.g., Gilbert *et al.,* 2006), reconstructions spanning recent centuries (Nahm *et al.,* 2010) to Holocene-length records (Brown *et al.,* 2000). Flood units are incorporated into the abyssal sedimentary record either preserved within seasonal to annual cycles or merged into the background sedimentation, with the potential to be blurred by variable rates of sediment accumulation. Recognition of flood events and the resolution of analysis is thus conditioned by the sedimentary system, with seasonal to annual flood signatures possibly identified in annually laminated or varved sediments (e.g., Swiercynski *et al.,* 2012; Czymzik *et al.,* 2013) and less clearly resolved sequences allowing identification of flood-rich phases over decadal/centennial timescales (e.g., Glur *et al.,* 2013).

A wealth of palaeoenvironmental data has been retrieved from lake sediments in the UK (e.g., Mackereth, 1966; Pennington, 1991) but their value for reconstructing past hydrological events has only been hinted at (e.g., Foster *et al.,* 2008). That is the motivation for this research: to produce robust reconstructions spanning centuries and potentially millennia of historical high-magnitude extreme floods based on their stratigraphic signatures preserved in UK lake sediment sequences. The approach offers the potential to make a significant but hitherto overlooked contribution to better understand long-term trends in flood frequency and magnitude in the UK.

1.2 AIMS, SCOPE AND RESEARCH QUESTIONS

The principal aim of this thesis is to assess for the first time in the UK the viability of using lake sediments to reconstruct the frequency and magnitude of historical flood imprints of high river flows. This will be conducted by examining whether distinctive palaeoflood laminations have been preserved in the sediments accumulating in two lake basins located in northern England and southern Scotland. Previous research at both study sites suggested a link between the sedimentation dynamics and the hydrological regime (Chambers, 1978; Foster *et al.,* 2008) underpinned by the hydrodynamic relationship known to exist between river flow and the entrainment and transport of particles of specific calibre (Hjülström, 1939). This thesis tests the potential for applying high-resolution particle size measurements to lake cores to discriminate coarser-grained laminations deposited under high-flow conditions. For one of the lakes, an eighteen month monitoring programme of the contemporary sediment dynamics tested the process mechanics of catchment to lake sediment delivery and in particular associations with river high flows. Multiple sediment characterisation techniques were applied to the sediment records in the lakes to assess whether the sedimentary record preserved an event-specific resolution, and explore how the system responded to longer term climatic or anthropogenic drivers that may pose challenges and potentially mask the preservation of an event-scale stratigraphy. The long legacy of mining in northern Britain has the potential to affect the sedimentary system so lake sediment records of ore exploitation will also be examined in detail. In conjunction with the development of well-constrained age-depth models for the sediment records integrating multiple and independent dating techniques, the two sediment palaeoflood records are compared to meteorological and historical sources of information on past floods in the study catchments, as well as regional and global climate histories. The thesis structure is framed around the following research questions:

I) Is there a catchment – lake configuration and methodological toolset that can routinely be applied to lake sediments to recover palaeoflood information?

Rationale: Records of palaeoflood frequency and magnitude are needed for centennial or millennial timescales to place flood occurrence and intensity into a longer-term context. Lake sediment sequences act as a relatively untapped archive of high-

magnitude floods over these longer timescales. Here a comprehensive review is undertaken of how flood frequency and magnitude data are recovered from lake sediments, the proxies available and the challenges that may hinder robust interpretation. The review explores flow processes, the physical controls affecting river sediment plume dispersal both to and within a lake, how process-controls map to the lake sediment record and attempts an evaluation of the proxies used to identify palaeoflood deposits. In reviewing a subset of lakes previously investigated for palaeoflood data, a conceptual model is proposed that uses the catchment –lake configuration as a basis to conceptualise the controls over production and preservation of palaeoflood sequences. Developing a decision protocol for selecting the optimum study site, locations within the lake and the most appropriate analytical procedures is a key inclusion that has conditioned the analysis undertaken in the remainder of the thesis.

II) What sedimentological and/or stratigraphical signatures can be identified within UK lake sediment cores that reflect past floods?

Rationale: The composition of lake sediments is highly heterogeneous through space and time, dependent on local geology, catchment-to-lake sediment regime, depositional mechanisms and landscape evolution (Håkanson and Jansson, 1983). Taking these factors into account, criteria will be established to ensure selected lakes have a high likelihood of flood-related material being preserved. High-resolution stratigraphical, particle size and geochemical analyses will be applied to a series of sediment cores to test whether discrete laminations can be identified that unambiguously reflect individual floods. The internal sedimentological structure and/or geochemical composition of these flood units will be classified. Evaluating to what extent and why the palaeoflood signature(s) differ(s) between sites is a core objective for this thesis.

III) Do lakes record a historical of industrial pollutant flux within their sediments?

Rationale: Human activity that modifies the sediment source area of a lake may alter the volume and characteristics of sediment depositing within the lake through time, potentially blurring palaeoflood laminations. The Lake District in particular has an extensive legacy of historical mining (Adams, 1988), and locally-sourced contamination has been found in other Cumbrian lakes (e.g., Grayson and Plater, 2008). Thus, assessing whether the abandoned mine at Hartsop Hall has impacted the

Brotherswater sediments is important. On the other hand, geochemical pollutant records have been used as a tool to correlate multiple cores across a lake, which could help map discrete flood units across a basin, and have provided geochronological markers to build improved age-depth models (e.g., Hammarlund *et al.,* 2008). A literature review will be undertaken in the first instance to examine approaches to measurement and flux calculations and evaluate the conditions most suitable for acquiring a geochemical record of heavy metal contaminations in lake sediments. Secondly, geochemical profiles of the Brotherswater sediment sequence will be compared with the documented history of Hartsop Hall Mine to test the representivity of the sediment record, assess whether mining activity has influenced sedimentation rates within the lake and examine whether a chronological signal can be extracted.

IV) Does the contemporary system show evidence for a hydrodynamic relationship between river flow and sediment delivered to the lake?

Rationale: Palaeoflood hydrology is underpinned by the assumption that a process (elevated river discharge) will lead to a response that will be preserved in the sedimentary record and can be characterised using proxy data sources in the sediments (Baker, 2008). In the case of lakes, this means demonstrating that sedimentologically-distinctive material is deposited and preserved at the lake bottom that reflects the hydrogeomorphic processes taking place in the catchment at the event scale (Gilli *et al.,* 2013). However, different catchment-lake configurations means that the interpretational protocols for discriminating palaeoflood deposits developed at other field sites may be inappropriate. Instead, explicitly demonstrating the link between low frequency, high-magnitude hydro-meteorological processes and the particle size, geochemical or other proxy data used to characterise materials delivered to lakes under high flows by monitoring contemporary sediment dynamics is critical on a site-specific basis (Schiefer *et al.,* 2006a). This is an important hypothesis tested in this thesis, particularly as sporadic decoupling between grain size and deposition rate has been identified in certain lakes (e.g., Cockburn and Lamoureux, 2008). This comparison is expanded by linking the recent sedimentary record with independent instrumental or documentary information of local and/or regional hydrological extremes over slightly longer timescales for which robust data exist (*sensu* Kämpf *et al.,* 2014).

V) How can the validity and application of μXRF scanning and the utility of geochemical proxies for grain size in palaeoflood research be effectively tested?

The recent proliferation of μXRF scanning within palaeoenvironmental research (Croudace *et al.,* 2006) has carried over to palaeoflood investigations of alluvial (Jones *et al.,* 2012) and lacustrine sequences (e.g., Vasskog *et al.,* 2011; Czymzik *et al.,* 2013). μXRF core scanning can determine the geochemical composition of sediments at unprecedented analytical resolution (the ITRAX can measure at 200 μm intervals), which could be invaluable for identifying flood layers too thin to detect and sub-sample manually, either through characterising the the geochemical signature of individual flood laminations (e.g., Swiercyniski *et al.*, 2012) or employing the ratio between two elements as a proxy for down-core variation in grain size (e.g., Vasskog et al., 2011). However, concerns have been raised about the reliability of the geochemical data obtained on a wet-sediment basis from μXRF scanners due to variable core composition, for example (e.g., Weltje and Tjallingii, 2008; Löwemark *et al.,* 2011). As a result, reconstructing palaeoflood histories from μXRF scanning without independent verification could yield erroneous results. One important element of this research will thus be to assess the suitability of μXRF scanning at the two study sites and potentially develop calibration tools that may improve data quality.

VI) Through the development of robust chronologies, to what extent can the frequency of floods in northern Britain be reconstructed for the timespan covered by the sedimentary records?

Rationale: Reconstructing the frequency of past high-magnitude floods is a key objective of palaeoflood research and it requires robust chronologies that are both precise and accurate at high-resolution over the timescale of investigation (Gilli *et al.,* 2013). Developing age-depth models that integrate multiple, independent dating techniques and tightly constrain the sediment sequences under investigation is thus a key primary objective. This will enable questions to be addressed such as how narrow an age window can be applied to discrete flood layers and to what extent do they correlate with independent regional flood records (e.g., Wilhelm *et al.,* 2012)? Assessing whether the maximum temporal resolution is more appropriate for dividing the record into flood-rich and flood-poor phases will also be important and the effects of antecedent conditions or successive floods on preservation potential will also be assessed.

VII) To what extent are catchments affected by changes in land-use or vegetation cover perturbing or influencing palaeoflood reconstructions?

Climatic variability and periods of intensive human activity can influence the supply of catchment-derived sediment to lakes (Dearing & Jones, 2003), potentially masking or altering the characteristics of palaeoflood units through time (Giguet-Covex *et al.,* 2011). Identifying drivers of long-term catchment-to-lake sediment flux will thus be undertaken in parallel to the palaeoflood research. Changes in the stability of a catchment characterise the last 2-3000 years of history in the northern British Uplands (Chiverrell, 2006), leading to a reduction of wood cover and more intensive land-use. These changes would alter the erodability of the land surface and potentially change the sources of sediment available in the catchment. A consequence of this is that sedimentary proxies in geochemistry or particle size may have a baseline and event spectra lain down under flood conditions that may differ through time. Palaeolimnologists have long (reviewed in Edwards and Whittington, 2001) used geochemical, environmental magnetic and palaeoecological techniques to reconstruct histories of anthropogenic activities affecting lakes and their catchments. These techniques are applied here to test whether data processing techniques can correct or adjust palaeoflood proxies (e.g. particle size indicators or element ratios) for changes in stationary states or catchment condition. A number of well-resolved climate proxy records exist for the UK (e.g., Proctor *et al.,* 2002; Charman *et al.,* 2006; Wilson *et al.,* 2013) as well as 1000-year records of North Atlantic Oscillation strength (Trouet *et al.,* 2009), one important driver of extremes in western Britain (Burt and Howden, 2013). Comparison of extracted palaeoflood signals with these reconstructions will be explored to infer potential climatic drivers of long-term flood frequency and magnitude patterns.

1.3 THESIS LAYOUT

This thesis is formatted as a series of journal articles and book chapters. Thus it comprises three peer-reviewed book chapters (one first-author) that have been accepted for publication (Chapters 2.2; 3.3; 3.4), one published journal article (Chapter 2.1) and four manuscript-style chapters (Chapters 4-8), essentially articles for imminent submission to international, peer-reviewed journals. The published paper is a detailed review of the prospects and challenges to lacustrine palaeoflood investigations. One of the book chapters is a co-authored review of mining and industrial activities and impacts on the sediment records in lakes. The other two book

chapters address important methodological issues related to the collection, processing and use of micro-scale X-ray fluorescence spectrometry (μXRF) scanning technology and the development of calibration tools to rigorous data quality in μXRF scanning, which underpins aspects of the PhD research.

Chapter 2:

Section 2.1: *Flood stratigraphies in lake sediments: a review (*Earth-Science Reviews **135**, pp 17-37, August 2014). This paper provides a comprehensive review of the sequence of considerations vital to successfully extracting palaeoflood information from lake sediments. It outlines physical controls on the behaviour and characteristics of depositing material, evaluates the proxies and dating techniques employed to date in palaeoflood research, presents two conceptual models to guide further research and presents five case studies where different interpretational protocols have been applied to reconstruct palaeofloods.

Section 2.2: *Lacustrine archives of metals from mining and other industrial activities- a geochemical approach. (*Boyle, JF., Chiverrell, RC., Schillereff, D. (2014, *In press*) Lacustrine archives of metals from mining and other industrial activities- a geochemical approach. In: Blais, JM, Rosen, MR and Smol, JP (eds). Environmental Contaminants: Using Natural Archives to Track Sources and Long-term Trends of Pollution. Dordrecht, Springer). The chapter reviews research on the recent stratigraphic changes of heavy metal concentrations in lake sediments, examining the recent methodological advances, placing them in the context of the historical development of the discipline, and exploring the various purposes to which such methods have been applied. The processes controlling natural variations in metal flux in lake sediments are introduced and techniques for measuring concentrations in sediments and calculating enrichment or fluxes from concentration data are reviewed. Applications of metal stratigraphies in lakes are explored focusing on: i) their use as geochronological markers in sediments; ii) quantifying pollution loading histories, or to identify pollutant sources and iii) assessing pre- and post-mining baseline conditions, and pollutant pathways or environmental processes regulating heavy metals.

Chapter 3: *Methodological context and data quality evaluation*. Detailed descriptions of the study sites as well as an overview of the field sampling and laboratory techniques employed in this thesis are provided, alongside guidance to the relevant Chapters in which these methods are described in greater detail where applicable.

Section 3.3: The prevalence of μXRF in contemporary palaeoenvironment research necessitates addressing imperfections in the scan data that arise because of its acquisition from wet sediments. This chapter outlines two calibration approaches to convert wet sediment concentrations or count rate collected by μXRF scanning to dry-mass equivalent output. Both approaches are applied to two lakes of differing sediment composition and their respective suitability is evaluated.

Section 3.4: A number of different μXRF core scanning instruments are currently in use in palaeolimnological research around the world. This chapter presents the results of a first inter-comparison of μXRF measurements made by an Olympus/Geotek and an ITRAX instrument on a sediment core extracted from Loch of the Lowes, Scotland.

Chapter 4: Lake sediments have been demonstrated to be effective tools for evaluating historical trends in anthropogenic-derived trace metal contamination within catchments. Here, geochemical data are presented from high-resolution analyses of multiple sediment cores extracted from Brotherswater, English Lake District. The development of a robust chronology for the Brotherswater sediment sequence is outlined, including the chronological markers that were employed, and uncertainties associated with the resultant age-depth model. High-resolution estimates of late-Holocene sediment flux to the lake, in particular mineral supply and mining-derived metal contamination, were calculated using the chronological data, and these are presented alongside proposed drivers of the highly variable accumulation rates. Insights into catchment-lake sediment dynamics, spatial patterns of sediment deposition across the basin and the persistent negative impacts of mining on the aquatic ecosystems evident in the sedimentary record are also highlighted. In terms of the mining history, sedimentary Pb concentrations in the sediment closely reflect the known record of historical mining at the now-closed Hartsop Hall Mine. Issues including whether Pb levels in the aquatic ecosystem have recovered or remain higher than pre-mining period are explored.

Chapter 5: This chapter explores the construction of a late-Holocene palaeoflood record from Brotherswater. The laboratory methods are detailed and multiple lines of evidence are presented that illustrate the detectable imprints of historical floods preserved in the sediment sequence. Trends in flood frequency and potential links to climatic and/or anthropogenic drivers are discussed. The temporal consistency between the Brotherswater record and regional, independent instrumental and

documentary palaeoflood data is assessed and some comments on reconstructing flood magnitude are made.

Chapter 6: The results from the 18 month sediment trapping programme at Brotherswater are presented in this chapter. Particle size measurements are used to assess whether the presumption that a hydrodynamic relationship exists between river discharge and the calibre of material delivered to the lake water column is valid at Brotherswater. The sediment trap data also yield insights into seasonal variability of within-lake depositional mechanisms and sediment provenance. A comparison of the particle size distributions between trapped material and adjacent sediment cores is performed and a particle size distribution representing total sedimentation that will be preserved in the abyssal sediments is presented.

Chapter 7: Results from the second study site, Loch of the Lowes, are presented in this chapter, as an opportunitity for testing the methodology developed at Brotherswater. The rationale for site selection is provided, the sediment sequence and depositional mechanisms are described in detail and the proposed palaeoflood signature is outlined. Some comments on trends in flood occurrence are offered in the context of the solely relative chronology currently available.

Chapter 8: This chapter presents **a**n extended discussion that ties the findings together from the two reviews (Chapter 2.2 and 2.3), the methodological papers (Chapters 3.3 and 3.4) and the four results sections (Chapters 4-8) and explicitly addresses the key scientific questions outlined in Chapter 1. Finally, key limitations to the research and several avenues of future work are highlighted.

1.4 AUTHOR CONTRIBUTION AND STATUS OF MANUSCRIPTS

At the time of submission, the status of the three book chapter and five papers is as follows:

Chapter 2.1

Schillereff, D., Chiverrell, R., Macdonald, N. and Hooke, J. (2014) Flood stratigraphies in lake sediments: a review. *Earth-Science Reviews* **135**, 17-37.

Author contribution:

Schillereff, D. - Main author, conducted the literature review, wrote the manuscript and collected and interpreted the data underpinning the case study.

Chiverrell, R. - Collected sediment cores from Brotherswater, in-depth discussions and detailed manuscript review.

Macdonald, N. - Collected sediment cores from Brotherswater, in-depth discussions and detailed manuscript review.

Hooke, J. - In-depth discussions and detailed manuscript review.

1st submission: 1 September 2013

Final submission (accepted): 24 March 2014

Published online: 14 April 2014

Chapter 2.2

Boyle, JF, Chiverrell, RC, **Schillereff, D.** (2014 In press) Lacustrine archives of metals from mining and other industrial activities- a geochemical approach. In: Blais, JM, Rosen, MR and Smol, JP ed(s). Environmental Contaminants: Using Natural Archives to Track Sources and Long-term Trends of Pollution. Dordrecht , Springer.

Author contribution:

Boyle, J. - Main author and wrote the bulk of the paper.

Chiverrell, R. - Detailed discussions and thorough manuscript review.

Schillereff, D. – Second author, wrote the section on measurement methods, detailed discussion and thorough manuscript review

1st submission: June 2013

Final submission (accepted): June 2014

Published online: Pending.

Chapter 3.3

Boyle, J., Chiverrell, R. and **Schillereff, D.** (*In Press*) Approaches to water content correction and calibration for μXRF core scanning: comparing x-ray scatter with simple regression of elemental concentrations. In: Rothwell, R.G., Croudace, I.W. (Eds.),

Developments in Palaeoenvironmental Research: Micro-XRF Studies of Sediment Cores. Springer, Dordrecht.

Author contribution:

Boyle, J. - Main author, collected, processed and interpreted the Lilla Öresjön data and wrote the bulk of the paper.

Chiverrell, R. - Data interpretation, detailed discussions and thorough manuscript review.

Schillereff, D. - Collected and interpreted the Brotherswater data, wrote the Brotherswater section and thorough manuscript review

1st submission: 30 May 2013

Final submission (accepted): 21 March 2014

Published online: Pending.

Chapter 3.4

Schillereff, D., Chiverrell, R., Boyle, J. and Croudace, I. (*In Press*) An inter-comparison of μXRF scanning analytical methods. In: Rothwell, R.G., Croudace, I.W. (Eds.), *Developments in Palaeoenvironmental Research: Micro-XRF Studies of Sediment Cores.* Springer, Dordrecht.

Author contribution:

Schillereff, D. - Collected, processed and interpreted the data, wrote the manuscript.

Chiverrell, R. - Collected the sediment cores, detailed discussions and thorough manuscript review.

Boyle, J. - Detailed discussions and thorough manuscript review.

Croudace, I. - Conducted the ITRAX μXRF scans and thorough manuscript review.

1st submission: 1 August 2014

Final submission (Accepted): 9 September 2014

Published online: Pending.

Chapter 4

Schillereff, D., Chiverrell, R., Macdonald, N., Hooke, J., Appleby, P., Piliposian and Welsh, K. (Manuscript for submission to **Journal of Paleolimnology**) Metal fluxes, sediment accumulation and Pb mining: lake sediment evidence from Brotherswater, northwest England.

Author contribution:

Schillereff, D. - Main author, collected, processed and interpreted the data and wrote the manuscript.

Chiverrell, R. - Collected sediment cores, provided assistance with radiocarbon sampling and GIS expertise, in-depth discussions and detailed manuscript review.

Macdonald, N. - Collected sediment cores, in-depth discussions and detailed manuscript review.

Hooke, J. - Collected bathymetric data and manuscript review.

Appleby, P. - Conducted and interpreted the ^{210}Pb measurements and reviewed the manuscript.

Piliposian, G. - Conducted and interpreted the ^{210}Pb measurements and reviewed the manuscript.

Welsh, K. - Provided the funding for the ^{210}Pb measurements and reviewed the manuscript.

Chapter 5

Schillereff, D., Chiverrell, R., Macdonald, N. and Hooke, J. (Manuscript for submission to **Quaternary Science Reviews).** A late-Holocene record of severe floods in northwest England

Author contribution:

Schillereff, D. - Main author, collected, processed and interpreted the data and wrote the manuscript.

Chiverrell, R. - Collected sediment cores, provided assistance with radiocarbon sampling and GIS expertise, in-depth discussions and detailed manuscript review.

Macdonald, N. - Collected sediment cores, in-depth discussions and detailed manuscript review.

Hooke, J. - Collected bathymetric data and manuscript review.

Chapter 6

Schillereff, D., Chiverrell, R. and Macdonald, N. (Manuscript for submission to **Sedimentology**). Contemporary sedimentation dynamics and provenance at Brotherswater.

Author contribution:

Schillereff, D. - Main author, collected, processed and interpreted the data and wrote the manuscript.

Chiverrell, R. - Collected sediment cores, provided assistance with radiocarbon sampling and GIS expertise, in-depth discussions and detailed manuscript review.

Macdonald, N. - Collected sediment cores, in-depth discussions and detailed manuscript review.

Chapter 7

Schillereff, D., Chiverrell, R., Macdonald, N. and Croudace, I. (Requires further radiocarbon dates prior to submission, potentially to **The Holocene).** Palaeoflood activity during the late-Holocene recorded by lake sediments in southern Scotland.

Author contribution:

Schillereff, D. - Main author, collected, processed and interpreted the data and wrote the manuscript.

Chiverrell, R. - Collected sediment cores, provided assistance with core scanning, in-depth discussions and detailed manuscript review.

Macdonald, N. - Provided assistance with Scottish historical flood records and detailed manuscript review.

Croudace, I. - Conducted the ITRAX μXRF scans and manuscript review.

2 REVIEWS OF PREVIOUS WORK

2.1 Flood stratigraphies in lake sediments: a review

Abstract

Records of the frequency and magnitude of floods are needed on centennial or millennial timescales to place increases in their occurrence and intensity into a longer-term context than is available from gauged river-flow and historical records. Recent research has highlighted the potential for lake sediment sequences to act as a relatively untapped archive of high-magnitude floods over these longer timescales. Abyssal lake sediments can record past floods in the form of coarser-grained laminations that reflect the capacity for river flows with greater hydrodynamic energy to transport larger particles into the lake. This paper presents a framework for investigating flood stratigraphies in lakes by reviewing the conditioning mechanisms in the lake and catchment, outlining the key analytical techniques used to recover flood records and highlighting the importance of appropriate field site and methodology selection. The processes of sediment movement from watershed to lake bed are complex, meaning relationships between measureable sedimentary characteristics and associated river discharge are not always clear. Stratigraphical palaeoflood records are all affected to some degree by catchment conditioning, fluvial connectivity, sequencing of high flows, delta dynamics as well as within-lake processes including river plume dispersal, sediment focussing, re-suspension and trapping efficiency. With regard to analytical techniques, the potential for direct (e.g., laser granulometry) and indirect (e.g.,

geochemical elemental ratios) measurements of particle size to reflect variations in river discharge is confirmed. We recommend care when interpreting fine-resolution geochemical data acquired via micro-scale X-ray fluorescence (μXRF) core scanning due to variable down-core water and organic matter content altering X-ray attenuation. We also recommend accounting for changes in sediment supply through time as new or differing sources of sediment release may affect the hydrodynamic relationship between particle size and/or geochemistry with stream power. Where these processes are considered and suitable dating control is obtained, discrete historical floods can be identified and characterised using palaeolimnological evidence. We outline a protocol for selecting suitable lakes and coring sites that integrates environmental setting, sediment transfer processes and depositional mechanisms to act as a rapid reference for future research into lacustrine palaeoflood records. We also present an interpretational protocol illustrating the analytical techniques available to palaeoflood researchers. To demonstrate their utility, we review five case studies of palaeoflood reconstructions from lakes in geographically varied regions; these show how lakes of different sizes and geomorphological contexts can produce comprehensive palaeoflood records. These were achieved by consistently applying site-validated direct and proxy grain-size measurements; well-established chronologies; validation of the proxy-process interpretation; and calibration of the palaeoflood record against instrumental or historical records.

Keywords: lake sediments, palaeoflood, geochemistry, particle size, limnology, extreme events

2.1.1 Introduction

2.1.1.1 Rationale behind lake palaeoflood research

Researchers (e.g., Milly *et al.,* 2002; Gorman and Schneider, 2009) have suggested that the frequency and intensity of extreme flood events may be increasing due to the high sensitivity of the hydrological cycle to a warming climate (Knox, 2000), triggering an intensification of the water cycle (Huntington, 2006). Recent modelling by Hirabayashi *et al.* (2013) projects a current 100-year return period flood is likely to occur every 10-50 years in the 21st Century. However, the complexity inherent in the climate-flood relationship, coupled with the infrequent and short-lived nature of extreme floods, means few data are available for evaluating long-term trends in their frequency and

magnitude (IPCC, 2012). Acquiring long-duration datasets of historical floods that extend beyond available instrumental records is clearly an important step in attributing trends in flood frequency and magnitude to climate change and addressing future flood risk. Conventional flood histories derived from instrumental data rarely span sufficiently long timescales to capture the most extreme events (Brázdil *et al.,* 1999; Macdonald, 2012) nor do they enable climatic (non-) stationarity or the attribution of the intensification of precipitation events by global warming to be assessed (Min *et al.,* 2011). Various sources are routinely accessed in order to acquire information on historical floods on timescales extending beyond the instrumental record, including documentary records (e.g., Benito *et al.,* 2004) and sedimentary records extracted from river flood-plains and slackwater deposits (e.g., Baker, 1987).

Lakes act as efficient repositories for clastic material eroded from catchment slopes and floodplains and subsequently transported through the fluvial system (Mackereth, 1966; Oldfield, 2005). If the hydrodynamic relationship between river discharge and entrainment potential of specific particle sizes is reflected in the materials received by the lake basin and incorporated into the sediment record, high-magnitude flows should appear as distinct laminations of coarse material. As a result, a growing number of palaeolimnologists are searching for lake sediment sequences from which records of past floods can be uncovered (e.g., Noren *et al.,* 2002; Czymzik *et al.,* 2013; Gilli *et al.,* 2013; Wilhelm *et al.,* 2013; Wirth *et al.,* 2013a; 2013b; Schlolaut *et al.,* 2014). Lake sediment records can contribute valuable data on flood frequency and, potentially, single-event magnitude over several millennia (Noren *et al.,* 2002). Improvements in the mechanics of coring technology (e.g., UWITEC-Niederreiter (Schultze and Niederreiter, 1990); Mingram *et al.,* 2006) and resolution of analytical methods (e.g., micro-scale X-ray fluorescence (μXRF); Croudace *et al.,* 2006) have aided the extraction of palaeoflood records from lakes in Africa (Baltzer, 1991; Reinwarth *et al.,* 2013), Asia (Ito *et al.,* 2009; Nahm *et al.,* 2010; Li *et al.,* 2013; Schlolaut *et al.,* 2014), Europe (Arnaud *et al.,* 2002; Bøe *et al.,* 2006; Wilhelm *et al.,* 2012; Wirth *et al.,* 2013a), New Zealand (Orpin *et al.,* 2010; Page *et al.,* 2010), North America (Brown *et al.,* 2000; Noren *et al.,* 2002; Osleger *et al.,* 2009) and South America (Chapron *et al.,* 2007; Kastner *et al.,* 2010).

A comprehensive review of the acquisition of flood frequency and magnitude data from lake sediments, the proxies available and the challenges that may hinder robust interpretation is thus timely. Here we outline the flow processes and physical controls

on river plume dispersal both to and within a lake, assess how process-controls map to the lake stratigraphical record and evaluate the proxies employed by palaeolimnologists to identify palaeoflood deposits. This paper presents a conceptual model that assesses the catchment-to-lake water and sediment flow pathways and their relative importance for the successful extraction of palaeoflood sequences. It also develops a decision tree outlining the analytical procedures available for identifying and interpreting these data and presents five case studies where these protocols have been applied to reconstruct palaeofloods at widely distributed lakes with different characteristics.

2.1.1.2 Non-lacustrine sources of flood data

Gauged river flow data are widely available for the last 30 – 40 years in Australia and most European countries (Benito *et al.,* 2004), a comprehensive hydrometric network (>3000 gauging stations) has existed in Canada since 1975 A.D. (Pyrce, 2004), and the United States Geological Survey (USGS) has operated an effective, centralised stream gauging programme since 1970 A.D. (Benson & Carter, 1973). In countries where an expansive network of hydrometric stations has existed for longer time periods, such as Switzerland (national hydrological service established in 1863 A.D., more than 30 stations established in the 19th century, more than 70 in operation since 1930 A.D.), more detailed assessments of trends in flood frequency can be undertaken (e.g., Schmocker-Fackel and Naef, 2010a). Elaborate monitoring networks enable good understanding of changes in hydrological regimes at hourly to annual timescales. Nevertheless, obtaining data for the short-duration, high-magnitude flow events is logistically challenging or, as a worst case scenario, monitoring stations can be damaged or destroyed by a flood. For example, the November 2009 extreme floods on the River Cocker in Cumbria, northwest UK, caused significant damage to the gauging station at Camerton on the River Derwent (National River Flow Archive Station #75002; http://www.ceh.ac.uk/data/nrfa/. Last accessed 27/08/2013). This suggests that the 200-year return period calculated for the flood (Everard, 2010) is likely to be an underestimate as the hydrological capacity of the gauging station was exceeded (Miller, J. *et al.,* 2013).

Historical data can be used to improve estimations of flood frequency and magnitude (NERC, 1975; Hooke and Kain, 1982; Bayliss and Reed, 2001; Schmocker-Fackel and Naef, 2010b) and have been acquired from sources including epigraphical markings of

peak flow stages on infrastructure adjacent to a river (Macdonald, 2007), paintings or photographs and written documents such as diaries or newspapers (Brázdil *et al.,* 2006). Documentary evidence often expresses an extreme event in terms of its impacts on society, which can be used as a reference for peak flow level, or to assess the recurrence intervals of such events (Benito *et al.,* 2004). Many flood histories extending back several centuries have been compiled using documentary sources in Europe; Brázdil *et al.* (2006) used historical records to identify a 20th century trend towards lower flood frequency due to regional warming reducing the number of winter floods and Wetter *et al.* (2011) showed that six catastrophic events (Q (discharge) > 6000 m^3 s^{-1}) occurred in the pre-instrumental period that exceeded all more recent events since 1877 A.D.. In the UK, Macdonald and Black (2010) demonstrated more robust flood frequency estimates were obtained for the River Ouse when data from historical sources were integrated with conventional gauged techniques, while Prieto and García Herrera (2009) reviewed the value of documentary sources for reconstructing climate in South America since its colonization by the Spanish.

Sedimentological techniques have been employed to decipher imprints of past flood events in incised floodplains or canyons, a research field termed 'palaeoflood hydrology' (Baker, 1987). One promising strand involves reconstructing floods recorded in slackwater deposits in floodplain settings. Under high flows, coarse-grained sediments are entrained and deposited in depressions along the floodplain that are separated from the river channel under normal flow conditions, and thus are positions of high sediment preservation potential (Baker, 2008). As a result, the highest magnitude floods are captured as discrete layers in cut-off meanders or in bedrock canyons. Granulometric analyses of these sediment sequences have generated centennial-scale records of meteorologically-generated floods (Werritty *et al.,* 2006) and ice-jam-generated floods (Wolfe *et al.,* 2006). Increasingly high-resolution core scanning techniques (e.g., ITRAX; Croudace *et al.,* 2006) have enabled channel fill sequences to be analysed in greater detail, with selected elemental ratios being utilised as indirect proxies of grain-size (e.g., Zr/Rb ratio in Welsh palaeochannels; Jones *et al.,* 2012).

Discrete landforms produced during high-flows, such as alluvial fans or upland boulder berms, can be dated using radiocarbon (^{14}C) and lichenometry, and these chronologies can produce fragmentary records of palaeofloods (e.g., Foulds *et al.,* 2013). Their precision and utility is limited by the available dating control and the validity of its

application (Chiverrell *et al.,* 2009; 2011) but case studies in the UK (e.g., Macklin *et al.,* 1992; Macklin and Rumsby, 2007) and Greece (e.g., Maas and Macklin, 2002) in part overcome these challenges.

Reconstructing peak discharges of jökulhlaups and 'superfloods' (potentially exceeding millions of cubic metres per second; Baker, 2002) through geomorphic investigations (Jarrett & England, 2002) and hydraulic numerical modelling (Carling *et al.,* 2010) has also been a focus of palaeoflood research, due to their capacity to abruptly modify vast landscapes. Examples of such Pleistocene megafloods include Glacial Lake Missoula in north-western USA (Baker, 1973), around the Altai Mountains, Siberia (Herget, 2005), and Glacial Lake Agassiz, constrained by the Laurentian ice sheet (Teller, 2004).

2.1.2 Flow processes and depositional mechanisms

2.1.2.1 Coupling of lakes with drainage basins

In the case of lakes, palaeoflood studies attempt to explicitly link low-frequency, high-magnitude flows to discrete sedimentary units recorded within long lake sediment profiles sampled by various coring equipment. Interpreting the sedimentary characteristics that represent a single historical flood requires confidence that the material accumulating at the lake bottom reflects the hydrogeomorphic processes taking place in the catchment at this event-specific temporal scale.

Catchment hydrological and sedimentological regimes appear to operate in a cascading manner, where material delivered to a lake as suspended sediment reflects the interplay between sources, transmission, storage and sediment sinks across the slope, gully, floodplain and fluviodeltaic systems (Fryirs, 2012). Both anthropogenic and natural factors can influence system connectivity within a drainage basin (Chiverrell, 2006; Foster *et al.,* 2008), for example by altering soil formation and its susceptibility to erosion (Giguet-Covex *et al.,* 2011). Floodplain sediment stores may subsequently introduce time-lags within the sediment conveyor (Fryirs *et al.,* 2007; Chiverrell *et al.,* 2010). The degree to which a river channel is well- or poorly-connected through time will also influence the nature of material moving downstream (Harvey, 1992; Hooke, 2003). For example, fluvial systems in which only exceptionally high flows generate a sediment pulse are classified as *unconnected* compared to those where sediment is readily transported by low-magnitude floods in more efficient, *connected* channels (Hooke, 2003). Changes in connectivity can potentially modify the geomorphic signal

transmitted along the sediment conveyor to the lake, altering the hydrodynamic relationship between lacustrine sedimentation and river discharge through time. The implications for discerning flood magnitude from discrete sedimentary units is that changes in sediment supply through time may result in flood events of equivalent magnitude depositing sedimentary units exhibiting different thicknesses, particle size distributions or geochemical composition. In this context, event sequencing can also be important. Where two floods of equivalent magnitude occur in close succession, the first may exhaust fluvial sediment stores, leaving the subsequent event deprived of material to transport. In summary, for lakes, river systems are best described as sources of sediment where the supply regime is inherently non-stationary.

Integrating multiple palaeoenvironmental proxies offers the most comprehensive approach to gaining a better understanding of changes in fluvial connectivity, soil erodibility and sediment supply as well as identifying shifts in the climate-vegetation-soil relationship (e.g., Koinig *et al.,* 2003). For example, pollen and plant macrofossil records will reflect changes in vegetation cover, which may alter sediment supply and provenance during phases of intensive agriculture (Dearing & Jones, 2003). Environmental magnetic measurements can be an effective sediment-source tracer, highlighting phases of greater topsoil delivery to a lake in response to the expansion of agriculture (e.g., Chiverrell *et al.,* 2008; Shen *et al.,* 2008). Inorganic and organic geochemical measurements also provide insights into catchment soil development and weathering and erosional processes (Giguet-Covex *et al.,* 2011) that may influence sediment supply through time. Without a robust understanding of changes in catchment conditioning through time, quantitative relationships identified between flow stage and sedimentary evidence of palaeofloods may be misinterpreted.

2.1.2.2 Sediment deposition in lakes

2.1.2.2.1 Mechanics of sediment deposition

Sediment plumes entering lakes are subjected to a number of physical and chemical processes that determine the nature and rate of deposition across the lake bed. Sediments extracted from a lake bed are typically comprised of clastic (i.e., terrestrially-derived) material as well as autochthonous biogenic compounds that can include silicates, carbonate and organic matter (Lowe & Walker, 1997).

Palaeoflood records are most effectively extracted from sediment sequences where sufficient river-borne material is delivered during a flood to overprint the near-continuous autogenic (internal) or allogenic (external) sedimentation pattern at the lake bed with a distinctive detrital lamination. Distinguishing the different sedimentary components lain on the lake bed is therefore an important first step but a non-trivial task. Lakes often exhibit a heterogeneous sediment matrix consisting of fine-grained allochthonous clay and silt, siliceous material (e.g., diatoms) and variable organic matter content, comprised of detrital plant material (leaves, wood, seeds) and humic substances as well as autogenic planktonic and benthic microbes (Håkanson and Jansson, 1983; Lowe and Walker, 1997). Sediment sequences in lakes that experience climatic conditions conducive to intensive photosynthetic activity, or where considerable Ca-rich bedrock is found in the catchment (including some upland lakes in the European Alps where palaeoflood studies have been undertaken; e.g., Lake Iso; Lauterbach *et al.,* 2012), are more strongly influenced by the precipitation of carbonate while other lakes display annually laminated (varved) sediment sequences (e.g., Czymzik *et al.,* 2013). Palaeoflood records have been extracted from each of these lake settings, although site-specific hydrogeomorphic processes, sediment provenance and within-lake depositional mechanisms must be considered. Broadly, catchments with considerable erodible soil cover and limited interruption of the sediment conveyor in the form of large deltas or extensive floodplains will receive greater allochthonous input (Dearing, 1997) and are therefore better suited to palaeoflood reconstruction (e.g., Foster *et al.,* 2008; Parris *et al.,* 2010).

2.1.2.2.2 Sediment dispersal and mixing pathways within lakes

Sediment load is a function of the relative production of autochthonous particles and the delivery of allochthonous material, a relationship that can change significantly through a lake's lifetime (Håkanson and Jansson, 1983). The pattern of sediment accumulation across a lake will be systematically altered based on the distance from the inflow acting as the dominant sediment source while basin morphology may result in selective deposition across the lake bed (Dearing, 1997). Sediment focusing at certain zones of small basins, reviewed extensively by Hilton (1985), poses a challenge when correlating thicknesses of individual palaeoflood units across multiple sediment cores from a single lake. Schiefer (2006) noted a non-linear decrease in sediment accumulation rates in Green Lake, British Columbia (a glacially-scoured upland lake ~2 km^2 in area) of 2 g cm^{-2} yr^{-1} at a delta proximal site declining to < 0.1 g cm^{-2} yr^{-1} at more

distal locations; results of a similar magnitude were found in Lake Geneva (Loizeau *et al.,* 2012). Thus, assessing the degree of spatial heterogeneity in sediment accumulation through stratigraphical correlation between multiple cores across a lake is crucial where high-resolution data are sought (Dearing, 1997).

The expression outlined by Stokes (1851) describing the frictional force exerted on a spherical particle of a certain diameter in a viscous fluid (Equation 1), known as hydraulic equivalence (Rubey, 1933), is the primary control on the rate of fallout from suspension of a sediment particle.

$$\boldsymbol{V = {g.\Delta m.Dm^2}/{18\eta}} \qquad \text{(Equation 1)}$$

where g = gravity, Δ_m = submerged density (mineral density δ_m – fluid density δ_f), D_m = diameter of the particle and η = fluid dynamic viscosity (in freshwater, δ_f = 1 g/cm^3 and η = 0.01 g/cm^{-1}/s^{-1}) (Garzanti *et al.,* 2008). Equation 1 is applicable when laminar flow conditions exist (i.e., Reynolds Number (Re) < 0.5; Håkanson and Jansson, 1983). In turbulent flows with higher Re values (> 0.5), settling velocities approach being independent of the drag coefficient (C_d) and Stokes' Law may be invalid. Several attempts to derive empirical equations applicable to turbulent flow exist (e.g., Cheng, 1997; Jiménez and Madsen, 2003). Flows that maintain turbulent momentum are capable of moving considerable distances across a lake bed while transporting high suspended sediment concentrations. These turbidity currents may take the form of high-density hyperpycnal flows, which are considered further in Section 2.2.4.

While settling velocity is primarily a function of particle size and fluid density and viscosity, differing mineral composition or particle shape can also affect settling velocity. In particular, where fluid density remains constant, particles composed of denser minerals (e.g., magnetite) will be deposited at an equivalent velocity to larger particles predominantly made up of common, less dense minerals such as quartz, feldspars or calcite (referred to as a *size shift*; Garzanti *et al.,* 2008). Furthermore, the influence of turbulence and viscosity on settling velocity varies between grains of silt, sand or gravel (Garzanti *et al.,* 2008). In the case of lakes (where gravel deposition is less likely), size shifts can be easily predicted for silt particles, but calculating correct settling velocities for sand which account for size shifts is much more challenging (e.g., Gibbs *et al.,* 1971; Cheng, 1997) as a result of circular interplay between particle size, the drag coefficient of the water column and the mineral composition of the sand

fraction. In addition, particles settling in natural settings are rarely spherical, leading Komar and Reimers (1978) to incorporate the Corey Shape Factor (CSF; quartz = 0.7, mica = 0.1 according to empirical estimates; Komar *et al.,* 1984) into Equation 1.

Mechanisms that generate turbulent flow within the water column, such as wind-induced waves and currents or thermal stratification (the warming of surface waters during summer while cold water remains at depth year-round), drive mixing between adjacent layers (Imboden and Wüest, 1995). These turbulent flows can result in settling velocities deviating from those predicted by Stokes' Law for quiescent fluids (Håkanson and Jansson, 1983).

Wind speed and fetch are the dominant forcings on the size and power of wind-generated waves and currents, respectively, in a lake. Particles at the lake bed may become re-suspended when shear-generated turbulence (controlled by wind speed and water depth) exceeds a frictional threshold (Figure 2.1) that depends on the density, size and cohesion of grains (Imboden & Wüest, 1995).

Sediment remobilization during periods of high wind-speeds can potentially create hiatuses in the sedimentary sequence or scour prior event deposits. Applying a multi-core extraction protocol across a lake can enable the degree of re-suspension across a basin to be assessed (Dearing, 1997).

Lakes with long wind fetch are also more susceptible to slumping along lake margins, which can generate extensive turbidity currents and leave sedimentological imprints that will complicate the stratigraphical sequence of 'background' and flood-derived sedimentation (Talbot & Allen, 1996). The turbulent effects of waves in small, deep lakes should be minimal, and thus represent a preferred study site characteristic. These effects should be considered, however, where shallow lakes are selected as field sites. Where data on local wind speed spanning long time periods are available, empirical equations have been developed describing the relationship between orbital velocity driven by wave action and fetch and their ability to entrain sediment, although these relationships are highly complex (Håkanson and Jansson, 1983). If wave motion has been calculated (see Håkanson and Jansson, 1983), Equation (2) relates its power to move particles smaller than 500 μm (Komar & Miller, 1975), which are typical of suspended sediments likely to reach a lake basin:

$$\boldsymbol{\rho}.\boldsymbol{u_m}^{\mathbf{2}}(\Delta_{\boldsymbol{m}}).\boldsymbol{g}.\boldsymbol{d} = \boldsymbol{C}.\sqrt{\mathbf{1}_{\boldsymbol{n}}}/\boldsymbol{d} \qquad \text{(Equation 2)}$$

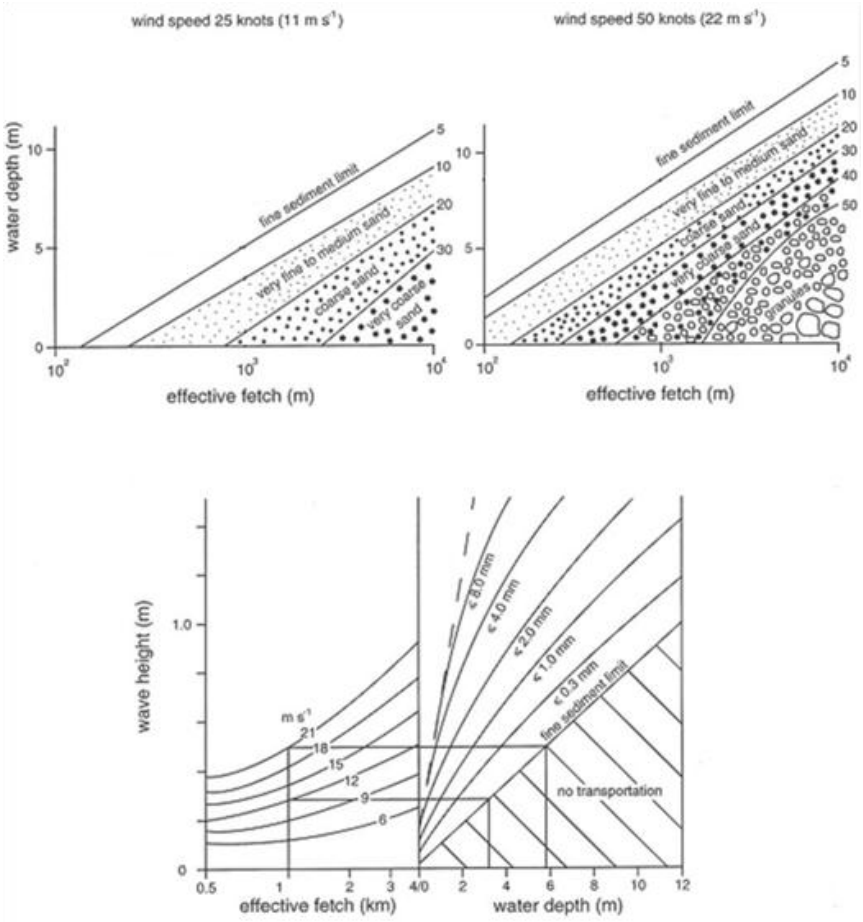

Figure 2-1 The relationship between effective fetch, water depth, wind speed and sedimentation thresholds in small lakes for different particle size fractions. Merged diagram modified from Dearing (1997), upper plate originally published by Johnson (1980) and lower diagram by Norrman (1964). Used with permission of Springer.

where u_m = horizontal wave velocity (m), d = grain diameter (mm), C = empirical constant reported to be 0.13 (Sternberg & Larsen, 1975), 1_n = horizontal displacement.

Turbulent flow driven by wind or surface heating is normally confined to the layer above the thermocline in well-stratified lakes. However, wind energy or a density differential between water masses can trigger the vertical or horizontal movement of the thermocline, creating interval waves (seiches) that can affect the entire waterbody (Larsen and Macdonald, 1993; Talbot and Allen, 1996), even in large lakes (e.g., Lake Geneva; Lemmin *et al.,* 2005). Importantly, the propagation of seiche waves across a lake applies shear stresses at the lake bed potentially capable of sediment re-mobilisation (Lemmin *et al.,* 2005). While the frequency, magnitude and effect on basal sediments of these interval waves are highly complex and depend on the stratification

of the water column and basin morphology (Larsen & Macdonald, 1993), their effects have been shown to be a prominent feature in the stratigraphical record (Pomar *et al.,* 2012).

The time available for suspended particles to be subjected to these diffusion mechanisms provides an additional control on spatial accumulation patterns. Residence time of water in lakes measures the average time taken for a single waterparcel to leave a waterbody from a specified location (Monsen *et al.,* 2002), and a change in this parameter of the hydrological budget, due to climatic change, land cover perturbation or lake-level change (Dearing, 1997) can alter the nature of deposited sediments. For example, fine suspended grains may be removed from lakes with short residence times via the outflow prior to deposition at the lake bed, imparting a negative skew (an excess of coarse grains in the sediment) on the particle size distribution.

Fish foraging at the lake bottom as well as the burrowing of microbes and macrofauna can also result in substantial post-depositional disturbance within the upper, biologically-active zone of profundal lake sediments (Davis, 1974; Håkanson and Jansson, 1983). Bioturbation poses a particular challenge for identifying distinctive laminations (Krantzberg, 1985) and calculating sediment ages using radionuclide techniques by flattening down-core ^{210}Pb concentration profiles and masking ^{137}Cs or ^{241}Am peaks (Appleby, 2001). The extent of lake-bottom benthic activity appears to be spatially variable (White & Miller, 2008) and extracting multiple cores across a lake basin can enable regions of more intensive bioturbation to be identified (e.g., Schiefer, 2006).

2.1.2.2.3 Controls on river plume flow patterns

River plumes entering lakes diffuse across the basin as hypopycnal (over-), inter- or hyperpycnal (under-) flows, controlled by the relative densities of the incoming plume and the water column (Figure 2.2). Interplay between the concentration of suspended sediment in the incoming plume and the stratification of the lake (due to thermal or density differentials) thus plays an important role in determining the dispersal of sediment (Talbot and Allen, 1996). Within-lake physical mechanisms (described in Section 2.2.2) subsequently control the movement of suspended particles. Annual temperature variability of lake surface waters is primarily driven by insolation

patterns and, on shorter timescales, by local weather conditions (particularly wind-driven mixing), and is an important control on lake stratification (Hostetler, 1995).

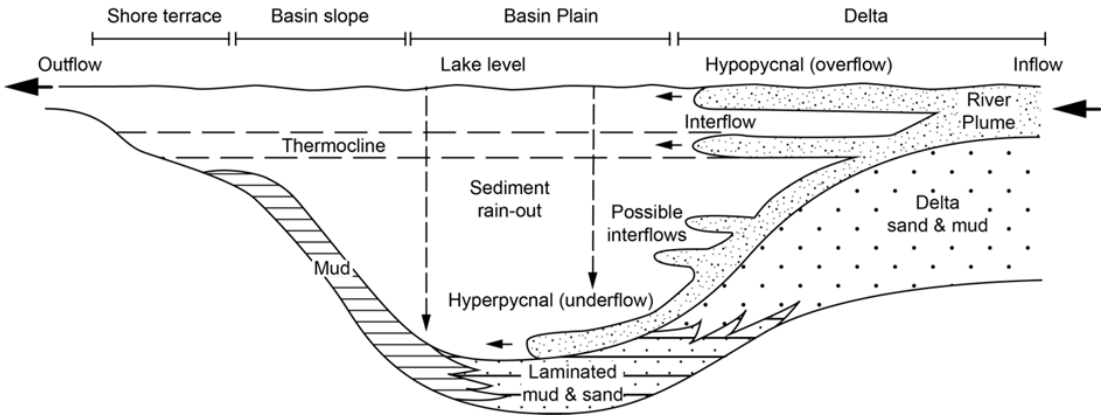

Figure 2-2 Processes of sediment dispersal and associated deposits within a lake basin dominated by clastic sedimentation. Lake dimensions and sediment thicknesses are not to scale. Re-drawn from Sturm and Matter (1978).

At depth, intra-annual temperature variability is normally much less pronounced, thus surface waters (epilimnion) are typically warmer and less dense than deep water (hypolimnion) (Boehrer and Schultze, 2008). The boundary that forms between these layers, most commonly during summer months, is called the thermocline (Figure 2.2). Lakes that display thermal stratification may generate interflows at the thermocline as fluvial discharge is often denser than the epilimnion but less dense than the bottom, unmixed hypolimnion (Sturm and Matter, 1978). Cooling of the epilimnion during autumn and winter often causes the water column to turn-over, degrading the thermocline. The potential for mixing is strongly influenced by lake basin morphology (Gorham & Boyce, 1989).

While the seasonality of floods can be explored where annually laminated sequences exist (e.g., Czymzik *et al.,* 2010; Swierczynski *et al.,* 2012), the nature of annual stratification can produce highly variable depositional features (Håkanson and Jansson, 1983) and may complicate the preservation of palaeoflood signatures. For example, if lake stratification breaks down during winter, high-density river flows are more likely to trigger an underflow than during summer, when plumes are more likely to disperse above the thermocline. Weakly or unstratified lakes can thus be advantageous for recording flood stratigraphies, as the hydrodynamic relationship between particle size and river discharge is less likely to be modified by internal processes in the water column.

In the largest lakes, the Coriolis effect will divert incoming river plumes in an anti-clockwise direction from the delta in the northern hemisphere (Håkanson and Jansson, 1983), which could alter the relationship between detrital layer thickness and distance from the delta if cores are extracted counter to the plume direction.

2.1.2.2.4 Importance of hyperpycnal flows

Energetic, sediment-laden underflow plumes, first noted by Forel (1885), have been identified as an important process in delivering sediment to submarine deltaic settings on the continental shelf (Mulder *et al.,* 2003; Best *et al.,* 2005; Migeon *et al.,* 2012). These hyperpycnal flows have also been identified in man-made reservoirs (Cesare *et al.,* 2001) and temperate lakes (e.g., Lake Tahoe; Osleger *et al.,* 2009). Hyperpycnal plumes often form when the suspended sediment concentration of the river exceeds the density of the lake water and down the delta, spreading across the basin floor (Mulder *et al.,* 2003). As a result, sedimentary signatures of high-magnitude discharge events have been attributed to hyperpycnal flows because as they are capable of rapidly delivering significant volumes of sediment to the lake bottom.

Hyperpycnal flows can be observed visually (e.g., Mulder *et al.,* 2003) or their potential to form in each lake can be calculated empirically based on suspended sediment load and river discharge measurements (Mulder *et al.,* 2003). Following the calculations of Mulder and Syvitski (1995), the probability of individual rivers to generate hyperpycnal flows can be estimated by comparing mean suspended sediment concentration to the critical concentration of 42 kg/m^3.

Deciphering the triggering mechanism for a sediment-laden hyperpycnal flow at some sites can prove challenging. While such flows have been noted in larger lakes with sediment-laden tributaries (e.g., the Rhone delta at Lake Geneva; Lambert and Giovanoli, 1988), thermally-driven density underflows are often observed in alpine or arctic lakes, where in-flowing rivers deliver water supplied from snow and ice melt that is considerably colder than the ambient lake water (Mulder *et al.,* 2003). Alternatively, the sliding or slumping of large and unstable river deltas (Lambert & Giovanoli, 1988) or subaqueous landslides triggered by seismic activity (e.g., St-Onge *et al.,* 2004; 2012) are capable of generating turbidity currents that traverse across the lake bottom.

In lakes where incoming river water under normal flow conditions is low density and thus disperses near or above the thermocline, the exceptional suspended sediment

load experienced during a phase of heightened river discharge (i.e., a flood) may be capable of generating a hyperpycnal underflow (Mulder *et al.,* 2003; Migeon *et al.,* 2012). Thus, if the formation of such hyperpycnal flows can be ascribed solely to high flows, the resulting sediment deposit will represent a palaeoflood signature (Brown *et al.,* 2000).

2.1.2.2.5 Role of deltas

Delta morphology can strongly influence the dynamics of river plumes (Talbot and Allen, 1996) but interplay between river discharge, lake morphology and deltaic sedimentation means delta form is in turn sculpted by incoming river flow, particularly where hyperpycnal flows occur during high discharge events (Olariu *et al.,* 2012).

Many freshwater lakes display steeply-graded, coarse-grained deltas exhibiting classic Gilbert-style morphologies (Gilbert, 1885; Figure 2.3), and sediment-laden hyperpycnal flows tend to move down steep deltas. Modelling work by Olariu *et al.* (2012) of the Red River delta flowing into Lake Texoma, southern USA, shows the direction of delta progradation and steepness of the foreset slope can significantly deflect the flowpath of descending hyperpycnal plumes (~80° from the inflow direction under low flow and steep slope angle, ~8% under highest flow and low slope angle). Lateral shifts in delta morphology may result in sediment being delivered to different areas of the lake through time (Sastre *et al.,* 2010) while the formation and evolution of multiple, branching channels on top of a river delta will generate highly distributive sediment deposition across the basin (Olariu & Bhattacharya, 2006). Delta morphology is strongly affected by the particle sizes delivered as bedload and suspended load, which in turn can alter sediment dispersal of subsequent events (Orton & Reading, 1993). Lake geometry is also important: in narrow basins or where sublacustrine channels are present, the confined flow may focus sediment deposition or erosion along a particular path (Girardclos *et al.,* 2012), compared to plumes dispersing into broad, circular lakes.

Delta progradation has particularly important implications over longer timescales (centuries or longer) for modifying the thickness and particle size distributions of deposited flood laminations. In lake sediment profiles dominated by river input, flood units are expected to thin and fine away from the delta. However, the zones where thicker and thinner layers are predicted to be deposited may migrate in response to delta progradation, even if flood magnitude remains constant (Figure 2.4). This process

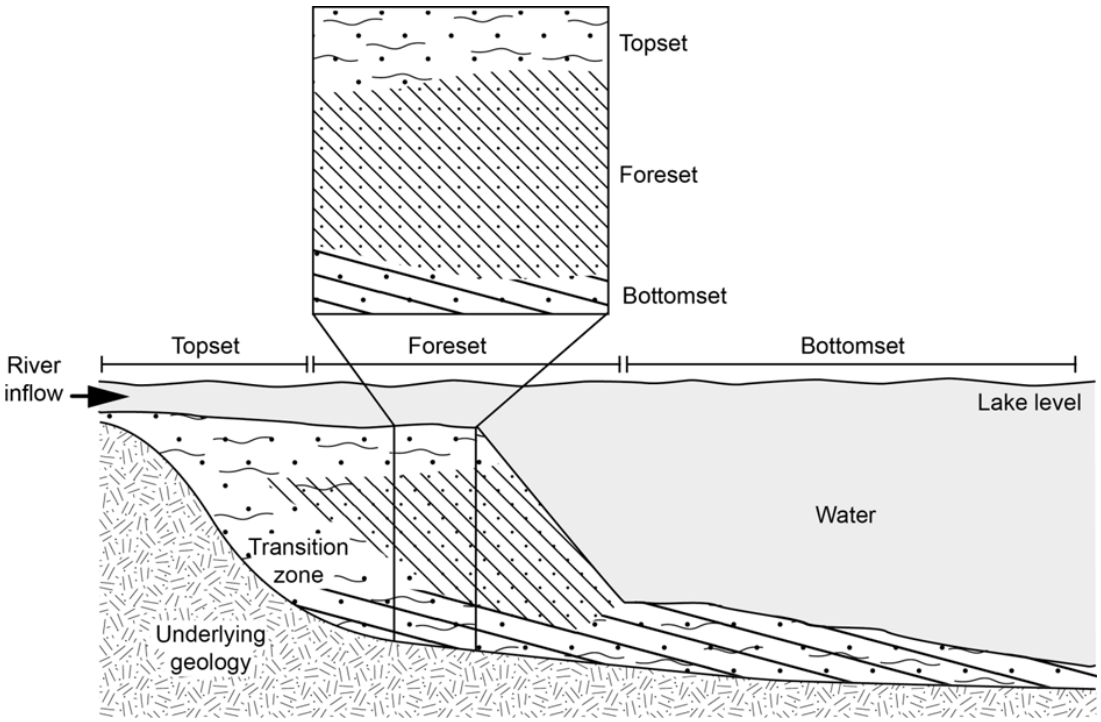

Figure 2-3 Conceptual model of the stratigraphy of a coarse-grained Gilbert-style lake delta. Modified from Friedman and Sanders (1978).

may render the use of layer thickness as a proxy of stream power problematic and must be considered through the use of multiple (at least three) core locations to characterise the three-dimensional geometry of flood deposits (Jenny *et al.,* 2013). Sites immediately adjacent to the inflow experiencing exceptionally high sediment accumulation rates may be particularly problematic, especially where multiple sublacustrine channels with erosive capabilities are active (Shaw *et al.,* 2013).

2.1.2.2.6 Influence of flocculation

Biological factors (e.g., the presence of microorganisms, faecal matter, dissolved and particulate organic matter), the chemical characteristics of the water (e.g., pH, ionic concentration, redox potential) or physical processes (including the turbulence, temperature and suspended sediment concentration of the flow), may trigger fine-silt, clay and organic particles to bind with other entrained grains, due to the electrical charges produced across their comparatively large surface areas and/or through microbial binding (Droppo *et al.,* 1997). This may occur prior to entering the river system (aggregates), or within the fluvial or lacustrine water column (flocculates) (Droppo *et al.,* 1997).

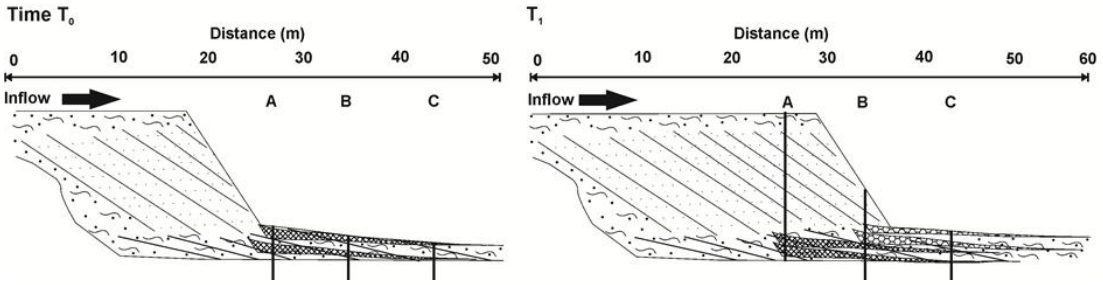

Figure 2-4 Schematic illustration of the role lacustrine delta progradation may exert on palaeoflood deposit thickness. At time T_0, recent floods have deposited a series of laminations which thin away from the delta. At time T_1, the delta has prograded substantially into the lake. When floods of similar magnitude to those at T_0 occur at T_1, the flood-related sedimentary units will be absent from core site A and significantly thicker at core sites B and C compared to those lain down at T_0. In essence, a sediment core extracted from site B soon after T_1 will contain multiple flood laminations of variable thickness that in fact reflect floods of equivalent magnitude.

Their heterogeneous nature can result in significant changes to particle shape, density and porosity (Droppo, 2001). Most importantly, flocculation can substantially alter the hydrodynamic relationship between particle size and settling velocity, as suspended flocs may settle more rapidly than predicted by Stokes' Law for the individual particles (Håkanson and Jansson, 1983).

The importance of this process in lacustrine settings has been documented by Hodder (2009), who identified macroflocs in the varved Lillooet Lake (British Columbia, Canada; Desloges and Gilbert, 1994) composed of particles two orders of magnitude smaller bound together. Micro- (10 μm – 35 μm) and macroflocs (200 μm – 280 μm) both make substantial contributions to annual sediment flux in Lillooet Lake.

However, detailed exploration of the mechanics of formation, internal floc architecture and rigorous assessment of the degree of flocculation in natural sediments are still on-going (Droppo, 2001) and traditional methods for measuring absolute particle size remain commonplace, but do not fully consider the issue of aggregate size (Haberlah and McTainsh, 2011). Experimental data from a flood-laminated alluvial terrace at Flinders Range, South Australia, in which mixed particle size distributions were decomposed into different end-members, showed that flocs settle out of suspension

first during flood events (Haberlah and McTainsh, 2011). Their decomposed distributions showed particle size variability across a flood deposit characterised by a light (sand-dominated) and a dark (silt) band. When considered as mixed distributions, no change in particle size across the bands was observed. This has significant implications when exploring particle size data for evidence of palaeofloods and highlights the value of applying statistical decompositional techniques to particle size datasets (e.g., Weltje and Prins, 2003; Haberlah and Mctainsh, 2011).

However, visual examination under a low-power microscope of sediment trap samples from Brotherswater, a small upland lake in northwest England (discussed further in section 4.2.1), highlights that dark-brown flocs, predominantly composed of bound fine-silts and organic matter, can be clearly distinguished from discrete sand grains (D. Schillereff, unpublished data). This confirms that the sand fraction settles through the water column and is deposited on the lake floor as individual particles, which differs from the observations of Hodder and Gilbert (2007) who found macroflocs of primary coarse particles bound to microflocs in Lillooet Lake. Absolute measurements of particle size in the laboratory can be acceptable for palaeoflood research in lakes where flood deposits are characterised by primary sand-sized particles within a finer matrix; laboratory tests or a sediment trapping protocol can be used to gauge the extent of this potential issue.

2.1.2.3 Conceptual model of palaeoflood analysis

Above, we have discussed the role of environmental setting, the sediment transfer processes and the depositional mechanisms that can regulate how stratigraphical flood signatures are preserved in lake basins. These are integrated here into a conceptual model to act as a rapid reference for researchers exploring the potential for a prospective field site to contain a robust palaeoflood record (Figure 2.5). While there will be considerable site-specific variation in terms of local geology, climate, degree of human disturbance or nature of the fluvial system (e.g., Parris *et al.,* 2010), this model outlines a set of considerations to guide field site selection.

Stable and unimpeded sediment transfer from catchment to lake is ideal, while desirable lake characteristics include a deep basin minimising sediment remobilisation, long residence time and weakly- or non-stratified water column, sufficient river-borne material delivered during a flood to overprint the normal sedimentation pattern, and size grading (fining) of particles from inflow-proximal to distal settings.

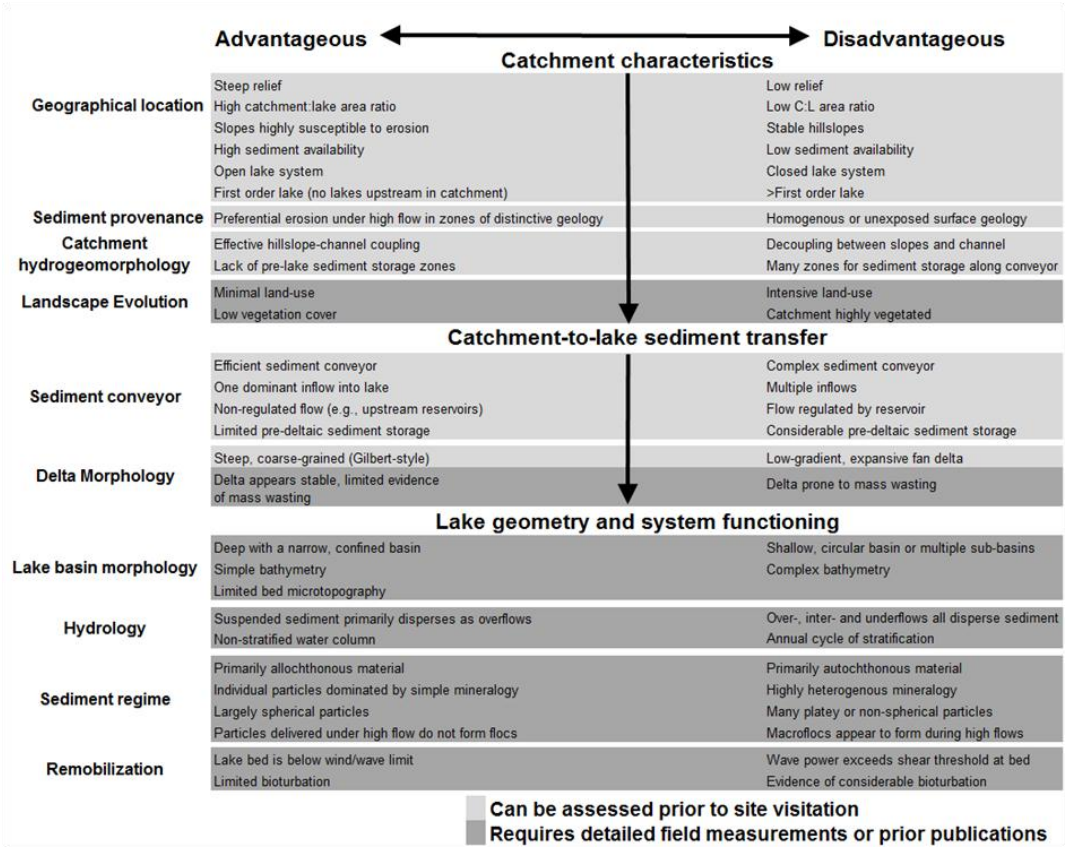

Figure 2-5 The physical landscape and lake basin characteristics and sediment delivery processes most advantageous or disadvantageous to the archiving of a palaeoflood sequence in lake sediments.

2.1.3 Review of analytical methods

A range of methodologies have been used to extract flood data from lake sediments (Brown *et al.,* 2000; Arnaud *et al.,* 2002; Noren *et al.,* 2002; Moreno *et al.,* 2008; Vasskog *et al.,* 2011; Kämpf *et al.,* 2012; Swierczynski *et al.,* 2012; Czymzik *et al.,* 2013; Simonneau *et al.,* 2013; Wilhelm *et al.,* 2013). The focus of the palaeoflood literature has largely been two-fold; either generating millennial-scale records of flood-rich and flood-poor phases for the Holocene and discussing their possible climatological forcings (e.g., Noren *et al.,* 2002; Czymzik *et al.,* 2010; 2013; Wilhelm *et al.,* 2012) or adopting an event-scale approach focussing on distinguishing the stratigraphical signature of discrete floods (Thorndycraft *et al.,* 1998; Arnaud *et al.,* 2002) from other mass movement deposits (e.g., Wirth *et al.,* 2011). In practice, many researchers achieve both of these objectives by identifying signatures of detrital layers, counting their frequency and subsequently identifying large-scale climatic or anthropogenic

forcings that explain the phases of more frequent high-magnitude floods. Lake sediment records have provided some of the best continental palaeoclimate records using other well-established palaeobiological or stable isotopic techniques (Leng and Marshall, 2004; Oldfield, 2005). However, using the calibre or provenance characteristics of inflow materials for environmental reconstructions presents different methodological challenges. Accounting for the range and variety of depositional mechanisms requires care during field site selection and sample recovery as well as the capability to acquire high-resolution data (Gilli *et al.,* 2013).

By overcoming issues of preservation, post-depositional processes and difficulties in obtaining sufficient analytical resolution, signatures of individual floods can be distinguished from the background sediment matrix. Once identified, confirming the event laminations are the result of repeated flooding rather than other geophysical events capable of producing similar depositional signatures is critical (Table 2.1).

2.1.3.1 Field procedures

Selecting an appropriate lake and subsequently identifying ideal sites for core extraction should be guided by a thorough knowledge of basin bathymetry. Lakes with broad, flat central basins, and sufficient sediment availability in a catchment well-coupled to a fluvial system capable of transporting material to the lake under high flow conditions are ideal (Section 2.3.; Gilli *et al.,* 2013). Identifying safe, secure and easily accessible launch points onto the lake are important to facilitate repeated site visits.

Seismic reflection (Abbott *et al.,* 2000) or multibeam bathymetric surveys of lake basins (Gardner and Mayer, 2000; Miller, H. *et al.,* 2013) that remotely sense the thickness and characteristics of basin sediment fill, can aid selection of coring sites (Debret *et al.,* 2010; Wirth *et al.,* 2011; Lauterbach *et al.,* 2012; Wilhelm *et al.,* 2013). Deposits from other lake proximal sediment sources, in particular delta mass-movement or lake-edge slumping, can often be identified from acoustic reflections and thus avoided (Schnellmann *et al.,* 2002; Girardclos *et al.,* 2007; Lauterbach *et al.,* 2012). These data may also enable subaqueous morphological evidence of palaeoflood deposits to be examined. Channel incision down delta foreset slopes or across the lake bed or the identification of levee formations may indicate past hyperpycnal flows (Talbot and Allen, 1996). Such morphological evidence should encourage further efforts to retrieve long sediment records for palaeoflood analysis.

Table 2-1 Geophysical processes previously noted as being capable of generating depositional stratigraphical signatures in lake sediment profiles.

Process	Proxy	Reference
Debris flows	Stratigraphy; Particle size	Irmler *et al.,* 2006
Hillslope fires	Geochemistry; Loss-on-ignition; Pollen; Charcoal	Macdonald *et al.,* 1991
Jökulhlaups	Stratigraphy; Particle size; μXRF geochemistry	Lewis *et al.,* 2007; 2009
Lake-edge slumping	Stratigraphy; ^{14}C dating	Hilton *et al.,* 1986; Schnellmann *et al.,* 2002
Seismic activity	Stratigraphy; Particle size; ^{210}Pb measurements	Doig, 1990; Arnaud *et al.,* 2002
Snow avalanches	Particle size	Nesje *et al.,* 2007; Vasskog *et al.,* 2011
Turbidity currents	Stratigraphy; Seismic profiles; Particle size	Lambert and Giovanoli, 1988; Girardclos *et al.,* 2007
Windstorms or hurricanes	Stratigraphy; Particle size	Eden and Page, 1998; Noren *et al.,* 2002; Besonen *et al.,* 2008

It is critical that discrete flood laminations are correlated and mapped across multiple cores within lake basins to confirm their origin from river plumes, their three-dimensional geometry (Jenny *et al.,* 2013) and to enable chronological control to be transferred between cores. High-resolution visual analysis of sediment cores (e.g., Czymzik *et al.,* 2013) and proxy measurements (e.g., magnetic susceptibility; Dearing, 1983; μXRF scanning geochemistry) are rapid and effective methods of cross-correlating between cores. Baltzer (1991) traced clastic sediment units across 43 cores extracted from Lake Tanganyika using particle size and X-ray diffraction measurements.

2.1.3.2 Stratigraphical analysis

Many proxy techniques have been applied to lake sediment sequences to identify and characterise detrital laminations, including measuring the thickness of visual layers (e.g., Bøe *et al.,* 2006), particle size analysis (e.g., Arnaud *et al.,* 2002), organic and inorganic geochemistry (e.g, Brown *et al.,* 2000; Vasskog *et al.,* 2011), magnetic susceptibility (e.g., Osleger *et al.,* 2009), loss-on-ignition (e.g., Nesje *et al.,* 2001) and density and luminosity measurements (Debret *et al.,* 2010).

2.1.3.2.1 Techniques for recording the visual stratigraphy

Logging the visible core stratigraphy prior to sub-sampling has is a valuable technique for deciphering potential event layers that are clearly different from the dominant sediment core material (e.g., Arnaud *et al.,* 2002). High-resolution photography (Cuven *et al.,* 2010), thin-section preparation (Swierczynski *et al.,* 2012; Czymzik *et al.,* 2013), Computer tomography (CT) X-ray scans (Støren *et al.,* 2010) and core scanning for a sediment density or reflectance (L*) signal (Debret *et al.,* 2010; Lauterbach *et al.,* 2012) have been used to characterise and quantify changes in colour, sediment matrix structure and mineralogically-different event layers.

Microfacies analysis of annually laminated sediments from Lake Ammersee (southern Germany) identified three types of detrital layers exhibiting different mineralogical composition and variable grading (Czymzik *et al.,* 2013). Erosional bases across some units are visible and the matrix-supported units are clearly distinguishable by the presence of primary clastic grains held within a calcite matrix. In other instances, thin sections of discrete detrital layers show a basal unit enriched in organic material and thin clay caps, such as at Lago del Desierto, Patagonia (Kastner *et al.,* 2010). CT scanning of sediment cores produces a three-dimensional image from which X-ray attenuation numbers correspond to sediment density at sub-mm scales, enabling extremely thin flood layers to be distinguished from a dark, organic-rich sediment matrix (Støren *et al.,* 2010). Similarly, down-core spectrophotometric measurements (denoted by L* a* b* values, reflecting total reflectance, chromacity along the green to red and blue to yellow visible light axes, respectively) can detect small changes in sediment colour due to greater clastic inputs during floods (Debret *et al.,* 2010).

2.1.3.2.2 Measuring detrital layer thickness

Where detrital laminations exhibit sharp contacts, individual layer thickness can be measured accurately (e.g., Kämpf *et al.,* 2012; Czymzik *et al.,* 2013). Flood-layer thickness theoretically depends on carrying capacity and the duration of the high discharge, but sediment supply also regulates this relationship. Bøe *et al.* (2006) showed a significant correlation between thickness, higher mean particle size and better sorting for clastic deposits, supporting increased stream power as the dominant delivery mechanism. Matching flood laminations between delta-proximal and distal cores and comparing layer thickness can also provide insight into the depositional mechanism (Czymzik *et al.,* 2013). For example, a unit displaying a thinning trend away from the delta indicates sediment was delivered in a river plume that decelerated as it dispersed and the volume of material settling out of suspension declined accordingly. Other research has been unable to find a positive correlation between layer thickness and river discharge (e.g., Lapointe *et al.* (2012) working at East Lake, Canadian Arctic), suggesting that measuring particle size within discrete layers is a more suitable proxy.

Accounting for variable sediment supply through the timescale of deposition, potentially driven by changes in land-use and/or climatic fluctuations, is critical because extreme events of similar magnitude may deposit layers of unequal thickness. Applying statistical techniques that account for temporal changes in background median values can be useful, allowing peaks relative to local background to be assigned as 'extreme values' within a time series. For example, Besonen *et al.* (2008) apply the CLIM-X-DETECT package (Mudelsee, 2006) to a varved lake sediment record from Massachusetts to identify anomalously thick flood deposits triggered by hurricanes over the past millennium.

2.1.3.3 Particle size as a palaeoflood proxy

In lake sediment sequences comprising clastic material as the primary component, an imprint of the hydrodynamic relationship between river discharge and the particle size distribution of the suspended sediment should be present. A positive relationship between higher discharge and coarser particles is often observed (e.g., Campbell, 1998; Lenzi and Marchi, 2000) but factors including selective sediment sources, intensity of erosion and local soils and bedrock lithologies may substantially alter this relationship (e.g., Walling and Moorehead, 1989). While some evidence of particle size - stream power decoupling from lake sediments has been published (Cockburn & Lamoureux,

2008), as rivers at low flow generally deliver very little sediment, sediment cores dominated by fine-grained silts and clays most likely reflect sedimentation during slightly elevated flows that commonly occur. Coarse-grained layers punctuating this matrix therefore reflect the highest-energy floods, so particle size analysis identifying the coarsest fraction appears a valuable palaeoflood proxy (Cockburn and Lamoureux, 2008). This approach has underpinned the development of robust palaeoflood records in Africa (Reinwarth *et al.,* 2013), the European Alps (Arnaud *et al.,* 2002; Wilhelm *et al.,* 2012; Wirth *et al.,* 2013a; 2013b), New Zealand (Eden and Page, 1998; Page *et al.,* 2010), Norway (Bøe *et al.,* 2006; Vasskog *et al.,* 2011) and North America (Osleger *et al.,* 2009; Hofmann and Hendrix 2010; Parris *et al.,* 2010). In some arctic or pre-alpine lakes capable of depositing annually laminated sediments, particle size measured at annual resolution has been directly correlated with rainfall amounts, including Cape Bounty, arctic Canada (Lapointe *et al.,* 2012) and Rock Lake, British Columbia (Schiefer *et al.,* 2010), enabling more comprehensive hydrogeomorphological interpretations to be drawn.

Measuring particle size at the micro-(sub-mm) and macro-structural (cm) scale has also provided detailed information on depositional processes (Vasskog *et al.,* 2011; Czymzik *et al.,* 2013). For example, graded layers reflecting hyperpycnal flows, finer-grained silt and clay layers settled out of suspension from overflows and matrix-supported layers requiring larger than normal sediment supply were distinguished by Czymzik *et al.* (2010; 2013) at varved Lake Ammersee, illustrating the ability for process interpretations to be drawn from microstratigraphical particle size measurements. Down-core variation in mean and sorting particle size values (e.g., Blott and Pye, 2001) enabled visually different laminations in Oldvatnet, Norway (Vasskog *et al.,* 2011) to be attributed to different triggering mechanisms, namely river floods, snow avalanches and density currents due to lake-edge slumping.

The graded nature of some lacustrine deposits is a particularly useful sedimentological characteristic for distinguishing flood layers. Thick (many cm's), siliciclastic facies in sharp contact with the organic- or carbonate-dominated sediment matrix and often exhibiting normal grading (i.e., classic Bouma (1962) turbidite) have been traditionally attributed to catastrophic events such as glacial outburst floods (jökulhlaups; Lewis *et al.,* 2009) or shelf-edge collapse triggered by earthquakes (Beck, 2009). In many studies, turbidic deposits have been interpreted as reflecting terrestrially-derived material delivered during episodic flood events (Brown *et al.,* 2000; Lauterbach *et al.,*

2012; Czymzik *et al.,* 2013; Gilli *et al.,* 2013; Wirth *et al.,* 2013a). Turbidites can be correlated across a lake basin (Brown *et al.,* 2000) or between multiple lakes (Noren *et al.,* 2002; Glur *et al.,* 2013), confirming their ability to record discrete events.

Some sedimentary units exhibit normal-grading overlying inverse-grading and have been interpreted as reflecting the hydrographs of individual, high-magnitude floods. Mulder and Alexander (2001) developed a classification scheme for the Var turbidite series in the Mediterranean (Mulder *et al.,* 2001; 2003; Migeon *et al.,* 2012) in which this distinctive sedimentation pattern was attributed to the waxing and waning phases of river flow that delivered sufficiently sediment-laden plumes to generate hyperpycnal flows upon entering the waterbody and then rapidly spread across the basin floor (Normark & Piper, 1991). The resulting deposit ("hyperpycnite") reflects the hydrodynamic conditions of the river, and similar facies have been identified in several lake sediment sequences (Ito *et al.,* 2009; Osleger *et al.,* 2009; Hofmann and Hendrix, 2010; Stewart *et al.,* 2011). The forcing mechanism follows a typical flood hydrograph: river flow velocity will steadily increase following the onset of a flood (i.e., waxing flow), depositing a sedimentary sequence of upwards-coarsening particles, reflecting the progressively coarser particles that can be transported as suspended load as river power increases. The subsequent diminishing discharge (i.e., waning flow) is reflected by an often thicker fining-upwards sequence (Mulder *et al.,* 2003). While these layers are normally mm- or cm-scale, a similar sedimentological structure is observed across a 30 cm thick layer in a sediment core extracted from Lake Puyehue, Chile (Chapron *et al.,* 2007), attributed to a dam-burst megaflood after the 1960 AD earthquake. Stewart *et al.* (2011) proposed the term 'inundite' for lacustrine flood deposits that exhibit this internal structure. Other stratigraphical signatures should be sought, including a basal erosional contact, bedded ripples or rippled, diagonal laminations (Mulder *et al.,* 2003), to confirm such deposits are indeed the result of hyperpycnal flows. Furthermore, the possibility of stacked inverse-to-normal grading units representing a single flood must also be considered, as shown by Saitoh and Masuda (2013) at Lake Shinji, Japan, due to lateral movement of the plunge point of a sediment-rich flood plume across a subaqueous delta.

Assessing particle size distributions alongside stratigraphic data can provide additional information on flood frequency/magnitude and sediment provenance. The degree of sorting, mean or median particle size and the sizes of prominent modes within particle size distributions has enabled deposits corresponding to river floods, shelf edge

slumping and snow avalanches to be distinguished (Arnaud *et al.,* 2002; Czymzik *et al.,* 2010; Vasskog *et al.,* 2011). Strong correlations between skewness and mean particle size (Bøe *et al.,* 2006) and sorting and mean particle size (Arnaud *et al.,* 2002) have been used as proxies for fluvial energy. Median (Q50) vs 90th percentile (P90) scatter plots (after Passega, 1964) display points representing low flow sedimentation, river floods and mass wastage events in different quadrants (Wilhelm *et al.,* 2012; 2013).

The tendency for deposited sediments to display mixed grain-size distributions as a result of the range of processes driving sedimentation can make it difficult to infer processes. Employing statistical models to unmix particle size distributions into multiple end-members, each of which represents a differing depositional mechanism, can address this issue (Sun *et al.,* 2002; Dietze *et al.,* 2012; Parris *et al.,* 2010), in conjunction with visual stratigraphical analysis to confirm the reality of each individual end-member. Flood laminations in lake sediment sequences from New England, USA, are clearly represented by the coarse end-member while background material appears as a fine-grained end-member (Parris *et al.,* 2010); standard frequency statistics were unable to effectively make this distinction.

2.1.3.4 Indirect particle size measurements

The susceptibility of different minerals to erosion is reflected in the bulk geochemical composition of sediments generated by erosion or weathering, based on the relative proportion of stable and unstable elements (Bloemsma *et al.,* 2012). This relationship can translate into a correlation between particle size and geochemical composition due to the grain-size specific nature of individual minerals. As a result, lake sediment sequences dominated by clastic material may enable certain geochemical signals to be used as a proxy of particle size. Furthermore, high-resolution core scanning devices (e.g., ITRAX; Croudace *et al.,* 2006) enable data at sub-mm scales to be extracted from sediment cores using X-ray fluorescence, potentially revealing sedimentary structures that proxies requiring manual sub-sampling are unable to access.

It is critical that analytical care is taken when interpreting μXRF measurements made on wet sediment because variable down-core water and organic matter contents may prevent precise dry mass elemental concentrations being obtained (Boyle *et al.,* in press, a; Chapter 3.3). The X-ray signal may also contain artefacts due to imperfections of the core surface or the development of a thin water film under the polypropylene cover (Hennekam & de Lange, 2012). In order to acquire more accurate dry mass

equivalent geochemical concentrations, Boyle *et al.* (in press; Chapter 3.3) outline two methods to apply in parallel: one applies a simple regression calibration, while the other is a novel technique that estimates water content for the full core from X-ray scatter data collected during the scanning process. We strongly recommend adopting this procedure where water content varies significantly along a wet sediment core. Other researchers have attempted to normalise elements of interest to either another element (e.g., Löwemark *et al.,* 2011) or to back-scatter peaks (e.g., Kylander *et al.,* 2012; 2013; Chawchai *et al.,* 2013). The potential for Fourier transform infrared spectroscopy (FTIR) to act as a rapid and cost-effective calibration technique alongside XRF scanning was demonstrated by Liu *et al.* (2013), who analysed inorganic and organic content of sediments from Lake Malawi (Africa) and Lake Qinghi (China).

Site-specific geochemical concentrations and, in some cases, ratios between selected elements, have been used to effectively characterise flood layers. For example, Czymzik *et al.* (2013) show elevated concentrations of Ti, K and Fe, normalised to back-scatter peaks, across cm-scale flood units at varved Lake Ammersee, where sedimentary rocks in the catchment supply significant volumes of detrital grains. A seasonal record was developed for Lake Mondsee, Austria (Swierczynski *et al.,* 2012), where elevated Ti and Mg concentrations in flood laminations were attributed to high river discharges from the northern siliciclastic-dominated and southern dolomite-rich catchments, respectively. The application of the Ca/Fe ratio as a particle size proxy has been microscopically confirmed via thin-section analysis at Lac Blanc, Belledonne Massif (Wilhelm *et al.,* 2012; Section 4.2.4). Similar assessments using the Zr/Fe ratio at Lac Blanc, Mont Blanc Range, (Wilhelm *et al.,* 2013) and K/Ti and Fe/Ti at Cape Bounty in the Canadian High Arctic, (Cuven *et al.,* 2010; Section 4.2.3) showed variations in these ratios were effective particle size proxies.

Vasskog *et al.* (2011; Section 4.2.2) matched the visual stratigraphical record of flood laminations at Oldevatnet, western Norway, to low Rb/Sr values, as Sr is more likely to be eroded from the catchment surface geology. Likewise, Rb is commonly associated with the clay fraction while Zr is often enriched in coarse silts, meaning higher Zr/Rb values should reflect coarser grains (Dypvik & Harris, 2001).

Mineral magnetic measurements have also been used as a particle size proxy, for example at Petit Lac d'Annecy where Foster *et al.* (2003) showed the χ_{LF} (low field) magnetic susceptibility parameter, measured on sediment trap and lake core samples, correlated positively with discharge-controlled variations in median particle size. An

equivalent positive relationship between χ_{LF} and the coarse silt-sand fraction was found at Taihu Lake, China (Li *et al.,* 2013). At Loch of the Lowes (southern Scotland), Foster *et al.* (2008) attribute the cyclical pattern of the HIRM (hard isothermal remanent magnetisation)/ χ_{LF} profile (reflecting the hematite to magnetite ratio) to reflect flood-rich and flood-poor phases. The potential for any single magnetic parameter to be controlled by sediment calibre, source or delivery process (Dearing, 1999) or the presence of bacterial magnetite (e.g., Oldfield and Wu, 2000) can pose interpretational challenges, however.

2.1.3.5 Adapting a multi-proxy approach

Combining multiple proxies in a single study can be particularly effective for distinguishing detrital laminations potentially linked to historical floods. High-resolution multi-proxy analysis of the Lake Suigetsu (Japan) sediment sequence (Schlolaut *et al.,* 2014) showed that discrete flood layers are represented by four sub-laminae, each characterised by changes in colour, the presence or absence of grading structure or diatoms and fragments of organic material, distinctive minerology, changes in grain size (assessed via thin section) and variable Ca, K, Si and Ti concentrations (measured via ITRAX core scanner). Thorndycraft *et al.* (1998) showed coincidental peaks in magnetic and geochemical indicators of clastic material and soil-derived pollen in four recent flood laminations at Lac d'Annecy (SE France), while sediment cores spanning the last 15, 000 years from Laguna Pallcacocha (Ecuador) were punctuated by numerous light-grey layers of clastic material characterised by low carbon content, coarse modal grain size and low biogenic silica concentrations, attributed to mobilization of sediment during El Niño-driven storm events (Rodbell *et al.,* 1999). Groupings of values on scatter plots of multiple proxies can also discriminate between depositional mechanisms (e.g., Støren *et al.,* 2010).

A good knowledge of catchment soil properties and surface geology may enable phases of greater clastic input during a flood to be identified on a site-specific basis (e.g., magnetic susceptibility record reflecting magnetite-rich catchment material; Osleger *et al.,* 2009). Where sedimentation does not record short-term magnetic susceptibility (MS) or loss-on-ignition (LOI) fluctuations, measuring sediment colour and reflectance has proved useful (e.g., Lac Le Bourget (SE France), Debret *et al.,* 2010; Taravilla Lake (NE Spain, Moreno *et al.,* 2008). Furthermore, down-core variability in carbon and nitrogen isotope ratios, reflecting the allogenic or autogenic supply of organic matter

(Meyers & Ishiwatari, 1993), can confirm the detrital provenance of flood deposits (Brown *et al.,* 2000; Ito *et al.,* 2009). Concurrent high dry density and low total inorganic and organic C values can also indicate flood layers (Gilli *et al.,* 2003). Combining spectrophotometric and Rock-Eval pyrolysis for discriminating detrital input from autogenic production of organic matter proved successful in two lakes in Gabon (Sebag *et al.,* 2013).

As mentioned in Section 3.2.2., variable sediment supply poses a challenge to deciphering a consistent palaeoflood trend through a core profile. Noren *et al.* (2002) use singular spectrum analysis to identify sediment deposits from 13 small lakes in New England, USA, that are greater than 1 σ from the first principal component of down-core measurements for multiple proxies (visual logging, X-radiography, MS, LOI and particle size). Most detrital layers display significantly high values in two or more proxy techniques, thus providing more confidence in the reconstructed storm record.

2.1.3.6 Developing robust chronologies

Establishing a well-constrained chronology is paramount in order to develop a flood history and extract data on event frequency. Palaeolimnologists use a number of chronostratigraphical techniques dependent on the timescales of the research interest and many dating methods and their associated challenges have been recently reviewed by Gilli *et al.* (2013). The timescales over which different dating tools are most applicable are presented in Figure 2.6. The most reliable chronologies are generated by integrating multiple, independent chronological tools and this approach is most successful on historical timescales (spanning, at most, the last few centuries) due to the number of independent techniques that can be employed concurrently.

Lake sediment sequences characterised by annually-deposited laminations (i.e., varves) are of great value to palaeoflood researchers as they offer high-resolution dating constraints (Ojala *et al.,* 2012). Additionally, instantaneous flood deposits create unique layers in the record that may differ substantially from typical varves. As a result, a number of detailed palaeoflood records of annual resolution have been generated (e.g., Czymzik *et al.,* 2010; 2013; Stewart *et al.,* 2011; Swierczynski *et al.,* 2012). Where climatic and limnological conditions generate seasonal-specific laminations, seasonally-resolved records of past floods have been obtained (Swierczynski *et al.,* 2012). Lakes often only produce varved sequences under specific conditions and, as depositional mechanisms may not be continuous over long

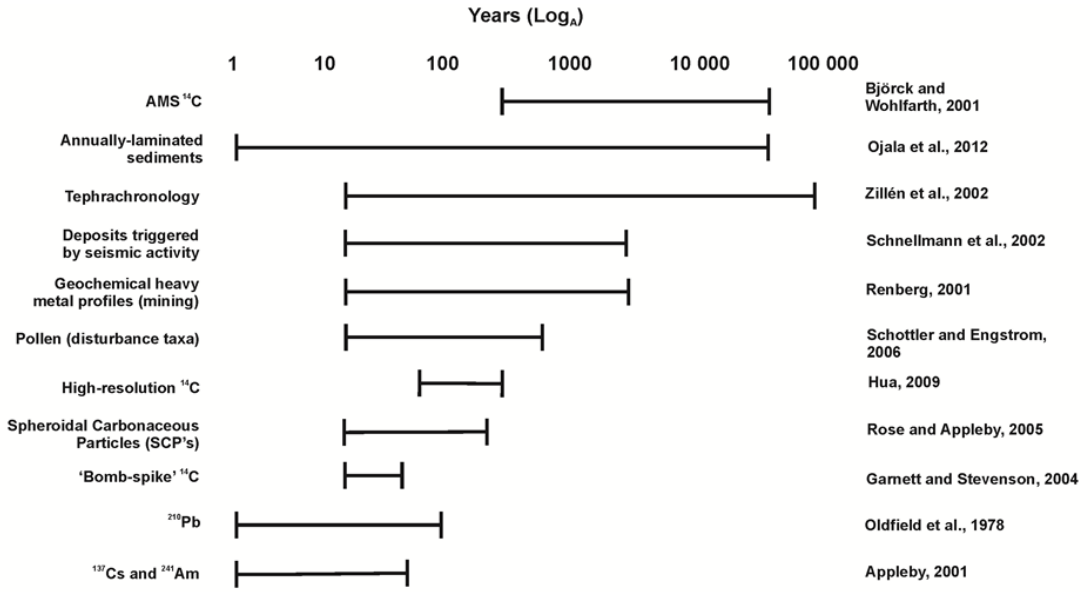

Figure 2-6 Timescales at which a range of chronological techniques can be effectively applied and relevant examples from the literature. Log scale on *x*-axis.

timescales, annually-resolved chronologies must be independently verified using other dating techniques (Ojala *et al.,* 2012).

Radiocarbon dating (^{14}C) is widely employed for dating lake sediment up to approximately 50 kyr BP (Bronk Ramsey *et al.,* 2012) and many palaeoflood reconstructions spanning the Holocene are underpinned by ^{14}C dating (e.g., Lauterbach *et al.,* 2012; Czymzik *et al.,* 2013, Gilli *et al.,* 2013). Radiocarbon dating faces a number of uncertainties (e.g., reservoir effects, 'old carbon', instrument precision; Björck and Wohlfarth, 2001) and identifying temporally precise markers in sediment sequences spanning several millennia is a significant challenge. As a result, such palaeoflood records are generally analysed in terms of flood-rich and flood-poor phases, as opposed to discrete flood events.

Conversely, natural and anthropogenic perturbations to the global carbon cycle during recent centuries (e.g., combustion of fossil fuels, release of nuclear weapons, changes in solar activity) have caused atmospheric ^{14}C concentrations to fluctuate through this time window, meaning calibration of a single radiocarbon date may yield multiple possible age ranges (Hua, 2009). Employing high-precision AMS ^{14}C dating can successfully disentangle recent core chronologies by *'wiggle-matching*' to these variations in atmospheric ^{14}C (e.g., Marshall *et al.,* 2007). This protocol offers substantial value when generating palaeoflood records spanning the past 200 to 300

hundred years, bridging the gap between shorter half-life radioisotopes (i.e., ^{210}Pb) and the conventional ^{14}C timescale. Similarly, nuclear weapons testing in the 1950s-60s released sufficient ^{14}C to significantly increase atmospheric concentrations before declining after the 1963 ban; this trend is recorded as fallout in upper profiles from different sedimentary environments (Garnett and Stevenson, 2004; Hua, 2009).

Measuring the gamma-activity of ^{210}Pb radionuclides is one of the most effective means of dating sediments lain down over the past century (Appleby, 2001). Although ^{210}Pb profiles can be affected by hiatuses in the sedimentary record resulting from periods of rapid sedimentation or instantaneous deposits triggered by seismic activity, mass-wasting or high-magnitude floods, they are usually a critical step when constructing core chronologies (e.g., Arnaud *et al.,* 2002). Importantly, Aalto and Nittrouer (2012) showed a clear response in ^{210}Pb profiles to individual flood events in floodplain sediment sequences. This non-steady-state accumulation means care must be taken when selecting a dating model (Constant Rate of ^{210}Pb Supply [CRS] or Constant Initial Concentration [CIC]; Oldfield *et al.,* 1978). Conversely, periodic spikes in ^{210}Pb concentrations down a lake sediment core, reflecting a response to elevated ^{210}Pb flux during high flows, could act as a palaeoflood indicator, although this would require more time-consuming and costly gamma detector measurements than aiming to calculate down-core sediment ages.

Measurements of ^{137}Cs and ^{241}Am activity are often run parallel to ^{210}Pb dating and the identification of two peaks in emission activity, attributed to fallout from atmospheric testing of nuclear weapons in the 1960s and emissions from the Chernobyl accident in 1986, respectively, provides precise chronostratigraphical markers for the late 20th century (Appleby *et al.,* 1991), although artificial radionuclide concentrations are often below detection levels in the southern hemisphere (most nuclear testing took place north of the equator; Humphries *et al.,* 2010). These markers have been used to verify ^{210}Pb profiles at sites where sediment accumulation rates have varied or where there has been downward migration of radionuclides through the sediment profile (Appleby, 2013). At sites where sediment accumulation may be non-uniform, radionuclide flux may be variable or concerns regarding mixing or slumping exist, other independent markers can validate recent radionuclide chronologies. Techniques previously employed include:

Attributing specific pollen-stratigraphical intervals to known phases of local vegetation change, particularly disturbance taxa (Schottler and Engstrom, 2006; Besonen *et al.,* 2008).

Elevated concentrations of industrial metals (e.g., Zn, Pb, Cd, As, Hg) deposited either from atmospheric fallout during industrialization or effluent from mining activity in the watershed (Renberg *et al.,* 2001; Schottler and Engstrom, 2006; Boyle *et al.,* in press, b; Chapter 2.2). Wilhelm *et al.* (2012) suggest normalizing Pb concentrations against Y in order to better differentiate natural- and anthropogenic-derived deposition. Artificial radionuclides (^{137}Cs, ^{60}Co) also serve as a chronological tool for recent decades where anomalously high down-core peaks in their concentrations are temporally correlated with discharges of radioactive substances from nuclear power plants directly into a river upstream of a lake that are known to have occurred at specific times (e.g., Thevenon *et al.,* 2013).

Counting spheroidal carbonaceous particles (SCP's) in the sediment profile, which reflect fossil fuel combustion (Rose & Appleby, 2005). Usefully, SCP's are widely dispersed geographically, are found in many sedimentary environments and display limited post-depositional degradation. Although regional differences are known, SCP measurements are generally useful from the initial rise after 1850 to peak concentrations in the late 20th century (Rose *et al.,* 1999). Down-core behaviour of polychlorinated biphenyls (PCBs), produced from 1927 until a global ban in 1976, can also provide chronostratigraphical markers (Schottler and Engstrom, 2006).

Seismic or volcanic activity can yield additional chronological markers in the form of tephra layers (e.g., Zillén *et al.,* 2002; Turney *et al.,* 2004) or thick, distinctive sedimentary layers which reflect lake-edge slumping trigged by earthquakes (Schnellmann *et al.,* 2002; Wilhelm *et al.,* 2012). Deposited tephras exhibit geochemical signatures unique to individual eruptions, enabling lake sediment chronologies to be refined (Orpin *et al.,* 2010). Chapron *et al.,* (2007) incorporate tephrostratigraphy into their age-depth model for a palaeoflood record at Lake Puyehue (Chile).

The most robust chronologies will often integrate multiple techniques and also consider stratigraphical context from which the samples for dating were extracted in order to better understand the sequencing of events. Such Bayesian approaches to age-depth modelling have been effectively applied on lake sediment sequences (e.g., Chawchai *et al.,* 2013) and slackwater palaeoflood deposits (Thorndycraft *et al.,* 2011),

whereby an age-depth model is built that incorporates prior knowledge pertaining to the order of deposition, sediment accumulation rates and depth of sampled intervals within the sediment column when calculating the probability distribution functions for individual points along the core (Bronk Ramsey, 2008). Geoscientific software developed recently facilitates simple application of Bayesian age-depth modelling with Markov Chain Monte Carlo simulations (e.g., Bacon; Blaauw and Andrés Christen, 2011; OxCal, Bronk Ramsey, 2009) to test various plausible age-depth models (e.g., Shen *et al.,* 2008).

The ultimate goal of sediment dating is to generate a well-constrained sequence that overlaps the instrumental river flow measurement period (second half of the 20th century), which may enable quantitative discharge values to be transferred to the palaeoflood record. Figure 2.6 highlights a number of techniques which may, in some cases, bridge the temporal gap between the ^{14}C record and the ^{210}Pb record (e.g., heavy metal signatures, pollen taxa, SCPs).

2.1.4 Interpretational protocol for flood palaeolimnological research

2.1.4.1 Schematic protocol

Researchers have described a number of characteristic sedimentary signatures attributed to historic floods, but local conditions and complex pre-depositional processes present interpretational challenges. We have developed a schematic protocol (Figure 2.7) to aid researchers with site and method selection and facilitate more rapid identification of typical flood laminations. Each stage of the model directs readers towards the relevant published material.

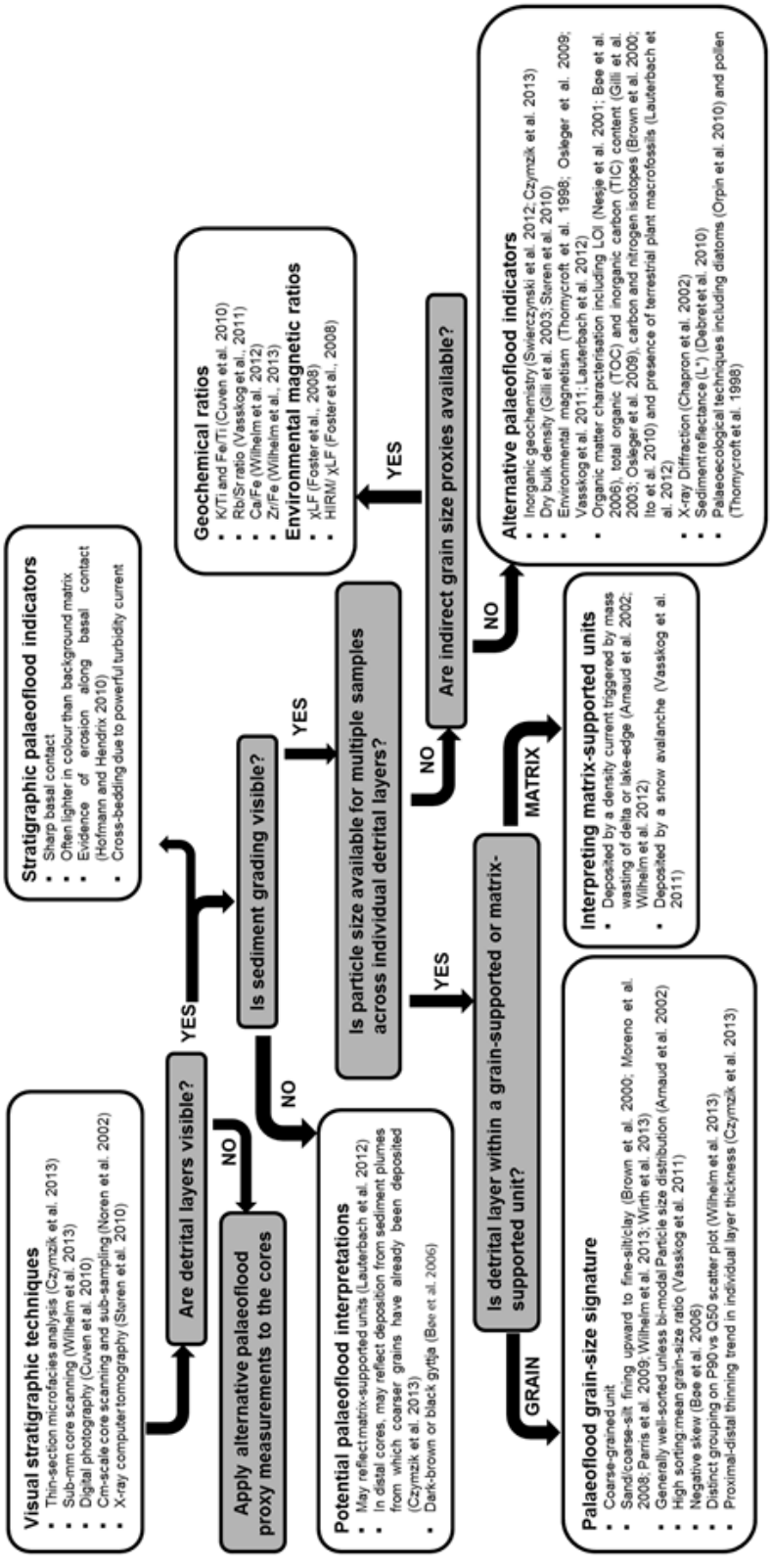

Figure 2-7 Schematic methodological pathway for interpreting palaeoflood deposits within lake sediment sequences.

2.1.4.2 Palaeoflood investigations from lakes: some case studies

To demonstrate the utility and functionality of the protocol for field site selection (Figure 2.5) and the interpretational schematic (Figure 2.7), and to further explore the mechanics of palaeoflood investigations using lake sediments, we present a series of case studies.

2.1.4.2.1 Brotherswater, northwest England

The lake (surface area 0.2 km^2) and catchment (surface area 12 km^2) morphology of Brotherswater (eastern Lake District, Northwest England) appears conducive to the preservation of palaeoflood deposits (D. Schillereff, unpublished), meeting the following key criteria (Figure 2.5): steep relief, large catchment area to lake area ratio (72:1), largely deforested slopes with ample sediment supply, a single inflow and limited pre-lake sediment storage. Furthermore, the flat central basin exceeds the depth (maximum 16 m) of potential wind-induced re-suspension for the dimensions of this water body, the lake appears weakly thermally stratified and sediment trap data show coarse sand is delivered as primary particles during phases of high river flow. On 24 March 1968, a severe flood affected much of the eastern Lake District, with a 43-year return period calculated for the River Eden flood levels at Carlisle (Smith & Tobin, 1979). In the Brotherswater sediment sequence (Figure 2.8a), two well-defined ^{137}Cs peaks (11-13 cm and 22-23 cm), the result of fallout from the 1986 Chernobyl incident and 1960s atmospheric weapons testing, respectively, bracket a coarser lamination at 14.75-18.75 cm depth that is attributed to this flood. There are no other candidate events in the historical record (Chronology of British Hydrological Events; Black and Law, 2004). The sediment signature of the flood forms a coarsening-upwards followed by fining-upwards grading couplet, seen in the particle size distributions (Figure 2.8b). The P90 particle size increases to ~435 μm near the delta and ~280 μm in the lake centre, indicating fluvial delivery as the dominant sediment source. Of the geochemical proxies, the Zr/K ratio (Figure 2.8c) mirrors the particle size data most closely, with highest values at 16.25 cm depth (similar to P90) suggesting an association of the ratio with grain size; a similar trend is seen in the Zr/Ti ratio. For other commonly used elemental ratios (e.g., Zr/Rb), this association is less clear or absent. Validating the indicative meaning of the geochemical ratios commonly used as proxies for grain size on a case-by-case basis appears prudent.

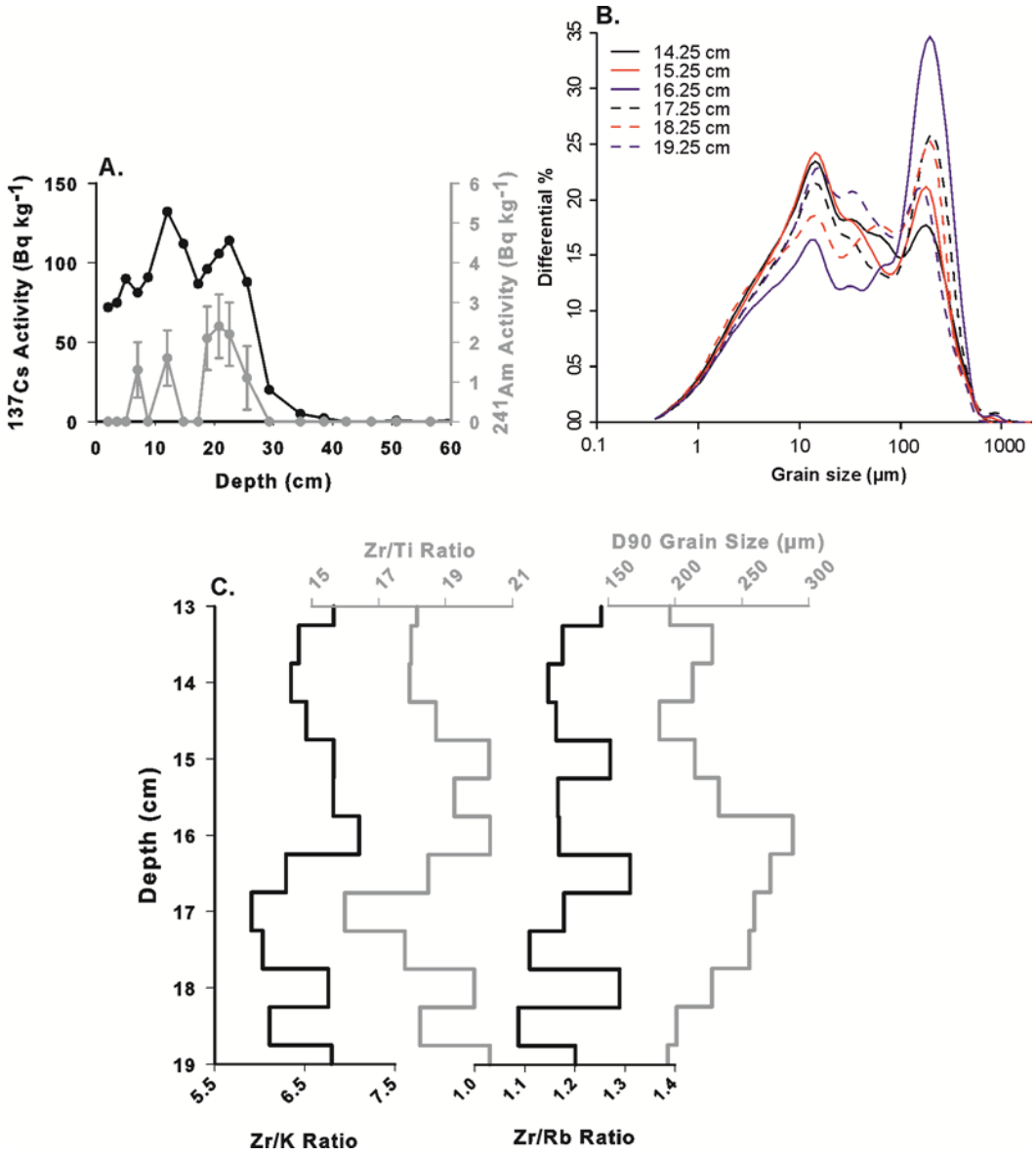

Figure 2-8 A) Fallout radionuclide concentrations (^{137}Cs and ^{241}Am) for the uppermost 40 cm of core BW11-2, extracted from Brotherswater, northwest England. The CE 1963 weapons testing peak falls at 21±1.5 cm and the CE 1986 Chernobyl peak appears at 11–13 cm. B) Particle size distributions for samples across the interval 14.25–18.75 cm depth in BW11-2. C) Selected geochemical ratios being tested as particle size proxies for the 1968 flood unit plotted against the P90 profile.

2.1.4.2.2 Oldevatnet, western Norway

Working at Oldnevatnet, a large (8 km^2) lake in the Jostedal Mountains in western Norway, Vasskog *et al.* (2011) established an event-based stratigraphy for the abyssal

(~40 m depth) sediments of this long narrow lake. The lake is flanked by mountain slopes rising steeply ~1300m and fed by glacial outwash from the Jostedal and Myklebust glaciers. At two core locations, background sedimentation is dominated by siliciclastic glacial-outwash materials that are very light in colour, with event layers darker in colour and often displaying higher organic matter content.

Visual stratigraphy and lower Rb/Sr ratio values (measured via ITRAX core scanner) were used to discriminate the darker-coloured event deposits, characterised by a greater supply of chemically-weathered material, from the lighter-coloured, Rb-rich, glacially-derived background sediment because Rb-bearing minerals are generally more resistant to weathering. The authors recognised that the geomorphic setting provides a context where event layers could be formed by snow avalanches directly entering the lake, by turbidity currents triggered by lake-edge debris flows or by (glacio-) fluvial floods. Thus, the key to developing a flood stratigraphy for Oldnevatnet was material characterisation and process understanding for these three different event types. Vasskog *et al.* (2011) used grain size analysis applied at one centimetre resolution to identify distinctive sedimentological signatures for each process based on grading across laminations and using the mean particle size compared to sorting ratio. The palaeoflood units have a single mode in the coarse-silt fraction and are better sorted than snow avalanche deposits (material transported during a snow avalanche would be highly heterogeneous), which have a strongly polymodal particle size distribution. The two debris flow units are much coarser (very coarse silt/very fine sand fraction) and better sorted. There remains a resolution mismatch between the particle size analysis (physically limited to 10 mm sub-samples) and the characterisation of the event stratigraphy by ITRAX geochemistry (200 μm) but the consistent match between the visual stratigraphy and Rb/Sr ratio supports their interpretation in this instance.

2.1.4.2.3 Cape Bounty East Lake, Canadian Arctic archipelago

Cape Bounty East Lake (Melville Island, western Canadian Arctic archipelago) presents an interesting contrast in the possible temporal resolution of palaeoflood reconstruction, revealing an annually-laminated sediment sequence that has accumulated throughout the last ~2845 years (Cuven *et al.,* 2010; 2011; Lapointe *et al.,* 2012). East Lake is a low altitude (5 m), small (1.5 km^2) and deep (32 m) lake, and has a relatively small non-glacial catchment (11.5km^2) producing a catchment to lake area

ratio of ~8:1. The gains in the temporal resolution of analysis are partially off-set by challenges in independently dating the deeper sediments, with a lack of terrestrial carbon negating the application of radiocarbon dating to validate the varve chronology at depth. The recent (~100 years) varve chronology was validated by comparison with a ^{210}Pb chronology and ^{137}Cs radionuclide markers (Cuven *et al.,* 2011). Eight erosive markers were discernible as interruptions to the varve couplets in the 2845 year sequence, thus the varve chronology is utilised with some confidence (Cuven *et al.,* 2011; Lapointe *et al.,* 2012). Identification of flood laminations in East Lake is enhanced by process monitoring at nearby lakes, including sediment trapping and measurements of fluvial suspended sediment concentrations (Cockburn and Lamoureux, 2008). These data show that intense summer rainfall events are capable of delivering coarser grains, producing hyperpycnal flows and higher sedimentation rates than annual snowmelt pulses. Lapointe *et al.* (2012) compared the annually-resolved particle size distributions, measured on discrete laminations from 7100 scanning electron microscope images, to 25 years of local precipitation data. They identified a statistically significant positive relationship between the largest annual rainfall events and the 98th percentile (P98) particle size fraction. The P98-rainfall regression model was used to reconstruct rainfall since AD 244 and they found anomalously high rainfall during the 20th century compared to preceding centuries, a finding with significant implications for contemporary climatic changes in the Arctic. Importantly, Lapointe *et al.* (2012) assessed the relationship between varve thickness and particle size and found a weak correlation, thus advocating linking grain size to single events instead of using layer thickness as a proxy for event magnitude. Detailed examination of geochemical data for the lake (collected by μXRF; Cuven *et al.* 2010) pinpointed distinct elemental signatures for each lithozone identified from their microstratigraphical analysis. Lithozones B and C, likely triggered by intensive rainfall, are characterised by high Si and Zr and low K and Fe.

Cuven *et al.* (2011) subsequently showed that higher Zr/K values correlated with coarser grains delivered under high flow for this system on longer timescales (since ~4000 yr BP). Comparison with subsequent grain-size data (Lapointe *et al.,* 2012) supports this interpretation to a certain extent, although the Zr/K ratio appears a better match to the median (Q50) than the P98, especially for the overall trend towards coarser particles since 500 yr BP. Conversely, peaks in Zr/K around 850 yr. BP (Figure 4 in Cuven *et al.,* 2011) lack an equivalent grain size marker (Figure 4 in Lapointe *et al.,*

2012). Variations in catchment sediment sources, storage and fluxes and the arid nature of the Canadian Arctic are possible causes of these differences. This work also demonstrates the value of building a comprehensive body of research at a single lake to more fully understand the hydrological and sedimentological variability and its implications for the sedimentary signatures deposited by floods.

2.1.4.2.4 Lac Blanc, western French Alps

Lac Blanc, lying in the Belledonne Massif in the western Alps (SE France), is small (0.1 km^2) with a flat central basin (~20 m depth), a relatively large catchment (3 km^2; catchment to lake area ratio 30:1) and a single dominant glacier-fed inflow with eroded morainic material and glacial flour as the primary sediment sources during summer (the lake is frozen from November to May). Using a multi-proxy approach that integrates μXRF measurements (1 mm resolution) with 5 mm resolution particle size measurements and visual microstratigraphical analysis from thin sections on three cores from different parts of the central basin, Wilhelm *et al.* (2012) produced a palaeoflood record spanning the past three centuries. They used the Ca/Fe ratio as a proxy of event deposits, citing Cuven *et al.* (2010), who showed that Fe was associated with finer particles at Cape Bounty East Lake (preceding case study). Transferring geochemical ratios between regions assumes similar sediment sources are active and similar depositional mechanisms are operating and thus is potentially problematic, but, critically, Wilhelm *et al.* (2012) validated this relationship for the Lac Blanc catchment by showing a strong, positive correlation between median grain size and the Ca/Fe ratio (averaged over 5 mm intervals). Frequency statistics on the particle size data (mean, sorting, Q50 and P99) distinguished three types of sediment deposits. Their 'Facies 2' exhibit fining-upward grading with a thin, light, fine-grained cap, are well-sorted and are positioned on the Q50:P99 scatter plot at points suggesting that phases of higher river discharge are the controlling depositional mechanism. In addition, these deposits can be mapped between three cores across the basin, supporting their flood event origin. An independent chronology was developed using artificial radionuclide markers (^{137}Cs and ^{241}Am), changes in down-core Pb concentrations reflecting atmospheric-derived fallout of known age and the identification of distinctive sedimentary deposits reflecting lake-edge slumping, most likely triggered by four well-dated earthquakes since the 18th century. The authors take the important step of attempting to temporally correlate the palaeoflood layers with fourteen historical events noted in written records from the 19th and 20th centuries and are able to

attribute almost all documented floods since 1851 to a corresponding sediment deposit. Uncertainties within the age-depth model before 1851 makes the task of extending the palaeoflood reconstruction more challenging.

2.1.4.2.5 Lago Maggiore, Italian-Swiss border

The recent sediments of Lago Maggiore, a large (area 212.5 km^2), deep (177 m mean and 370 m maximum) and low elevation (194 m) montane lake with a relatively large catchment to lake area ratio (31:1) have been used to reconstruct a well-constrained flood history for the last 50 years (Kämpf *et al.,* 2012). Investigations focused on the western shallower basin (~152 m deep), which is proximal to a major inflow, the River Toce, which drains 1551 km^2 to the south of the Alps (maximum elevation 4600 m at Monte Rosa). Glaciers comprise ~1% of the catchment area, and high magnitude river flows driven by heavy precipitation are common from September to November. Sediment trap data (Kulbe *et al.,* 2008) showed that the maximum sedimentation rate during a two-year period occurred as a result of the October/November 2004 flood. The stratigraphy of multiple short (~60 cm) cores was discerned by visual inspection, thin-section microscopic analysis and μXRF, with a robust geochronology secured by ^{210}Pb and ^{137}Cs isotope analysis and biological markers including changes in diatom composition and enhanced nutrient loading during known years. Flood layers 1-12 mm in thickness were discerned from the background sediments as lighter in colour and richer in detrital elements (e.g., Al, Ti and K). Focusing on the uppermost layers, Kämpf *et al.* (2012) identified 20 detrital layers spanning 1965 – 2006 and interpreted these as flood laminations, based on their strong basin-wide correlation, increases in detrital elements (Al, Ti and K), fining-upward grain size to 100 μm, and the presence of abundant quartz and feldspars in the basal part of each flood layer. The authors further supported their flood reconstruction by comparison of the sediment record with lake level data, where water levels exceeding a 195.5 m threshold reflect flood events. The authors were able to relate elevated lake levels to 18 of the 20 synchronous event laminations in the sediment record. Two detrital laminations do not correspond with times of elevated lake levels, and conversely four lake level maxima do not appear in the sedimentary record. A similar comparison with recorded (1977-2006) daily river discharges for the outflow (River Toce), with discharges >600 m^3s^{-1} assigned as floods, noted 13 out of 15 instances produced an event layer in the lake and five high discharge events left no discernible event lamination in the lake sediment sequence.

A limited relationship was found between layer thickness and the magnitude of river discharge and lake level maxima, with environmental changes in the catchment and lake basin likely degrading the association of sediment transmission with the hydrological regime. Validation of the flood control for laminations in the recent sediments in Lago Maggiore offers the prospect of extending the record back in time, though Kämpf *et al.* (2012) display caution in this regard given the lack of precise age control and increased minerogenic sediment content for their the deeper record.

2.1.4.2.6 Implications for palaeoflood research

These case studies illustrate that lakes of many sizes (surface area of Brotherswater is 0.25 km^2, Lago Maggione is 212.5 km^2) can contain useful palaeoflood records, provided other important physiographical criteria are met. For example, their watersheds tend to be steep, they have one dominant inflow and a single, flat central basin. While sediment sources may differ (e.g., glacially-derived material, eroded soils) and some lakes are frozen for part of the year or experience little background sedimentation under normal or low flow conditions, each lake episodically also receives high detrital sediment flux. This means that sediment transport to the lake under flood conditions should exceed typical autogenic and allogenic sedimentation and thus leave a visible imprint.

Each of the above case studies evaluates in detail the accuracy and precision of the chronological methods used. Multiple and independent techniques have been employed in each case, with short-lived (^{210}Pb, ^{137}Cs) and longer half-life (^{14}C) isotopes most common and integrated with biological (e.g., disturbance pollen taxa), chemical (e.g., mining contamination) and stratigraphical (e.g., earthquake-triggered slump deposits) markers to verify the chronology. Annually-laminated lakes (e.g., East Lake; Cuven *et al.,* 2011; Lapointe *et al.,* 2012) are especially useful for chronological purposes but also because discrete flood deposits exhibit different sedimentological characteristics to the recurring seasonal laminations.

The structure of a flood unit deposited by a known event has been shown at Brotherswater, and this signature can thus be used as an analogue to seek similar deposits deeper in the core. Other case studies used microstratigraphical analyses of thin-sections to show the graded nature of the flood deposits (e.g., Wilhelm *et al.,* 2012) or μXRF measurements showing trends in detrital elements related to phases of sediment delivery during a flood (Cuven *et al.,* 2010). In addition, sediment trap data

from Brotherswater, East Lake and Lago Maggiore were used to confirm that elevated river discharges are capable of supplying coarser grains.

Correlating the sediment record with local instrumental data provides tremendous support for palaeoflood reconstructions. Where gauged lake level or river discharge data are available (e.g., Lago Maggiore; Kämpf *et al.,* 2012), discrete flood units that have been accurately dated can be compared on an individual basis to years where an extreme flood was known to occur. Precipitation records may also be useful but it is important to keep in mind that intense rainfall does not always lead to flooding or may be localised. Lapointe *et al.* (2012) used meteorological data from stations 100 km and 320 km away and found strong positive correlations between grain size and periods of intense precipitation. Regions with highly spatially variable rainfall patterns may require more local meteorological data for any similar trends to emerge. Older flood laminations can be compared to historically documented floods normally over timescales of 100 to 300 years (e.g., Wilhelm *et al.,* 2012).

Clearly, the use of any one proxy is site-specific and palaeoflood signatures must be interpreted in a similar manner; i.e., avoid citing research from another lake that employed a certain proxy to discriminate palaeoflood laminations without demonstrating that down-core variability in that proxy does in fact respond to changes in river discharge at the lake under investigation. For example, the background sediment in many temperate lakes is dark-brown and organic-rich; thus, detrital palaeoflood layers appear lighter in colour. The opposite is the case at Oldevatnet, where the dark layers in fact relate to extreme events (Vasskog *et al.,* 2011). In particular, reliance on geochemical ratios as a proxy for particle size, and its subsequent use as a flood proxy, must be informed by a comprehensive understanding of the catchment geology and sediment provenance and, critically, the relationship should be explicitly demonstrated for contemporary processes and/or in the palaeo record.

2.1.5 Conclusions

We have presented a conceptual model and reviewed methodological protocols for using lake sediment sequences as recorders of past floods and thus hope to contribute a better understanding of flood frequency and magnitude over centennial to millennial timescales. The paper highlights recent advances made by palaeoflood researchers and discusses key challenges for on-going and future research.

1) While a number of detailed, high-resolution lake sediment palaeoflood records have emerged recently from many regions of the world, pressing concern over future trends in extreme events means there is a need to increase the number and extend the timespans of these records. They potentially provide river managers and decision makers with greater context to assess current flood risk and augment flood rating curves. The presented case studies highlight the value of lake sediment sequences as an archive of past floods and building a palaeoflood database that addresses the global geographical distribution of lakes (all latitudes, lowland and alpine, near urban areas and more remote settings) is a challenge requiring substantial future effort.

2) We present a framework for selecting appropriate study sites and identifying lakes most predisposed to preserving palaeoflood stratigraphies. The potential for a flood to deposit a distinctive, undisturbed sedimentological unit at the lake bed is a function of catchment processes and within-lake mechanisms. Thus, knowledge of local geology, the efficiency of the sediment conveyor, past inflow or delta migration and progradation, basin morphology and characteristics including water residence time and thermal stratification and the potential for sediment re-suspension are important factors. Understanding changes in catchment conditioning through time is of critical importance, as the sedimentary signature of floods can vary with changes in sediment supply or provenance and, thus, independently of event magnitude.

3) The dispersal of a sediment-laden river plume across a lake basin is influenced by numerous processes and acquiring sufficient process-based understanding from the sediment record is challenging. Field and laboratory experiments have enabled simplified empirical equations to be developed for many of these processes, such as calculating critical depths for wind-induced sediment re-suspension, but the range of variables means they are not globally applicable and that site-specific data should be obtained. Contemporary sediment trap studies characterising current processes of sediment flux and deposition can aid interpretation of the longer sediment record while recovering sedimentary units associated with known floods confers greater confidence to the process interpretation. Extracting multiple cores across a lake provides the three-dimensional sediment geometry of individual flood laminations, ideally following an inflow-proximal-to-distal transect and the repeatability of sediment signatures between core sites and along depositional gradients (e.g., proximal to distal fining of sediments) can also help confirm the palaeoflood interpretation.

4) Many analytical techniques have been used to discern flood deposits from the background sediment matrix. Visual analysis of the sediment cores can provide important context, with the structure and grading of sedimentary units capable of distinguishing flood layers. Measurements of particle size are critical as they can directly reflect changes in river discharge through time, however more research is needed investigating how floccules in the water column may degrade relationships between particle size and river discharge. Indirect proxies of grain size, particularly ratios between selected geochemical elements increasingly recovered with ease by high-resolution μXRF core scanning are effective but these data must be interpreted with caution as several factors, including variable water and organic matter content, can impede the X-ray signal. The basis for the association of grain size with geochemistry must be proven for specific sites: (i) in a process domain through sediment trapping or (ii) for the palaeorecord by correlating geochemical ratios with particle size across individual flood signatures

5) Developing a well-constrained chronology is challenging but critical for obtaining meaningful data on flood frequency. Integration of multiple chronological markers (e.g., radionuclides, environmental pollution and pollen markers) is preferable and normally most feasible over the past 200 to 300 years. A well-dated, overlapping validation period between the lake sediment sequence and local river flow records can enable the proxy palaeoflood data to be calibrated quantitatively; this should be the ultimate goal of palaeoflood research. Longer-duration palaeoflood records generally have a temporal resolution sufficient to decipher flood-rich and flood-poor phases as opposed to discrete events, although annually- or seasonally-laminated core profiles are especially useful for producing event-scale reconstructions over millennial timescales.

6) We describe five case studies of palaeoflood reconstructions undertaken at lakes in different geomorphic settings and from geographically widespread regions (England, Norway, Canadian Arctic, French Alps and northern Italy). The selected records were analysed at variable resolutions and span different temporal scales, but illustrate how independent chronological techniques and multiple lines of sedimentological evidence can be integrated to successfully distinguish palaeoflood signatures. Whilst these case studies highlight the feasibility of undertaking palaeoflood research at various locations, we emphasise that each lake meets many of the physical characteristics shown to be most conducive to palaeoflood record preservation.

7) A key challenge for lake sediment palaeoflood researchers is the extraction of data on flood frequency from these sedimentary records and its incorporation into flood risk assessments. Using these long datasets to refine thresholds of flood magnitude on either a qualitative (e.g., threshold categories) or fully quantitative (e.g., discharge-calibrated particle size metrics) basis will enable the research field to contribute more fully to our understanding of long-term trends in flood frequency and magnitude.

Acknowledgements

DNS would like to thank the School of Environmental Sciences, University of Liverpool for funding this research via a PhD Studentship. DNS is also grateful for additional financial support from the British Society for Geomorphology. Many thanks are also extended to Jan Bloemendal, Jordon Royce and Beverley Todd for assistance with fieldwork and to Suzanne Yee for assistance with producing selected diagrams. We gratefully acknowledge the thoughtful and constructive comments of Stéphanie Girardclos and two anonymous reviewers that significantly improved the final manuscript, as well as valuable guidance from the Editor André Strasser.

2.2 Lacustrine archives of metals from mining and other industrial activities – a geochemical approach

Abstract

Since the first studies (Thomas, 1972) reporting recent stratigraphic changes of metal concentration in lake sediments, many hundreds of studies have been published in the peer-reviewed literature. It is an impossible task to do justice to all of these works here; instead we 1) examine recent methodological advances and place these in the context of the historical development of the discipline, and 2) explore the various purposes to which such methods have been applied. Such a historical emphasis may appear in conflict with the needs of a review of new approaches; however, this is not in fact the case for two main reasons. First, most new advances supplement rather than replace traditional methods, such that a thorough understanding of the practical and theoretical issues impacting these is still essential for reliable interpretation of palaeolimnological data. Second, while many of the new methods purport to circumvent problems, they achieve this only under favourable conditions, not dissimilar to the conditions that influence the earlier methods, so the same lesson must be learned anyway. Consequently, we use this historical narrative to address the fundamentals of the discipline.

The chapter comprises two main parts; the first addressing methodology, and the second, applications. The methodological part comprises three mains subsections:

i) Processes: an introduction to processes controlling natural variations in metal fluxes and concentrations in lake sediments;

ii) Approaches to the measurement of metal concentrations in sediments;

iii) Approaches to the calculation of enrichment or fluxes from sediment metal concentration data.

The applications part comprise four main subsections focusing on the value of lake sediment records of metals derived from mining or industry for:

i) Geochronological markers in sediments providing temporal support for other research aims;

ii) Lake sediment heavy metal records to quantify pollution loading histories, or to identify pollution sources;

iii) Identifying and quantifying pre and post mining baseline states;

iv) Identifying pollutant pathways or environmental processes regulating heavy metals.

2.2.1 Methods

Analytical approaches for the evaluation of heavy metal pollution records preserved in lake sediments fall into two categories: methods for measurement of metal concentrations, and methods to obtain useful information from such measurements. However, a number of issues impact both of these, depending on natural dynamics of heavy metals within a lake catchment. So important are these to the reliable interpretation of heavy metal pollution records that we start with a brief introduction to natural processes.

2.2.1.1 Processes

2.2.1.1.1 Parent material heterogeneity

Natural materials are highly variable in elemental composition. Though biological entities such as plant tissues have relatively limited variability in major element concentrations, most soil or rock types are classified only in terms of function or physical characteristics, and may exhibit a wide range of geochemical compositions. Even the better-defined igneous rock classification terms, such as “granite”, actually have multiple meanings, and even when strictly specified are defined in terms of their component minerals, which themselves may be highly variable in composition. Most other terms, such as “sandstone”, convey very little compositional meaning at all; though likely dominated by quartz, they may contain any other minerals including calcite, provide the particles fall in the size class for sand. Even when qualified by terms like “volcaniclastic”, the type of volcanic rock comprising the sandstone is commonly not mentioned, and thus an extremely wide compositional range is possible.

To make matters worse, geological maps are generally chronostratigraphic in purpose, accurately reflecting what is known of rock age, but saying little or nothing of what the mapped units are made of. Thus geological maps provide little compositional information to the palaeolimnologist in terms of natural metal concentrations in the

parent rock types. The result is that direct assessment of parent material composition is required if natural heavy metal contributions are to be fully understood. Without this it may be very difficult to separate a potential pollutant signal from natural variation. Nevertheless, geological maps do sometimes list specific rock types, particularly maps that represent small spatial extents, and thus rock classification may be used as a starting point. Table 2.2 shows the element concentrations of a small number of selected rock types. It is highly incomplete and, more importantly, represents only the average condition and thus may be a very poor guide to the composition of a specific instance of one of the listed types. Nevertheless, the values in the table serve to illustrate likely ranges in element concentration given some knowledge of the geological make-up of the catchment. It is striking that some elements differ little across the rock types (except in the case of carbonate, in which all elements except Ca, Cd, Mg, Mn, Sr and Zn – are strongly depleted). However, most heavy metals show substantial differences. Thus, Cu, Cr, Ni and Zn are enriched in basic (basaltic) rock types, Cr and Ni strikingly so in ultrabasic rocks, while As, Hg and Cd are most enriched in shale (and other rocks formed from clays including slate and schist). Pb is depleted in basic rock types, and equally enriched in granite and shale. This information is useful when choosing study sites as careful screening of bedrock type improves the chance of finding the low natural heavy metal concentrations and fluxes, and thus providing a site with maximum sensitivity to metal pollution.

The information in Table 2.2 provides the average compositions for rock materials that may underlie a catchment. However, several processes cause a lake's sediment to be quite different in composition to its parent rock. This is partly because little if any of the sediment comprises fragments – termed lithoclasts - of that rock. In the case of coarse-grained rock types such as granite no lithic fragments are small enough to reach the profundal mud. Thus, most lithogenic particles in the sediment comprise individual minerals. This would make little difference if the mineral assemblage in the sediment comprised an unbiased sample of the rock minerals. However, this is not the case for coarse parent rock, as only the finer primary crystals reach the sediment, and these are generally atypical (Figure 2.9). In the case of fine-grained rock types, such as siltstone, shale/mudstone/slate or volcanic rocks types, the lake sediment lithogenic particles may indeed be whole rock fragments, but even then are unlikely to be identical to the parent material. These lithogenic particles will have been altered by chemical weathering prior to erosion, except in cold or rapidly eroding settings such as under

Table 2-2 The elemental composition of some common rock types.

		Granite	Basalt	Shale	Ultrabasic	Basaltic	Granitic high Ca	Granitic Low Ca	Syenite	Shale	Sandstone	Carbonate
		1	1	1	2	2	2	2	2	2	2	2
Si	mg g^{-1}	323	230	238	205	230	314	347	291	273	368	24
Al	mg g^{-1}	77	84	92	20	78	82	72	88	80	25	4.2
Fe	mg g^{-1}	27	86	47	94.3	86.5	29.6	14.2	36.7	47.2	9.8	3.8
Ca	mg g^{-1}	16	72	25	25	76	25.3	5.1	18	22.1	39.1	302.3
Mg	mg g^{-1}	4	45	14	204	46	9.4	1.6	5.8	15	7	47
K	mg g^{-1}	32	8	25	0.04	8.3	25.2	42	48	26.6	10.7	2.7
Na	mg g^{-1}	28	19	9	4.2	18	28.4	25.8	40.4	9.6	3.3	0.4
Ti	mg g^{-1}	2.1	9.0	4.5	0.3	13.8	3.4	1.2	3.5	4.6	1.5	0.4
Mn	μg g^{-1}	500	1700	850	1620	1500	540	390	850	850		1100
As	μg g^{-1}				1	2	1.9	1.5	1.4	13	1	1
Ba	μg g^{-1}				0.4	330	420	840	1600	580		10

Cd	$\mu g\ g^{-1}$	0.1	0.2	0.3		0.22	0.13	0.13	0.13	0.3		0.035
Cr	$\mu g\ g^{-1}$	20	200	100	1600	170	22	4.1	2	90	35	11
Cu	$\mu g\ g^{-1}$	12	100	50	10	87	30	10	5	45		4
Pb	$\mu g\ g^{-1}$	20	3.5	20	1	6	15	19	12	20	7	9
Hg	$\mu g\ g^{-1}$	0.03	0.01	0.3		0.09	0.08	0.08		0.4	0.03	0.04
Ni	$\mu g\ g^{-1}$	0.8	150	80	2000	130	15	4.5	4	68	2	20
Rb	$\mu g\ g^{-1}$	150	30	140	0.2	30	110	170	110	140	60	3
Sr	$\mu g\ g^{-1}$	300	450	400	1	465	440	100	200	300	20	610
Zn	$\mu g\ g^{-1}$	50	100	90	50	105	60	39	130	95	16	20
Zr	$\mu g\ g^{-1}$	180	140	180	45	140	140	175	500	160	220	19

1 = Krauskopf

2 = Turekian and Wedepohl, 1961

glacial conditions. They will probably have lost their most weatherable minerals such as sulphides, carbonates and apatite, may have partially or wholly lost minerals of intermediate weatherability such as plagioclase and chlorite (and other mafic minerals), and will have acquired secondary "clay" minerals in the process. Thus, to understand the range of likely compositions for lithogenic sediments, it is necessary to know something of the composition of the rock forming minerals; those that make up the bulk of the common rocks; and of the commoner secondary minerals. Clearly, in mining regions we may find rarer mineral types in abundance, but it is beyond the scope this chapter to review the vast array of such minerals.

Table 2.3 shows the compositions of a selection of minerals. This table must be interpreted with caution for two reasons. First, to simplify the table only single examples are given, even for the very large mineral families such as the pyroxenes, amphiboles and chlorites. Averages of common types within these families are presented, but even these types commonly show great natural variability. The values thus serve to distinguish difference in typical mineral compositions, but may be incorrect in any specific case. Second, the mineral data set on which the trace element analysis is derived is incomplete, likely comprises an unrepresentative sample, and displays great variability in composition. The values shown are log means of highly skewed data, so any particular specimen of a mineral may differ greatly from these. Nevertheless, as in the case of the rock compositions in Table 2.2, the generalities are useful. Thus the strong association of V with magnetite, of Cu and Zn with mafic minerals, of Pb with potassium bearing minerals, particularly K-feldspars, is reliable and this information is useful when interpreting natural concentrations and fluxes of heavy minerals.

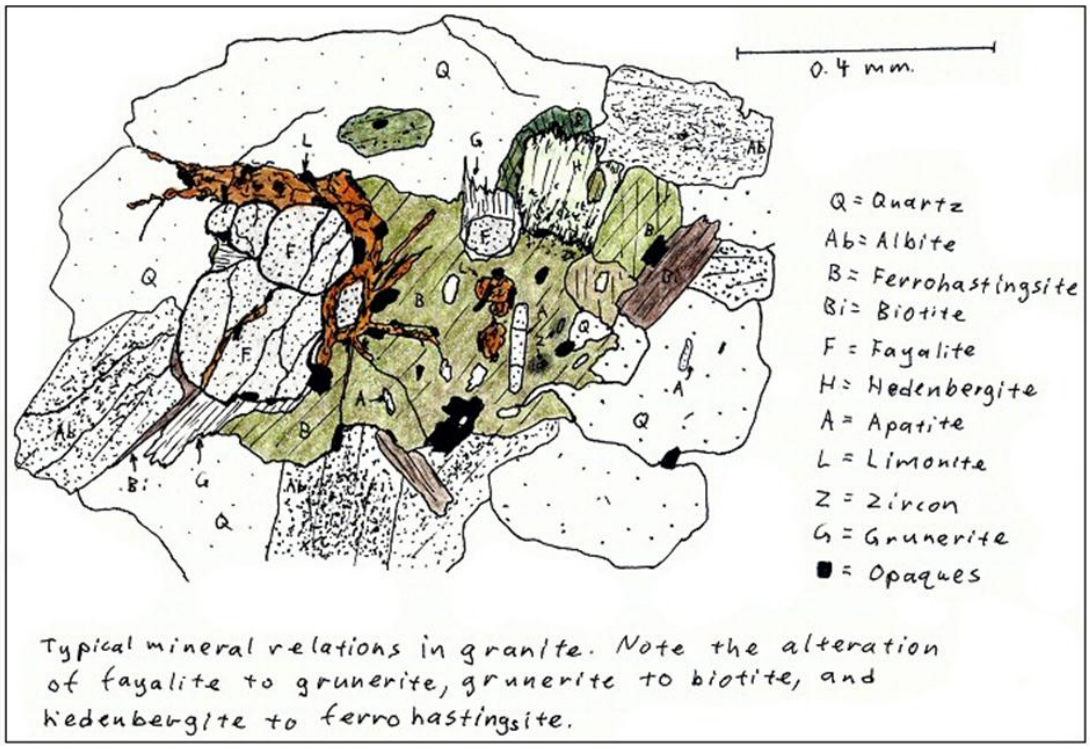

Figure 2-9 Sketch thin section of granitic rock (reproduced with permission of Kurt Hollocher). This alkali fayalite granite illustrates the mix of crystal sizes. Mainly large crystals of quartz, feldspar (albite), amphiboles (ferrohastingsite and grunerite), pyro pyroxene (hedenbergite), olivine (fayalite) and biotite, enclose an assemblage of smaller crystals of apatite, zircon and opaques (mainly ilmenite and magnetite). Other common small crystals are various oxides of Ti (rutile, anatase and brookite). During weathering micas readily disintegrate to smaller particles; quartz and feldspar tend to remain intact.

Table 2-3 Elemental composition of some common rock forming minerals.

	Si[1]	Al[1]	Fe[1]	Ca[1]	Mg[1]	K[1]	Na[1]	Ti[1]	Mn[1]	P[1]
	mg g^{-1}	mg g^{-1}	mg g^{-1}	mg g^{-1}	mg g^{-1}	mg g^{-1}	mg g^{-1}	mg g^{-1}	mg g^{-1}	mg g^{-1}
Olivine	147.4	1.9	435.5	9.8	49.7	0.0	0.0	2.7	13.2	
Garnet	176.9	86.7	149.4	152.0	16.2	0.0	0.0	1.2	8.5	
Pyroxene	235.5	9.0	177.6	52.2	93.1	1.0	3.5	1.8	4.3	
Amphibole	220.4	42.2	128.3	58.6	89.4	5.1	7.3	7.8	2.4	
Biotite	174.7	80.8	181.0	4.7	48.8	66.1	3.1	19.5	0.8	
Muscovite	201.7	144.8	77.0	0.4	15.0	84.1	3.5	6.5	0.6	
Chlorite	125.0	107.8	183.4	0.9	98.7	0.2	0.4	2.9	1.0	
Kaolinite	213.7	209.4	5.4	2.9	0.8	0.2	0.0	0.0	0.0	
Illite	241.4	145.2	22.4	6.5	7.7	54.6	3.3	2.9	1.4	
K-feldspar	301.6	103.8	0.9	3.2	0.0	97.3	25.0	0.0	0.0	

Albite	316.6	104.0	0.4	0.0	0.2	2.4	82.1	0.0	0.0			
Oligoclase	299.1	120.0	2.3	23.3	1.5	0.4	73.4	0.0	0.0			
Andesine	271.1	140.0	1.4	56.0	0.2	9.1	48.1	0.0	0.0			
Labradorite	247.1	157.3	7.0	87.7	0.0	1.1	31.2	0.0	0.0			
Apatite	0.0	0.0	0.2	399.1	0.1	1.1	31.2	0.0	0.0	183.3		
Magnetite	1.3	1.1	721.4	0.0	0.0	0.0	0.0	0.0	0.0			

	As[2]	Ba[2]	Cd[2]	Cr[2]	Cu[2]	Pb[2]	Hg[2]	Ni[2]	Rb[3]	Sr[2]	V[2]	Zn[2]
	µg g^{-1}	µg g^{-1}	µg g^{-1}	µg g^{-1}	µg g^{-1}	µg g^{-1}	µg g^{-1}	µg g^{-1}	µg g^{-1}	µg g^{-1}	µg g^{-1}	µg g^{-1}
Olivine	0.11		0.37		71			1280				60
Garnet					19			116			2	451
Pyroxene	0.36	75	0.43		72	6		250	2.2		69	139
Amphibole	1.7	214			29	13			3.5	59	174	507
Biotite	1.4	1198	1.51		57	26			612	18	186	412
Muscovite		1057			32	27			339			24

Chlorite		83		100			700				512
Kaolinite				23							59
Illite											120
K-feldspar		957		3	45			280	210	2	5
Albite		16		5					482		
Oligoclase	0.71	355		53	22	0.27	15	0.63	1002	3	14
Andesine		471							906		
Labradorite		168	0.15						1013		
Apatite	0.4	248	0.15			0.052			1512	80	
Magnetite	3.6		0.12	89	7	0.65				1965	204

2.2.1.1.2 Pedogenic materials

In general, lithogenic particles in lake sediments have been derived from soil rather than directly from bedrock. Thus the compositional transformations that occur within soils must be fully understood if we are to understand the composition of lake sediments. Weathering of many rock-forming minerals generates secondary solid phases. As these secondary minerals generally occur as very small particles, they contribute disproportionately to profundal lake sediments. Unfortunately, relatively little is known about the heavy metal content of these materials. While the minerals they are composed of are often well-studied, at least in the case of the more crystalline examples, the specimens of these mineral have generally not been collected from soils, rather from mineralised veins where natural enrichment has occurred. In soils, the same secondary minerals are likely mixed with other materials, particularly humic substances that coat their surfaces and control their adsorption properties. This is particularly important in the case of secondary oxides, hydroxides and oxyhydroxides of Fe, Mn and Al. Thus, our secondary minerals have not only inherited elements directly from their parent minerals, but have also adsorbed some elements released from the decay of other minerals. Thus Cu, Cd and Zn released from parent material sulphides, and Pb released from partial dissolution of micas and feldspars, are partially or wholly retained in the soil, chemically bound to the pedogenic phases. It is unclear just what proportion of Cu, for example, is held this way rather than released to the exported runoff from soil. However, some preliminary modelling using the Windermere Humic Acid Model (WHAM), which assesses binding of metals to humic substances coating sediment particles (Steve Lofts, Pers. Comm.) suggests a high degree of retention.

In the event that heavy metals are also being supplied to the soil by pollution, they will be fixed in the sediment by the same secondary phases that hold the natural component. This similarity of process is highly significant when it come to the characterisation of pollutant metals, because there is no difference between the natural and pedogenic metal in terms of chemical speciation in the soil, though both may readily be distinguished from any metal bound with the lattices of lithogenic minerals.

2.2.1.1.3 Element fractionation during transport from parent rock to lake sediment

We have quickly looked (above) at heterogeneity of parent materials, both by rock type, their component minerals, and by pedogenic transformation. This heterogeneity contributes to fractionation of elements as they make their way from bedrock to the lake bed, and this profoundly impacts how we must interpret natural baseline element fluxes, enrichment factors, and other concepts or methods used to understand heavy metal pollution using lake sediment records. Three driving mechanisms control this fractionation: 1) contrasts in element "solubility" between soil and lake water; 2) interactions of element composition size-profiles with hydrodynamic sorting, and 3) solubility contrasts between buried sediment and the sediment surface. All three must be properly understood if stratigraphical changes in element composition are to be correctly interpreted.

Fractionation by solubility contrast. Mackereth (1966) makes the point that the ease by which an element can be dissolved in the catchment soil, and the ease by which it may be re-precipitated with the lake or sediment, are both fundamentally important to understanding sediment composition. He particularly contrasts elements such as K, Na and Ca, which are readily leached from the soil and transferred to the lake, but which are poorly captured by the sediment (in soft-water systems at least) with elements such as P and heavy metals, which may be readily dissolved but also readily captured by sediment within the lake. In the former case, the element concentrations in the sediment are unaffected by the dissolved load, and are controlled instead by the supply of eroded soil particles. In the latter case, a more complex pattern of variation is expected arising from both allogenic (eroded particles) and authigenic (formation of or capture by particles in the water column) delivery.

This useful conceptual system can be extended in two ways. First, elements such as Ti and Zr, not considered by Mackereth (1966) and which are commonly assumed to be wholly insoluble, can be treated as a third case. In their mechanism of delivery to the lake bed they resemble K, Na and Ca. However, while the latter are subject to gradual source-area depletion through time by leaching (Boyle *et al.,* 2013a), Ti and Zr are not, and thus potentially remain at high concentrations throughout a long (~103 plus years) sediment record. Second, Mackereth's second category can be subdivided by capture efficiency. Thus, a significant proportion of P delivered to a lake may exit with any out-flowing water (see Kirchner and Dillon (1975), for a useful empirical model),

while the proportion of heavy metals captured is generally very high (though varying between metals – see Boyle and Birks, 1999; Rippey, 2010). This last point is crucial for quantitative interpretation of heavy metal sedimentation fluxes, which may be quite different from short-term supply fluxes (see Boyle *et al.* (1998) for an approach to calculating this in deep lakes). However, it is also relevant to the interpretation of long sediment records of heavy metals. First reported by Mackereth (1966), the strong early Holocene sediment enrichment by Cu and Zn has been attributed to changing metal solubility within soil and sediment brought about by warming-induced increases in dissolved organic carbon fluxes (Wolfe and Hartling 1997).

2.2.1.1.4 Fractionation by size effects

The data in Table 2, showing widely differing element concentrations across the common minerals, suggests that hydrodynamic sorting of allogenic particles will result in changing sediment heavy metal concentrations. Clays, micas and chlorites are all enriched in Cu and Zn such that sediment fining, whether due to enhanced mobilisation of fine sediment or reduced mobilisation of coarse sediment, will cause elevated Cu and Zn concentrations. The strength of the particle size effect is illustrated for two soil and two Younger Dryas sediment samples from Kråkenes Lake, Norway (Figure 2.10, unpublished data and Boyle *et al.,* 2013). Derived from a mixed assemblage of schist, granitic gneiss, and amphibolite, Cu, Ni, Pb and Zn are strongly enriched in the finest size fractions. The samples have been treated to remove the organic matter and adsorbed ions so the result is due to size variation in what the lake will experience as allogenic particles. For comparison, Al, Ti, Rb and Zr, all elements proposed for use as passive tracers of the natural heavy metal flux, show widely varying size dependence. Rb is similar to the heavy metals, particularly to Cu and Zn, in showing both a strong enrichment in the fine fraction, and a degree of enrichment in the coarse sediment, here dominated by weathered biotite. At the other extreme is Zr which is depleted in both coarse and fine sediment but strongly enriched in silt. Aluminium shows a presence across all size fractions, with a tendency to enrichment at the fine end. Ti is similar but with a peak in the silt size reflecting primary Ti oxide minerals. Clearly, at this site changing hydrodynamic sorting will strongly impact the heavy metal ratios to Al, Ti and Zr but much less so for Rb. At other sites, however, very different results might be expected. Where Al and Ti are dominantly in clays rather than primary oxides then they may provide good analogues to the heavy metals. Crucially, it is clear that

such size sorting effects may invalidate enrichment factor procedures (see below) and so must be assessed carefully.

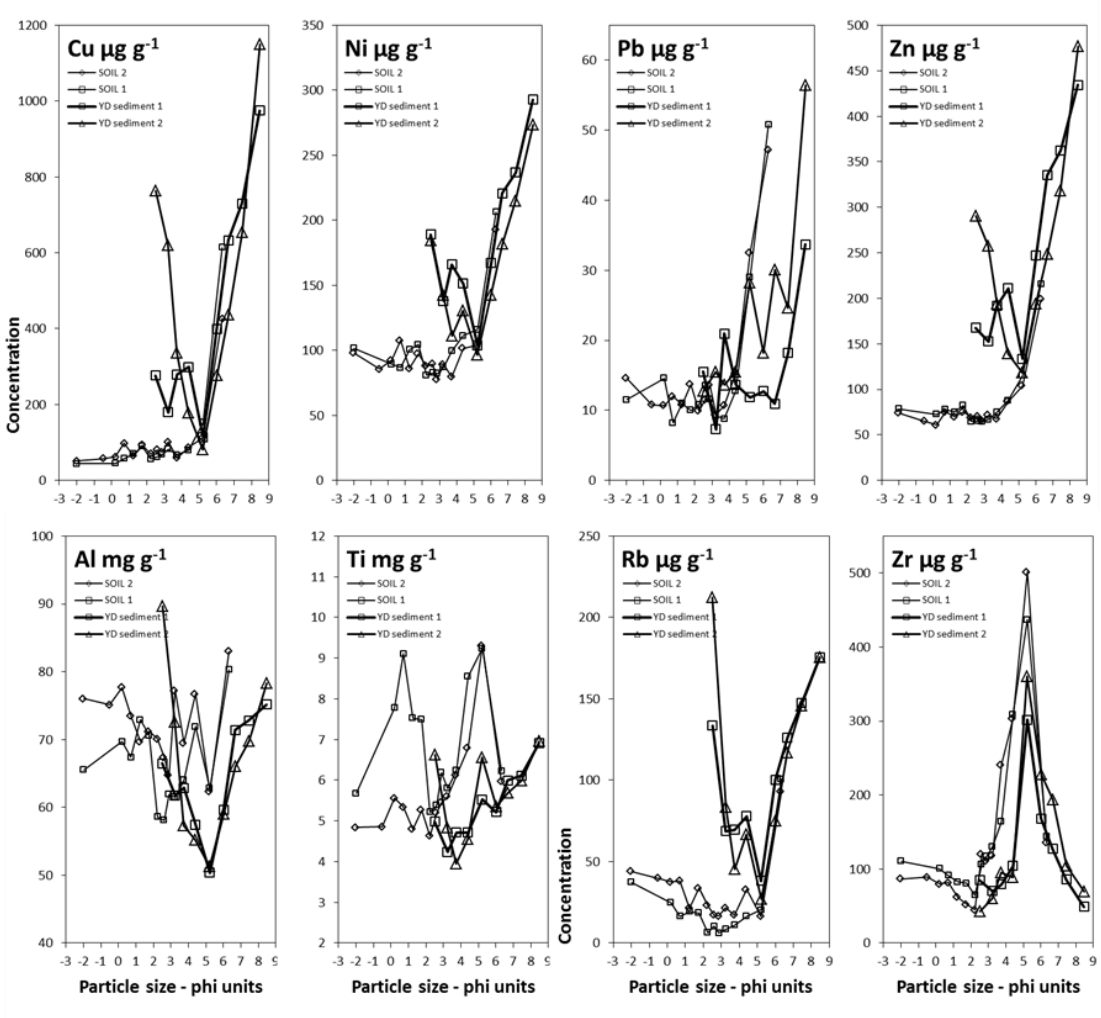

Figure 2-10 Soil and sediment particle size fractions at Kråkenes Lake, western Norway.

2.2.1.1.5 Fractionation of elements by diagenesis

If element solubility can change after sedimentation then post-deposition change can also occur. The effect is best seen for Fe, Mn, As, Co, Cr and V because changes in oxidation state so profoundly change the solubility (Boyle, 2001a; Boyle, 2001b). It is less certain whether elements that occur in a single oxidation state (under natural conditions) are also subject to such powerful migration. Based on a simple model Boyle (2001a) argues that Cu, Zn and Pb profile might indeed be modified by changing Fe and Mn sediment concentrations, but only to a noticeable degree in very slowly accumulating sediments (sediment mass accumulation rate < 50 g m^{-2} yr^{-1}). Empirical

studies comparing known heavy metal pollution histories with the sediment record support the view the records are generally reliable for Cu, Cd and Zn (Couillard *et al.,* 2004) and Hg (Lockhart *et al.,* 2000). However appropriate caution should always be applied in considering possible causes of metal migration. For example, in the exceptionally acidic lakes near Sudbury (Canada) the combination of elevated lake-water Cu and Zn concentration and sulphate reduction in the sediment causes diagenetic enrichment of the sediment with these elements (Carignan and Tessier, 1985; Tessier *et al.,* 1989).

2.2.1.1.6 Concentration versus flux

The debate about whether sediment geochemical records should be expressed as fluxes rather than concentrations is addressed in detail by Engstrom and Wright (1984), and further visited by Boyle (2001b). The broad conclusion of both is that concentration is the primary form being more precise, less open to interference and generally easier to interpret. However, accumulation rate data are invaluable for the interpretation of the elemental concentrations, and a case can be made for displaying both where needed.

It is worth reiterating that if sediment accumulation rate is critically important, then it is unlikely that a single core will be sufficient. Rowan *et al.* (1995a) and Rowan *et al.,* (1995b) discuss this at length and propose an approach to estimating the optimum number of cores.

Finally, it is worth observing something that appears commonly to be misunderstood. Concentration and flux are not unrelated. If concentration is viewed in terms of relative flux – that is, the flux of the element of interest divided the total sediment flux - it is easier to conceptualise possible causes of the compositional variation. An increase in heavy metal concentration is frequently mistaken for an increase in heavy metal flux, while it may be equally well explained by a decrease in the total sedimentation rate.

2.2.1.2 Approaches to measurement

Having considered the processes and pathways in the catchment that may modify the pollutant signal reaching a lake sediment core, the methods which will most effectively determine their concentrations must be considered.

Two main approaches exist (Boyle, 2001b) which can be categorised as one, determining elemental concentrations on the original solid material and two, determining the elemental concentrations of solutions extracted from the original material. The decision regarding which approach to employ largely depends on the research question being asked and whether there is a need for non-destructive analyses. In general, analysing sediment directly returns values that reflect a total concentration and some methods are non-destructive, conserving sediment and minimising the risk of contamination. However, for elements that are abundant both in loosely bound form and within primary mineral lattices, total concentrations can be difficult to interpret. In such cases, analysing extracts can be more versatile as total or partial components can be considered as required. However, such procedures are always destructive resulting in a loss of sample, though the sample size required may be very small. Furthermore, hazardous reagents are used in many of the chemical extraction methods, particularly hydrofluoric and perchloric acids. Completing appropriate risk assessments prior to commencing the work and employing safe working practices are essential.

2.2.1.2.1 Extraction methods

2.2.1.2.1.1 Total digestion using acid digestion

Where the total extraction of mineral-bearing material is desired, the preferable method is acid attack using a mixture of nitric (HNO3), perchloric ($HClO_4$) and hydrofluoric (HF) acids (Boyle, 2001b; Couillard *et al.,* 2004). Two methods of mixture preparation have been proposed; Allen *et al.* (1974) used open vessels, enabling HF acid to be fumigated and also results in removal of silica, reducing matrix interferences in the subsequent analysis. More commonly used are sealed acid bombs which should ensure complete dissolution (e.g., Garçon *et al.* (2012)) before boric acid (H3BO3) is applied to make the solution safe.

2.2.1.2.1.2 Partial or sequential extraction

The aim of applying partial extraction techniques to sediment samples is to separate readily available elements from inert ones. One recommended procedure (Engstrom and Wright, 1984) initially uses 0.3 M HCl as an extraction reagent followed by oxidation by adding hydrogen peroxide (H_2O_2). Alternative acid digestion methods include aqua regia (HCl + HNO_3 mixture; Skierszkan *et al.,* 2013). A comparative study

by Peña-Icart *et al.,* (2011), investigating the relative extraction efficiencies of aqua regia and EPA Method 3050B which applies a mixture of nitric acid (HNO_3), hydrogen peroxide (H_2O_2) and HCl, concluded that both methods extracted similar amounts of Cu while Ni and Pb showed different rates of extraction. Importantly, both of these methods are effective at minimising the dissolution of the silicate component.

Sequential extractions are time-consuming, so it is important to assess the value of the information gained this way. Boyle (2001b) points out that little evidence exists that the components separated by sequential extraction, created and extensively tested for freshly deposited sediments or soils, are preserved in lake sediment cores. Furthermore, there is no evidence suggesting that such extractions can separate pollutant from naturally derived heavy metals (See Pedogenic Materials, in the Methods section). Nevertheless, partial dissolution can separate the wholly inert primary mineral component from the rest, and this is both useful and likely preserved in the sediment record. These reasons lend support to the conclusion of Arain *et al.* (2008) who argue that a single extraction delivered results for a number of heavy metals (Cd, Cr, Ni, Pb and Zn) as useful as more complex multiple extractions, greatly reducing the total preparation time.

Some elements may require special extraction procedures which are detailed below for specific instruments or are cited in Boyle (2001b).

2.2.1.2.2 Analysing solid samples

Two principal approaches have been used to analyse samples consisting of solid material. These are underpinned by different physical processes, nuclear and atomic, where a sample is irradiated by neutron or x-ray stimulation respectively, the latter being more commonly applied. More recently, laser ablation has been added to various instruments, permitting analysis of solid materials. These methods and some others are described here.

2.2.1.2.2.1 X-ray fluorescence spectrometry (XRF)

All XRF techniques are underpinned by the irradiation of solid material by primary photons from an x-ray source. This triggers the photoelectric fluorescence of secondary x-rays with energies characteristic of the elements present in the sample. Signal processing by the XRF system converts count rates of individual elemental signatures into element concentrations. The x-ray count rate is primarily controlled by elemental

concentration, excitation and detector efficiency and instrument geometry, but also by effective x-ray absorption by the material which must be corrected for. XRF systems deliver primary x-rays either from an isotope source or x-ray tube source and may also differ in their method of x-ray detection. Wavelength dispersive instruments (XRF-WD) are more precise, but more time consuming, while energy-dispersive instruments (XRF-ED) are more rapid but commonly have lower detection limits and for some elements yield less precise results.

The poorer detection limits of XRF techniques for many elements when compared to procedures that measure elemental concentrations from solutions is highlighted by Boyle (2001b). For most palaeolimnological applications, however, concentrations vastly exceed detection limits and this is indeed the case for many heavy metalloid elements likely to be found in mining effluent.

Traditional XRF equipment has been designed for use in laboratories, being large in size with helium or other coolant gases required. More recently, field portable XRF guns (e.g. Thermo-Niton, Olympus Delta, and Bruker) have become common which in general offer lower detection limits but high-precision and good accuracy nevertheless. These offer the advantages of rapid data acquisition in the field or laboratory, either on split cores or sub-samples in bags. Beneficial implications on field expeditions include identifying preferred locations for extraction of master core(s) based on preliminary geochemical stratigraphies acquired during the same coring expedition.

2.2.1.2.2.2 Scanning XRF

The appearance of X-ray fluorescence core scanning in the last decade is proving a valuable addition to palaeolimnological research (as well as in marine or other sedimentary settings). These technologies offer a method for rapid, non-destructive acquisition of geochemical data on wet sediment cores at very fine resolution, down to sub-millimetre scale in some instances (Croudace *et al.,* 2006).

Two main types of core scanner, manufactured by Geotek and ITRAX are regularly used. The Geotek Multi-core logger measures elemental concentrations directly using an Olympus Delta portable XRF gun mounted on a mechanised arm that tracks along the core. This applies XRF measurements and returns total concentrations after applying a series of algorithms to convert count rate into total concentrations. Compared with the ITRAX this instrument has low resolution (best ~ 5 mm). A critical

assessment of instrument accuracy and calculation of dry mass concentration values is presented in Chapter 3.3.

The ITRAX technology operates in a different manner (Croudace *et al.,* 2006), using a fixed dedicated Energy-Dispersive XRF (using a Mo or Cr x-ray tube) under which the sediment core is passed. This configuration has the disadvantage that the instrument occupies a space twice the length of the core track. Compared with the Geotek system, the ITRAX has the additional disadvantage of reporting only x-ray count rates rather than element concentrations. Conversely, the exceptionally high analytical resolution (minimum ~200 μm) and measurement speed are great advantages.

Despite the recent substantial volume of research underpinned by XRF core scanning, potentially significant measurement uncertainties have been highlighted only recently. Hennekam and de Lange (2012), and references therein, list a number of problems which may result in unpredictable deviations in measurements, including the heterogeneous nature of the wet sediments, grain size variability, uneven core surface, interstitial water content and the formation of a water film between the sediment surface and covering polypropylene film. The x-ray tubes can also change with age meaning measurements performed with significant time gaps should not be compared directly (Löwemark *et al.,* 2011).

Variable water content can negatively impact instrument precision in two ways; overall element concentrations will be diluted due to the presence of water and wet sediment elemental concentrations may appear to vary along a core but whether this reflects a change in composition or simply water content is unknown. Furthermore, water can absorb the x-ray radiation, reducing instrument performance and detection limits (Hennekam and de Lange, 2012).

Some potential solutions have recently appeared, focusing on accounting for variable water content and verifying effective x-ray operation. Normalising the raw data to the ratio between incoherent and coherent backscatter to account for changes in water content along a core appears sufficiently rapid to offer a practical solution (Chapter 3.3; Kylander *et al.,* 2011). Using elemental ratios can be an effective solution. However, a good understanding of the chemical properties being analysed is crucial to ensure signal is not lost and that the ratios reflect true values (Hennekam and de Lange, 2012; Löwemark *et al.,* 2011).

It is worth emphasising that the undesirable absorption of fluorescence by water predominantly influences weaker energies (Tjallingii *et al.,* 2007) and therefore poses a greater problem to the precision of measuring elements with a lower atomic number. The heavier elements associated with industrial effluent are likely to be less affected by this potential source of measurement error (Hennekam and de Lange, 2012).

2.2.1.2.2.3 Laser ablation ICP Mass Spectrometry (LA-ICP-MS)

Detailed discussion of ICP procedures is contained in the following section (analysis of solutions) but the recent development of laser ablation (LA) techniques has enabled solid, powdered samples to be analysed by ICP-MS for a number of major elements, trace metals Ba, Cr, Cu, Zn, As (Rauch *et al.* (2006) and Shaheen and Fryer (2011)) and Pb isotopes (Sheppard *et al.,* 2009). This technique shows great promise for minimising the complications inherent to ICP analyses of extracted solutions introduced by pre-treatment, sample handling and spectral interference (Shaheen *et al.,* 2012). LA-ICP-MS enables sub-millimetre resolution geochemical analyses to be conducted although where water content is high or the core surface has been disturbed, effective laser profiling may be more problematic.

A number of methods have been proposed for creating an effective flat surface for scanning by the laser system. Powdered samples can be compressed into small disc-shaped briquettes using a styrene-wax binder (Sheppard *et al.,* 2009) while Rauch *et al.* (2006) propose using thin-sections sub-sampled 1.5 cm below the surface of frozen sediment cores and dried at low temperature (40°C) to ensure sediment structure is maintained. Alternatively, dried sediment can be directly impregnated with epoxy resin (Shaheen and Fryer, 2011). The LA system operates by placing samples in a sealed cell through which a stream of Ar gas is pumped. A narrow laser beam (50 - 100 μm) is focused on the sediment surface and moves incrementally (5 - 10 μm) causing ablation along a linear transect. These ablated particles are carried under Ar flow to the plasma torch for analysis by ICP-MS.

Usefully, instrumental setup parameters are published by Rauch *et al.* (2006) and Shaheen and Fryer (2011) for their particular systems and enabling a degree of inter-lab data comparison to be conducted.

2.2.1.2.2.4 Direct Mercury Analyser

This piece of equipment offers a simple method for determining total Hg concentrations from solid material with no pre-treatment required. Quoted measurement precision is ng g^{-1}. The instrument performs all necessary procedures including drying and oxidation of the original sample, reduction of elemental mercury and the measurement of the resultant total Hg vapour (Couillard *et al.,* 2008).

2.2.1.2.2.5 Instrumental neutron activation analysis (INAA)

Different procedures and system setups exist (e.g. Negi *et al.,* 1997; Mader and Koeberl, 2009) which irradiate samples by neutrons adjacent to a nuclear core, initially forming highly-excited nuclei before subsequent gamma ray emission upon deexcitation. Decay energies of the gamma emissions are a function of elemental composition, enabling elemental speciation and concentrations to be measured (Li *et al.,* 2012). INAA is useful as both short-lived and long-lived isotopes, including many trace elements and heavy metals, can be measured with high degrees of precision by exposing samples to differing irradiation time intervals (few seconds or up to 30 days, respectively). Li *et al.* (2012), however, note Cu and Pb were below detection limits on their particular system.

Measurement uncertainties associated with neutron flux mean this method is not in common use (Negi *et al.,* 1997). However, a number of recent papers have successfully used NAA to measure concentrations of heavy metals in sediments (Li *et al.,* 2012; Matsapaeva *et al.,* 2010; Waheed *et al.,* 2010).

2.2.1.2.2.6 Thermogravimetry Analysis (TGA)

Thermal analysis, in which solid sediment samples are heated at a controlled rate (5 - 20 °C/min) across a specified temperature range (usually 30° - 950°C) under an oxygen or nitrogen atmosphere, has been demonstrated to contain signals of heavy metal pollution in marine sediments (Rodríguez-Barroso *et al.,* 2010; Rodríguez-Barroso *et al.,* 2008). Provided geochemical data obtained using a secondary technique is available for correlation purposes, applying their procedures to lake sediments offers an automated and low-cost methodology.

2.2.1.2.3 Analysis of solutions

2.2.1.2.3.1 Atomic Absorption Spectroscopy (AAS)

Measuring the absorption of light at a specific wavelength by a sample is the basis for AAS and geochemical data are obtained as each element absorbs a unique energy wavelength linearly related to concentration (Boyle, 2001b).

The atomization of a sample can be achieved in two ways, either flame atomic absorption spectrometry (FAAS) in which the radiation beam passes through a flame which aspirates metallic ions within the sample or electrothermal atomic absorption (EAAS) which involves placing the sample in a graphite tube which is briefly heated by a high-current electric supply. In general, EAAS delivers better detection limits but is prone to greater matrix interference than FAAS and significant technological advances in FAAS now enable a number of trace metal elements to be measured more effectively. For example, using a flow injection or sequential injection method enables ultra-trace concentrations of heavy metals to be determined (Zhang and Adeloju, 2008). Furthermore, the cold-vapour AAS technique enables very low concentrations of mercury (Hg) in the parts-per-billion range to be determined.

2.2.1.2.3.2 Cold-Vapour Atomic fluorescence spectrometry (CVAFS)

Coupling the cold-vapour principle with atomic fluorescence spectrometry, which involves exciting electrons using a beam of ultraviolet light, is particularly effective for measuring trace amounts of mercury (Ma *et al.,* 2013). Published literature generally follows the EPA method 1631, initially involving oxidation by bromine monochloride (BrCl) and subsequent two-step reduction procedure using hydroxylamine hydrochloride ($NH_2OH.HCl$) and stannous chloride ($SnCl_2$) prior to collection of the Hg vapours in a gold trap. Suggested experimental setup to achieve picogram detection levels is described by Bloom and Fitzgerald (1988) while a comprehensive review of different techniques for the speciation and measurement of Hg in environmental samples is provided by Leermakers *et al.* (2005).

2.2.1.2.3.3 Inductively coupled plasma Atomic Emission Spectrometry (ICP-AES)

Subjecting atoms to thermal excitation causes radiation lines to be emitted at particular wavelengths according to the elemental composition of the solution. The line

wavelength intensity should be proportional to concentration of each element within the sample.

The integration of ICP and AES systems promotes greater emissions than traditional AES and hence is capable of measuring a wide range of elements simultaneously at detection levels reaching parts-per-billion. A similar digestion procedure is usually employed involving sequential HClO4-HF-HCl treatment (Couillard *et al.,* 2004).

The high number of emission lines (i.e., spectral interference) presents a significant challenge to robust interpretation of highly heterogeneous materials like lake sediments. In addition, high operating costs limits the number of samples which can feasibly be run. This is particularly problematic if the spatial distribution of mining pollution across a lake is being assessed using many sediment cores.

Inductively coupled plasma mass spectrometry (ICP-MS). The accuracy and detection limits of these techniques are vastly superior when coupled with ICP which uses high-temperature plasma to atomize samples for analysis by mass spectrometry (Boyle, 2001b). The high cost and greater sample handling are disadvantageous when compared to AAS and XRF, however.

Sample preparation prior to ICP-MS usually follows USEPA Method 3501 which involves leaching the sediment via microwave-assisted HNO3 digestion to remove sulphides, carbonates and some clays while avoiding the dissolution of silicates (Parviainen *et al.,* 2012). Conducting sample preparation in the sealed microwave environment minimises vaporisation of certain pollutant elements which are highly volatile at temperatures <60°C (As, Hg, Cr).

2.2.1.2.4 Isotopic Determination (Hg and Pb)

Using a multicollector ICP-MS permits isotopes of pollutant elements including mercury (^{199}Hg, ^{200}Hg, ^{201}Hg or ^{202}Hg) and lead (^{204}Pb, ^{206}Pb, ^{207}Pb and ^{208}Pb) to be determined (Garçon *et al.,* 2012; Ma *et al.,* 2013). Analyses of isotopic composition are a powerful tool for detecting provenance of pollution fluxes (Renberg *et al.,* 2001) and Komarek *et al.* (2008) provide a detailed overview of Pb isotope analyses on environmental samples.

Solution preparation for Pb isotopes also involves digestion using HF, $HClO_4$ and HNO_3 before Pb is isolated using an anion exchange technique involving HCl and phosphoric acid (H_3PO_4) following Manhes *et al.* (1984).

It is worth pointing out that these techniques can be applied in conjunction to negate their relative advantages and disadvantages, with cost and time being the greatest barriers. Calibration against known standards is crucial and, where internationally-recognised standardized materials have been used, direct comparisons between trace element geochemical data acquired using different instruments can be used confidently (Ayuso *et al.,* 2013).

2.2.1.2.5 Quality control

All instruments must be calibrated, samples must be prepared (though minimally in the case of XRF), and commonly quite elaborate signal processing is required to correct for matrix effects and inter-element interferences. How sure can we be that all of this is being performed correctly? A full treatment of quality control procedures is beyond the scope of this chapter; each instrument and manufacturer generally has comprehensive guidance. However, the role of blanks and certified reference materials is pivotal and is worth discussing in brief here.

2.2.1.2.5.1 Analytical blanks

Perhaps counter intuitively, an instrument is unlikely to yield zero signal for an element that is effectively at zero concentration. Spectral background and inter-element interferences lead to a measurable signal even in the absence of the element of interest. Therefore, to prove that an observed signal does indeed indicate the detectable presence of an element it is essential that analytical blanks have been correctly prepared and measured as unknowns. These must have the same matrix as the samples being measured; generally this means treating an aliquot of nothing (empty crucible, for example) identically to the samples, with the same reagent additions and treatments. Measuring such a blank as if it were an unknown sample serves to assess simultaneously both instrument calibration and any introduced contamination (from reagents or environment). Measuring a suite of such analytical blanks provides a statistical characterisation of the zero measurement, and is essential for calculation of the true detection limit.

Note: a zero calibration standard, generally also matrix matched, will be included in the calibration of the instrument. This is NOT the same as an analytical blank, which must be treated as an unknown sample. Note too that for solid sample methods, such as XRF, analytical blanks are problematic for two reasons. First, it is practically impossible to

create a solid material whose matrix is similar to lake sediment but which contains none of a particular heavy metal – even spectrographically pure reagents contain trace contamination. Second, the matrix (major components such as quartz, organic matter, etc.) of lake sediment is highly variable; thus a large number of analytical blanks would be needed to cover all possibilities. Generally the best option is to seek Certified Reference Materials (see below) that have low concentration of specific elements and a range of matrices, from which the zero condition can be reliably approximated.

2.2.1.2.5.2 Certified Reference Materials (CRMs)

Many organisations exist that manufacture large batches of homogenised sediment that have been analysed for specified elements by multiple laboratories using multiple methods. Statistical analysis of the suite of values obtained this way is used to generate certified values for element concentrations. These materials provide the corner stone of reliable sediment analysis. Small subsamples of CRMs must be included with each batch of unknowns, and treated identically. The readings obtained can then be compared with the certified values, and any problems can be identified and addressed. The choice of CRM, and the number of different ones to include, will depend on the purpose of the analysis. Ideally, the matrix of the CRM should be similar to the unknown. This is problematic for highly organic sediments, particularly for mineral-poor peats, as there are no generally available CRMs. Various plant tissue CRMs provide a partial solution, but these are mineral-poor compared with typical highly organic lake sediments.

2.2.1.3 Approaches to calculation

Reliable measurement of heavy metal concentrations in lake sediment, with appropriate accuracy and precision, is a prerequisite to reliable interpretation. However, it is not enough. Heavy metals are present in unpolluted sediments, and may naturally show stratigraphic variation. How certain are we that any metal enrichment derives from pollution? A series of procedures have been developed address this question; these are reviewed here starting with the earliest.

2.2.1.3.1 Raw concentrations

The earliest studies to use lake sediment records to infer recent changes in heavy metal pollution explored variations in the concentrations of Hg and Pb (Aston *et al.,* 1973;

Kemp and Thomas, 1976; Thomas, 1972). Their interpretations are based on the trends and timing of concentration changes, allowing them to infer an increasing pollution load. This simple approach succeeds because the signal is strong; Hg and Pb have very low natural concentrations at the studied sites, so a pollution contribution can readily add substantially to the total, leaving a clear, simple signal. In cases where these conditions are met, this simple approach is still applicable and widely used. Hammarlund *et al.* (2008), for example, apply this approach in Sweden at a location where the pollution signal is strong. This situation is illustrated in Figure 2.11a for the Pb sediment concentration record at Lilla Öresjön (unpublished data). However, where pollution signals are weak, or in the case of elements that have strong natural components, separating natural from pollution drivers is more difficult. Mackereth (1966) showed that Cu, Ni and Zn showed strong systematic concentration changes through the Holocene; and while he did not investigate modern pollution, it is clear

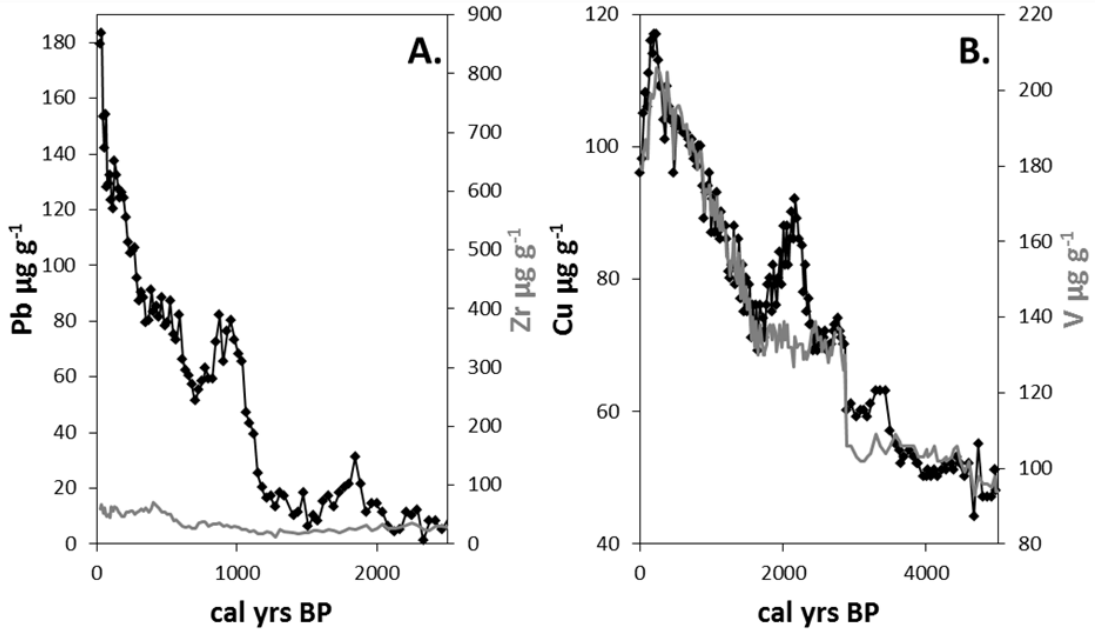

Figure 2-11 A) 2500 years of Pb concentration variation shows a series of abrupt increases. These are far in excess of any passive tracers (only Zr shown). B) At Er Hai (Dearing *et al.,* 2008) Cu concentrations also increase steadily. However, V, which shows no sign of contamination, closely follows the Cu increase except for some episodes of elevated Cu concentration.

that the patterns he revealed must be allowed for if pollution is to be identified. This situation is illustrated in Figure 2.11b for Cu in Er Hai, Yunnan Province, China. The Cu concentration rises strongly over the last 3000 years; however, most of this rise can be

attributed to natural causes (erosion of basaltic soils rich in magnetite) as is shown by the V concentration signal.

2.2.1.3.2 Ratio to passive tracer

On the basis that lithogenic element fluxes should remain constant in the face of pollution, expressing heavy metal concentrations as ratios to a lithogenic tracer element should correct for any changes in concentration arising from dilution effects. Thus, Bruland *et al.* (1974), interpreting sediment heavy metal records from near-shore marine sediments in California, use ratios to aluminium concentration to support their case for enhanced pollution. Kemp and Thomas (1976) develop this approach for their Great Lake records, applying a normalisation that retained the original concentration units. Norton and Kahl (1987) formalised this approach, using equation 1:

$$M_{a,x} = M_{total,x} - M_{total,bg}\frac{[T_x]}{[T_{bg}]} \qquad \textbf{Equation 1}$$

where M = a heavy metal, T = passive tracer element, suffix a = anthropogenic, x is any depth, bg = background (usually, basal sediment values).

They also switch from Al to Ti as the passive tracer. Does this matter? Indeed, is either of these elements suitable for this purpose? Renberg (1986) showed for sites in Sweden that loss on ignition (LOI, a proxy for organic matter concentration) provided a better tracer than any of the lithogenic elements. Ochsenbein *et al.* (1983) showed that for Blelham Tarn (English Lake District) natural Cu variation was controlled by the mineral chlorite, such that Mg provided an excellent passive tracer for it. Dearing *et al.* (2008) found that V, which showed no pollution enrichment, provided an excellent passive tracer for natural Cu variations in Er Hai, Yunnan Province, owing to the enrichment of both in catchment-derived primary magnetite (Fig 2.11b). Such a strong association, is however, likely to be a rare occurrence. Boes *et al.* (2011) compare Ti, Zr, Rb and Al as passive tracers in Swedish lakes. They find substantial differences between these and recommend using all four to inform a critical interpretation. How can this diversity be reconciled? The element concentrations shown in Table 2 help explain why different passive tracers are needed for different heavy metals, and that the best tracer will vary with parent material composition. Combining the information

in Table 2.2 with the data in Figure 2.9 (Kråkenes, Norway) is still more informative; choice of passive tracer must take particle size into account. Most heavy metals, even under natural conditions, are strongly enriched in the finest particle size fractions. At Kråkenes Lake, we can see that most possible passive tracers fail to match the size-composition properties of the heavy metals; only Rb is at all suitable. Zr, enriched in the silt fraction, is wholly unsuitable, and would only yield accurate results if there are no changes in particle size associated with recent human impacts. Rb, Ti and Al are enriched in the fine sediment, though not so strongly as the heavy metals, but they are also enriched in the coarse sediment. If any changes in sediment particle size did not extend to the largest size fractions, all three could make usable tracers. Such issues are of great practical importance. Boyle *et al.,* (2004) find large stratigraphical variations in heavy metals concentrations in six cores from Svalbard, but are able to rule out natural causes for these at only one site, and only for Pb. The literature is full of examples where a less cautious approach has led to potentially erroneous (unsafe) inference of human impacts.

A useful empirical approach for the numerical optimisation of passive tracer methods is given by Hilton *et al.* (1985). It must be noted, however, that while this improves the precision of the method, and tests its numerical validity, it does not avoid the conceptual pitfalls described above.

In conclusion, the passive tracer approach constitutes a valuable empirical approximation that should be approached cautiously and critically. The information discussed above provides a framework for identifying likely passive tracers, but this is no substitute for critically testing the suitability of any candidates. That said, the method has wide effective application, as illustrated by a number of recent case studies, each using different passive tracers. Thus, Ahmed *et al.* (2005) (Dhaka City, Bangladesh) ratio to Fe, while von Gunten *et al.* (2009) (Chile) ratio to Rb and Zr. Krom *et al.* (2009), for studying pollution signals in Sea Lochs normalise Pb and Zn to Al to great effect.

2.2.1.3.3 Enrichment factors

Enrichment factors are somewhat problematic. Numerically, they are essentially the same as the ratio methods described in the preceding section. The difference is in the use of terminology that implies process. The reality is that no matter the extent to which a statistical analysis demonstrates that one part of a sediment sequence has a

greater heavy metal quotient than another part; "enrichment" has NOT been demonstrated. A strong case can be made that the term "enrichment factor" is never appropriate, and should be discarded as unhelpful. Nevertheless, these methods are so widely used that a brief review is necessary.

Various enrichment factors have been proposed, each intended to show whether or not sediments have been enriched in specific element due to pollution. The approaches fall into two general classes depending on the nature of the benchmark against which enrichment is judged, which may be either local or global.

The Anthropogenic Factor (AF) of Szefer and Skwarzec (1988) is directly analogous the normalisation procedure of Kemp and Thomas (1976), equation 2:

$$\boldsymbol{AF = \frac{C_{s,M}/C_{s,Zr}}{C_{d,M}/C_{d,Zr}}} \qquad \textbf{Equation 2}$$

where C = concentration, suffix s refers to surface sediment (0 – 5 cm) and suffix d to deeper sediment (below 15 cm). M is the metal under investigation, and Zr is the normalisation element.

This approach is therefore local, and differs from Kemp and Thomas (1976) only in its genetic nomenclature. The alternative method is to benchmark against a global reference material, commonly the Wedepohl (1995) estimate of average crustal rock. Thus the Enrichment Factor (EF) of Sinex and Helz (1981) uses the same formulation as for AF, but with D referring crustal average values rather than deep sediment. Other methods normalise to crustal average values but avoid additional normalisation to passive tracer elements. One influential implementation of this is the Geoaccumulation index of Müller (1979). This is based on the logarithm of the element concentration (c) normalised to global shale concentration (B), adjusted slightly to allow for uncertainty in natural concentrations (Eq. 3). Such methods are assessed by Das *et al.* (2008),

$$\boldsymbol{AF = \frac{C_{s,M}/C_{s,Zr}}{C_{d,M}/C_{d,Zr}}} \qquad \textbf{Equation 3}$$

Both of these approaches are in widespread use, though the terms used vary substantially. Thus the EF of Camarero *et al.* (2009) is identical to the AF of Szefer and Skwarzec (1988), though with Ti as a normalising factor rather than Zr. Both are locally referenced. Local reference methods are useful where element concentration varies due to changing dilution by biogenic or authigenic sediment. However, there are two issues weaken this approach. First, just as in the case of ratios to passive tracers, EF

normalisation only corrects for natural fluctuations if there is no change in the sediment particle size characteristics. The magnitude of this effect is illustrated for the Kråkenes particle size fraction data (see Figure 2.10), converted to enrichment factors relative to the mean concentrations (Figure 2.12). Across the four normalising elements (Al, Ti, Rb and Zr), the apparent EF values range from 0.3 to 5.1 for Cu and from 0.4 to 3.3 for Pb. Given the pervasive character of most human impacts on catchments, changes in sediment particle size must occur often. Second, the term Enrichment Factor conveys a causal mechanism which cannot be readily tested. If its magnitude is significantly higher in the surface sediment, then the pattern is consistent with enrichment. However, there is no way of rejecting the alternative explanation,

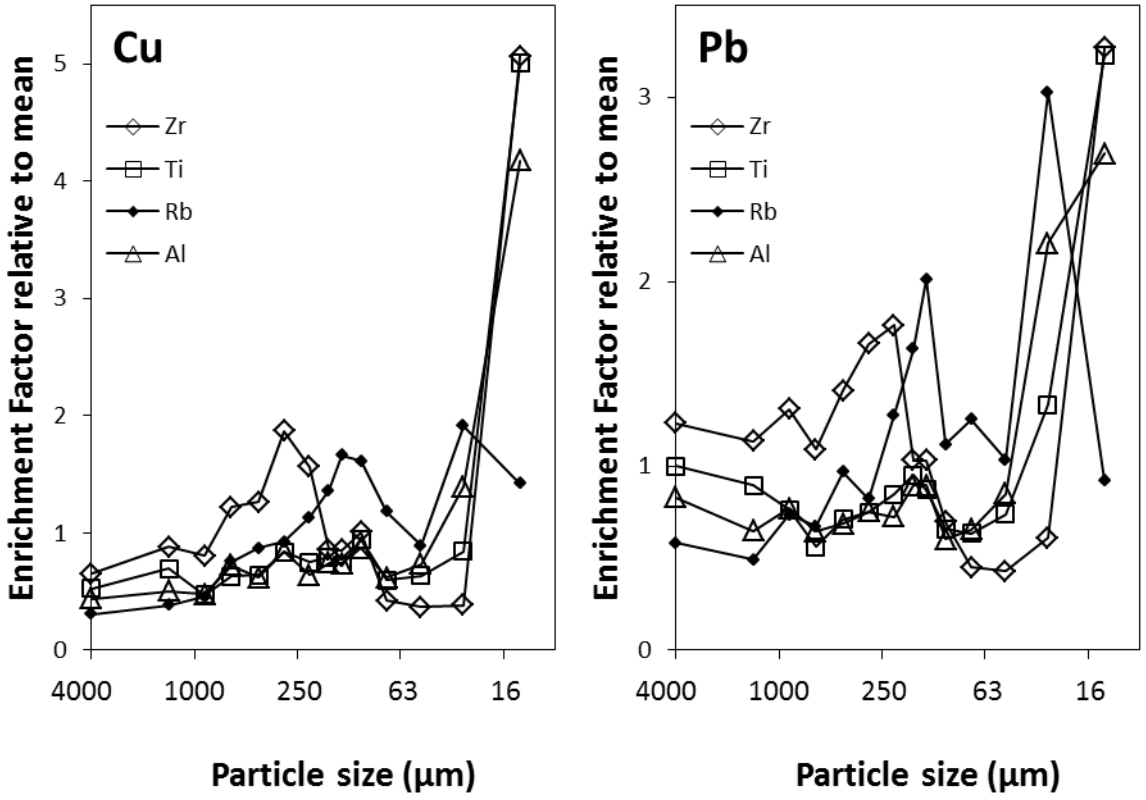

Figure 2-12 Enrichment factors by particle size fraction relative to mean concentrations (data from Kråkenes, unpublished data and Boyle *et al.* (2013). These are calculated according to Equation 2, substituting size fraction for depth (s) and mean concentration for the deep sample (d). This serves to show the potential for particle size sorting to lead to changes in enrichment factor values.

that the normalising element is depleted in the surface sediment while the heavy metal remains constant. Thus the term "Depletion Factor" would be a little less logically

reasonable. This is not to say that the numerical procedure is without value, only that its cautious application might be better encouraged if a more descriptive term were used. Globally referenced enrichment factors suffer from the same drawbacks as their locally referenced counter parts. However, they suffer from the additional problem that local compositions are generally very different from the global average due to very great natural heterogeneity. Tapia *et al.* (2012), for example, amply demonstrate that average crustal concentrations are of no use in assessing heavy metal enrichments in the mineralised regions of Bolivia.

Enrichment factors, whether locally or globally referenced must always be treated sceptically. A high or low EF tells us no more about local pollution than about local bedrock characteristics. If weathering does indeed also come into play, as suggested by Das *et al.* (2008), then the EF values depend on even more unknowns and unrelated properties and must be interpreted only with the very greatest of caution. To illustrate this point one need only look at the widely varying preindustrial sediment concentrations seen for Cu, Ni and Zn in arctic Canada (Wolfe and Hartling, 1997), the English Lake District (Mackereth, 1966), the Alps (Koinig *et al.,* 2003) and in Er Hai, Yunnan Province, China (Figure 2.11b), and for Hg in Greenland (Lindeberg *et al.,* 2006). All of these would be revealed as pollution according to any of the published EF schemes, and yet are of wholly natural origin.

2.2.1.3.4 Fluxes and mass balance

The methods described above are wholly empirical, and referenced to local benchmarks that smooth out geographical factors, or to global benchmarks that are generally a poor guide to actual catchment materials. This means that there is no theoretical framework by which to interpret the results, and no interpretation can be judged more reasonable than any other as there is no mechanism for assessing reasonableness. An alternative approach is to apply a mass balance method which provides externally referenced estimates of expected result. Thus, Gallagher *et al.* (2004), studying 6 lakes from British Columbia, use not just concentrations but mass fluxes to assess plausible sources. With quantitative estimates of fluxes, though they cannot rule out natural change, they can at least compare observed with expected pollutant loading, allowing plausibility to be established. Conversely, Boyle *et al.* (2004) in failing to observe any clear anthropogenic heavy metals signal in five of size cores in Svalbard are able to show that the likely atmospheric fluxes are too weak to be

detected (Figure 2.13). Curiously, this powerful approach, put to great effect by Garrels and Mackenzie (1971) in application to global fluxes, have been little used in the analysis of sediment heavy metal records. Two exceptions to this are with the increasing use of Pb isotopes, which will be addressed below, and some mass balance modelling of lake sediment heavy metal fluxes (Boyle and Birks, 1999; Boyle *et al.,* 1998; Rippey, 2010). A powerful argument in favour of this approach has been presented recently by Engstrom and Rose (2013).

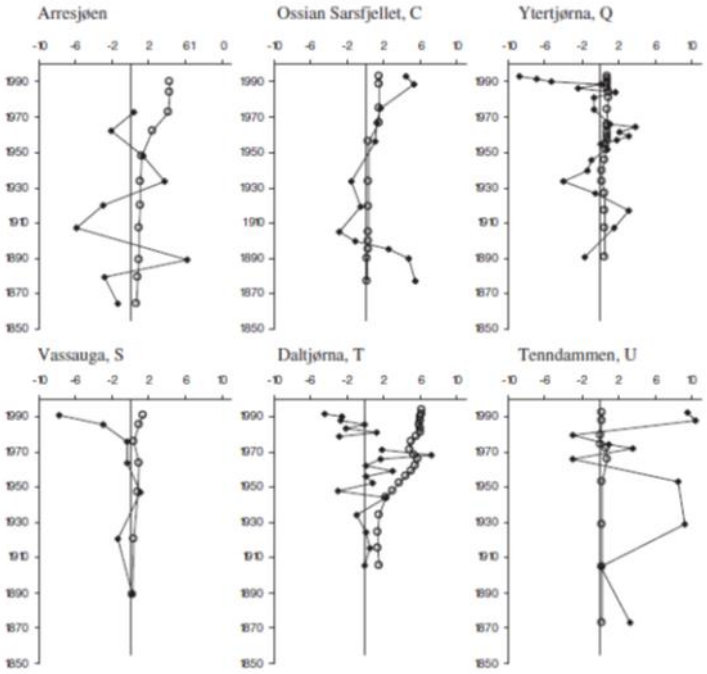

Figure 2-13 Using mass balance methods to test for expected pollution signals in lake sediments from Svalbard (Boyle *et al.,* 2004).

2.2.1.3.5 Normalisation to ^{210}Pb

Quantitative treatment of heavy metal fluxes in lake sediment raises the problem of interpreting sediment accumulation rates. A measured sediment mass accumulation rate for a single core partially reflects the average lake-wide sedimentation flux, and partly local factors that result in sediment focussing. In general, it is the lake-wide flux that is needed (to assess pollution loading, for example), so any focussing effects must be quantified and corrected for. Various predictive models have been developed over the years (Håkanson, 1977; 1981; Rowan *et al.,* 1992), but while the general trends are well known, prediction of focussing at specific coring location remains highly uncertain (Terasmaa, 2011). The alternative is to use 210Pb inventories as a direct measure of

focusing (Rowan *et al.,* 1995a), improving estimation of lake-wide sediment fluxes from single cores. While not as good as using multiple cores, 5 – 10 cores being recommended (Rowan *et al.,* 1995b) sensible values can be obtained with single cores, as was shown by Krom *et al.* (2009) in Scottish sea lochs in their assessment Zn and Pb pollution.

2.2.1.3.6 Isotopic signature and mixing models

Studies in which heavy metal isotopes are used in conjunction with their concentration values (e.g., Figure 2.14) show far greater interpretational values than either alone (Brännvall *et al.,* 1997; Brännvall *et al.,* 2001; Renberg *et al.,* 2002). The more recent application of binary mixing models to these data are proving very powerful (Brugam *et al.,* 2012) as a tool in source quantification.

The long established Pb isotopes method has more recently been added to by isotopic studies of both Cu and Zn (Thapalia *et al.,* 2010), showing similar power for discrimination of heavy metals sources.

2.2.2 Applications

Heavy metals records in lake sediment have been used for nearly 50 years, and have been applied to an extraordinarily wide range of environmental questions. The topics listed here are intended to represent the breadth and depth of this work, but inevitably is limited in scope by both space and the authors' experience. The section is divided into six broad themes each with rather differing objectives, though the reader will quickly notice that there is considerable overlap.

2.2.2.1 Chronological markers for other research

Where pollution histories are well known, either from extensive palaeoenvironmental research or from documentary records, the stratigraphy of heavy metals in lake sediments can provide a method for establishing, or contributing to the establishment of, sediment chronologies. Indeed, many studies use sediment records of heavy metal pollution solely to obtain chronological information, typically relying on mining/industrial production data to secure the chronology. Such an approach may be regional in scope, as with the exemplary nation-wide investigation of Pb concentration and isotopic character in Sweden (Brännvall *et al.,* 2001; Renberg *et al.,* 1994), leading

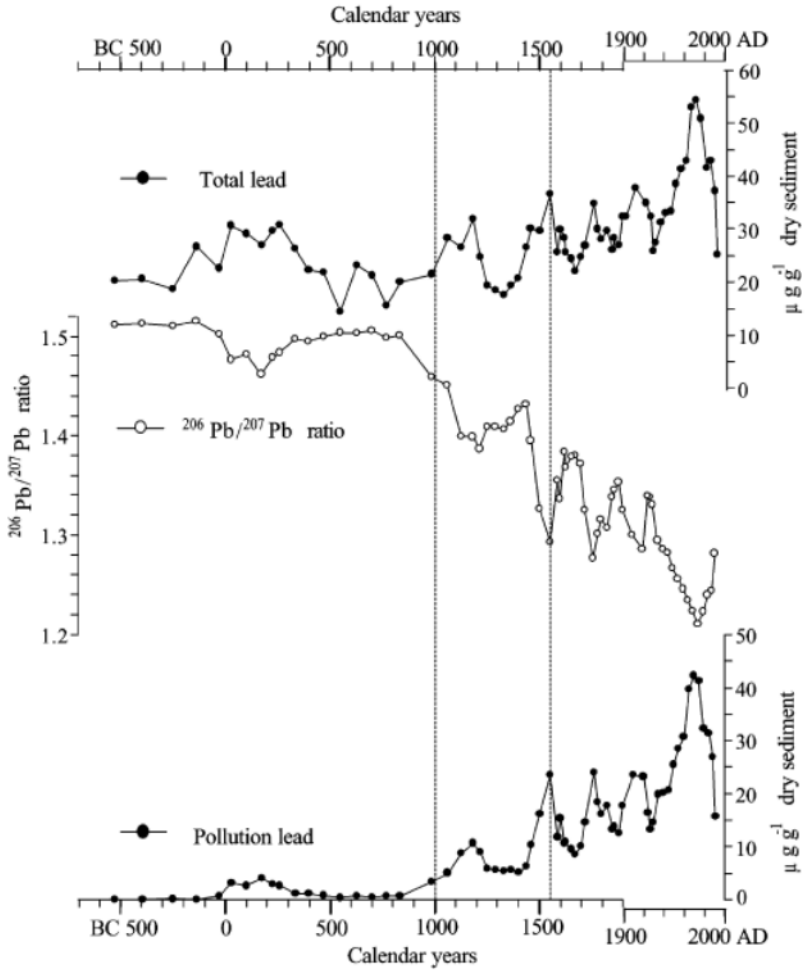

Figure 2-14 Combining Pb concentration data with Pb isotope values greatly increases confidence in interpretations (Data from Renberg *et al.,* 2002). The small Roman enrichment would be implausible without the corresponding excursion in isotopic ratios.

to concepts that are applicable at least as far away as Britain (Eades *et al.,* 2002; Oldfield *et al.,* 2003; Yang *et al.,* 2002). Or it may be local in character, exploiting the known history of specific mines or industries. This latter may take the form of chronological links between single elements and specific events in the mining record (Dearing, 1992; Grayson and Plater, 2009), or may include multiple elements and multiple phases of mining as illustrated in Figure 2.15 for Lake Verkasjön, Sweden. Though not the primary purpose of the study, Bäckstrom *et al.* (2006) by relating different elements to stages in the industrial development of the Salaån River catchment, are able to provide a far more robust chronology for Verkasjön than would be possible for a single metal or phase of mining. In another example, where the main

objective was to document the impacts of mining and the subsequent recovery on mine closure, the Pb pollution record was used by Hammarlund *et al.* (2008) to improve their sediment chronology. Once established a metal pollutant history that is well constrained in time provides an excellent means for correlation of cores in an individual lake basin. These chronological markers can then underpin assessment of spatial patterns of lake sediment accumulation, for example at Brotherswater (NW England) correlation of 12 cores shows there are sharp reductions in sediment accumulation rate with distance from the inflow delta (Chapter 4).

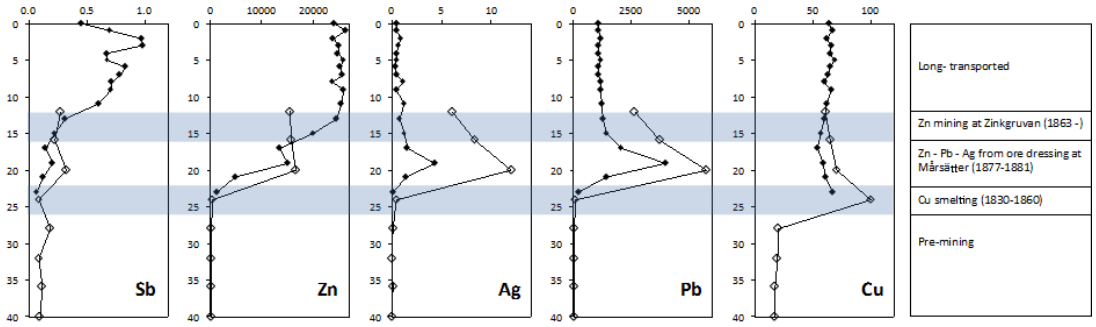

Figure 2-15 Complex heavy metal record at Verkasjön (Bäckstrom *et al.,* 2006)

2.2.2.2 Lake sediment heavy metal records to quantify pollution loading histories, or to identify pollution sources

With due care in choice of lake site, coring location, number of cores, and independent sediment chronologies, and with an informed approach to understanding natural heavy metal dynamics, lake sediments provide a uniquely high quality source of historical information about heavy metal pollution. The earliest studies focussed on known regional pollution hotspots, on metals known to be scarce in nature, and aimed to establish the pollution history or demonstrate the importance of local factors within the broader story. The studies of Hg and Pb described above (Aston *et al.,* 1973; Kemp and Thomas, 1976; Thomas, 1972) broadly fit this category. Such work continues, but increasingly studies address specific local questions or the impact of long-transported heavy metal pollution at sites remote from industry. A particularly fruitful area has been the establishment of reliable pollution records in areas of historic and prehistoric mining or industry.

In Britain, Farmer *et al.* (1997a) studied the historical Cu, Pb and Zn mining legacy of the southern Scottish Highlands in Loch Tay, showing the link to metal mining in the wider catchment. Eades *et al.* (2002) use both concentrations and isotopic composition

of Pb to extend this analysis more widely across Scotland, showing stages in evolving contamination starting with coal burning before 1820, through local mining and smelting during the 19th century, to international sources of Pb for fuel later. Further south, the impact of 19th century copper mining on the composition of sediment in Coniston, English Lake District, was studied by Davison *et al.* (1985). It was shown both that the Cu was transported in particulate sulphide form, and also that is dispersed quite efficiently throughout the lake, though most concentrated near the source. Investigations at both Brotherswater (Chapter 4) and Bassenthwaite Lake (Chiverrell, Sear, Dearing, Warburton and Schillereff, unpublished data) show a strong match between historical mining production metrics (e.g., Tyler, 2005) and metal concentrations preserved in the lake sediment record. In the case of Bassenthwaite Lake this recorded successive phases of Cu, Zn, Pb and Ba extraction. For lowland Britain, the magnitude of Pb and Zn pollution from heavy industry was demonstrated by Foster and Charlesworth (1996). This is illustrated for a small rural lake, Hatchmere (Cheshire, UK, Figure 2.16), showing a suite of changes starting in the Bronze Age, but dominated by the legacy of the Industrial Revolution that dwarfs even the impact of leaded fuel.

In Sweden, a number of large studies have investigated long and complex mining histories. Ek and Renberg (2001) use a multi-lake study of the region around the Falun copper mine in central Sweden, demonstrating acidification in the early 17th century

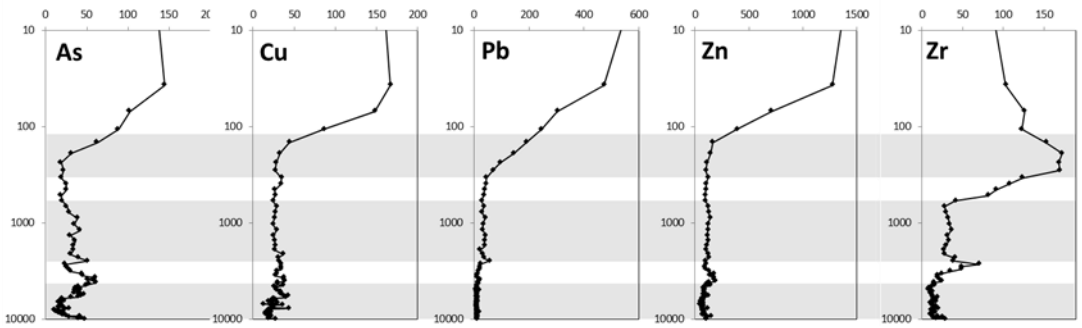

Figure 2-16 Mining and metal working pollution at Hatchmere, Cheshire, UK (unpublished data, D. Alderson). This reveals erosion (Zr) and Zn mining in Bronze Age (4ka), Pb mining Iron Age (2.7 ka), enhanced soil erosion (1400 AD), onset of recent Pb pollution (1660), and onset of Zn and Cu pollution (ca. 1800 BP).

associated with rapid expansion of the already ancient mine. More than 300 years later, the region remains severely polluted. Later, Bindler *et al.* (2009) used a large multi-lake study of an entire catchment draining this region to show that water transport dominated the local signal for Cu, Zn, Pb and Hg. In the same area, but looking at the whole Holocene, Hammarlund *et al.* (2008) used the Fe, Pb and Zn sediment records to link to the Cu and Fe mining of region, and to long transported Pb. Bindler *et al.* (2011b) focus more specifically of the 1000 year history of Swedish iron working using lake sediments. The detailed study at Lake Verkasjön, further south in Sweden (Bäckstrom *et al.,* 2006), has been addressed above. Together, these studies build up an accurate record of both the industrial history and the environmental consequences for a large area of central Sweden. Across the Baltic in Estonia, the legacy of oil shale mining and power generation in terms of heavy metal fluxes was assessed by Punning *et al.* (1997).

In a rather different setting and with a far shorter history, a suite of studies has investigated the legacy of heavy industry in North America. Sprenke *et al.* (2000) provide a quantitative characterisation of late nineteenth and early twentieth century heavy metal contamination in lateral lakes along the Coeur d'Alene River, Idaho, a legacy of upstream mining. Further east, at St Louis, Missouri, Vermillion *et al.* (2005) evaluate the impact of Pb smelting, active since the late eighteenth century. Combining concentration data, Pb/Ti ratios and Pb isotopes, they successfully demonstrate a progressive intensification of smelting impacts leading to a peak around 1950s. Recycling of battery lead after 1950 then led to a distinctive change in the isotopic signature demonstrating the power of the method for source discrimination. Further south, in Colorado, Gray *et al.* (2005) use sediment records of the late 20th century to assess possible sources of Hg contamination. They show that coal burning is the most likely explanation. At a larger spatial scale, detailed analysis of Cu and Hg in multiple short cores from Lake Superior show the complex interplay or early mining and metal working, followed by later long transported atmospheric pollution (Kerfoot *et al.,* 1999; Kerfoot *et al.,* 2004). This work also reveals high natural baselines, as might be expected for a region suitable for mining.

The preceding examples all depend on good chronological control for the sediment record in order to link to the documented environmental data. A subset of studies into sediment records of heavy metal impacts, though using sediment chronology for other reasons, use the same sediment core to measure both the disturbance driver (Heavy

metal contamination) and ecological response thereby avoid the problem of synchronising records. For example, Kauppila (2006) assess Ni loadings near smelters in western Finland to assess whether cessation of activity has changes the loading, and whether this in turn has reduced ecological stress. Salonen *et al.* (2006) do this for algae near a Cu mine in Finland. Effect of mine tailings from gold mining, including large qualities of Hg, were assessed in Nova Scotia (Wong *et al.,* 1999).

Many other such studies exist, far too numerous to list here, much less describe and discuss. These range from regions in central Europe with long mining histories (e.g., Tylmann (2005), Thevenon *et al.* (2011), Thevenon and Poté (2012), areas with current rapid expansion of industrial activity (Rose *et al.,* 2004), and polar regions where long-transported pollution is surprisingly evident (Muir and Rose, 2004). It is this field of geochemical palaeolimnology which has proved the most successful, a consequence of its sound theoretical basis; its continuing application seems certain.

2.2.2.3 Identifying and quantifying pre and post mining baseline states

It has been recognised in recent decades that industrial activity has contaminated the terrestrial ecosystem to an extent that ecological harm has occurred, and that such contamination predates any attempt at environmental monitoring. As governments have come to accept the need to restore soils, rivers and lakes to their pre-contamination state, the question has arisen of exactly what this means. Palaeoecology is ideally suited to this task, as amply demonstrated in the cases of acidification (Battarbee *et al.,* 1996; Battarbee *et al.,* 2005) and eutrophication (Battarbee, 1997; Bennion *et al.,* 2011; Bennion *et al.,* 2004). More recently, several research groups have started the task of characterising pristine environmental heavy metal concentrations. Catalan *et al.* (2013) review evidence for metal pollution (and other substances) at lake sites across Europe and North America remote from local disturbance, stressing their role in providing benchmarks against which to evaluate current trends. Bindler *et al.* (2011a) use lake sediment records of Cd, Cu, Hg and Pb to assess the meaning of the European Union's Water Framework Directive "reference conditions", and conclude that it is important to distinguish between "natural background conditions" which are those existing prior to human disturbance, and "reference conditions" which may constitute any well-defined point of comparison. They show that far deeper levels in the sediment must be sought for Pb natural conditions than is the case for Hg and Cd. Wei and Wen (2012) present a thorough analysis of sediment from Dianchi and Taihu

to determine baseline conditions for central China. Tapia *et al.* (2012) do the same for a mineralised region of Bolivia. This is a field of research that shows great scope for further development; it offers the potential to go beyond simple characterisation of "natural" or "reference" conditions, to assessment of mechanisms that might help assess the feasibility of achieving specific remediation targets. This is further addressed in section 2.2.2.4.

This generalising research builds on a longer history of identifying the dates and environmental characteristics of pre-industrial conditions at specific sites. For example, Farmer *et al.* (1997a) use lake sediment records of Cu, Pb and Zn to provide a benchmark for the onset of renewed mining on the Scottish Highlands at Tyndrum. Audry *et al.* (2004) show strong enrichment in Cd and Zn in three reservoirs of the Lot River (southwest France) due to smelting and mining. They use their data to determine pre-mining baseline Cd and Zn concentrations for the Lot-Garonne fluvial system, using the Geoaccumulation Index (see Eq. 3) of Müller (1979) to classify the state of metal pollution. Ahmed *et al.* (2005) assess pre-pollution conditions in Dhaka City for Pb and Zn using two lake sediment records.

2.2.2.4 Identifying pollutant pathways or environmental processes regulating heavy metals

The applications described in the preceding sections are essentially empirical in purpose; studies designed to generate evidence needed to define system states and test for change. However, these same, or similar, studies can be used to formulate, parameterise or test process models describing the fluxes and fate of heavy metals in soils, rivers and lakes. The following studies illustrate this approach to assess the migration of heavy metals through soil to watercourses. Shotbolt *et al.* (2006) used reservoir sediment records of Pb and Zn to demonstrate delayed supply of Pb to the lake from its catchment. The delayed delivery of Pb and Hg from catchments to lakes was clearly shown for both long transported contamination of mountain soils (Yang and Rose, 2005; Yang *et al.,* 2002) and localised Hg pollution associated with the weaving industry in Diss, UK (Yang, 2010). Data of this type has been used to generate a conceptual model of transfer mechanisms for Pb and Hg (Rose *et al.,* 2012).

At the still longer time scale Bindler *et al.* (2008) develop a conceptual model of pollutant supply, storage and fate in Sweden over the last 4 millennia. They show that even following current emissions reductions atmospheric Pb fluxes are still 2 to 3

orders of magnitude above the natural baseline, and that despite this recent aggravation, more than half the total atmospheric loading in Sweden was deposited prior to modern industrialisation. This allows them to provide robust estimates of recovery rates for catchment soils, finding the legacy of at 150-500 years of deposition dominates topsoil inventories, making recent emission reductions of little practical significance.

This delay effect is still more striking in mining districts. Thus, Wong *et al.* (1999) find no decrease in the export of As, Hg, Pb to lakes from gold mine tailings at the Goldenville, Nova Scotia, 50 years after mining ceased. At Bassenthwaite Lake and Brotherswater in the English Lake District, present day Pb concentrations are 300-400 ppm, down from the 19th century peak of 3000-4000 ppm, but still 10-15 times higher than the pre-mining values (Chiverrell and Schillereff, unpublished data).

2.2.3 Concluding statement

The assessment of heavy metal pollution is one of the most successful and widely used applications of palaeolimnology. It holds this position owing to its sound theoretical basis, and straightforward procedures. Provided sediment mass accumulation rates are well constrained and natural heavy metal fluxes can be reliably established, then chemical palaeolimnology provides accurate and reliable quantification of environmental heavy metal fluxes.

Nevertheless, there is much potential for error. Natural heavy metal fluxes are variable and can be large relative to pollution fluxes. In such cases, reliable interpretation of heavy metal concentration records requires a thorough understanding of natural processes. The various enrichment factor methods, all validly applicable under suitable conditions, may readily lead to misinterpretations where their underlying assumptions invalid. This is particularly likely where there are changes in sediment particle size and thus particularly likely in recent sediments over the time frames over which heavy metal contamination records are of interest.

It might be supposed that Pb-isotope approach would avoid this problem. However, this need not be the case. Pb-isotopes are fractionated between rock forming minerals, and so are also subject to particle size sorting effects. It is preferable then that particle size effects are properly investigated and correctly handled.

All existing methods for the interpretation of heavy metal pollution records in lake sediment would be more reliable if appropriate mass balance modelling were done in conjunction. This would serve to assess the geochemical plausibility of any interpretations.

Isotopic procedures, though not without their methodological issues, have revolutionised heavy metal sediment record interpretations by avoiding dilution effects when assessing potential sources. Further development of these methods has great potential for the future.

3 METHODOLOGICAL CONTEXT AND DATA QUALITY EVALUATION

3.1 Linking the research objectives to the methodology

Chapter 2 outlined in detail a range of criteria conducive to the preservation of palaeoflood layers in abyssal lake sediments and emphasised not all lakes may be suitable. The study sites for this thesis, Brotherswater in the Lake District National Park, northwest England (54.5066°N, 2.9249°W), and Loch of the Lowes, in the Southern Uplands of Scotland (55.2756°N, 3.1226°W), were selected in part based on previous work at both lakes (Chambers, 1978; Rae and Parker, 1996; Oldfield and Wu, 2000; Foster *et al.,* 2008) that suggested a signal of the hydrological regime may be preserved in their sediments, as well as the suitability of the physical settings of both lakes and their basin characteristics to those specified in Figure 2.5. More detailed site descriptions and how the selected lakes meet these criteria are highlighted in Chapter 3.2 as well as the Study Site sections of Chapters 5 (Brotherswater) and 7 (Loch of the Lowes).

The field and laboratory methods utilised throughout this thesis are introduced in Section 3.2 and more detailed descriptions are included in the respective results sections (Chapters 4-7) in which each method is employed.

The potential value of μXRF core scanning to palaeoflood research has been highlighted in Chapter 2 and a growing body of publications (Vasskog *et al.,* 2011; Lapointe *et al.,* 2012; Swierczynski *et al.,* 2012; Czymzik *et al.,* 2013; Wilhelm *et al.,* 2013; Wirth *et al.,* 2013a). This technique contributes a substantial volume of data to the thesis but questions remain regarding operational aspects and data quality of core scanning devices (Weltje and Tjallingii, 2008; Löwemark *et al.,* 2011). Thus, the final two sections in Chapter 3 (3.3 and 3.4) address methodological uncertainties associated with μXRF scanning in order to grasp a better handle on the quality of data output. While the non-destructive and high-resolution capabilities of core scanning devices are powerful, the wet nature of the sediment core will affect XRF determinations, in particular if water content varies substantially down-core. Section 3.3 presents two calibration methods to convert wet-sediment concentrations into their dry-weight equivalents, either using the ratio of Compton and Raleigh back-scatter intensities or a more simple regression correction. Secondly, both an Olympus portable XRF gun mounted on a Geotek platform and an ITRAX scanner were used to acquire data for this thesis; a detailed inter-comparison is presented in Chapter 3.4.

3.2 Study sites

3.2.1 Brotherswater

Brotherswater (54.5066°N, 2.9249°W, 158 m above sea level [asl])is a small, oligo- to mesotrophic upland lake (Maberly *et al.,* 2011) and a Site of Special Scientific Interest SSSI) located in the eastern Lake District National Park, Cumbria, Northwest England (Figures 3.1 and 3.2). The catchment and lake dimensions (Table 3.1) provide a high catchment:lake area ratio of 72:1, yielding substantial sediment supply, highlighted in Figure 2.5 as an important condition to maximise flood lamination preservation. A single inflow (Kirkstone Beck) fed by five tributaries draining the upper hills enters Brotherswater at the southeast corner, where a Gilbert-style delta has developed, characterised by a gravel top-set (Figure 3.3a) and steeply-dipping foreset slope. The deep, bowl-like basin with a flat, central abyssal zone has a maximum water depth of 16 m (Figure 3.1), limiting the potential for wind or wave-induced remobilisation of profundal sediments for a water-body of these dimensions (Dearing, 1997). Moderate thermal stratification occurs in the lake during the summer months (Maberly *et al.,* 2011).

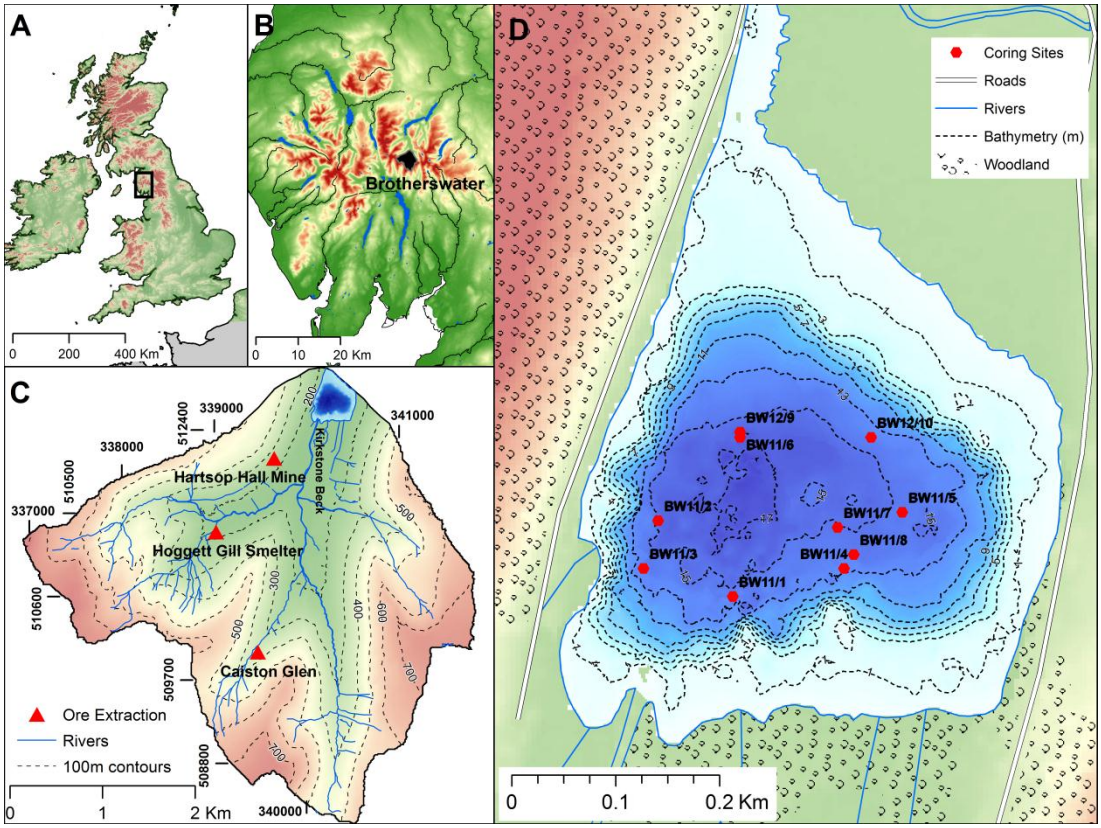

Figure 3-1 A) Location of the English Lake District within the UK. B) Topography and waterbodies within the English Lake District. The extent of the Brotherswater catchment is highlighted. C) Catchment Digital Elevation Model highlighting the location of ore extraction sites mentioned in the text. D) Bathymetric map of Brotherswater showing the location of ten coring locations.

Figure 3-2 Photograph of Brotherswater looking south towards its watershed. Inflow enters at the far right-hand side.

Table 3-1 Lake and catchment physical characteristics of the study sites

Parameter	Brotherswater	Loch of the Lowes	Lilla Öresjön
Catchment area (km^2)	13.01	27	4.55
Lake area (km^2)	0.18	0.47	0.67
Max water depth (m)	16	15	17
Mean water depth (m)	7.4		4
Catchment – lake area ratio	72:1	57:1	7:1
Lake elevation (m)	158	243	107
Maximum catchment elevation (m)	792	610	

Catchment geology is dominated by Ordovician volcani-clastic sandstones of the Borrowdale Volcanic Series, comprising andesitic tufts (96%) interspersed with occasional andesitic and rhyolitic flows (4%), overlain by Younger Dryas glacigenic sediments and landforms and shallow podzolic-brown earth soils. Forest cover in the catchment has been almost entirely replaced by open hill grazing and some pasture, although the southern shore is lined by an alder-willow fen.

Considerable variations of flow into Brotherswater are illustrated in Figures 3.3 and 3.4, while the November 2009 flood (Figure 3.5) highlights that high-magnitude events occur locally.

Figure 3-3 A) Kirkstone Beck under low-flow conditions in July 2013. B) The inflow delta of Kirkstone Beck exposed under low flow conditions in July 2013.

Figure 3-4 The inflow delta of Kirkstone Beck under higher flow conditions in February 2014.

Figure 3-5 Hartsop village during the November 2009 flood. Photo by Sarah Brockbank.

3.2.2 Loch of the Lowes

Loch of the Lowes lies in the Tweedsmuir Hills (55.2756°N, 3.1226°W), in the central Southern Uplands of Scotland (Figures 3.6 and 3.7), and occupies a headwater of the large River Tweed watershed, the second largest in Scotland (total area ~5000 km^2). The small loch (area 0.47 km^2) receives flows from five sub-catchments (total area 27 km^2, C:L ratio ~57) with a maximum elevation 610 m (Table 3.1). Most drainage enters the southern shore along with two smaller inflows at the northeast and northwest. The loch is adjoined to the downstream larger St Mary's Loch by a small stream. An alluvial fan separates the two water-bodies that probably developed during the early-Holocene (Murray and Pullar, 1910). Yarrow Water is the outflow of St Mary's Loch and its confluence with the Tweed is 20 km downstream. The lake is oligotrophic and has an elongated basin dominated by a single, flat central basin 12 – 15 m depth and with limited littoral area (Murray and Pullar, 1908). Catchment bedrock geology is dominated by Lower Palaeozoic greywacke sand/silt/mud-stones, which have been sculpted by Quaternary glacial erosion into an upland terrain comprising U-shaped valleys and more rounded summits.

Land cover today is a mixture of managed blanket moorland on hill tops and grazing pasture growing on podzolic soils that have developed on hillslopes artificially drained through the 18th and 19th centuries (Tipping, 1994; McEwen, 1990). Forest cover is largely absent except for small conifer plantations.

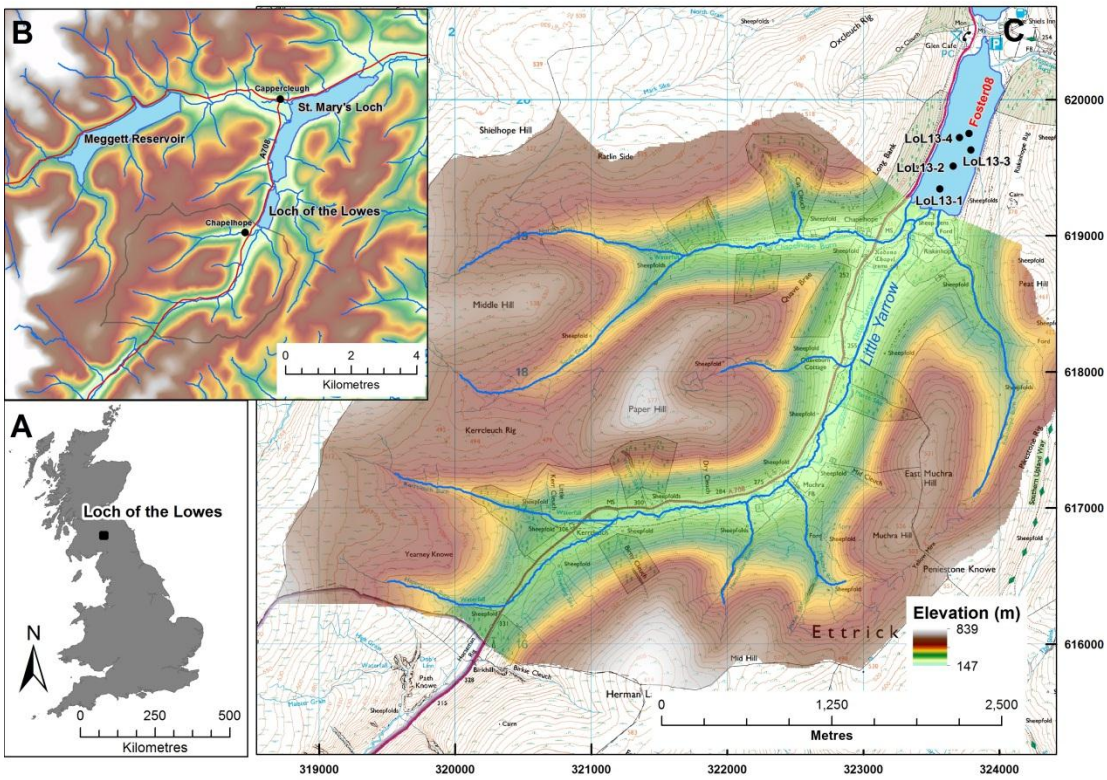

Figure 3-6 A) Location of the study site within the UK. B) The topography of the catchment and wider area around Loch of the Lowes. C) Core locations, catchment morphology and the main, southern drainage system entering the loch.

Figure 3-7 Photograph of Loch of the Lowes looking southwest towards its watershed. The main inflow enters near centre of photo, smaller streams flow through reed beds to the left and right.

3.3 Field and laboratory techniques

3.3.1 Field techniques

3.3.1.1 Sediment coring

Coring locations were determined after detailed bathymetric surveys at both lakes using a Garmin dual frequency echo-sounder and conducted along delta-proximal to distal transects. Lake bathymetries and the locations of ten coring sites at Brotherswater and four at Loch of the Lowes are highlighted on Figures 3.1 and 3.6. A Russian-style coring device (0.075 m diameter) was used to extract long cores from both lakes. A 1.5 m chamber was used at Loch of the Lowes while both 1 and 1.5 segments were obtained at Brotherswater (Table 3.2). Short gravity cores (0.16 – 0.25 m length, 0.08 m diameter; Boyle, 1995) were also obtained wherever possible to capture intact sediment-water interfaces (high sand content prevented successful extraction in some instances). Core handling and sub-sampling intervals are detailed in Chapters 4, 5 and 7.

Table 3-2 Details of the sub-sampling intervals and XRF procedure applied to each Brotherswater core.

Core ID	Total length (cm)	Sub-sampling interval (cm)	XRF measurement technique
BW11-2	339	0.5	Bruker (dried samples)
BW11-3	264.5	0.5	Thermo-Niton XLt3 (wet core)
BW11-5 (Drive 1)	152	0.5	Geotek (wet core)
BW11-7	142	4	Bruker (dried samples)
BW12-9A (Drive 1)	134	0.5	Geotek (wet core)
BW11-8	132	1	Bruker (dried samples)
BW12-9D	128	0.5	Geotek (wet core)
BW11-4 (Drive 1)	72	0.5	Geotek (wet core)
BW11-1	60	0.5	Geotek (wet core)
BW11-6s	26	0.5	Bruker (dried samples)
BW12-10s	25	0.5	Bruker (dried samples)
BW12-9s	24.5	0.5	Bruker (dried samples)
BW11-5s	19.5	0.5	Bruker (dried samples)

3.3.1.2 Sediment trapping

The sediment traps were installed in Brotherswater in July 2013 and collection intervals were broadly monthly (some intervals were much longer; Table 6.1) in part

regulated by logistical difficulties and inclement weather. Trap design followed the recommendations of Blomqvist and Håkanson (1981), Håkanson and Jansson (1983) and Ohlendorf and Sturm (2001) and consist of cylindrical tubing with diameter:length ratio of 6.8:1 and removable beakers. Detailed schematics are presented in Chapter 6. Traps were installed at three different water depths, ideally in order to capture over, inter- or underflows, and at a delta-proximal and distal location (their locations are highlighted in Figure 6.1).

3.3.2 Laboratory

3.3.2.1 Particle size analysis

The premise that high-resolution particle size measurements may yield information on palaeoflood pulses is central to this thesis. In this case, particle size distributions were determined via laser granulometry. As a result, considerable effort has been invested to assess the quality of the particle size data (see Chapter 5), especially in light of on-going debate surrounding the suitability of Coulter machines for discriminating between certain grain size classes (Roberson & Weltje, 2014). The detailed protocol is provided in Chapter 5; in brief, measurements of the Brotherswater cores and sediment trap samples were made on a Beckman Coulter™ LS200 while the Loch of the Lowes measurements were performed on a Beckman Coulter™ LS320. Sensitivity testing revealed the LS320 produced slightly coarser particle size distributions than the LS200 so direct comparisons between datasets were avoided. Samples were pre-treated to thoroughly remove the organic component, dispersed using sodium hexametaphosphate and run under sonicating conditions during measurement. Final results were averaged from three runs to ensure intra-sample noise remained low and particle size frequency statistics were calculated using the geometric formulae of Folk and Ward (1957) with the GRADISTAT 8.0 software (Blott and Pye, 2001).

3.3.2.2 XRF Geochemistry

Geochemical composition of sediment cores and sediment trap samples was determined via X-ray fluorescence (XRF) applied using three different instruments. All 0.5 cm sub-samples from Brotherswater core BW11-2 (3.5 m total length) were weighed, freeze-dried and re-weighed after drying to estimate moisture content, and subsequently analysed on a dry-mass basin on the desktop Bruker S2 Ranger energy-

dispersive instrument (Geography, University of Liverpool). Instrument specifications and sample preparation procedures are described in Section 3.3. The Brotherswater and Loch of the Lowes calibration datasets, as well as all sediment trap samples, were also measured on the Bruker device. All samples were corrected for their organic matter contents.

Long cores from Brotherswater and Loch of the Lowes were measured on a wet sediment basis prior to sub-sampling using an Olympus portable XRF gun mounted on a Geotek platform (Liverpool) and, in the case of the Loch of the Lowes cores, an ITRAX scanner (National Oceanography Centre, Southampton) also. A description of the Geotek device is provided in Chapters 3.3 and 3.4 and the ITRAX configuration is described in Chapter 3.4. Brotherswater cores were scanned at 5 mm intervals and scans of the Loch of the Lowes cores were carried out using step sizes of 5 mm, 1 mm (both Geotek) and 300 μm (ITRAX). Tests to correct for water content were performed using the procedures outlined in Chapter 3.3. A detailed inter-comparison (Chapter 3.4) illustrates a broadly consistent signal is obtained for most elements.

3.3.2.3 Visual analysis

The Brotherswater cores were photographed in the field immediately upon extraction using a Canon EOS600D camera. The Loch of the Lowes cores (Chapter 7) were photographed at 100 μm resolution using a Canon EOS 600D Line-scan (LS) camera fitted to a Geotek XZ MSCL instrument, after calibration to 18% grey and white plates.

3.3.2.4 Thermogravimetry

Organic matter (OM) content, or loss-on-ignition (LOI), of selected core samples and all sediment trap material was determined by thermogravimetry (TGA)/differential scanning calorimetry (DSC) on a PerkinElmer STA6000. TGA/DSC measurements were performed on the calibration samples (5 cm intervals) for BW12-9 (Chapters 3.3, 5 and 6), LoL13-4-1 (Chapters 3.4 and 7) and at 0.5 cm resolution for BW11-2 to correct Bruker XRF measurements for OM content. LOI values reflect the mass loss of freeze dried subsamples (~20-40 mg) recorded under a nitrogen atmosphere as the sample was heated from 30° to 995°C at 20°C min^{-1}. Sample mass is measured at 1-5°C intervals. The heating curve for each TGA/DSC measurement runs from 30°C to 150.00°C before a 5 minute hold at 150.00°C to equilibrate the programme and sample chamber temperatures and to drive off residual water. The heating cycle from 150°C to

995°C at 20.00°C min^{-1} under nitrogen includes multiple thermal composition phases depending on the character of the sediments, with plant tissue and soil organic fraction typically undergoing pyrolysis between 150° and 530°C. Charcoal and carbonates decompose thermally between 550-750 and 750-990°C respectively. The final phase of the TGA/DSC involves switching the atmosphere to air and holding at 995°C for 10 minutes to burn off products of the 30-995°C heating under nitrogen. Samples are then cooled to room temperature. Thermal decomposition between 150° and 530°C is used to represent organic content or loss-on-ignition. There is further information in the mass loss curves in the form of phases with more rapid and slow thermal decomposition, but their interpretation is beyond the scope of this thesis.

3.3.2.5 Sediment dating techniques

Two sediment cores from Brotherswater (one delta-proximal, the other from the lake centre) were dated using shorter-lived isotopes (^{210}Pb, ^{137}Cs, ^{241}Am) measured at the Liverpool Environmental Radioactivity Laboratory (Appleby *et al.,* 1986) and thirteen radiocarbon ages were obtained for core BW11-2 on hand-picked terrestrial plant macrofossils. Preparation methods are outlined in Chapter 4 and ^{14}C measurement data is listed in Table 4.1. The resultant age-depth model is also presented in Chapter 4 which used the Bayesion routine 'Bacon' (Blaauw & Andrés Christen, 2011) to integrate the radioisotopic information with chronological markers inferred from the geochemical profiles of Pb, Zn and Cu that reflected intensive mining in the catchment. The mining data and the Bayesian modelling approach are discussed further in Chapter 4.

Unfortunately radiocarbon dates have yet to be acquired for the Loch of the Lowes due to insufficient carbon in the plant macrofossil samples. Some chronological information is available from a previously ^{210}Pb dated core from the lake (Foster *et al.,* 2008) and a pollution signal reflecting atmospheric deposition probably after ~CE 1860 is identified in all four LoL cores (Chapter 7). The tentative chronology can be transferred between cores on the basis of stratigraphic and geochemical matches outlined in Chapter 7.

3.4 Approaches to water content correction and calibration for µXRF core scanning: comparing x-ray scatter with simple regression of elemental concentrations

Abstract

Geochemical evaluation of sediment records traditionally exploits dry mass concentration data; the new generation of scanning XRF devices, however, are generally presented with wet sediment cores. Therefore, conversion of wet core measured XRF data to dry mass concentrations will aid the palaeoenvironmental interpretation, provided the method used is reliable and avoids loss of data quality. Here, we perform measurements on sediment cores extracted from two lakes, Lilla Öresjön (southern Sweden) and Brotherswater (northwest England) using a GEOTEK/Olympus DELTA scanning µXRF device (approximately 5 mm resolution) and we compare two correction methods: 1) correction by simple regression, calibrated using dry sediment elemental concentration data measured for 'training set' of subsamples, and 2) a novel technique that corrects for water content estimated using x-ray scattering data obtained during scanning. We show that where sediment water contents are highly variable the regression method fails while water content correction methods can be highly effective. Where water sediment water contents are relatively constant, the elemental regression is as effective and introduces less noise.

3.4.1 Introduction

The last decade has seen a proliferation in the use of high resolution or micro-scanning XRF data to discern stratigraphical changes in alluvial, lacustrine and marine sediment, work that exploits a growing family of µXRF equipment that includes the ITRAX core scanner (0.2 mm resolution) originally developed by Croudace, Rothwell and Cox Analytical (Croudace *et al.,* 2006; http://coxsys.se/), the Avaatek XRF core scanner (0.1 mm resolution) (Richter *et al.,* 2006; http://www.avaatech.com/), developed over the last two decade for rapid analysis of marine sediment cores, and systems that automate (e.g., GEOTEK: http://www.geotek.co.uk/) the application of Handheld XRF Analysers such as the Olympus Delta XRF and Thermo-Niton XL3t (3-6 mm resolution). As µXRF scanning becomes an increasingly popular way of measuring element

composition data in sediment cores over "conventional" XRF analysis (Boyle, 2000) the question is raised of whether they generate sufficiently accurate quantitative composition data. The answer to this is far from simple, depending as much on the application or purpose of the measurements as to other considerations. The palaeoecologist with cores of wet sediment who asks whether scanning μXRF is as good as conventional XRF methods must first specify the question and expectations of the data. If these involve assessing the meaning of relative variations in element concentration, and considering only elements that are well-measured by μXRF, then the answer may be a simple, yes. However, the device will clearly not produce precise and accurate dry mass concentration values, and if these quantitative data are required then the answer is, no.

These two end-member cases are unlikely to change in the near future, because the issues do not arise from technological limitations. Rather, the problem is that conventional methods in sediment geochemical evaluation (Boyle, 2001b) are based on dry mass concentrations, where the concentration of an element, X, is defined as the mass of X divided by the dry mass of sample in which it is measured (Note this remains true even if the mass of X is expressed in molar units). It is a convenient fact of XRF analysis that such dry mass concentration values are obtained without the need to know the sample mass, provided the sample is both dry and of "infinite" thickness (Tertian, 1969) relative to x-ray penetration (generally a few millimetres of dry sediment will achieve this). μXRF scans of wet sediment do not meet this requirement. They still measure elements as concentrations or raw counts, but this concentration is relative to the density of wet sediment. In the case of typical organic lake sediment, where water contents may exceed 95%, the wet mass concentration may be only 5% of the dry mass concentration for a particular element.

This diluting of the concentration by water presents a challenge when interpreting wet-core μXRF data. Consider the case of a sediment record which contains high frequency variations in the carbonate to silicate ratio, but which also has highly variable water content. The x-ray signal for, say, Ca, will vary both with the Ca concentration in the dry matter and with the water content of the sediment. Furthermore, the signal will also contain variations resulting from imperfections of the core surface, and may contain artefacts arising from x-ray detection and correction for spectral background (Boyle, 2000). As the geochemist is interested only in the dry mass concentration component, it is necessary to process the signal to reduce the

contribution of other sources of variation. The most widely used approach is to normalise the element of interest to either another element (Löwemark *et al.,* 2011; Richter *et al.,* 2006) or to back-scatter peaks (Kylander *et al.,* 2012). Working with element ratios has the advantage of eliminating several unknowns; the diluting water content and surface imperfections in particular. However, as x-ray mass attenuation by water varies with photon energy, element ratios do not wholly avoid water content artefacts. Furthermore, when working with element ratios it is easy to overlook associated variations in major components that alter the geochemical interpretation. Furthermore, direct comparison of results with other data is difficult or impossible unless the element composition data are expressed as absolute concentrations, and ideally in dry mass form. Thus, the element ratio solution to the water content problem is far from ideal.

It would be desirable, therefore, if wet sediment core scanning XRF signals could be reliably converted to a dry sediment basis. In relatively uniform and consistent stratigraphical sequences the absence of large changes in content of water or organic matter means this conversion to a dry sediment equivalent basis can be achieved by simple correlation as demonstrated by Croudace *et al.* (2006) and Weltje and Tjallingii (2008). This is because under such constraints the dry and wet mass concentrations are proportional. This simple approach can be used regardless of whether the XRF output is given in concentration units (as is typical for Handheld XRF devices) or as raw x-ray count data. However, if water content in the sediment varies systematically, then simple regression will lead to an invalid correction, potentially producing an apparent chemical stratigraphy that is highly misleading. Where water content varies strongly, such as at the sediment-water interface, or across the transition from inorganic to very organic sediments in lakes during the early Holocene (Shen *et al.,* 2008), then wet and dry mass concentrations are not proportional, and an alternative approach must be taken which is capable first of estimating the water content of the wet sediment, and then correcting the XRF signal for this. Fortunately, all energy dispersive XRF spectra contain information that is strongly associated with the water content, offering the possibility that direct correction could be achieved. This information is contained in the part of the signal that arises from scattering of the primary x-rays rather than from fluorescence effects. Figure 3.8 shows the scattering of primary rhodium x-rays in two sediments with different water contents. Two different types of scattering can be seen Rayleigh (or coherent) scattering leaves the photon

energy unchanged, while Compton (or incoherent) scattering transfers some of the photon energy to electrons in the irradiated material, slightly lowering the energy of the photons. The amount and relative proportions of the different scattering mechanism varies with atomic number (Duvauchelle *et al.,* 1999); high water content (thus low mean atomic number) causes more scattering and favours the Compton mechanism. If sediment water content is the primary control over mean atomic mass, then the sediment water content may be estimated using this scattering ratio.

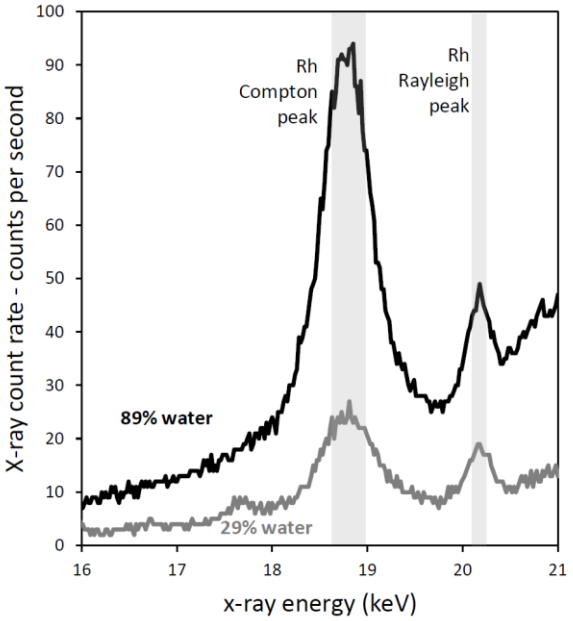

Figure 3-8 Scattering of primary rhodium x-rays as a function of sediment water content. The sediments are from the LOR3 core. The Rayleigh peak represents coherently (without loss of energy) scattered photons, while the Compton peaks represents incoherently (with partial energy loss) scattered photons. The wetter sample has a greater proportion of incoherent x-ray scattering.

Particle size also impacts the x-ray fluorescence signal (Finkelshtein & Brjansky, 2009). We neglect this effect for two reasons. First, range of the particle size variation in our lake sediment cores (as is typical for deep water cores) is sufficiently narrow that a large particle size effect of x-ray signal is not expected. At Lilla Öresjön a systematic particle size varies, with water content, between the late glacial sediment below 12.7 m (median size 10 μm) and the overlying early Holocene sediment (median size 34 μm). At Brotherswater, the modal size varies through the core alternating between 16 μm and 38 μm in response to palaeo-floods. These ranges are sufficient to cause changes in signal, but these are small compared with the effect of varying water content.

Furthermore, while the substantial water content effect can be readily corrected, as shown here, from information already collected (x-ray scattering), no equivalent method is available for the particle size effect.

In this paper we present a procedure for estimating dry mass concentrations for wet core sediment developed for the GEOTEK MSCL-XZ system driving an Olympus Delta XRF Analyser as a scanning μXRF, and we assess the implications of this for the analysis of lake sediments by comparison with parallel analysis of the sediments by conventional dry loose-powder measurements.

3.4.2 The Instruments

A Bruker S2 Ranger energy dispersive x-ray fluorescence analyser (ED-XRF) was used to measure the dry mass composition of sediment subsamples (freeze dried) from the scanned cores. This instrument has a Pd x-ray tube and Peltier-cooled silicon drift detector. The instrument was run at three different measurement conditions (20, 40 and 50 keV tube excitement) on loose powder under helium. Powder cups were prepared with spectroscopic grade 6 μm polypropylene film (Chemplex Cat. No. 425). Calibration used a set of up to 18 certified reference materials (Table 3.1). Mass attenuation correction used theoretical alphas, with organic matter concentrations estimated by LOI.

Table 3-3 Data for precision and accuracy of the S2 Ranger and Olympus DELTA XRF systems. The slope (certified/measured value) and root mean square difference (RMSD) indicate accuracy and precision. The number of certified reference materials used (N) and their mean and maximum concentrations are shown.

Element		Bruker S2 Ranger					Olympus DELTA				
		Measured v. Standards certified					Measured v. Standards certified				
		Slope	RMSD	Mean	Max	N	Slope	RMSD	Mean	Max	N
Al	mg g^{-1}	1.004	2.17	42.9	85.0	16	0.984	4.29	49.8	88.7	6
Si	mg g^{-1}	1.003	5.48	198.5	370.0	14	0.934	13.32	270.2	467.0	7
P	mg g^{-1}	0.963	0.05	1.1	4.1	11	Non-significant correlation				

S	mg g^{-1}	0.970	0.11	0.8	2.5	12	1.326	0.04	4.8	12.6	3
K	mg g^{-1}	1.049	0.91	20.1	43.0	12	1.128	0.98	15.6	33.8	7
Ca	mg g^{-1}	0.997	1.85	51.4	300.0	16	1.160	0.68	10.6	26.0	6
Ti	mg g^{-1}	0.994	0.16	2.9	5.6	17	1.002	0.16	3.1	7.0	6
Mn	mg g^{-1}	0.993	0.03	0.7	2.5	16	1.049	0.02	0.4	1.0	7
Fe	mg g^{-1}	0.961	1.26	21.5	93.8	14	0.925	0.59	25.0	39.4	7
Cu	µg g^{-1}	0.997	5.42	108.3	247.0	18	0.891	6.87	82.1	237.0	7
Zn	µg g^{-1}	0.988	3.43	72.8	373.0	15	0.861	3.54	88.3	251.0	6
Rb	µg g^{-1}	0.999	2.23	101.1	466.0	18	1.066	3.96	81.9	175.0	7
Sr	µg g^{-1}	0.993	10.30	275.7	790.0	17	1.022	11.27	151.0	239.0	6
Y	µg g^{-1}	0.990	0.98	16.8	62.0	14	0.939	0.37	12.8	33.0	4
Zr	µg g^{-1}	0.982	6.31	146.2	370.0	14	1.206	18.93	151.2	385.0	5
Pb	µg g^{-1}	0.995	2.56	65.0	698.0	14	0.975	3.66	96.3	500.0	8

The Geotek MSCL-XZ is a compact bench-top core-scanning system, located in the Central Teaching Laboratory of the University of Liverpool, that can conduct non-destructive measurements on split sediment core lengths (up to 1.55 m) obtaining multiple data sets simultaneously (XRF geochemistry, Colour photospectrometry, Magnetic Susceptibility and Line-scan high resolution imaging). The Olympus Delta is a handheld energy dispersive XRF Analyser fitted to the Geotek MSCL-XZ, which has a 4 watt rhodium x-ray tube (8-40 keV 5-200 µA excitement) and a thermoelectrically cooled large-area Si drift detector. The detector window is covered with a Mylar film. The XRF was run in 2 modes; the first, Soil mode, uses three beam conditions: 40 kV, 40 kV (filtered) and 15 kV each for 20 seconds to optimise beam conditions for materials where the elements of interest are relatively heavy, relatively dilute, and in a matrix of lighter elements. Elements are calibrated individually on a linear basis after spectra have been normalized to the Compton scattering peak to partially correct for mass attenuation effects. . For the second mode, MiningPlus, the spectrometer performs two measurements in succession: 40 kV and 15 kV beam conditions each for 20 seconds, and in a configuration suited to measuring the overall composition of the rock or

sediment. This mode uses a method of fundamental parameters, where the software assumes that certain elements are present in the sample and iteratively fits a model to the spectra. This approach is better suited to samples with high concentrations of the target elements (rock, or mineral-rich soil/sediment). The Olympus Delta completes a daily calibration check against a known standard (Alloy 316 Stainless Steel), and will not measure unless within tolerance. For both modes of operation local consistency checks have been made using a set of up to 8 certified reference materials (Table 3.1).

3.4.3 The Experiment

Two sediment cores have been investigated from lakes (Figure 3.9) that were selected to exemplify the two cases of 1) systematic variation in water content, and 2) relatively uniform water content (Figure 3.10; Table 3.4). The sediment at Lilla Öresjön, Sweden (In the boreal forest zone, Västra Götaland, core location 57.5514° N, 12.3166° E) is predominantly organic, but with an abrupt transition at the base of the Holocene from basal high-density glacial clays to low density wet organic gyttja (Figure 3.10). The sediment core LOR3 taken in August 2009 (Figure 3.9) samples the abyssal inflow-proximal sediments. A 1.5 m long, 70 mm diameter Russian corer was used. The core was tightly wrapped to prevent drying, and stored in darkness at 4 °C. The Brotherswater site (Cumbria, UK, 54.5066°N, -2.9249°E) was chosen for its more mineral-rich character and lack of systematic variation in water content (Figure 3.10). The core drive BW12-9A (1.35 m total length) was extracted in October 2012 from the flat bottomed central basin using 1.5 m long, 70 mm diameter Russian corer.

The wet cores were scanned using the Olympus Delta instrument using the two measurement modes described above. The Mining Plus mode was used for Al, Si, P, and Ca; the Soil mode was used for the other elements. For both modes the instrument

Figure 3-9 Location of the study sites.

Table 3-4 Lake and catchment physical parameters

Parameter	**Lilla Öresjön**	**Brotherswater**
Catchment area (km^2)	4.55	13.01
Lake area (km^2)	0.67	0.18
Max water depth (m)	17	16
Mean water depth (m)	4	7.4
Catchment – lake area ratio	7:1	72:1

automatically converts x-ray signals to elemental concentrations using factory-set calibrations. Split core lengths (up to 1.55 m length) were cleaned and covered with spectroscopic grade 6 µm polypropylene film (Chemplex Cat. No. 425) with measurements conducted at 5 mm intervals. Subsets of samples at intervals of 100 mm for Lilla Öresjön and 50 mm for Brotherswater were freeze dried, further oven dried at 50° C to ensure constant dryness, and measured using the Bruker S2 Ranger under the

conditions described above. Samples were weighed before and after drying to measure the water content of the sediment.

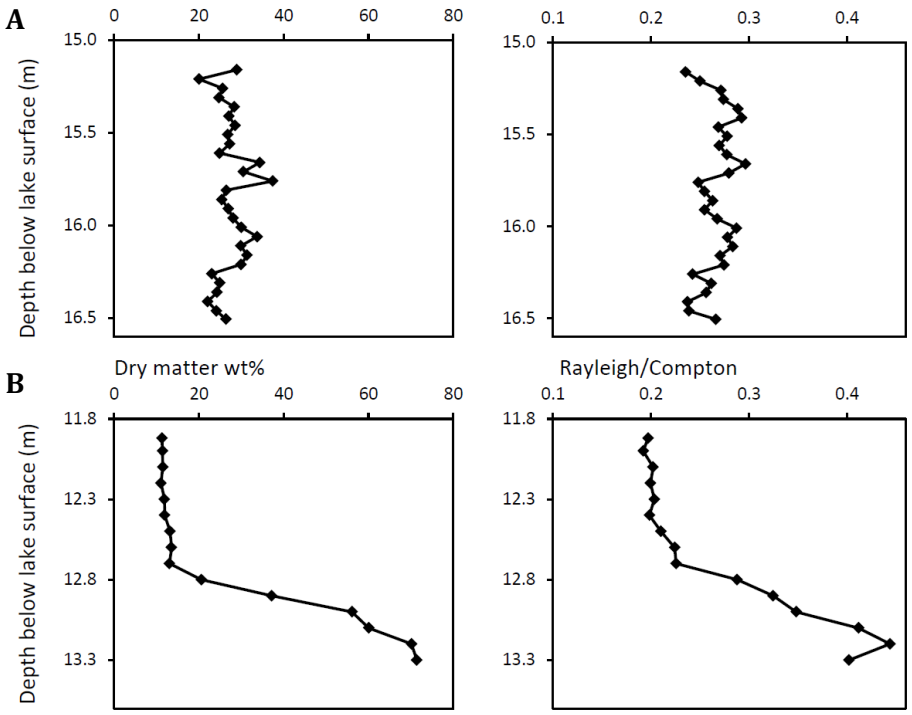

Figure 3-10 Dry matter content (wt %) for the subsamples, and coherent/incoherent backscatter ratio (Olympus DELTA scanning XRF) for the corresponding core interval for A) Brotherswater and B) Lilla Öresjön.

A series of tests were applied to the data collected.

1. Comparison of GEOTEK/Olympus DELTA XRF system wet core scanned concentrations with those measured on dried subsamples using the Bruker S2 Ranger XRF. The scanned data are compared both with 1) dry mass concentrations, and b) calculated wet mass concentrations (C_{wet}, based on the measured percentage water content, W, of the sediment and S2 Ranger dry mass concentrations, C_{dry}, using equation 1).

$$C_{wet} = C_{dry} \times \frac{100}{(100 - W)} \qquad \textbf{(Equation 1)}$$

These comparisons serve to test a) whether μXRF scanning yields usually accurate wet concentration data, and b) whether simple regression methods can be used to convert wet to dry mass concentrations.

2. Comparison of the ratio of coherent to incoherent x-ray scattering (coherent/incoherent) for the main tube line (Rh kα) of the Olympus DELTA XRF with a) water content and b) mean atomic mass.
3. Recalculation of the scanned XRF data on a dry mass basis by a) direct simple regression using the coefficients from test 1, and b) calculation using the water content estimate of test 2. This is achieved using equation 1 in reverse.
4. A brief assessment of the geochemical interpretation of a) uncorrected wet sediment concentrations, b) dry concentrations determined by simple regression, and c) dry concentrations determined from back-scatter estimated water contents, for two different sediment cores.

3.4.4 Results

3.4.4.1 Correlation of GEOTEK/Olympus DELTA scanned XRF data with subsample dry and wet mass concentrations

Figure 3.11 compares the measured concentration values obtained using the Olympus DELTA XRF and the Bruker S2 Ranger for the Lilla Öresjön LOR3 core. The S2 data were measured on subsamples; the Olympus DELTA XRF data used for the comparison is the mean value of scan data for the depth corresponding to the subsample. For each element there are two graphs. The left hand graph is based on the measured S2 Ranger value for the dried subsample. The right hand graphs uses the same measurements but recalculated to a wet composition basis, making the S2 data more comparable with the Olympus DELTA XRF data. The wet and dry basis-comparisons yield very different results.

In the dry mass comparison, elements displayed highly variable responses. Si, Al, Sr, Ca, K, Rb and Zr yield strong positive relationships, all exponential in form except for Sr which showed a linear relationship. P showed a weaker but statistically significant relationship. Fe, Mn, Cu, and Zn showed generally positive but highly scattered relationships that were not statistically significant. Y and Pb showed an organised but non-linear relationship. S showed a negative relationship. In the wet mass comparison all elements showed positive straight-line relationships. All are statistically significant,

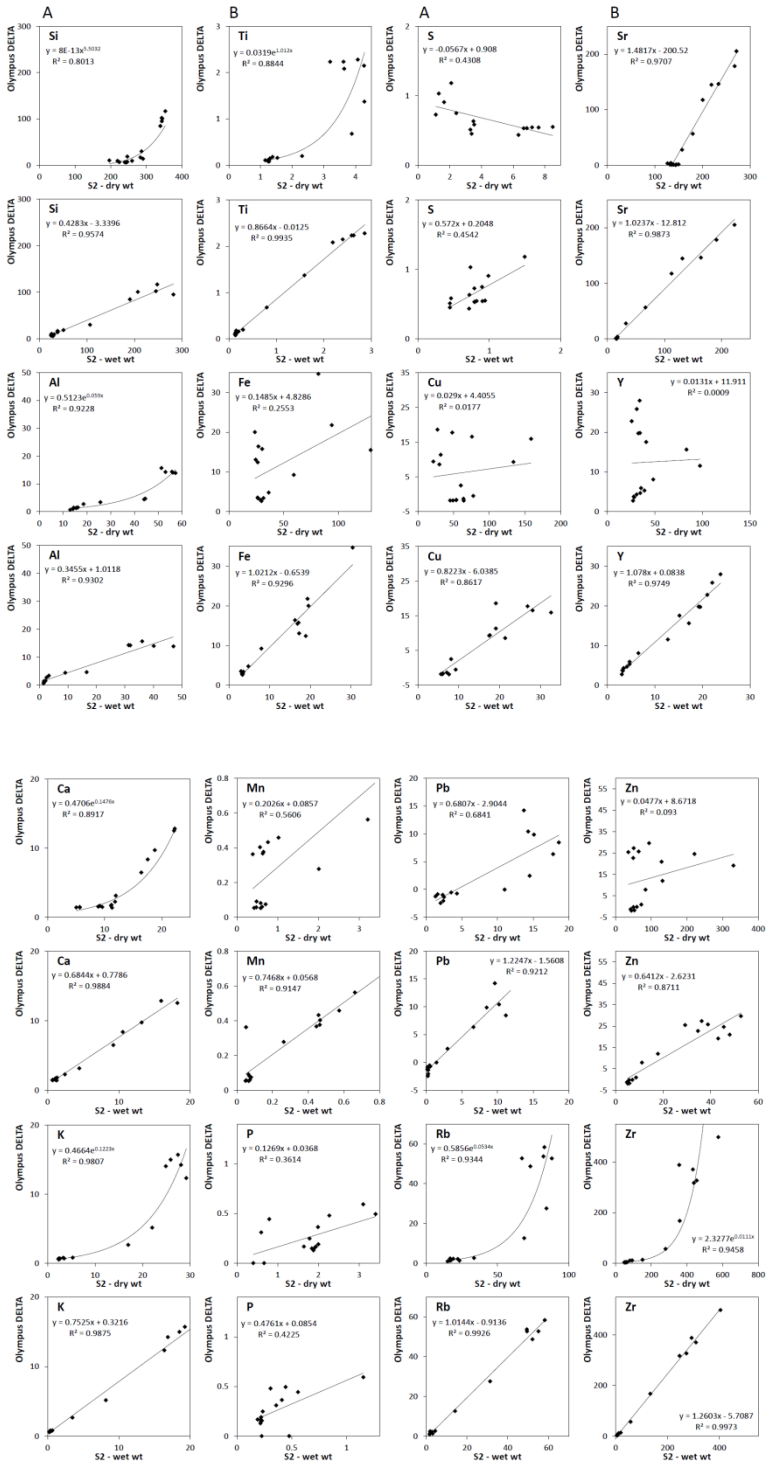

Figure 3-11 Correlations for the Lilla Öresjön core of element concentrations (ppm) measured by Olympus DELTA and by Bruker S2 Ranger. A) Wet core Olympus DELTA v. dry sample Bruker S2, and B) wet core Olympus DELTA v. wet concentration calculated from Bruker S2 dry sample measurements.

though for S and P this was weak. The lightest elements (Al, Si, P and S) all have low measured values by Olympus DELTA XRF relative to the S2 Ranger, with slopes ranging 0.3 to 0.5. Most other elements yield slopes between 0.8 and 1.25, and have coefficients of variation (R) greater than 0.9. The heaviest elements (Rb, Sr, Y and Zr) have coefficients of variation close to 0.99.

The data for Brotherswater (Figure 3.12) show some similarities with the results for LOR3, but with less striking differences between the wet and dry mass results. For most elements a stronger correlation is seen with the wet mass S2 data than for dry. However, none of the correlations are as good as for the LOR3 core. For Pb a similar degree of correlation was found for both, while for K the dry mass correlation was the better of the two.

The better fit between the scanned XRF data with the calculated wet concentrations is directly analogous to the finding of Tjallingii *et al.,* (2007) who performed a similar experiment in reverse, comparing dry scanned data with conventional XRF data on dry material. This shows that better results are obtained when concentrations are expressed in terms of the same matrix type (wet or dry).

3.4.4.2 Sediment core water content and x-ray back-scattering

The data in Figure 3.10 show a clear positive association between the ratio of coherent to incoherent back-scattering and the sediment dry mass concentration (wt%). Figure 3.13 shows the correlation between the dry matter concentration and the back-scatter ratio, revealing a coefficient of variation is 0.89. A linear regression line generated for the combined data sets passes through the points for both cores showing a strong similarity in the dependence of x-ray scattering on water content for these two rather different sediments. The slightly better relationship seen with mean atomic mass, as conforms with theory, shows that variations in mineral matter composition and organic matter content (which are taken into account in calculating the mean atomic mass) only marginally improves prediction of scattering properties. This shows that variation in water content is the main factor driving variations in mean atomic mass. This in turn allows the measured x-ray back-scattering to be used to estimate the water content of the sediment core material.

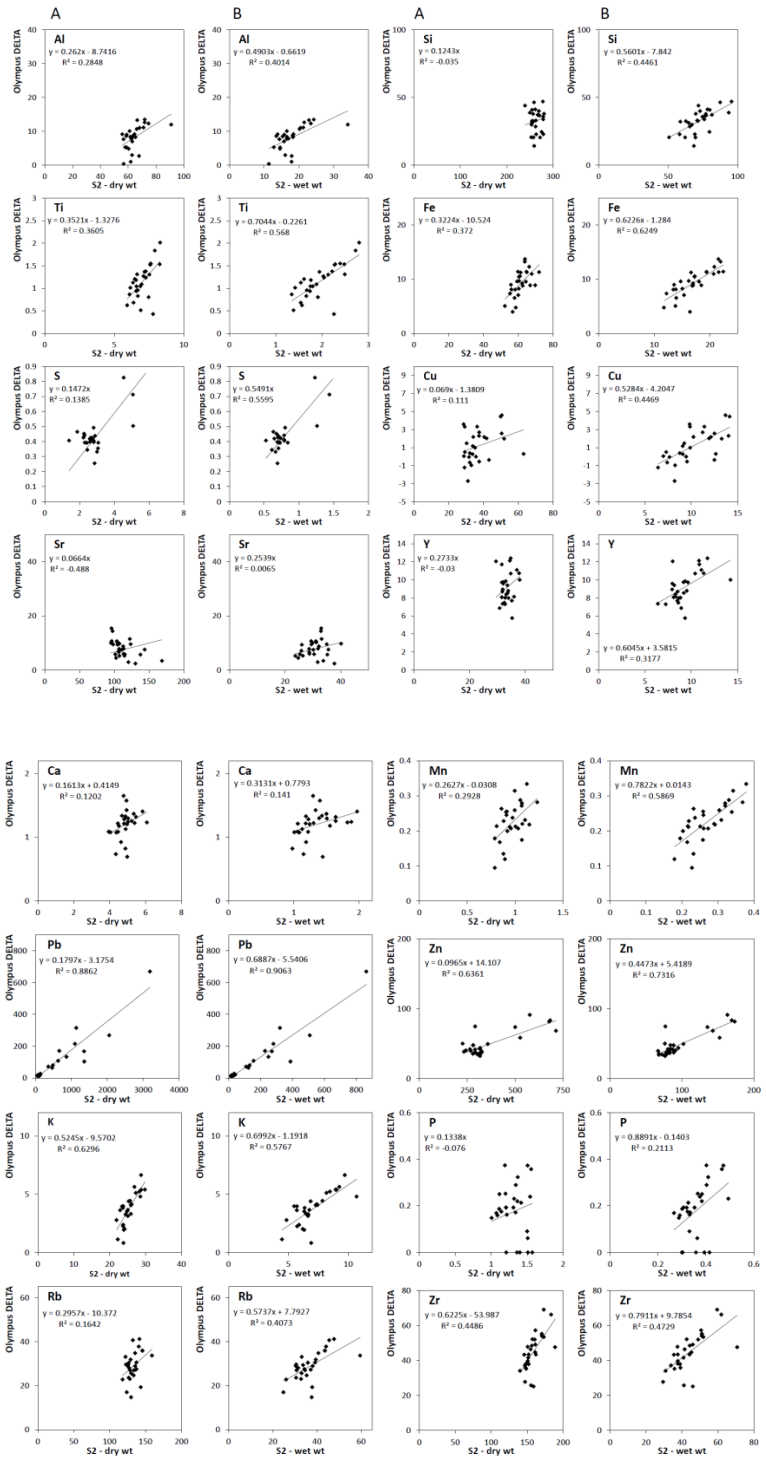

Figure 3-12 Correlations for the Brotherswater core of element concentrations (ppm) measured by Olympus DELTA and by Bruker S2 Ranger. A) Wet core Olympus DELTA v. dry sample Bruker S2, and B) wet core Olympus DELTA v. wet concentration calculated from Bruker S2 dry sample measurements.

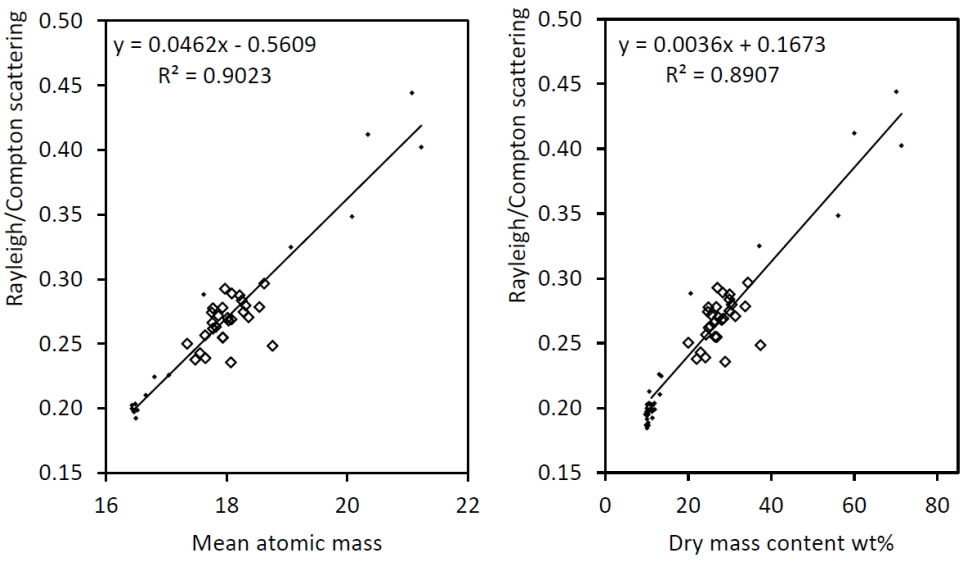

Figure 3-13 Relationship between measured subsample water content and the corresponding DELTA x-ray back-scatter ratios for Lilla Öresjön (points) and Brotherswater (diamonds). The regression coefficients are used to generate high resolution water content estimates for the scanned cores using the measured x-ray back-scatter peaks.

3.4.4.3 Conversion of GEOTEK/Olympus DELTA XRF scanned data to dry mass basis

Figures 3.14 and 3.15 show, for the LOR3 and BW cores respectively, the dry mass concentration estimates for the two procedures, and compare these with both the uncorrected data and sub-sample dry mass concentration values.

The simple regression correction has been applied using the coefficients (b_0 and b_1) shown on Figures 3.11 and 3.12 according to equation 2.

$$C_{dry,GEOTEK} = \frac{(C_{wet,GEOTEK} - b_0)}{b_1} \qquad \textbf{(Equation 2)}$$

The water content correction was applied by combining equations 3, 4 and 5, where the regression coefficients (b_0 and b_1) were taken from the wet-wet comparison on Figs 4 and 5 .

$$C_{dry,GEOTEK} = C_{wet,GEOTEK,corrected}\frac{(100)}{(100 - W)} \quad \textbf{(Equation 3)}$$

$$C_{wet,GEOTEK,corrected} = \frac{(C_{wet,GEOTEK} - b_0)}{b_1} \quad \textbf{(Equation 4)}$$

$$W = \frac{\left(\left(coherent/_{incoherent}\right) - 0.167\right)}{0.0036} \quad \textbf{(Equation 5)}$$

At Lilla Öresjön (Figure 3.14) it can be seen that correction to dry mass basis brings the GEOTEK data in line with the subsample measurements, the uncorrected data having very much lower values. For the corrected values the elements may be divided into three classes. 1) Al and Zr show essentially identical patterns but with the simple regression (Eq. 2) yielding the best agreement with the subsample measurements, and very much the least noise. 2) For Si, Ca, K, Ti, Mn, P, S, Rb and Sr the two methods show similar degrees of agreement with the subsample data, though with clearly poorer capture of underlying trends for the simple regression method but rather lower noise. 3) For Fe, Cu, Pb, Y and Zn the simple regression method could not be used owing to lack of correlation, but the water content correction method works well. In this last case there is a very great difference between the uncorrected (wet) and corrected (dry) sediment concentrations.

Membership within these three classes is associated with the relationship between the element concentration profile and the water content (Figure 3.10). Where an element correlates well with the sediment water content, positively or negatively (class 1), the simple regression method (Eq. 2) works well. Where these two are uncorrelated (class 3), the relationship between wet and dry mass concentrations is weak or non-existent, and the simple regression method is inapplicable.

At Brotherswater (Figure 3.15) the two methods yield a similar degree of fit with the subsample dry concentration values. They differ in the level of noise, which is far lower for the simple regression method.

For geochemical interpretation the two cores lead to different conclusions. At Brotherswater, the pattern of variation is similar for all three forms of the scanned data

(uncorrected, and both corrected data sets). Except for considerations of magnitude (absolute dry mass concentration), the correction have no impact on the geochemical

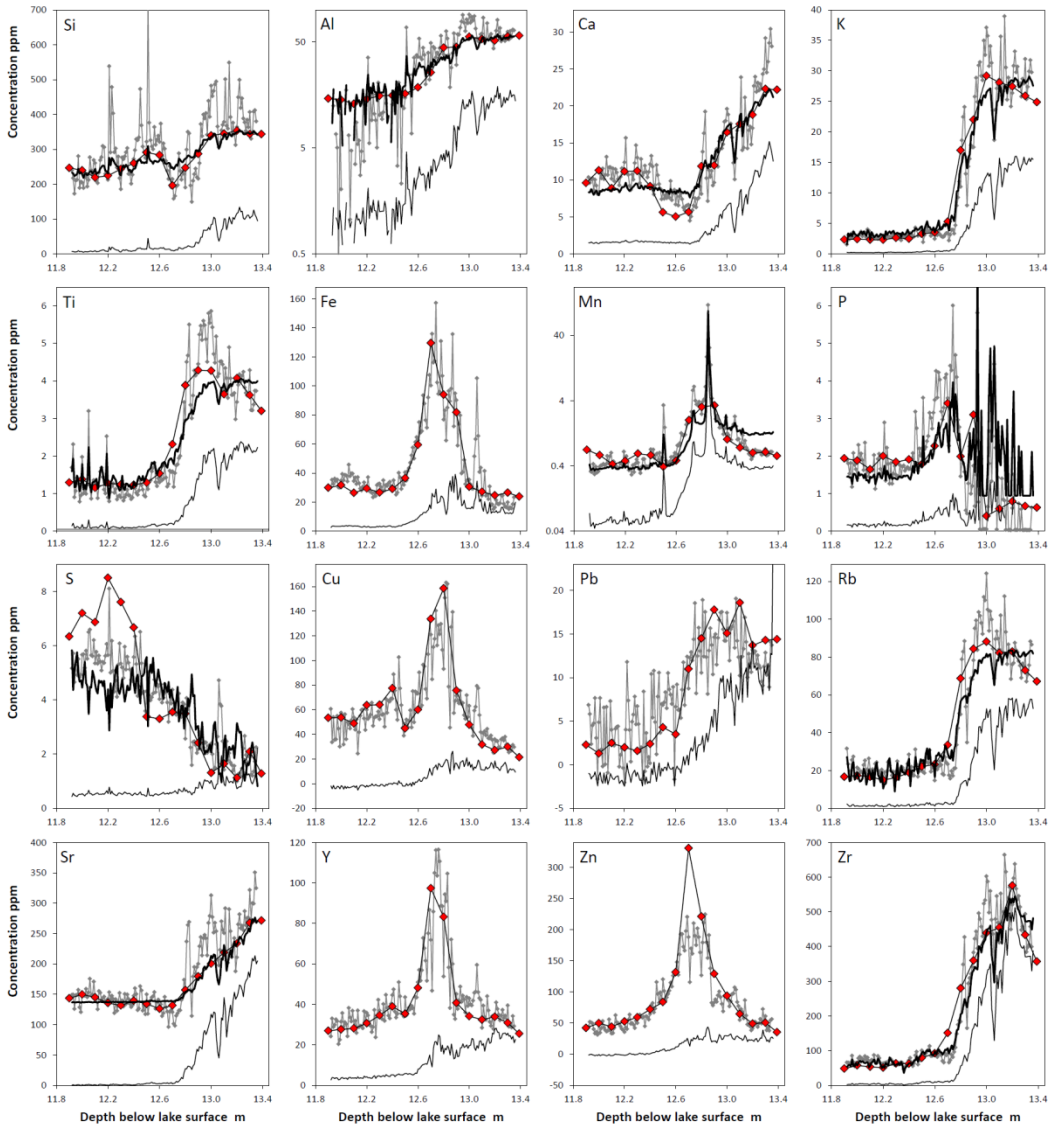

Figure 3-14 Lilla Öresjön element concentration data. Red symbols are S2 Ranger subsample data, accurate but low resolution dry mass concentration values. Thin black line represents- Olympus DELTA uncorrected data. Thick black line reflects Olympus DELTA corrected by regression on dry S2 data (only shown for cases that showed statistically significant correlations). Grey line GEOTEK corrected using water contents inferred from back-scatter x-ray data.

interpretation. However, at Lilla Öresjön the situation is very different. The uncorrected and regression-corrected data both fail to show the trends of variation

through the late glacial, and both fail to detect the enrichment in Fe, Cu, Zn, P and Y during the earliest Holocene, and thus fail to show a signal of substantial

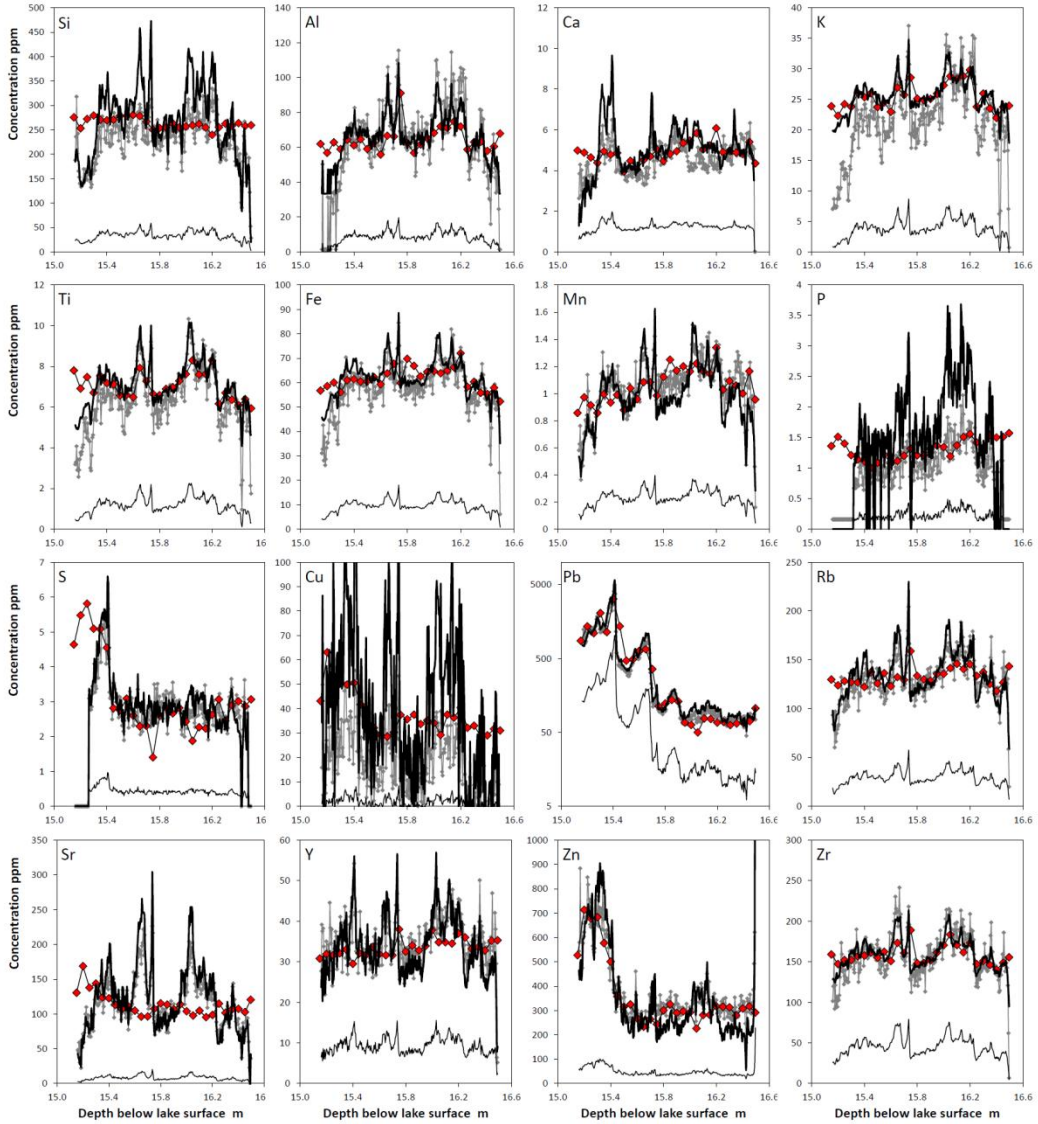

Figure 3-15 Brotherswater element concentration data. Red symbols are S2 Ranger subsample data, accurate but low resolution dry mass concentration values. Thin black line represents Olympus DELTA uncorrected data. Thick black line reflects Olympus DELTA corrected by regression on dry S2 data (only shown for cases that showed statistically significant correlations). Grey line GEOTEK corrected using water contents inferred from back-scatter x-ray data.

environmental significance (Boyle *et al.,* 2013). Thus the successful dry mass correction obtained using the x-ray back-scatter water content estimate profoundly improves the geochemical interpretation.

3.4.5 Discussion

The results from Lilla Öresjön (Figure 3.14) show that where the correlation between wet core XRF and dry sediment XRF concentration is poor (illustrated on Figure 3.11), then a) failure to correct for water content will lead to highly distorted depth-concentration profiles, and b) that water content estimation from x-ray back-scattering provides a useful degree of correction. A similar finding can be expected in any case where substantial systematic shifts in water contents are found through a core. We may also expect a comparable benefit from applying such a correction where large non-systematic shifts in water content are found; erratic signals resulting from erratic variation in water content will be reduced. However, this procedure comes at a price; the back-scatter signal is relatively noisy such that considerable noise is added to an element concentration profile through application of the method (Eq. 3-5). Thus for any particular case, both methods should be applied. Where both reveal a similar underlying data structure, the lower noise of the direct simple regression gives it a distinct advantage. This case is well illustrated at Brotherswater (Figure 3.15). There, it is apparent that both correction methods reveal patterns that are rather different from the subsampled dry mass data, which likely relates to imperfections in the core surface, but it is clear that the less noisy direct correction (Eq. 2) is better than the back-scatter approach (Eq. 3 to 5).

The pros and cons of conversion to dry mass concentrations are also well illustrated by the two cores. The concentrations and Fe, Cu, Zn, P and Y in the mid-profile "spike" in LOR3 are exceptionally high by comparison with other lake sediments. Expressed as wet mass concentrations, element ratios or raw counts this phenomenon is much less clear. Of course, this alone could be achieved simply by measuring only the subsamples. However, it is also clear for LOR3 that considerable fine scale compositional structure would be missed by coarse subsampling. It is similar at Brotherswater; the wet concentrations reveal very high Pb enrichment, but it is the dry mass values that can be compared with other cores and neighboring sites.

To apply dry mass correction with confidence it is necessary to analyse subsamples, ideally measured for both water content and element composition. This provides both

a training set and a means of evaluating performance. There is some advantage to analyzing the subsample independently. However, our Olympus DELTA XRF produces sufficiently accurate dry mass concentration data that subsamples can be dried and presented loose-powder form (pressed into loose "pellets" in inverted XRF cups) for scanning, allowing it to be used to generate test or calibration data (Table 3.1).

The procedure we have developed for the GEOTEK system is equally applicable for other scanning XRF instruments. Even where these present results as x-ray count rather than concentration data, normalization to dry matter content estimated from x-ray scatter peaks (which can be readily extracted from the raw x-ray spectra files generated by each instrument) will correct for systematic variation in water content, and is an essential first step before recalculation of the x-ray count scans to dry mass concentration.

3.4.6 Conclusions

Proliferation in the use of scanning μXRF has seen significant research gains in terms of resolution of analysis and examining fine structure within sediment profiles. However reliance on elemental ratios in interpretation of count or concentration data loses important information on the dry mass concentration of elements, sometimes negating correlation between and within sites. Correction of scanned data to a 'quantitative' dry mass equivalent form offers potential benefits for the understanding of elemental concentrations and fluxes. Our analysis of the two cores reveals that x-ray back-scatter correction for water content can be usefully applied to convert Olympus DELTA XRF wet concentration data to a dry mass basis where large variations, in this case around 50%, in water content are present. Although the correction procedure introduces noise at finer resolution, there is a very great improved accuracy in relation to the underlying trends. Where water contents are less variable (less than 10%), simple regression of wet and dry sediment element mass concentrations is likely the best approach.

3.5 An inter-comparison of μXRF scanning analytical methods

Abstract

The acquisition of high-resolution geochemical data from wet sediment cores through μXRF scanning is an increasingly important analytical tool. A number of μXRF core scanners are in use today that measure elemental concentrations using slightly different methods and several correction methods have been proposed in order to generate more precise and quantitative geochemical data. However, no inter-device comparison has been undertaken to date; this chapter is thus a first attempt. The results are based on a sediment core 1.44 m in length extracted from Loch of the Lowes, Southern Uplands of Scotland, and analysed using a Geotek XZ MSCL carrying an Olympus Delta XRF (University of Liverpool) and an ITRAX core scanner (National Oceanography Centre – Southampton). The core is strongly laminated but layers are not consistent in terms of thickness or frequency, thus it provides a good test of the comparative analytical resolution of the devices. The cores were measured at 5 mm and 1 mm intervals using the Geotek scanner and steps of 0.3 mm on the ITRAX instrument. Seven elements were selected for this inter-comparison: the Geotek 5 mm measurements of Ti, Zr, K and Rb concentration picked up all phases of enhanced mineral supply to the lake as characterised by light-coloured sediments. The finer detail (mm-scale laminations) was more effectively captured by the Geotek 1 mm and ITRAX scans, however Zr, Sr and Rb measured on the ITRAX were significantly more spikey or noisy in character; in particular, peaks and troughs in ITRAX count rate of similar amplitude to the light/dark layers also appeared across intervals with no visible stratigraphic variability. The Geotek less effectively discriminated thin layers within a sediment matrix of geochemically-different lithology. The decision as to which scanner to use thus depends on the research question being asked: if abrupt sedimentological or climatic transitions are not under investigation, more rapid 5 mm Geotek runs are likely to be sufficient to capture clear signals of palaeoenvironmental change. The regression correction method proposed by Boyle *et al.,* (in press; Chapter 3.3) was tested and consistent dry-mass equivalent concentrations were found for both techniques despite variable statistical relationships. We thus recommend future research presents μXRF data in terms of dry-mass concentration to facilitate more effective method and field site inter-comparison. A final instrument comparability test

was performed by measuring a short laminated sandstone section and a homogenous obsidian piece on the ITRAX, the Geotek and an Eagle III core scanner. The Ti profiles through the laminated sandstone output from the three instruments showed some differences: clear peaks and troughs in the ITRAX measurements effectively tracked the alternating light and dark layers while the Geotek returned a more smoothed signal. Interestingly, the Eagle III data exhibit several Ti peaks that do not fully correspond to layer thickness. For the obsidian piece, the signal-to-noise ratio was good in all cases but the relative major element composition varied between devices, possibly due to different instrument configurations' keeping this firmly in mind when comparing geochemical data thus seems critical.

3.5.1 Introduction

X-ray fluorescence (XRF) is a well-established geoscientific technique (Boyle, 2001b) used to characterise the chemical composition of rocks or soft sediments traditionally measuring dried materials presented as powders or pressed pellets. The proliferation of μXRF core scanning devices has seen the approach become the optimal preliminary and in many cases the primary tool for analysing wet sediment cores extracted from fluvial, lacustrine or marine settings. The ability to examine the chemical composition of sediments rapidly, at extremely high resolutions (e.g., Croudace *et al.,* 2006) and in a non-destructive manner are the primary reasons for the increasing popularity of core scanning. This popularity has been gained notwithstanding that approaches using wet sediment lack the ability to routinely produce accurate quantitative elemental concentrations, though correlation and data processing by comparison to parallel to dry and mass specific measurements improve this aspect (Chapter 3.3). Since the installation of the first core scanner in 1998 (Jansen *et al.,* 1998), several different manufacturers have produced commercial core scanners, and these include the Avaatech (Richter *et al.,* 2006; http://www.avaatech.com/), the ITRAX from Cox Analytical (Croudace *et al.,* 2006; http://coxsys.se/), the Eagle III BKA (Haschke, 2006) and the Geotek Multi-sensor core logger (http://www.geotek.co.uk/).

The speed of data acquisition offers an effective means for conducting exploratory analysis to rapidly obtain stratigraphic information from long cores. In the case of lake sediments, this could inform later field sampling and enable rapid stratigraphical correlation between cores across a basin. The μXRF resolution is of value, for example analysing annually-laminated sequences consisting of sub-laminations too thin to

manually sub-sample (Ojala *et al.,* 2012). μXRF also enables event-scale stratigraphic investigations to be undertaken, discriminating historical flood layers from the background sediment matrix at Lake Ammersee (Czymzik *et al.,* 2013) or Lake Suigetsu (Marshall *et al.,* 2012; Schlolaut *et al.,* 2014). μXRF data have also proved valuable for supporting sedimentological analysis of turbidite layers, such as deposits linked with the 1755 Lisbon earthquake (Cuven *et al.,* 2013). Longer term patterns of change in sediments are also revealed in μXRF data, such as Sr/Ca ratios reflecting increased salinity and the progressive drying of the Sahara through the Holocene in Lake Yoa (Chad) sediments (Francus *et al.,* 2013).

It is clear the rapid acquisition of geochemical data using μXRF core scanning techniques is a tremendous time-saving exercise provided data quality are maintained when compared to sub-samples measured individually on a dry-mass basis via conventional XRF. However, there are several potential impediments that may introduce artefacts into core scanning datasets, including surface irregularities along the core surface or gaps in the sediment sequence (Weltje & Tjallingii, 2008), non-homogenous mineral and grain size composition (Hennekam & de Lange, 2012) and variable down-core water and organic content (Boyle *et al.,* in press; Chapter 3.3). The μXRF platforms differ themselves in the mechanics of data acquisition and the format of data output. For example, hand-held XRF analysers such as the Olympus Delta XRF and Thermo-Niton XL3t output concentrations of various elements based on internal calibrations from raw X-ray spectra whereas raw data obtained using the ITRAX device are based on total counts per second. These methodological differences have the potential to introduce confusion and at worst erroneous interpretation, more so with direct comparison of results obtained from different platforms and where precise and/or accurate elemental concentrations are needed.

Here we present an assessment of the performance of two different core scanning platforms, the Geotek Multi-Sensor Core Logger (MSCL) carrying an Olympus Delta XRF and the ITRAX, with a calibration dataset obtained by conventional energy dispersive XRF (Bruker S2 Ranger), through analysis of a sediment core extracted from Loch of the Lowes, Southern Uplands of Scotland. We consider the analytical resolution of the devices, the trade-off that exists between higher-resolution but more time-consuming and costly scans, the similarities and differences that emerge across multiple elements and the impact of these issues in palaeoenvironmental research. We also assess the effectiveness of employing established dry-mass equivalent conversion techniques for

both devices and, finally, to assess µXRF inter-comparison on a dry, whole rock basis we ran two further samples, a heterogeneous laminated sandstone and a highly homogenous section of obsidian on three instruments: Geotek MSCL, ITRAX and an Eagle III core scanner.

3.5.2 The study site

Loch of the Lowes (Figure 3.16) lies in the headwaters of the River Tweed catchment in the Southern Uplands of Scotland. The lake (0.47 km^2) has a large upland catchment (area 27 km^2; maximum elevation 610 m; lake elevation 243 m; catchment to lake area ratio 57:1).

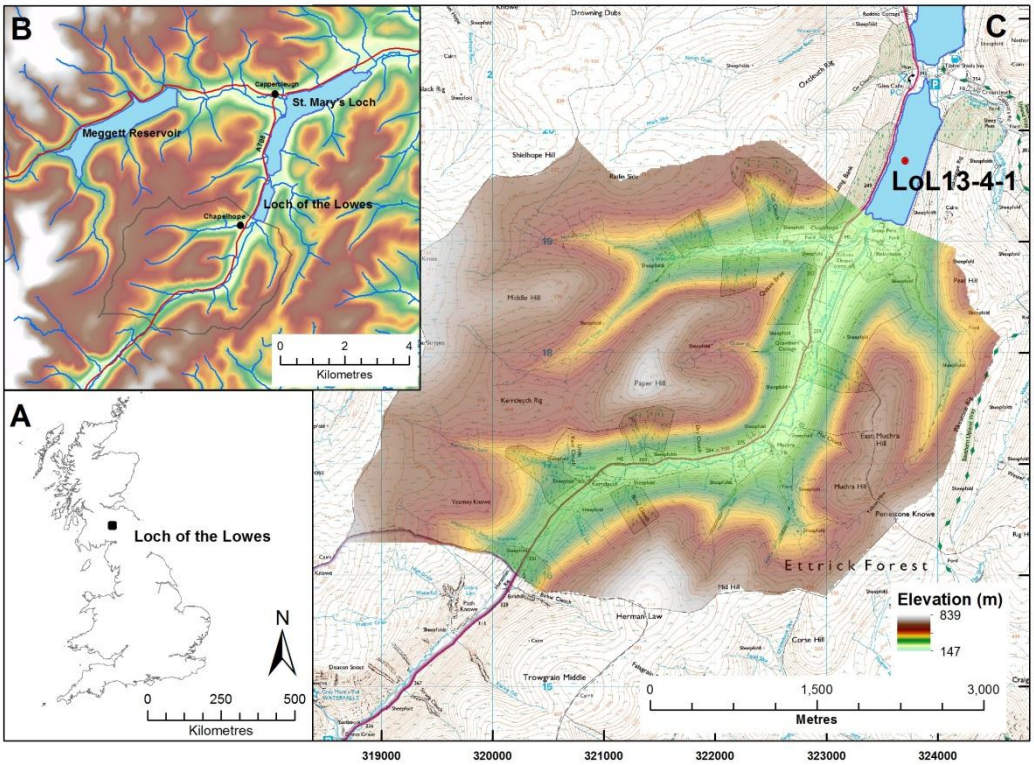

Figure 3-16 Location of the study site within the UK (a) and the adjacent St. Mary's Loch and Meggett Reservoir (b). Loch of the Lowes catchment elevation and position of the lake core (c).

The lake is oligotrophic and comprises a simple bathymetry dominated by a flat central plain at water depths 12–15 m(Murray & Pullar, 1910). Drainage enters the lake from five sub-catchments, three at the south shore (Little Yarrow, Chapelhope, Riskinhope) and two at the north (Crosscleugh, Oxcleugh) (Figure 3.16) (Foster *et al.,* 2008). Loch of the Lowes drains north into the adjacent St Mary's Loch via a small stream outflow.

Catchment bedrock geology is dominated by Lower Palaeozoic greywacke sand/silt/mud-stones, which have been sculpted by Quaternary glacial erosion into an upland terrain comprising U-shaped valleys and more rounded summits. Previous lake sediment investigations at the site (Foster *et al.,* 2008) using 1m Mackereth mini-cores identified flood-related indications in environmental magnetic and geochemical data that suggested an association with the North Atlantic Oscillation (NAO). Parallel investigations in the catchment (Foster *et al.,* 2008) show phases of extensive region-wide slope instability AD 700–900, 1100–1300 and after AD 1450–1550 and gully stabilization over the last 150 years. Loch of the Lowes thus meets many of the traits conducive to the effective recording of changes in catchment sediment flux in the profundal sediments, and flood stratigraphies in particular (Schillereff *et al.,* 2014), and thus offers a good test case for reconstructing high-resolution environmental change including flood laminations using μXRF scanning techniques.

3.5.3 Field and laboratory methods

The core data were obtained using the University of Liverpool Geotek Multi-Sensor Core Scanner (MSCL-XZ), a bench-top instrument capable of line-scan high-resolution imagery as well as simultaneous acquisition of XRF geochemistry, point magnetic susceptibility and visual light diffuse reflectance spectrometry (DRS) on split sediments cores (max length 1.53 m). The XRF measurements were undertaken using an Olympus Delta Energy-Dispersive XRF (ED-XRF) analyser fitted to a robotic arm. The XRF has a 4 watt rhodium x-ray tube (8-40 keV; 5-200 μA excitement) and a thermo-electrically cooled large-area silicon drift detector and the detector window is covered with a thin (6 μm) polypropylene film to avoid contamination of the internal measurement sensors. The Olympus Delta in 'Soil' mode applies three successive x-ray intensities (15, 40 and 40 (filtered) keV beam condition) and for 'Mining plus' two successive x-ray intensities (15 and 40 keV beam condition).

μXRF measurements on the same split core were carried out on the ITRAX system housed in the National Oceanography Centre (Southampton) using a step size of 300 μm and occupation time of 30 seconds. The ITRAX has a rectangular beam footprint of 20x0.2 mm focused through a flat-beam optical device (not a collimator) with the long axis perpendicular to the sample main axis thus 0.2 mm sampling resolutions are possible (Croudace *et al.,* 2006). ITRAX uses a 3 kW X-ray generator, with the current

system using a 3 kW molybdenum target tube that operated over a 30 kV and 30 mA range and a silicon drift detector.

To calibrate these μXRF scanning data to mass specific values a calibration training-set was subsampled from the core. Elemental analyses were performed on a dry-mass basis using the University of Liverpool Bruker S2 Ranger Energy-Dispersive XRF. This instrument has a palladium x-ray tube with a maximum current of 2000 μA, a Peltier-cooled silicon drift detector and it applies three successive x-ray intensities (20, 40 and 50 keV tube excitement) under a helium atmosphere to each sample. Samples were homogenised using a mortar and pestle and the powdered pellets were compressed into cups sealed with polypropylene film. A certified set of 18 calibration samples were measured (see Table 3.1) and concentrations were adjusted for organic matter content measured using thermogravimetry (Perkin Elmer STA6000), using the mass loss between 150° and 530°C in a nitrogen atmosphere.

A sediment core 1.38 m in length was extracted in April 2013 from the central basin of the lake in water depths of 13 m (core plots are expressed in metres below lake surface) using a Russian-type device with a diameter of 70 mm. The core was tightly wrapped to prevent drying, and stored in darkness at 4 °C at the University of Liverpool. The core were cleaned and photographed at 100 μm resolution after calibration to grey and white plates using the Line-scan camera fitted to the Geotek instrument. The core was covered with 5μm polypropylene film and measured at 5 mm intervals using the Olympus Delta device using factory defined Soil and MiningPlus modes as described above. The Mining Plus mode was used for Al, Si, P, and Ca; the Soil mode was used for the other elements. The core was then measured on the ITRAX core scanner (December 2013) at the National Oceanography Centre, Southampton. Finally, the core was re-measured on the Geotek/Olympus at 1 mm resolution (April 2014), increasing the time span between machine standardisation to 24 hours compared with 12 hour standardisation for the 5 mm interval runs. The calibration dataset was developed from sub-samples taken at 50 mm intervals from the core. These were weighed, freeze-dried and reweighed after drying to calculate moisture content and dry mass, and then measured as hand-pressed powders using the Bruker S2 Ranger. Dry masses were calculated assuming a mineral density of 2.65 g cm^{-3}.

3.5.4 Whole core data from μXRF scanning methods

The sediments largely comprise gyttja-type material, essentially a lightish-brown silty matrix that is heavily laminated throughout (Figure 3.17). The uppermost 65 cm in particular are characterised by very fine (often ≤1 mm thick) light (very light brown to grey) and dark (very dark brown to black) laminations, occasionally interspersed with thicker layers (≥ 5 mm thick). Light, thicker bands are more common through the lower portion of the core, although the black band at 14.34 – 14.36 cm is especially prominent. Organic matter concentrations are modest throughout (<10 %). The mean grain sizes lie predominantly in the fine to medium silt fraction (~8 - 20 μm) but display some variation in grain size between the lighter, finer-grained (~8-12 μm) layers and the coarser (~15-25 μm) dark units. For this whole core comparison, seven elements were selected: Ca, Fe, K, Rb, Sr, Ti and Zr. Their profiles (Figure 3.17) appear to divide into two groupings; Fe, K, Rb, Ti and Zr largely co-vary throughout and reflect variations of catchment-derived mineral in-wash. While the ITRAX data range for Fe and noise present in the Zr and Rb ITRAX datasets means the co-variance is somewhat less apparent for these elements, the major stratigraphic structures are identified in each of the ITRAX 0.3 mm and Geotek/Olympus 1 mm and 5 mm μXRF scans. In particular, well defined in all three scanning datasets are the elevated Ca and Sr concentrations above 13.40 m, a distinct band at 14.36 cm which corresponds with a thick black organic layer and a thick lighter sediment layer at 13.70 m that shows peaks in terrigenous elements (K, Sr, Ti and Zr).

In Figure 3.17, there are similar trends for all seven elements in both the 1 mm and 5 mm runs on the Geotek/Olympus. The 1 mm scans returned higher concentrations for Fe, K and Ti and slightly lower concentrations of Sr and Zr, in part this reflects the drying and reduced water content of the core over the nine month gap in measurement. These issues notwithstanding, most of the finer detail is captured at both resolutions. For example, five small peaks in Fe between 14.05 – 14.20 m are visible and the relative magnitude of the peaks is similar at both scanning resolutions. The Sr measurements at 1 mm resolution exhibit the most marked differences from the 5mm scans. For example, sub-cm scale fluctuations between 13.5-14 m are only visible in the 1 mm run superimposed on larger scale variations in Sr concentration. Zr exhibits similar characteristics in comparing 5 mm and 1 mm scans across this interval. Measurements made at 1 mm resolution return values that are averaged across the beam area (10 mm diameter), thus 5 mm intervals requires a 50% measurement

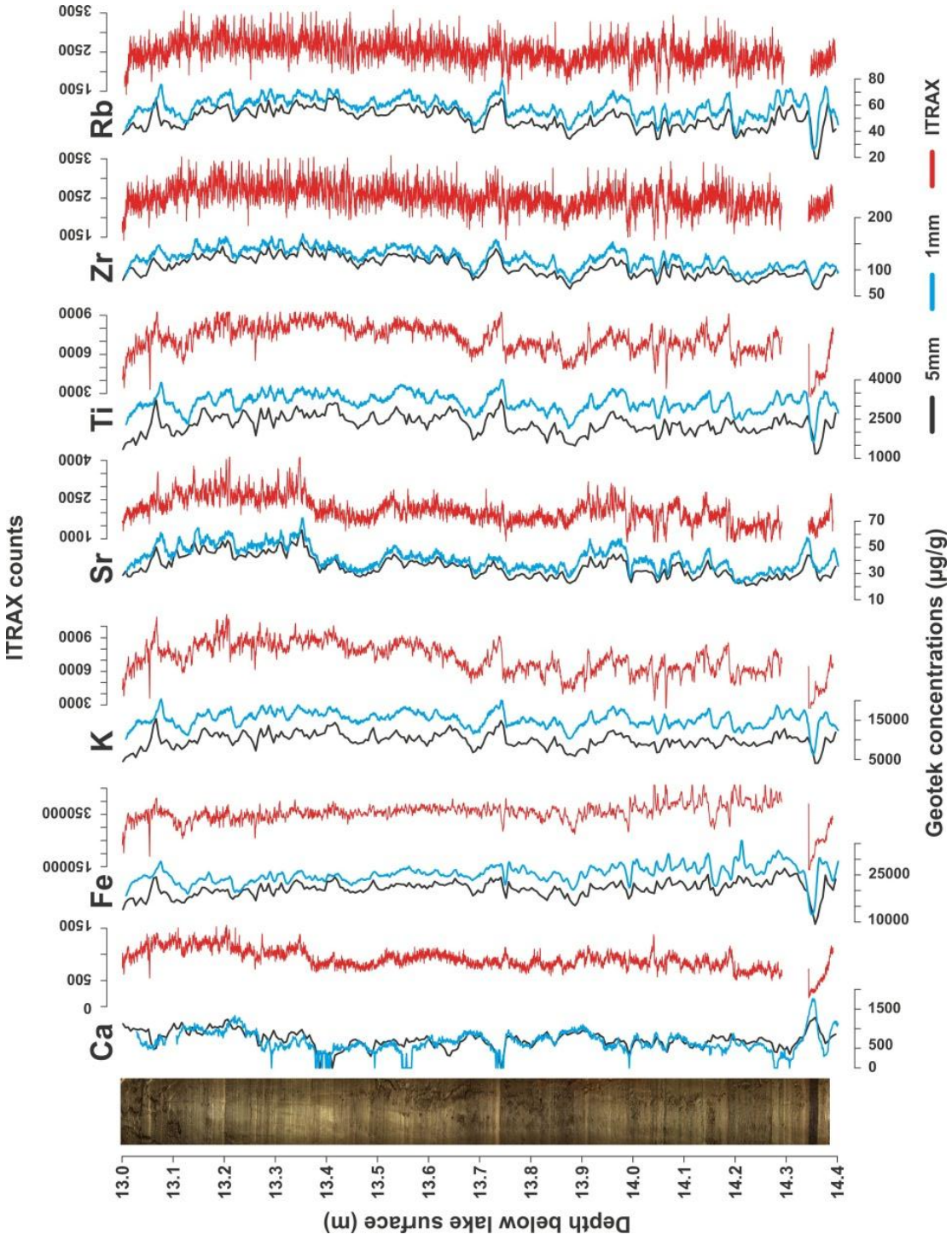

Figure 3-17 High-resolution photograph of core LoL13-4-1 obtained using the line-scan camera mounted on the Geotek platform and concentrations/counts for seven elements measured at 5 mm and 1 mm intervals on the Geotek and the ITRAX, respectively.

overlap and 1 mm a 90% measurement overlap. Fine resolution detail is captured with greater clarity for the heavier atomic mass elements e.g. Sr and Zr. For other elements the detail is smoothed within the measurement overlap. The Olympus Delta XRF range includes models with a beam collimator that focuses to a 3 mm diameter footprint, but signal is attenuated requiring longer count times. In summary, comparison of the full-core results shows benefits of operating the Geotek/Olympus at fine resolution, with ~1 mm runs for cores recovering finer detail evidence for environmental change, but it offers improved results for many elements (e.g., Zr, Sr, Ti, Rb).

Given the 300 μm resolution of the ITRAX scanning (Figure 3.17) it is not surprising that the geochemical profiles have an appearance that is more spikey or noisy in character. Initially (Figure 3.17) we have applied no smoothing to the whole core data which were collected as counts per second for defined element peaks, and broadly there is a strong correspondence with the Geotek/Olympus measurements. Sub-cm scale oscillations in Fe between 14.05-14.2 m are clearly defined in the ITRAX data (Figure 3.17) and mirrored in the Geotek/Olympus 1 mm output, but the relative magnitudes of the peaks vary between techniques. Perhaps this reflects the different machine configurations, particularly the 2x0.3 mm (ITRAX) and 10 mm diameter (Geotek/Olympus) beam footprints and the ITRAX output as x-ray count rather than ppm on the Olympus Delta XRF. In summary for the selected elements there is a strong correspondence between the ITRAX and Geotek/Olympus, but at a whole core scale there appears greater clarity in the Ti, K and Fe compared to Ca, Rb, Sr and Zr in the ITRAX data. However, it is not clear whether this reflects greater between-sample variability, a phenomenon not detected in the Geotek/Olympus 1mm scans, or simply greater analytical noise. Whether these issues persist when examined at fine resolution is explored in the following section using subsections of the core.

A final consideration is that with the more routine use of μXRF as a first stage to the analysis of core materials, researchers face an unfamiliar question as to whether they are presented with too much data. For fine resolution patterns across short core lengths this concern does not apply, but interpreting longer duration patterns of geochemistry for the Loch of the Lowes (Figure 3.17) data collected at lower analytical resolutions gives a clearer story (e.g. Zr and Sr) and given longer XRF count times is potentially more precise. Smoothing or aggregating the ITRAX data to 2-3 measurement intervals (600-900 μm) would increase the count times to 60-90 seconds and may enhance the signal.

3.5.5 Micro-structures revealed by μXRF of laminated lake sediments

The real strength and original motivation for μXRF lies in discerning detail of geochemistry at very fine resolutions. Here we have selected two short 10-26 cm length sections of the Loch of the Lowes core to exemplify this. The stratigraphy (Figure 3.18) between 13.2-13.46 m shows detrital flood laminations in the profundal sediments of the lake with numerous sub-cm laminations with lighter beige layers punctuating the accumulation of darker mineral and organic (<20%) gyttja. The 13.7-13.8 m section (Figure 3.19) shows ~5 cm of dark brown organic sediment with weak laminations giving way to 4.5 cm containing four sub-cm light laminations overlain by a further 2.5 cm of dark brown organic gyttja. The laminations mentioned occur throughout the core but not consistently and are unlikely to represent annual-laminations; more likely they reflect high magnitude river flows (floods) driven by either synoptic rainfall or snow-melt in this upland catchment. Figures 3.18 and 3.19 show high resolution photographs taken with the Geotek MSCL Linescan Camera (pixel resolution 100 μm) overlain by Zr, Ti and Rb concentrations (Olympus/Geotek) or counts (ITRAX). The elements selected are often used as proxies for the delivery of fine-grained soil derived materials (Rb and Ti) and coarser grained materials (Zr) in this region and type of lake (Boyle *et al.,* this volume; Schillereff *et al.,* 2014).

For the finely-laminated sediments 13.2-13.46 m there is a strong correspondence between the visible stratigraphy and variations in Ti detected in all three scans. Geotek/Olympus 5 mm scan has identified all phases with light-coloured laminations and these are also characterised by higher Ti concentrations. The data resolution cannot discern the structure within intervals containing multiple discrete sub-laminations (e.g. 13.41-13.43 m), but the light layers at 13.22, 13.28, 13.31, 13.35, 13.385, 13.40 and 13.41-13.43 m correspond with positive spikes in Ti concentration. This affirms the value of using low resolution scans, e.g. the 5 mm Geotek/Olympus data shown here, to rapidly (3-4 hours per 1.5 m) characterise sequences and in circumstances where the research objectives or chronological control do not require mm resolution, this level of analysis might be all that is required.

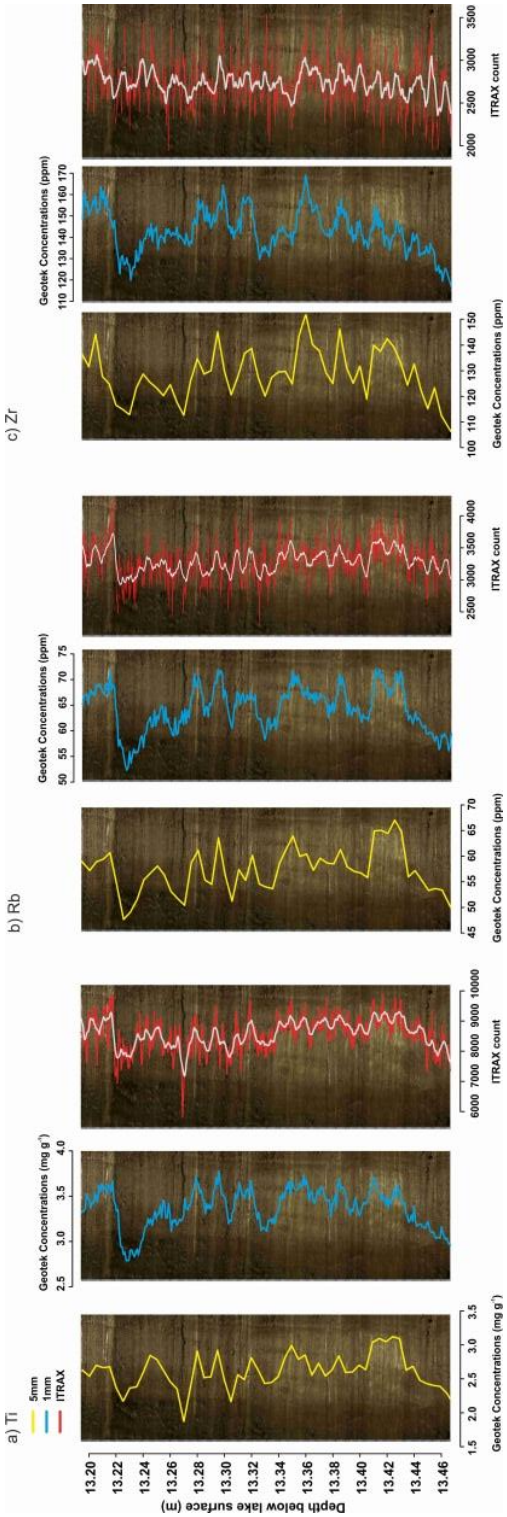

Figure 3-18 High-resolution line-scan image of a core section from 13.20 – 13.46 m depth overlain by a) Ti; b) Rb and c) Zr concentrations for the 5 mm (yellow) and 1 mm (blue) Geotek scans and the ITRAX count (red). The 15-point moving average is superimposed (light grey) on the ITRAX data.

The ITRAX and 1mm Geotek/Olympus scans both appear particularly powerful techniques for analysing heavily laminated sediments, with the Ti data exhibiting numerous peaks that correspond to the lighter layers. Our interpretation is that the Ti is being eroded as finer grained materials in catchment soils. The 1 mm Geotek/Olympus scans appear to have captured the majority of the light bands, although in the heavily-laminated section at 13.41 – 13.43 m depth, the ITRAX scan picks out four discrete laminations based on maximum Ti count rates while the 1 mm Geotek/Olympus curve only has three peaks. The ITRAX scan data appear more spiky or noisy when contrasted with the 1 mm Geotek/Olympus scans. These differences most likely reflect the configuration of the respective beams. The 1 mm Geotek/Olympus scans were collected by moving a circular 10mm diameter beam window at 1mm increments across the micro-laminated sediments. It is very encouraging the level of detail collected notwithstanding the inherent smoothing in this scanning process. The beam passed up the centre of the shown photograph and so the location of the beam matters, for example the peak in Ti at 13.40m corresponds with a lighter layer that is less clearly represented towards the edge of the core. Conversely a second lighter lamination ~4-5 mm below is clear towards the edge of the core but less so in the centre; the Geotek/Olympus scans fail to discern the second lamination probably lost in the smoothing. The ITRAX data were sampled from a 2x0.3 mm window that also moved across the centre of the core. It samples every aspect of the sediment structure and benefits from a lack of overlap in using a contiguous moving sampling window but is susceptible to discontinuous structure across the core segment. In addition a crack in the core at 13.27 m plots as a trough in Ti reflecting low count rate across the gap, whereas the Geotek/Olympus integrates data from a larger window and is less affected. Both datasets need careful checking for data integrity in the form of discontinuous layers and gaps or blemishes in the core surface.

Rb is also sourced from fine grained materials, probably clay minerals in soils, and shows a very strong correspondence between the photograph and the 1mm Geotek/Olympus scan data. All lighter layers correspond with peaks in Rb and dark layers troughs in Rb concentration. The resolution of the scan discerns almost all light coloured units, with the exception at 13.40 m where discontinuous laminations are not sampled or smoothed from the moving 10 mm diameter window. The ITRAX Rb data are intriguing, with the data smoothed to 1 mm showing a strong correspondence to the Geotek/Olympus 1 mm scans. The raw ITRAX data show a very spiky profile that

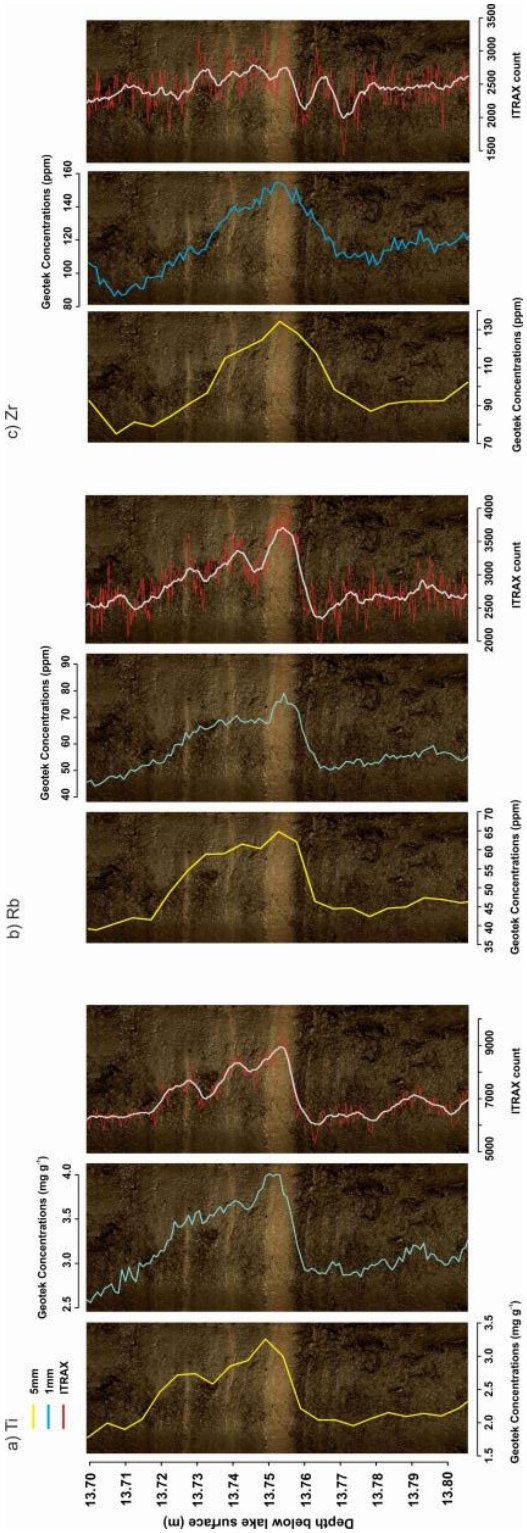

Figure 3-19 High-resolution line-scan image of a core section from 13.70-13.80 m depth overlain by a) Ti; b) Rb and c) Zr concentrations for the 5 mm (yellow) and 1 mm (blue) Geotek scans and ITRAX count (red). The 15-point moving average is superimposed (light grey) on the ITRAX data.

resembles noise. The improved agreement with the Geotek scans resulting from aggregating counts by smoothing suggests that there is structure within the noise of the ITRAX output. Zr reflects the flux of coarser grained materials to the lake, displays some similarities to the other elements (Rb and Ti), though some of the light layers, e.g. 13.33-13.35 m, do not correspond with peaks in Zr, most layers do. Comparison of the 1 mm Geotek/Olympus and ITRAX Zr profiles shows again a noisy raw ITRAX Zr profile that on smoothing better resembles the Geotek/Olympus. There are some notable discrepancies with pronounced shifts from dark to light sediment at 13.22, 13.32 and 13.39 m showing a less clear response in the ITRAX Zr profile.

The sub-section 13.70 – 13.80 m depth contains two thin, light bands as well as a major stratigraphic feature in the form of a 1.5 cm-thick light-brown unit overlying a 0.5 cm dark black unit (Figure 3.19). All methods show low values at the bottom of this sub-section, a sharp rise across the black band to maximum concentrations or counts in the light unit and then steadily declining upwards through the core. The slope of the steep rise is similar across all three datasets despite the different data acquisition resolutions. The most prominent feature in the ITRAX data not present in the Geotek/Olympus scans is the internal structure of the light unit. While peak values occurs in the middle of the unit in all plots, the ITRAX data shows a steep rise to the peak and a steadier decline, perhaps reflecting changes in grain size, Ti is often associated geochemically with the fine-grained fraction (Taboada *et al.,* 2006). The absence of a clear signal in the Geotek/Olympus data reflecting the two thin bands likely relates to the beam diameter not discriminating finer structure. The noisy character to the Rb and Zr ITRAX curves identified in Figure 3.18 repeats in Figure 3.19, smoothing the ITRAX data (in essence, extending the count time) produces a stronger match to the Geotek/Olympus data. There is also comparatively lower amplitude noise in the Ti data, visible in particular a dark brown unit below 13.76 m that lacks for laminated structures. Regular fluctuations in count rates for all elements have amplitudes in some cases equivalent to that characterising the thin laminations at 13.726 and 13.738 m. Fluctuations in the 5 mm and 1 mm Geotek/Olympus data are much more muted across this interval. These results suggest caution should be used when interpreting μXRF data from an ITRAX where supporting high-resolution stratigraphic data (photography, radiography or computerised tomography) are not available.

Published deep core records utilising ITRAX data often plot a running mean (e.g., white line: Figure 3.18 and 3.19) through the dataset to aid visual presentation of long-term datasets (e.g., Kylander *et al.,* 2013). Figure 3.20 compares the 5 mm Geotek data for Rb, Ti and Zr with the corresponding ITRAX counts smoothed using a 15-point running average to generate a dataset of equivalent analytical resolution. The 5 mm Geotek and smoothed ITRAX data show highly comparable patterning, most prominent stratigraphic features are identified and fluctuations are predominantly of a similar magnitude between all techniques. Four major troughs in Rb between 14.05 and 14.15 m featured in the ITRAX profile are not as prominent in the Geotek data. Thus we propose that where longer-term palaeoenvironmental changes are the primary research objective, lower resolution but substantially more rapid Geotek scans may be a more appropriate data acquisition approach.

3.5.6 Correcting µXRF scan data to mass specific values

The XRF geochemical data presented here could be for a variety of purposes, but for the most part interest lies in dry mass concentrations for a range of elements, with all expressed as the element concentration divided by the dry mass of sample. µXRF scanning of wet sediment does not operate in this manner, however, with elements typically (semi-)quantified as concentrations (including the ITRAX X-ray count per second), but these values are relative to the density of wet sediment. Boyle *et al.,* (this volume) proposed two correction methods, one of which is novel employing the relative intensities of x-ray backscatter emitted from the XRF instrument mounted on a Geotek/Olympus platform to estimate sediment water content the full-length of a scanned core. This procedure assumes the ratio between Rayleigh (or coherent) and Compton (incoherent) scattering processes varies primarily in response to water content. The ITRAX instrument also collects coherent and incoherent backscatter data. Here we have assessed the relationship between the Geotek/Olympus (1 and 5 mm) and ITRAX backscatter intensities for each of the scans and the general pattern of coherent/incoherent appears repeatable between the ITRAX and Geotek/Olympus. The actual water contents, estimated before and after freeze drying, are low (50-60%) and vary minimally; as the correction procedure works well for sediment sequences characterised by significant changes in water content (Boyle *et al.,* this volume), the second approach to correcting µXRF data advocated by the authors appears therefore more appropriate. This uses regression equations derived from µXRF element

concentrations and equivalent dry mass geochemical data collected for subsamples on a Bruker S2 Ranger ED-XRF (Figure 3.21).

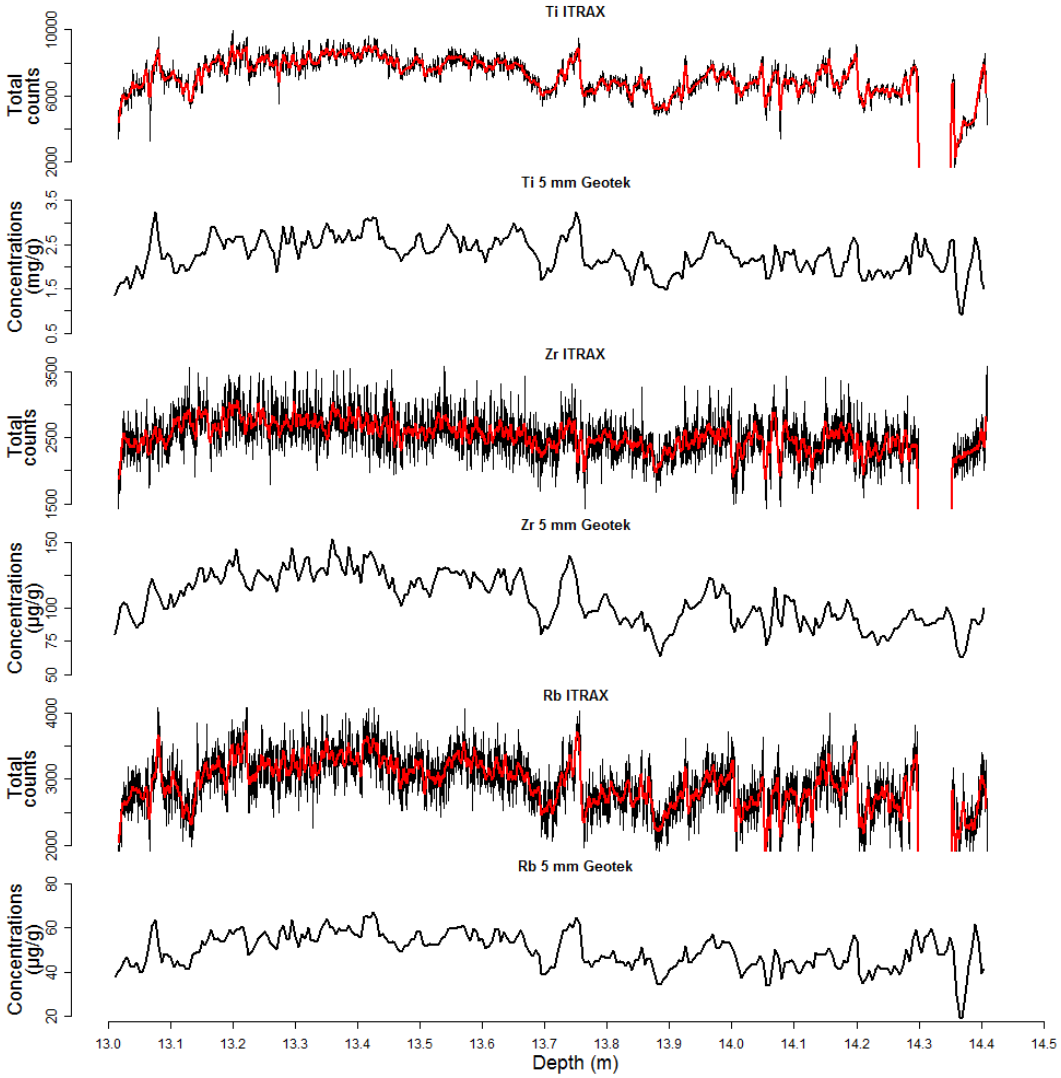

Figure 3-20 Count rate and concentrations(black lines) for core LoL13-4-1 measured on the ITRAX (top) at 0.3 mm and the Geotek (bottom) at 5 mm intervals for Ti, Zr and Rb. A 15-point running average has been applied to the ITRAX data (red line), plotting the data at a 5 mm equivalent analytical resolution.

Overall, six elements yield moderately positive relationships, although the responses are variable between element and instrument, and a relationship is absent for Rb. Overall, the Geotek/Olympus scans produce stronger correlations than the ITRAX device, except for Ca (R^2 = 0.53). K (R^2 = 0.757 for the Geotek/Olympus 5 mm) and Zr

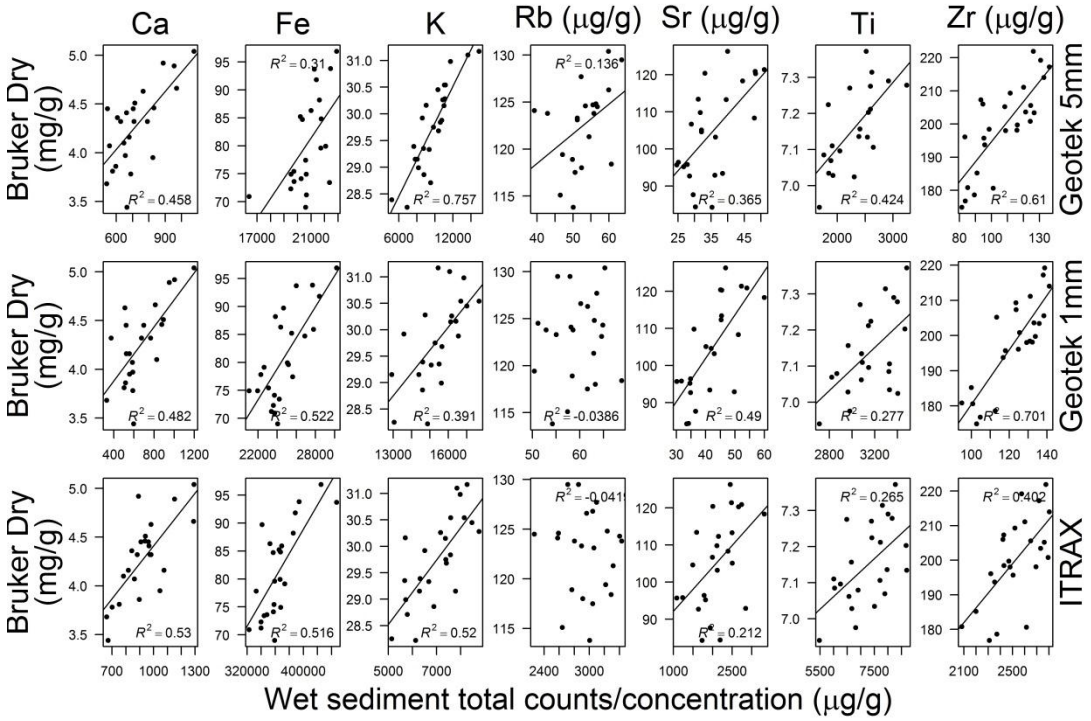

Figure 3-21 Scatter plots illustrating the linear relationships and regression coefficients between wet sediment concentrations measured by the Geotek scanner at 5 mm and 1 mm intervals, count rates emitted by the ITRAX instrument and dry-mass concentrations for 5 cm intervals measured on the Bruker S2 Ranger. *Y*-axis units are mg/g except Rb, Sr and Zr, which use μg/g as specified in heading.

(R^2 > 0.6 for 1 mm and 5 mm Geotek/Olympus) generally return the strongest correlations while the 5 mm Geotek/Olympus R^2 value for Ti significantly exceeds the other measurements. The fluctuating geochemical profiles visible in the ITRAX dataset throughout the core, not simply characterising the light and dark laminations, likely account for the observed weaker statistical relationships. Nevertheless, Figure 3.22 illustrates that the regression equations derived from these relationships are sufficiently strong to generate consistent dry-mass corrected concentrations for Ti and Zr. The variable ITRAX Zr curve is derived from the more noisy raw data (Figure 3.17). This is an encouraging finding as these calibrated concentrations are much more appropriate for comparison to other published μXRF data than attempting to infer similarities and differences between two datasets presented in counts per second, for example.

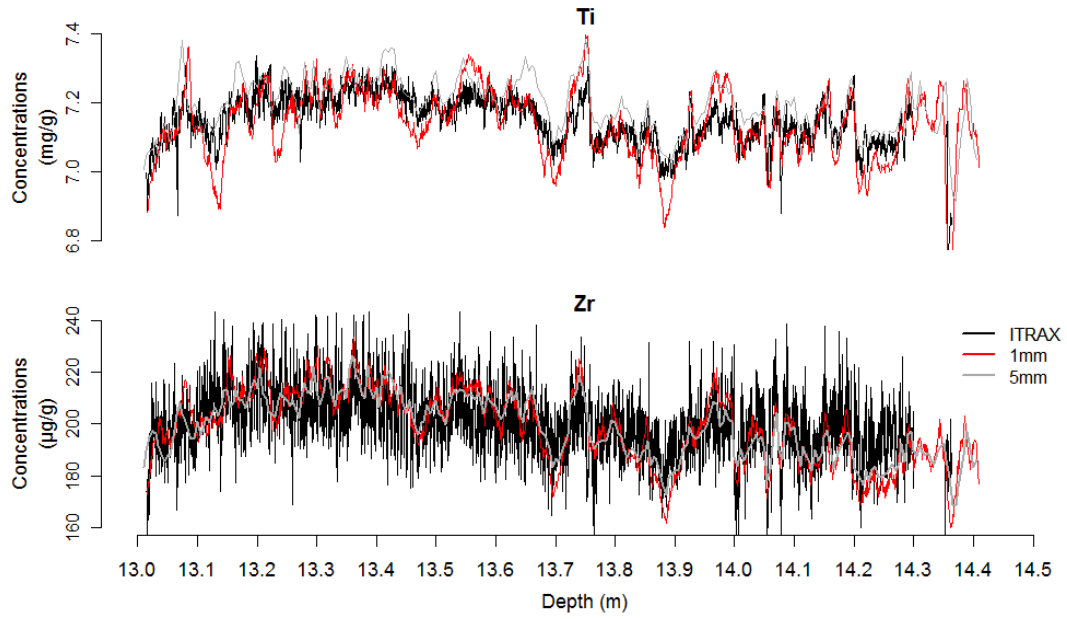

Figure 3-22 Profiles of Ti and Zr for core LoL13-4-1 using the three analytical methods and displaying concentrations (mg g-1 and µg g-1) that have been calibrated to dry-mass equivalent values using the regression correction method. The more variable Zr ITRAX values are derived from the noiser raw dataset.

3.5.7 µXRF inter-comparison for rock samples (laminated sandstone and obsidian)

To assess the comparative performance of three µXRF platforms without the complication of variable water and organic content we ran a short section of heavily laminated North Sea sandstone (57 mm length) and a piece of obsidian glass (52 mm length) on the ITRAX held at NOC-S, the Geotek/Olympus at Liverpool and an Eagle III core scanner (Haschke, 2006). The laminations visible within the sandstone (Figure 3.23) are generally 2 – 4 mm thick (occasionally < 1 mm). The dark layers are picked out well by peaks in Ti concentrations measured on the ITRAX and Eagle III, a function of their narrow step size (200 and 180 µm, respectively, compared to the 1 mm interval measurements on the Geotek/Olympus). As a result, the pattern of laminations is difficult to decipher from the Geotek/Olympus data, although the three thicker black layers at 12.4, 12.7 and 13.0 cm depth are represented by subtle peaks. Interestingly, the magnitude between the peaks and troughs is markedly different between the Eagle and ITRAX data and the Eagle III measurements do not appear to fully capture the variable thickness of the dark laminations, for example at 13.7 cm.

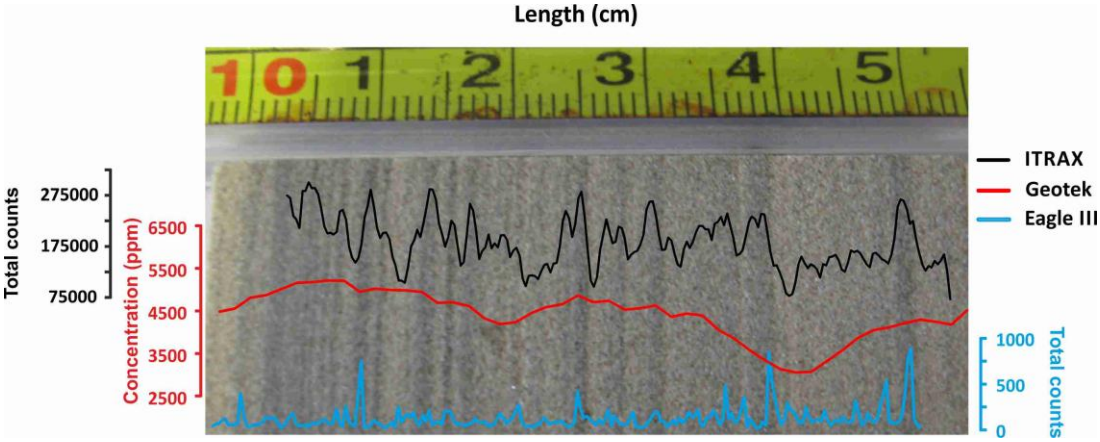

Figure 3-23 Photo of the laminated North Sea sandstone section overlain by Ti measurements from the ITRAX, Geotek and Eagle III core scanners.

A similar background trend in Ti content is observed between the ITRAX and Geotek/Olympus data, with lower values at 12 – 12.5 and 14 – 14.5 cm. However, while the majority of the dark laminations are represented by a Ti peak, lower resolution variability is absent in the Eagle III dataset. Instead, the discrete peaks rise from background values that rarely exceed 100 counts throughout the section. Whilst this is useful for recognizing the discrete laminations, any longer-term variability in sediment supply or changes in sediment provenance may be missed.

The obsidian is a useful quality control due to its largely homogenous composition and high Si content, as well as moderate values of other major elements (Table 3.3). The shard was also measured using WD-XRF enabling a quantitative comparison of the geochemical composition. While the Eagle III, ITRAX and Geotek/Olympus geochemical profiles are clearly analogous with minimal variability, differences emerge when the measurements are compared to the WD-XRF composition data. For example, mean Si content of the obsidian measured on the Eagle is 70.38%, close to the WD-XRF value (73.58%), and 71.3% on the Geotek/Olympus under MiningPlus mode (expressed as % with average light element (LE) content removed). Raw data from the Geotek/Olympus under MiningPlus mode are in ppm, but include a substantial contribution from LE (mean 57.73%); note SOIL mode does not help in this instance as neither Si nor Al is measured. Expressing each element as a percentage of the total non-LE composition (Table 3.3) produces values very similar to the Eagle III and a very close match to the WD-XRF measurements. The relative major element composition measured on the Eagle III and Geotek/Olympus data is equivalent to the WD-XRF data while the ITRAX

counts do not follow a similar pattern. It is important to keep in mind that the number of elements chosen to be measured by the operator can influence the data output. The signal-to-noise ratios assessed by comparing the standard deviations of the three scans are impressive, with comparative poorer performance from the Geotek/Olympus probably a function of fewer data points and lower scan resolution. For Si, the Geotek/Olympus σ was 1.93%, 0.6% on the Eagle and 0.99% on the ITRAX. For Fe, the Geotek/Olympus σ was 1.08%, 0.005% on the Eagle and 0.41% on the ITRAX.

Table 3-5 Major element composition for the 52 mm length piece of Obsidian glass measured on three different core scanning devices as well as via WD-XRF. The Geotek/Olympus values were obtained using the MiningPlus mode and converted from parts per million for display purposes. The final column are the converted concentrations of each element less the LE content of the sample (mean = 57.73%).

Element	WD-XRF (%)	ITRAX (counts)	Eagle III (%)	Geotek/Olympus (% of non-LE composition)
SiO_2	73.58	31734	70.38	71.30
Al_2O_3	11.61	1834	9.34	11.24
Fe_2O_3	3.57	1704780	7.76	6.22
K_2O	2.66	79283	5.97	5.94
CaO	1.64	72640	3.38	3.38
TiO_2	0.23	23761	0.46	0.40

Conclusions

The results from Loch of the Lowes show that, at this site, the geochemical composition of a wet sediment core is well estimated using both a Geotek/Olympus and an ITRAX core scanner. Most importantly, we show for the first time that μXRF data acquired using different instruments exhibit similar patterning, overall. One useful result is that the 5 mm scans performed using the Geotek/Olympus platform captured the vast majority of prominent stratigraphic features, despite its comparatively low analytical

resolution, as all phases of lighter, more mineral-rich laminations were characterised by higher concentrations of Ti, Rb and Zr (Figures 3.18 and 3.19). A key question we sought to address in this chapter is whether the finer resolution geochemical data offered insight into environmental changes missed by other techniques. Our results suggest the answer will depend on the research objectives of individual projects: 5 mm runs are sufficient to geochemically characterise most sedimentological shifts instead of plotting smoothed ITRAX data. Analysing annually-laminated sequences or identifying geochemical shifts across event layers will require finer resolution data acquisition, however, and the associated increased time and costs.

The diameter of the Geotek/Olympus laser aperture means some overlap between samples is inevitable. As a result, some fine laminations were not captured by the 1 mm runs, especially where they are located within a matrix of geochemically-different material. The ITRAX measurements (undertaken at 300 μm intervals) were able to distinguish these mm-/sub-mm scale light and dark bands, confirming its value when annually-laminated sequences, event deposits or tephra layers are being analysed. However, the ITRAX data also showed peaks and troughs with similar amplitudes to the laminated sections across intervals where no stratigraphic changes were visible (Figure 3.19). This may be a particular issue for long cores with no visible stratigraphic boundaries but highly fluctuating geochemical profiles. Our data also show that μXRF core scanning devices are sensitive to non-continuous laminations; operators should pay particular attention where discrete layers do not extend across the full core width.

The geochemical characterisation of sediments is often most effective when dry material is being measured. Our results are encouraging, indicating that despite the statistical relationships between the Geotek/Olympus or ITRAX measurements and the calibration dataset varying in strength (Figure 3.20), the dry-mass corrected values were very similar. We thus advocate that future published μXRF data is presented as concentrations calibrated to the dry sediment equivalent to facilitate more robust inter-comparison regardless of the method employed.

Finally, the μXRF scanning for whole rock samples (sandstone and obsidian) show a strong inter-comparability, but reinforce the need for careful assessment of μXRF data quality and indicate that directly comparing published geochemical data from sedimentary sequences without fully considering differences in instrument configuration and sample characteristics should be avoided. There is clearly scope to

conduct more detailed inter-comparisons of the different μXRF core scanners currently used by palaeoenvironmental scientists.

Acknowledgements

D. Schillereff is the recipient of a PhD Graduate Teaching Assistantship from the School of Environmental Sciences at the University of Liverpool. D. Schillereff also gratefully acknowledges financial support from The British Society of Geomorphology to conduct the ITRAX scans at the National Oceanography Centre Southampton under the guidance of Professor Ian Croudace. We also appreciate the thoughtful and constructive comments of Professor Andy Cundy that greatly improved the final manuscript.

4 METAL FLUXES, SEDIMENT ACCUMULATION AND PB MINING: LAKE SEDIMENT EVIDENCE FROM BROTHERSWATER, NORTHWEST ENGLAND

Abstract

Geochemical data for multiple sediment cores from Brotherswater (English Lake District) shows that lakes can record (pre-) historical trends in catchment metal flux in their sediments. This stratigraphy correlates with ore (Pb, Zn, Cu) production at Hartsop Hall Mine (~0.5 km away). Cores were independently dated using natural and artificial radioisotopes (^{14}C, ^{241}Am, ^{137}Cs, ^{210}Pb) and the trace metal stratigraphy provides supplementary geochronological control for the last 250 years, as well as aiding correlation between cores. Down-core zones with elevated K, Ti and Zr concentrations reflect greater supply of terrigenous sediment and coincide with periods of more intensive local agricultural and mining activity. Sediment accumulation

rates (SAR) decline sharply away from the inflow throughout the last 1500 years, but rates overall vary with human activity e.g., high SAR (0.06 cm yr^{-1}) coincident with CE 1863-71 mining. The timing of peak Pb concentrations and flux, exceeding 10000 ppm and 40 g m^{-2} yr^{-1}, respectively, in the delta-proximal profundal sediments also corresponds with intensive mining from AD 1863-1871. Later patterns in Pb reflect innovations in mining technology, especially mechanisation, 20th century effluent mediation and closure of the mine CE 1942. Metal profiles repeat in cores across the basin, but decline in concentration away from the inflow. Since mining ceased, core Pb concentrations declined marginally but remained higher than recorded in pre-mining sediments (i.e., 'background levels'). Inflow sediments trapped monthly (2012-14) in the lake centre show that elevated catchment-to-lake Pb flux persists today at an order of magnitude higher than background. This developed higher base level for trace metals delivered to the lake, coupled with the legacy preserved in hillslope, floodplain and lake-marginal soils, are of sufficient magnitude to constitute a marker for the onset of the Anthropocene. Precursor changes in sediment supply most likely driven by catchment agriculture during the last 1500 years are of an equivalent magnitude in terms of quantifiable anthropogenic impact, however.

4.1 Introduction

Adverse water quality arising from the historical legacy of mining and metal ore processing is driven by the release of toxic particulates from chemical and bacterial weathering of sulphide-rich waste rock into waterways and lakes (Martin & Meybeck, 1979). European Union Water Framework (2000/06/EC) and Mining Waste (2006/21/EC) Directives require mediation of contaminated runoff from abandoned industrial sites (Environment Agency, 2008). The English Lake District (Adams, 1988) experienced small-scale Bronze Age and Roman Era metal extraction followed by more extensive operations during the Medieval Era (CE 1200 – 1400) and an intensifying industrial phase from the 16th century. Falling metal prices, depleted reserves and competition led to the decline of ore extraction in the UK in the early 20th century (Byrne *et al.,* 2010). Baseline historical data on metal production are available for individual mines (e.g., Tyler, 1992), but equivalent data on the contaminant flux to watercourses is lacking. Measurements of trace element concentrations in sedimentary archives could make a valuable contribution enabling (pre-) historical metal extraction trends to be reconstructed (von Gunten *et al.,* 1997) and reference states (i.e.,

disturbed or pristine) for metals in aquatic ecosystems to be established (Bindler *et al.,* 2011a). These longer time-span data could also be used to assess the remediation efforts required to achieve pre-disturbance conditions (Förstner, 1976; Bindler *et al.,* 2011a).

Sediment pollutant records from lakes reflect either regional and/or hemisphere-scale atmospheric deposition of particulates (e.g., Brännvall *et al.,* 2001; Hammarlund *et al.,* 2007; Martínez Cortizas *et al.,* 2013; Oldfield *et al.,* 2003; Renberg *et al.,* 2001, 1994; Rippey and Douglas, 2004) or more focused water-borne effluent from proximal mining sites (e.g., Audry *et al.,* 2004; Couillard *et al.,* 2007; Ek and Renberg, 2001; Farmer *et al.,* 1997a). Assessment of various water bodies in the English Lake District (northwest England) show mining-derived signals in their sediments (e.g., Davison *et al.,* 1985; Grayson and Plater, 2008; Hamilton-Taylor, 2008; Hatfield *et al.,* 2008; Miller *et al.,* 2014; Rippey and Douglas, 2004; Yang and Rose, 2005). Here the history of catchment-to-lake metal flux (Pb, Zn, Cu) preserved in the late-Holocene sediment sequence at Brotherswater, English Lake District (Figure 4.1) is presented and interpret alongside the documented mining history of Hartsop Hall (Tyler, 1992, 2001, 2006). Metal mining during the 18-20th centuries delivered a significant metal and particulate load to the lake that vastly exceeded pre-industrial levels. Preservation of repeatable geochemical profiles between sites allows precise core correlation and the calculation of sediment and metal accumulation rates at the basin scale. Sedimentary basins of this nature have the potential to reveal the degree of system recovery and/or adjustment to human perturbations, including industrialisation or agricultural expansion, with relevance to ongoing debate about the Anthropocene (*sensu* Crutzen, 2002) markers and baseline states.

4.2 Brotherswater and the Hartsop Hall mining record

Brotherswater is a small upland lake (0.18 km^2) with a comparatively large catchment (13.01 km^2) in the headwaters of the River Eden, northwest England (Figures 4a and 4b). There is a single dominant inflow in the southwestern sector with a gravel steep-fronted Gilbert-style delta, although palaeochannels on the delta floodplain testify to a more complex past inflow channel geometry. The lake and catchment morphology are conducive to both efficient trapping of fluvially-transported sediments and the preservation of palaeoflood laminations (Chapter 2; Schillereff *et al.,* 2014). In particular, the limited littoral area and a bathymetry dominated by a single flat central

basin deeper (~16 m) than the high-risk zone for wind-induced re-suspension for the dimensions of this water body (Dearing, 1997). Brotherswater displays weak seasonal thermal stratification and is classified close to the oligo/meso-trophic boundary (Maberly *et al.,* 2011). The catchment displays steep relief, largely deforested slopes and a substantial mantle of glacial sediment and soil providing ample sediment supply.

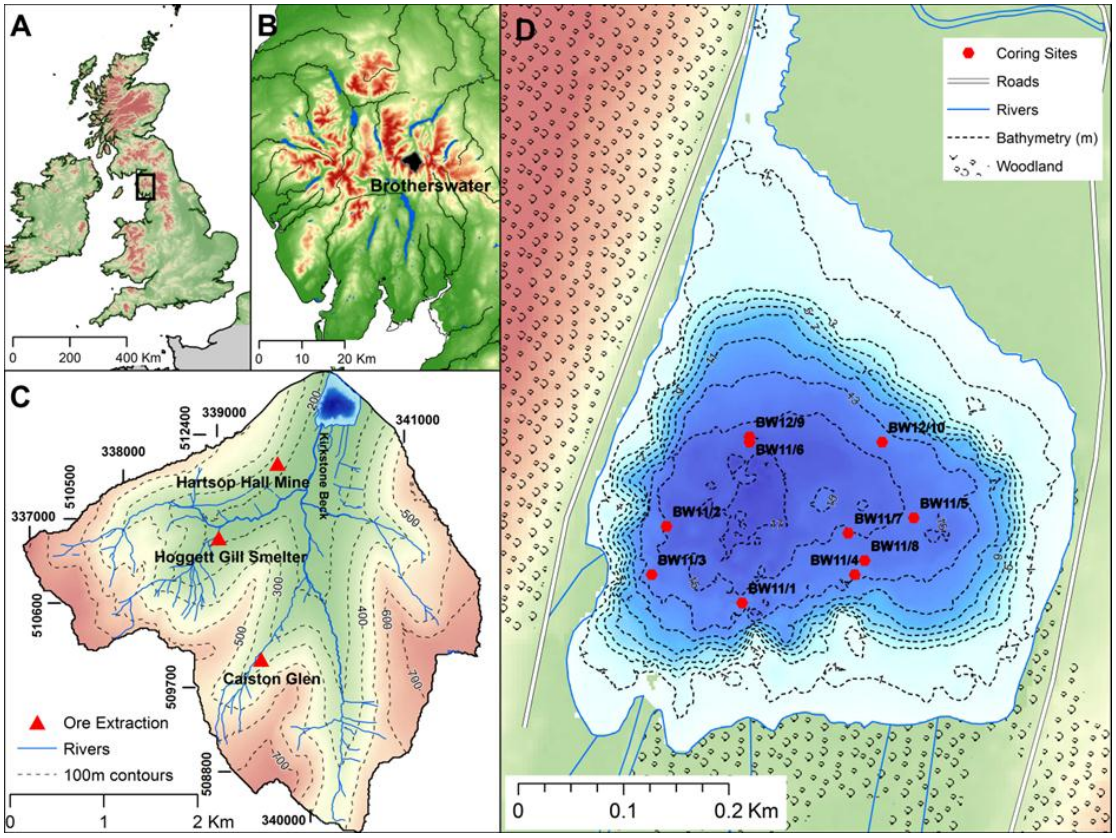

Figure 4-1 A) Location of the English Lake District within the UK. B) Topography and waterbodies within the English Lake District. The extent of the Brotherswater catchment is highlighted. C) Catchment Digital Elevation Model highlighting the location of ore extraction sites mentioned in the text. D) Bathymetric map of Brotherswater showing the location of ten coring locations.

Lincomb Tarns and Esk Pike Sandstones of the Borrowdale Volcanic Series of Ordovician age (*circa* 450 Mya) dominate the catchment geology. They are dissected by a NE-SW argentiferous galena (PbS) vein (<1 m thick) that relates to a regional 'galena-sphalerite' highly saline (marine waters), low temperature (110-130°C) mineralization phase during the early Carboniferous (Stanley & Vaughan, 1982). Ores were set in quartz and are predominantly composed of galena, moderate amounts of sphalerite (ZnS) and baryte (barium oxide; $BaSO_4$) and limited silver (Ag) (Tyler, 1992). Minor

quantities of copper (Cu), wulfenite ($PbMoO_4$) and fluorite (CaF_2) were below extractable quantities (Adams, 1988; Tyler, 1992). Abandonded mining infrastructure and exposed waste materials litter the hillslopes at Hartsop Hall Mine (54°29'55"N, 2°56'9.74"W), ~600 m SW of the lake (Figure 1). Limited extraction of Cu occurred CE 1870-80 further south at Caiston Glen Copper Mine (54°28'59N, 2°56'4"W). Tyler's (1992) collated history of Hartsop Hall Mine, though not including ore production figures, gives lease and operation dates. The first short-term lease dates from 17th April CE 1696, broadly concurrent with operations at a 17th century smelter at Hogget Gill (54°29'33" N, 2°56'42" W) (Figure 4.1c). Galena ore extraction volumes of *circa* 2450 kg (CE 1802-4) and 6230 kg (CE 1830-2) are estimated for short-lived 19th century ventures at Hartsop Hall that failed due to inclement weather and inadequate financing. Water-powered milling (CE 1863-71) allowed Hartsop Hall to operate at peak capacity (24,000 kg yr^{-1}) and coincides with anecdotal evidence for discolouration of Kirkstone Beck, fish deaths and poisoned livestock (Chambers, 1978; Tyler, 1992). Later efforts (CE 1931-1942) were mechanically enhanced, typified by more efficient Pb recovery from harvested ores and partially processes at the nearby larger Greenside Mine draining into Ullswater (Tyler, 1992; Grayson and Plater, 2008). Geochemical measurements of stream sediments (British Geological Survey, 1992) and soils (Hardy, 2013) across the catchment show Pb levels rarely exceed 250 ppm except near mining sites. Recent measurements of metal concentrations (January, April, July and October 2010) in water samples show Pb values at Brotherswater below their limit of detection (2 mg m^{-3}), but high Zn (<5 mg m^{-3}) levels (Maberly *et al.,* 2011) .

4.3 Methods

Sediment cores (3 to 4.5 m length) were extracted from ten profundal locations (Figure 4.1d) using overlapping (1 and 1.5 x 0.075 m) hand-percussive Russian-style drives and short (≤0.25 x 0.08 m) gravity cores captured the sediment water–interface intact (Boyle, 1995). Coring sites radiate from delta-proximal to more distal locations to encompass all sediment dispersal from Kirkstone Beck (Figure 4.1c and d). Near-monthly lake sediment trapping since August 2012 collected material at three heights (100, 75 and 25% of water depth) near the delta (~75 m from the inflow) and a mid-lake site (~300 m). The 1:8 (width:depth) aspect ratio traps consisted of cylindrical PVC tubing with removable basal sampling cups (after Bloesch and Bums, 1980).

Major element and trace metal concentrations were determined by X-ray Fluorescence (XRF) for core and sediment trap samples. Core subsamples taken at 0.5, 1 or 4 cm intervals and all sediment trap samples were freeze dried, collecting moisture content and dry bulk density data (assuming grain density = 2.65 g cm^{-3}), and measured on a Bruker S2 Ranger energy dispersive X-ray fluorescence (ED-XRF) analyser under helium using a Pd x-ray tube and Peltier-cooled silicon drift detector. The dry mass concentrations were corrected for organic matter content (Boyle, 2000). Long cores were μXRF-scanned at 0.5 cm intervals on a wet sediment basis using a Olympus Delta ED-XRF housed within a Geotek MSCL-XZ core scanner. Wet sediment element concentrations were converted to dry-weight equivalent (following the procedures outlined in Chapter 3.3), using dried samples (BW12-9A) measured on the S2 Ranger as a training set for correcting the wider wet sediment dataset. Both XRF undergo regular laboratory consistency checks using certified reference materials (Chapter 3.3).

Delta-proximal (BW11-2) and distal (BW12-9) cores were dated radiometrically (^{210}Pb, ^{137}Cs, ^{241}Am) at the Liverpool Environmental Radioactivity Laboratory (Appleby *et al.,* 1986). BW11-2 (Figure 2a) shows clear CE 1963 (atmospheric weapons testing) and CE 1986 (Chernobyl) peaks in ^{137}Cs and ^{241}Am but sudden fluctuations in unsupported ^{210}Pb levels and unexplained variations in sediment accumulation rates before the CE 1940s negated calculation of consistent ^{210}Pb ages from the deeper sediments. BW12-9 (Figure 4.2b) produced a more coherent Constant Rate of Supply model (Appleby and Oldfield, 1978), and the age/depth model constrains the stable lead spike at the base of the core to before CE 1880, coinciding with intensive mining CE 1863-71 (Figure 4.2b). Stratigraphic correlation of geochemical profiles allowed the transfer of ages from BW12-9 to BW11-2, correcting the problematic BW11-2 ^{210}Pb record. The longer BW11-2 sequence is dated using thirteen ^{14}C measurements (Natural Environmental Research Council Radiocarbon Laboratory at East Kilbride) targeting hand-picked terrestrial plant macrofossils (Table 4.1). All ^{14}C samples were pre-treated using the standard Acid-Alkali-Acid wash to remove dissolved humic acids, converted to carbon dioxide by combustion in quartz tubes and graphitised by iron-zinc reduction. A surface age (CE 2011), the radiocarbon ages, markers for the anthropogenic radioisotopes ^{137}Cs and ^{241}Am, ^{210}Pb dating transferred from BW12-9 and the well-defined 1860s mining horizon were integrated into a Bayesian age-depth model for BW11-2 (Figure 4.3) using the Bayesian routine 'Bacon' (Blaauw and Andrés Christen, 2011). This modelling approach partitioned the core into 5 cm-thick sections and

estimated the accumulation rate for each segment using a Markov Chain Monte Carlo (MCMC) approach, constrained by prior information on accumulation rate (a gamma distribution with mean 5 yr cm^{-1} and shape 2) and its variability (memory, a beta distribution with mean 0.5 and shape 20). ^{14}C ages were calibrated using the IntCal13 curve (Reimer *et al.,* 2013) and modelled within 'Bacon' using a Student-t distribution, which better takes into account scatter in the dates and allows for statistical outliers (Christen & Pérez, 2009). Geochemical profiles for the ten core sites show repeatable

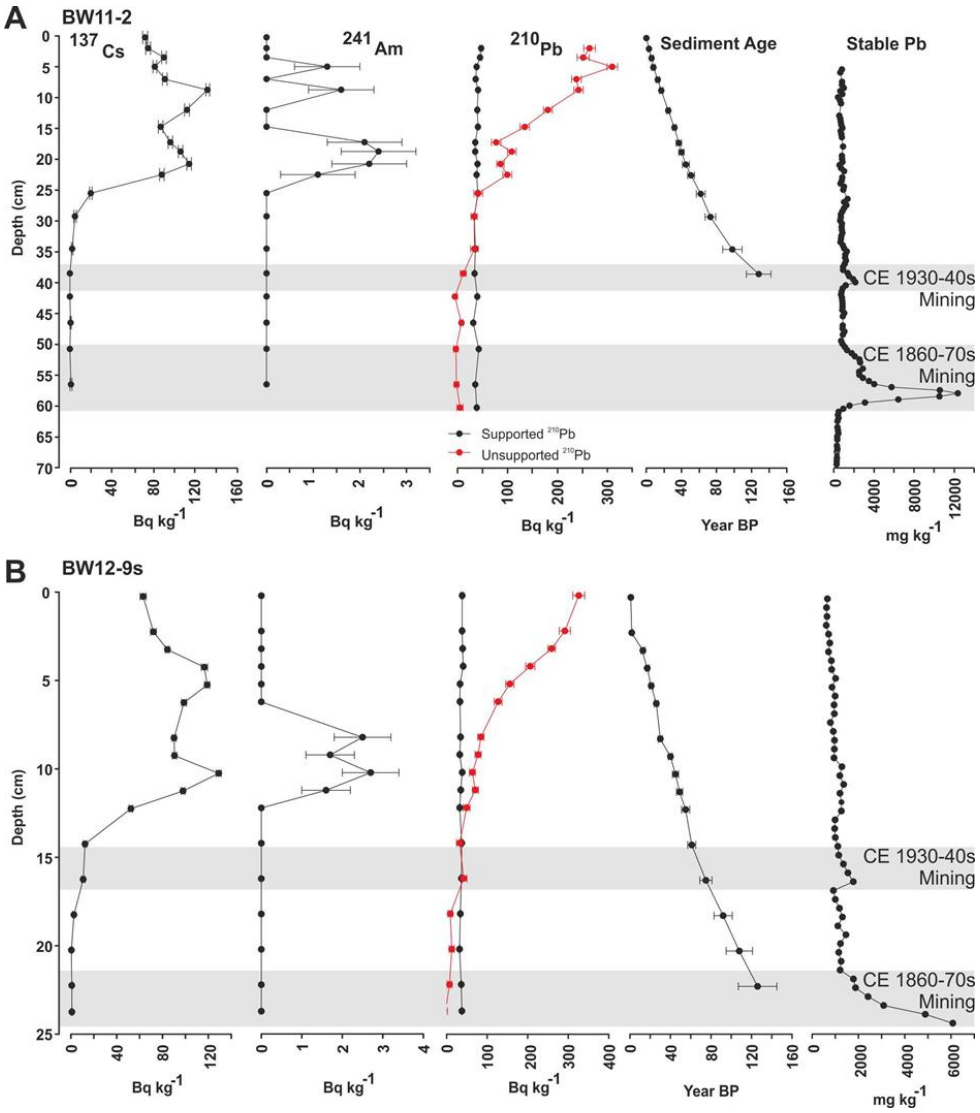

Figure 4-2 Artificial radionuclide measurements of ^{241}Am, ^{137}Cs and ^{210}Pb for cores BW11-2 (A) and BW12-9 (B) and the calculated sediment ages. Pb measurements made on dried sediment via ED-XRF are shown at right with the stable Pb peaks reflecting historic mining mining activity highlighted by grey bands.

Table 4-1 Radiocarbon dates used for the construction of the age model for the Brotherswater sequence. Dates were integrated into a Bacon Bayesian model (Blaauw and Andrés Christen, 2011) and calibrated using the IntCal13 calibration curve (Reimer *et al.,* 2013).

Publication Code	Sample Identifier	14C Enrichment (% Modern ±1σ)	Conventional Radiocarbon Age (years BP±1σ)	Carbon content (% by wt.)	$\delta^{13}C_{VPDB}$ ‰ ± 0.1
SUERC-48896	BW11-2 RC1 41-42	95.42 ± 0.53	377 ± 45	46.3	-27.765
SUERC-48897	BW11-2 RC2 49-50.5	95.48 ± 0.53	371 ± 45	43.7	-27.879
SUERC-48898	BW11-2 RC3 61-62.5	97.55 ± 0.54	199 ± 45	48.7	-28.3
SUERC-48899	BW11-2 RC4 81-81.5	97.02 ± 0.54	243 ± 45	44.2	-26.098
SUERC-48903	BW11-2 RC6 127-128.5	89.84 ± 0.50	860 ± 45	40.6	-27.351
SUERC-48904	BW11-2 RC7 150-151	90.38 ± 0.51	812 ± 45	41.2	-29.119
SUERC-48906	BW11-2 RC9 172-174	92.26 ± 0.52	647 ± 45	50.5	-28.752
SUERC-48907	BW11-2 RC10 197-198.5	90.85 ± 0.52	771 ± 46	46.1	-27.862
SUERC-48908	BW11-2 RC11 224-224.5	92.99 ± 0.54	584 ± 47	54.9	-30.719
SUERC-48909	BW11-2 RC12 269-270	87.03 ± 0.49	1116 ± 45	53.7	-28.506
SUERC-48910	BW11-2 RC13 321.5-323.5	84.08 ± 0.47	1393 ± 45	50.4	-28.959
SUERC-48913	BW11-2 RC14 335.5-336	82.66 ± 0.46	1530 ± 45	52.5	-28.384
SUERC-35378	BW11-2 (3) 258		930 ± 30		-25.0
SUERC-37679	BW11-3 137.5-138.5		200 ± 30		-28

patterning in Pb concentrations for the historical period and in Ti, K and Zr for the longer record (see Results and Discussion). These enable the transfer of the chronology between cores. Partial validation of the cross-correlation is provided from a single ^{14}C age from BW11-3 (Table 4.1) and a previous radiocarbon-dated core from Brotherswater (Chambers, 1978).

4.4 Results and Discussion

4.4.1 Geochronology and the fluxes of metals

The age-depth model for BW11-2 (Figure 4.3) shows a largely coherent integration of the radiometric dating techniques (^{14}C, ^{210}Pb, ^{137}Cs and ^{241}Am). Five ^{14}C ages in the last 500 years appear anomalous and were down-weighted in the Bayesian age-depth model; the four dates that appear to old most likely reflect erosion of 'old carbon' from catchment soils driven by woodland clearance and hillslope destabilisation (Edwards and Whittington, 2001; Chiverrell, 2006; Chiverrell *et al.,* 2007) and late 19th century modifications of Kirkstone Beck near the lake (Ordnance Survey, 1899). One date appears to be too young (SUERC-48908), most likely explained through contamination of the sample with modern material during lab processing. There are challenges in ^{14}C dating the last 250 years because their calibration produces wide probability distributions and multiple equally-likely age solutions for individual samples, driven by fluctuations in atmospheric ^{14}C concentrations due to fossil fuel combustion (Hua, 2009). This issue appears present in the ^{14}C measurements at 61 cm (SUERC-48898) and 81 cm (SUERC-48899) (Figure 4.3).

Pb, Zn and Cu concentrations in Brotherswater sediments exceed published values for atmospheric fallout of anthropogenic Pb and other metals recorded in European peat bogs (<400 ppm: Farmer *et al.,* 1997; Mighall *et al.,* 2002) and lake sediments (<600 ppm Pb: Renberg *et al.,* 2001; Rippey and Douglas, 2004; Yang and Rose, 2005). Metal loading at Brotherswater is almost certainly derived locally and maximum values (>10 000 ppm Pb, >1000 ppm Zn) are similar to other lakes receiving point-source contamination from abandoned mines, e.g., Ullswater (>30 000 ppm Pb; Grayson and Plater, 2008) and Lac Caron, Canada (>1000 ppm Zn; Couillard *et al.,* 2007). The oldest ^{210}Pb ages in BW12-9 (Figure 4.2b) tie the most prominent Pb marker to intensive mining at CE 1863-71; the onset of this increase forms a stratigraphical marker assigned an age of CE 1863. Using a narrow probability distribution for this marker in

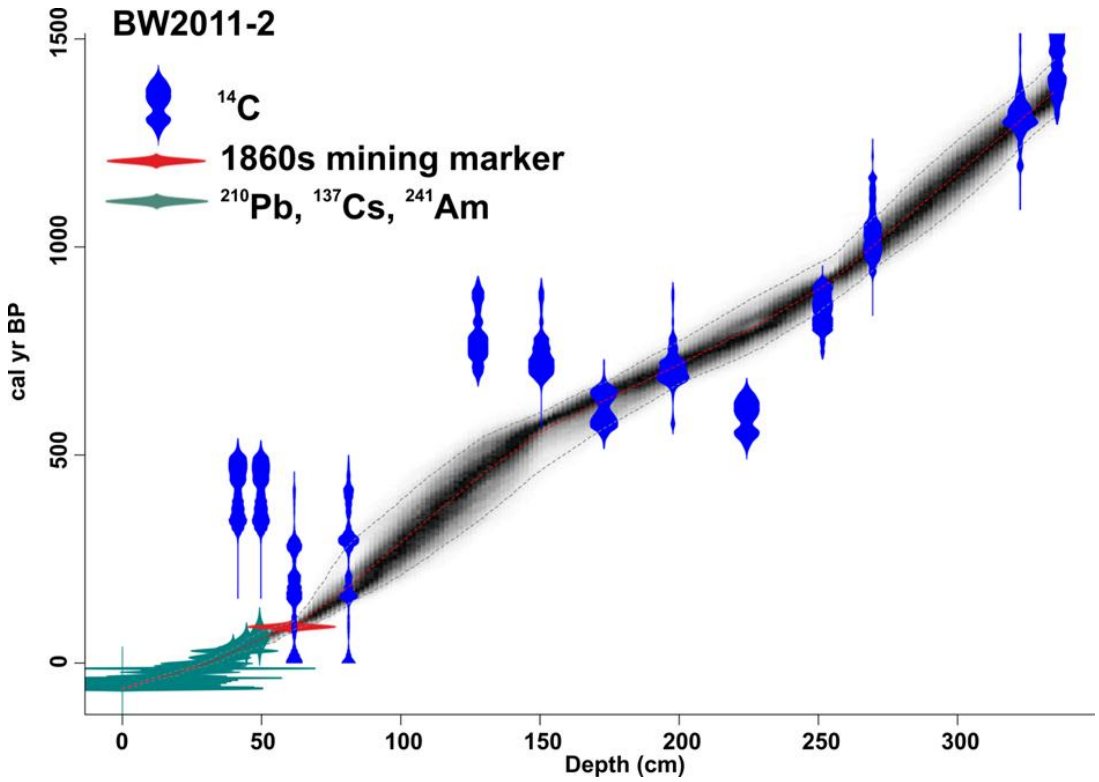

Figure 4-3 Age-depth model for core BW11-2 incorporating thirteen radiocarbon ages (blue symbols), ^{210}Pb and ^{137}Cs radionuclide dating for recent sediments (teal) and the 1860s mining marker in red.

the Bayesian modelling (red diamond) resolves the temporal uncertainty in the model and produces good convergence of ^{14}C ages at 61 and 81 cm (Figure 4.3).

Financial stress and inclement weather constrained operations at Hartsop Hall to brief periods (2 – 10 years) and the sedimentary imprint of these phases are observed in cores across the lake (Figure 4.4). Pb flux profiles for BW11-3, 11-2 and 12-9 (delta proximal to distal) show low, stable levels (<0.1 g m^{-2} y^{-1}) at depth, interpreted as the pre-mining baseline, before increasing ~AD 1700 to exceed 1, 0.3 and 0.2 g m^{-2} y^{-1}, respectively. Early smelting techniques were inefficient, leaving substantial waste ore in surface spoil heaps, accelerating the delivery of weathered sulphides to the water courses notwithstanding low extraction volumes (e.g., Loch Tay; Farmer *et al.,* 1997a), and producing considerable airborne contaminated particulates during processing (e.g., Ek and Renberg, 2001). Successive increases in Pb flux correspond with early 19th Century mining episodes (1802-1804; 1830-1832) before the maximum flux of stable Pb (80, 58 and 26 cm depth in BW11-3, 11-2 and 12-9, respectively), constrained to the AD 1863-1871 episode. While company records indicate peak ore production

occurred at this time (~24 000 kg yr^{-1}), the exceptional Pb flux probably also reflects spillage of contaminated effluent into Kirkstone Beck from a new crushing mill and open cast excavations at Hartsop Hall Mine level 3 (Tyler, 1992). Pb peaks during CE 1930s show a more muted sedimentary response, with documents indicating more mechanised ore extraction processes (Tyler, 1992) able to harvest a greater proportion of the ore from the host rock and leave less surface waste. There appears an imprint of ore production by volume in the pollutant sedimentary record, but the sediments reflect also technical innovations in the local mining technology. After mine closure in the 1940's, smaller scale peaks in Pb (e.g., 27 cm in BW11-2) could relate to leaded petrol usage in automotives in the 1950s – 70s (von Storch *et al.,* 2003) or the mobilisation of mining waste in the catchment during severe floods in the 1960s (Schillereff *et al.,* 2014), although palaeolimnological data from nearby Ullswater showed flood events flushing through mining regions do not always leave a clear heavy metal imprint in the sediments (Anderton *et al.*, 1998). Stable isotopic Pb measurements would be needed to discriminate leaded fuel emissions from mining sources but the local contribution overprints any 20th Century atmospheric Pb signal at Brotherswater. Previous research at Brotherswater shows neither evidence for post-depositional remobilisation within the sediment column (Rae & Parker, 1993, 1996) nor bottom-water redox conditioning driven by ferromanganese enrichment (no correlation is observed between Fe and Pb ($p > 0.6$) and Mn and Pb ($p > 0.4$)). These are processes that have altered stratigraphic pollution records at other lakes (e.g., Boyle *et al.,* 1998). We hypothesise that post-depositional diffusion is unlikely at Brotherswater as the point-source solid-phase concentrations of these metals are so high (Couillard *et al.,* 2004).

Zn and Cu fluxes also increase in the sediment record at the onset of elevated Pb (Figure 4.4), but they do not substantially exceed pre-industrial levels and so their down-core pattern could instead relate to more intensive soil erosion driven by human activity at this time. Both Zn and Cu fluxes do increase markedly at the Pb peak associated with CE 1860s. While these trends can be explained in part by higher sediment accumulation rates, the highest Cu flux probably includes a signal from operations at Caiston Glen Copper Mine (active CE 1860 – 1870). Zn levels since the 1860s remain high, unlike the Pb profile, a trend potentially explained by chemical reactions occurring during the oxidisation of surficial mining waste at Hartsop Hall.

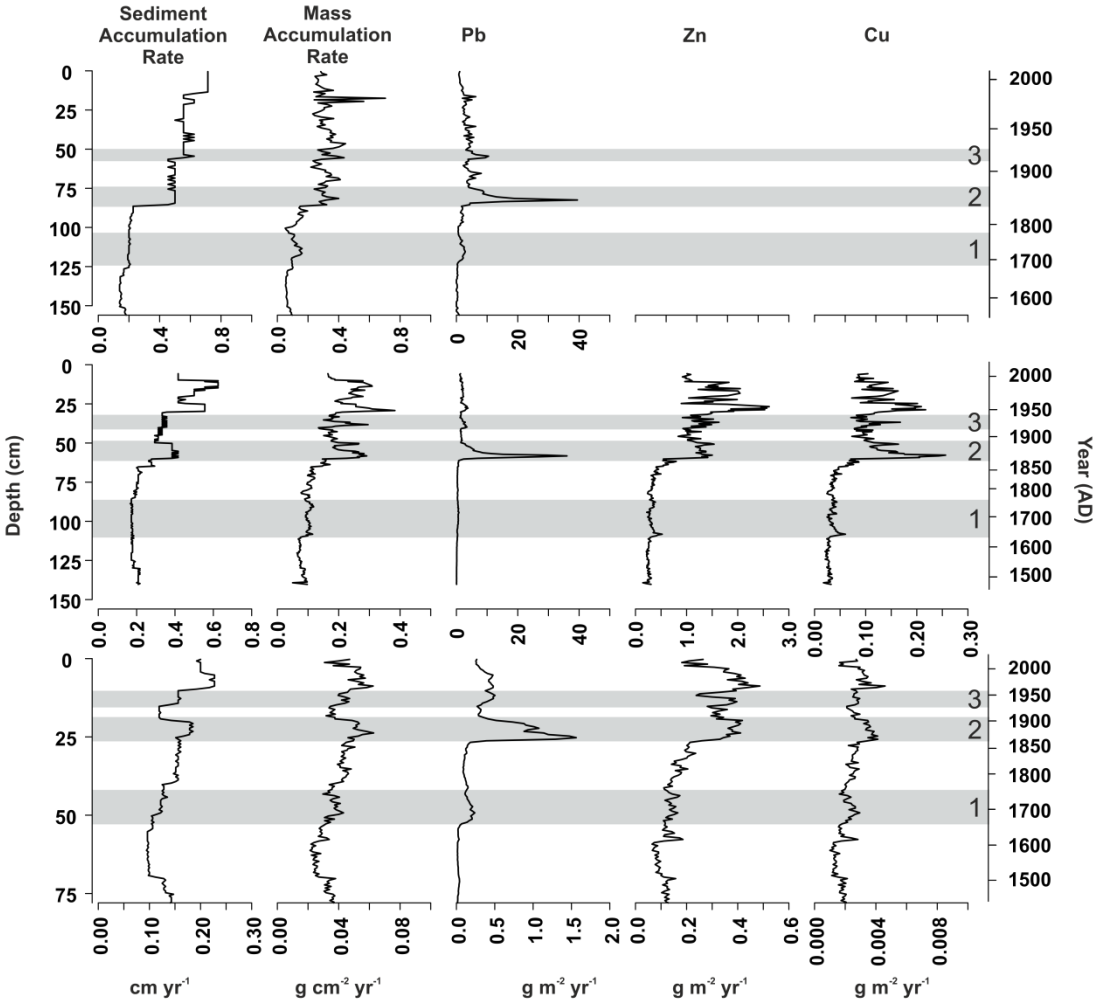

Figure 4-4 Pb, Zn and Cu flux to Brotherswater plotted alongside sediment and mass accumulation rates for cores BW11-3, BW11-2 and BW12-9. Zn and Cu were below the limit of detection for measurements performed on BW11-3. Note the converted metal flux units (g m^{-2} yr^{-1}) to avoid excessive decimal places.

The oxidisation of galena tends to form secondary minerals that reduce the potential for further weathering (Jones *et al.,* 2013), thus galena is normally less mobile and soluble than sphalerite (Nuttall & Younger, 1999). Furthermore, the mine operators primarily extracted galena ore and so greater quantities of sphalerite may have been left as unworked spoil thus leading to a proportional greater dissolution of Zn after mining operations ended (Mayes *et al.,* 2010).

Sediment trap (Aug 2012 – Aug 2013) data expressed as total monthly sedimentation and elemental concentrations for the central basin of Brotherswater show that monthly Pb concentrations regularly exceed 500 ppm and total annual Pb fluxes are

0.614 (top), 0.482 (middle) and 18.451 (bottom) g m^2 yr^{-1}. Higher values in the lower trap reflect either transport as a plume in the lower water column, secondary sedimentation or focusing of sediment within the lake. The upper and middle traps collected concentrations that are close to the Pb fluxes estimated for the top 10 cm of the nearby sediment record (BW12-9: 0.257-0.502 g m^2 yr^{-1}) and are significantly higher than pre-industrial levels. Furthermore, we suspect Pb is being delivered to Brotherswater as particulates as water monitoring (Maberly *et al.,* 2011) found Pb levels below their instrumental limits of detection. Physical sediment trapping is thus a sensible approach to assess the legacy of metals delivered from abandoned mining sites to aquatic ecosystems.

4.4.2 Variations in sediment accumulation rate

Coherent patterns in the wider geochemical stratigraphy include episodic increases in sediment flux affecting both fine-grained (Ti, K) and coarser (Zr) elements (zone 1 – 5: Figure 4.5). The phases with elevated minerogenic sediment flux appear to tie in with known periods of human-driven, more intensive land-use. These phases are recorded in sediment and landform records across northwest England, and coincide with periods characterised by enhanced soil and hillslope erosion (e.g., Chiverrell, 2006; Chiverrell *et al.,* 2007; Edwards and Whittington, 2001; Hatfield and Maher, 2009; Pennington, 1981; Shen *et al.,* 2008). Increases in the flux of Ti, K and Zr in BW11-2 around CE 950-1200 (zone 1) correspond with previous findings at Brotherswater (Chambers, 1978; Rae and Parker, 1996) and were likely driven by population and agricultural expansion during the Norse and subsequent Medieval Period (Winchester, 1987, Chiverrell, 2006) and probably the introduction of hill sheep farming practices. These timings are concurrent with palynological evidence from other lakes in the region for reductions in woodland cover (Pennington, 1981, 1991, 1997) and mineral magnetic evidence for increased soil erosion (Shen *et al.,* 2008). Climatic variability as a driver for these observed changes in sedimentation is also possible, though shifts to wetter conditions in peat sequences to the north and south of the Lake District occur typically later, around 400-500 years ago (Charman *et al.,* 2006).

Higher mass accumulation rates around CE 1400 – 1600 are present in all cores (zone 2) and coincide with age reversals in the ^{14}C measurements from BW11-2 (Figure 4.3). This radiocarbon phenomenon, present in many lake sediment profiles across Cumbria (Pennington, 1981, 1991; Langdon *et al.,* 2004; Chiverrell, 2006) has been interpreted

as the product of human-induced landscape disturbance driving influx of eroded soil and 'old carbon' (Pennington, 1991). Sediment flux at this time was greater than the

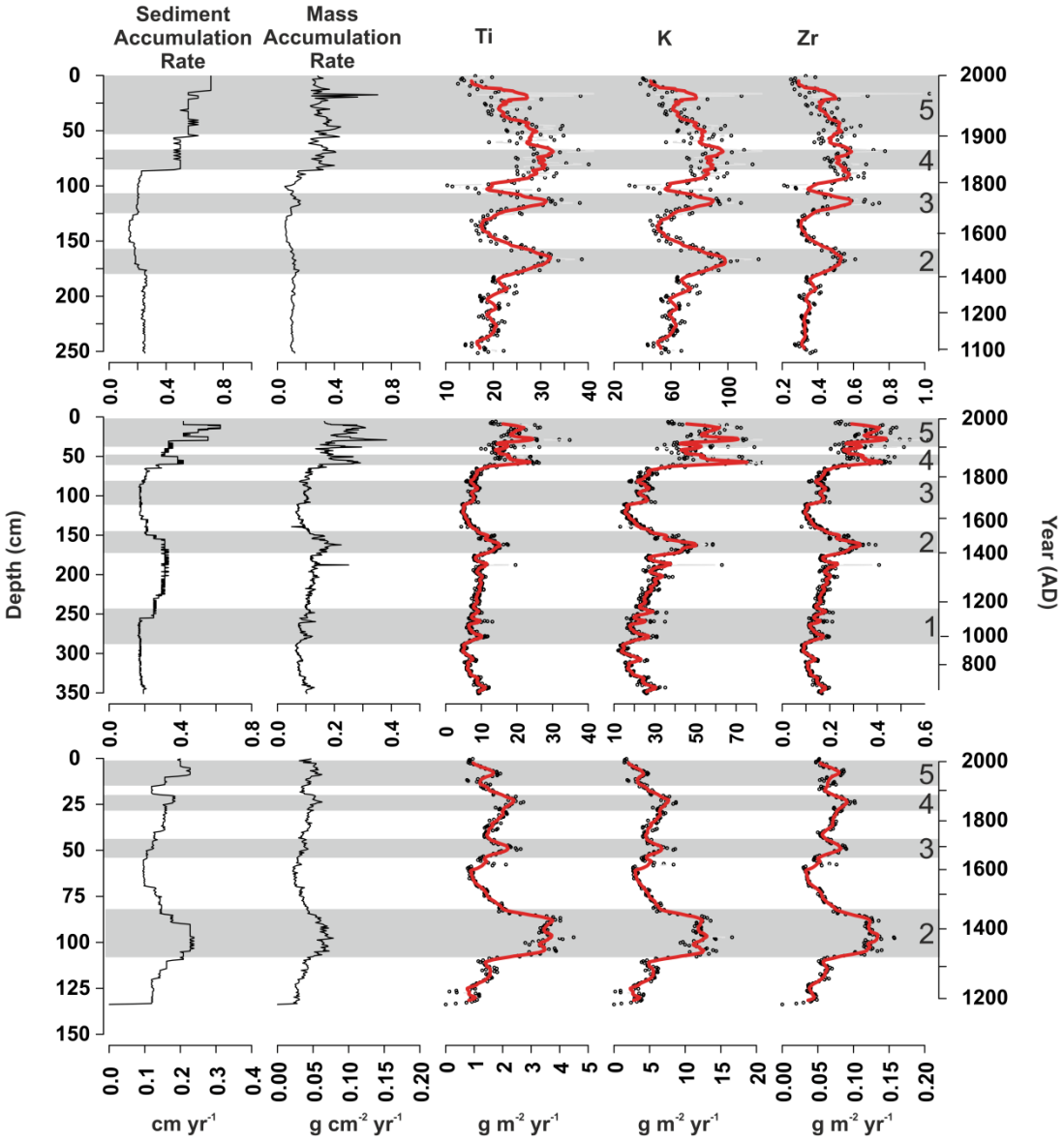

Figure 4-5 Elemental flux profiles for minerogenic supply indicators Ti, K and Zr for cores BW11-3, BW11-2 and BW12-9. Highlighted zones represent periods of enhanced mineral supply that appear to correspond with periods of more intensive land-use or population expansion. Note the converted minerogenic flux units (g m^{-2} yr^{-1}) to avoid excessive decimal places.

preceding episode in BW11-2, mirroring patterns at Blelham Tarn (Pennington & Lishman, 1984) and Bassenthwaite Lake (Hatfield and Maher, 2009). This phase is broadly coincident with a major phase of gully initiation from CE 1500-1600 in NW

England (Chiverrell *et al.,* 2007; 2008) attributed to rural land-use change and demographic expansion (Winchester, 1987) after lulls and modest woodland vegetational recovery linked to the Black Death, poor harvests and Anglo-Scottish border conflict (Chiverrell *et al.,* 2007; Coombes *et al.,* 2009). Increases in sediment flux are more muted around CE 1700 (zone 3), though much more prominent in the inflow zone BW11-3. These changes coincide with large increases in the intensity of upland agriculture (Pennington, 1991; Winchester, 1987) that impact the Esthwaite Water sediments somewhat later (~ CE 1750) (Dong *et al.,* 2011). This episode also overlaps with the onset of mining at Hartsop Hall and, although initial activity was limited, it no doubt produced landscape disturbance (e.g., tree felling for smelter fuel or access) and could be responsible for the enhanced MAR. Whether due to past changes in the agricultural landscape or industrial activity in these uplands, it appears the impacts are greatest at the event with gradual adjustment to the altered regime, as has been recognised in other lacustrine and geomorphological records (Dearing, 1991). The sharpest increase and greatest sediment flux in delta proximal cores represents the phase of most intensive mining at AD 1863-71 (zone 4). Despite the localised geographical scale of this activity, the use of open-cast mining, the construction of an access road along the western lake edge, the installation of leats (slope-parallel conduits for focusing water) to power the crushing mill and probably tree felling for smelter fuel all appear to have contributed to trigger increased sediment supply and flux to the lake. Flux of sediment and minerogenic elements (Ti, K and Zr) remained high through much of the 20th Century (zone 5), which match results from Bassenthwaite Lake (Hatfield *et al.,* 2009) and coincides with increasing mechanisation of agriculture and the highest sheep stocking densities (Bennion & Winchester, 2010). The mid-20th century peak in terrigenous flux corresponds with increased eroded soils and rapid sediment accumulation shown in mineral magnetic measurements on Brotherswater sediments (Oldfield and Wu, 2000).

4.4.3 Spatial patterns of sediment accumulation

Pb profiles display a repeatable stratigraphy across the 12 cores (Figure 4.6). Concentrations tend to decline with distance from the inflow, although the use of the conversion procedures outlined in Chapter 3.3 to calibrate those cores measured on a wet sediment basis (Geotek) appears to overestimate maximum Pb concentrations, which negates this trend somewhat. The longer profiles display low Pb concentrations

and flux at depth (<100 ppm; <0.1 g m^{-2} yr^{-1}), and probably reflect the natural, pre-mining baseline for this system. Pb concentrations then rise through one or two peaks (reaching ~2000 ppm; 0.81 g m^{-2} yr^{-1}) to the single, major 1860s peak. While the conversion of μXRF scan data appears to overestimate maximum Pb concentrations, the peak exceeds 10000 ppm (36.02 g m^{-2} yr^{-1}) in delta-proximal cores and exceeds 4000 ppm (~1.5 g m^{-2} yr^{-1}) more generally across the basin. After the AD 1860-70s Pb concentrations decline sharply and values fluctuate towards the present but around much higher mean concentrations than the pre-mining baseline. The thickness of sediment over which this stratigraphy is displayed varies across the lake, with less sediment accumulating with increasing distance from the delta. Peak Pb occurs at 80 cm depth in BW11-3 (delta proximal), whereas it occurs 17 – 22 cm beyond 350 m distance of the inflow. Sedimentation rates since 1860s have thus been four times more rapid near the delta and sediment focusing (Engstrom & Rose, 2013) in the central basin does not appear to be a major depositional process. There is a down-lake declining gradient in sediment mass accumulation rate (MAR), although the rate of decline is not constant (Figure 4.5). Instead, throughout the mining period, BW11-2 MAR (0.15 – 0.25 g cm^{-2} yr^{-1}) is only slightly lower than BW11-3 (0.2 – 0.4 g cm^{-2} yr^{-1}) whereas the MAR for the same interval from the centre of Brotherswater (BW12-9) is much lower, never exceeding 0.07 g cm^{-2} yr^{-1}. These data indicate the river-borne sediment plumes decelerate rapidly on entering the lake, depositing the majority of their sediment load near the delta and reducing sharply to the central basin. A similar trend is observed in the Pb flux data, with concentrations somewhat lower at BW11-2 than BW11-3 across all time-steps, for example maximum values reaching 36.02 compared to 39.43 g m^{-2} yr^{-1} during the 1860s mining period, but substantially lower in the central basin: maximum 1.6 g m^{-2} yr^{-1} during the 1860s mining phase, rarely exceeding 0.2 and 0.5 g m^{-2} yr^{-1} during the period of early mining and the 20th century, respectively. As trace metals will be transported into the lake bound to suspended particulate matter in the sediment plume, the process of sediment diffusion across Brotherswater exerts a strong control on the spatial distribution of Pb and this is consistent with theory on the rates of particle settling for heavy metals in profundal sediments (e.g. Boyle *et al.,* 1998).

This pattern differs from larger lakes in the Lake District contaminated by mining waste; at Ullswater, Pb concentrations decline moderately with distance from inflows receiving waste from Greenside Mine but sediment accumulation rates vary little

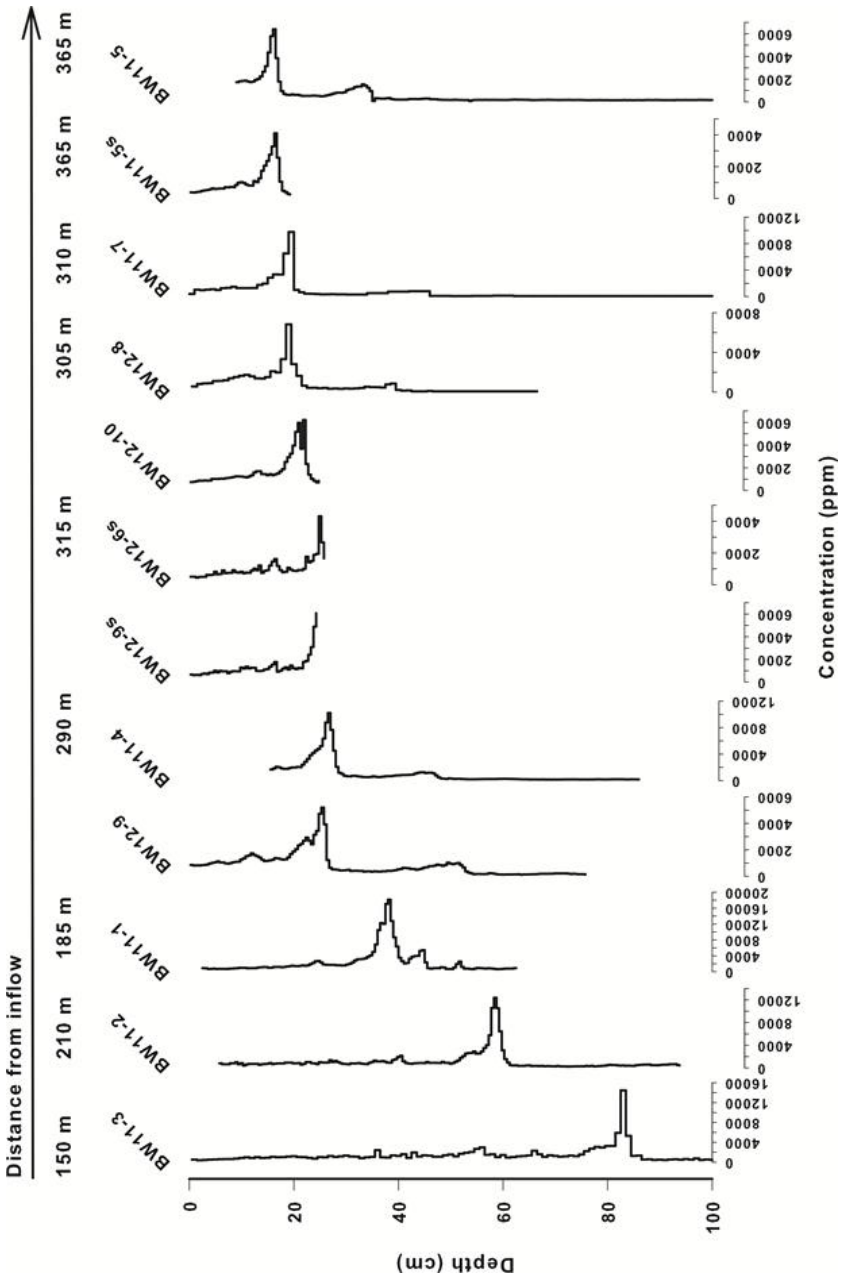

Figure 4-6 Pb profiles for twelve sediment cores extracted from Brotherswater, plotted from left to right according to distance from the delta. The major spike in each plot almost certainly corresponds to the episode of intense ore extraction during the CE 1860-70s at Hartsop Hall Mine. Where XRF measurements were performed on a wet-sediment basis, concentrations have been converted to dry weight equivalent following the procedures outlined in Chapter 3.3. As a result, the expected pattern of more diluted Pb concentrations with distance from the inflow is not fully coherent due to over-estimation of higher values in the regression model.

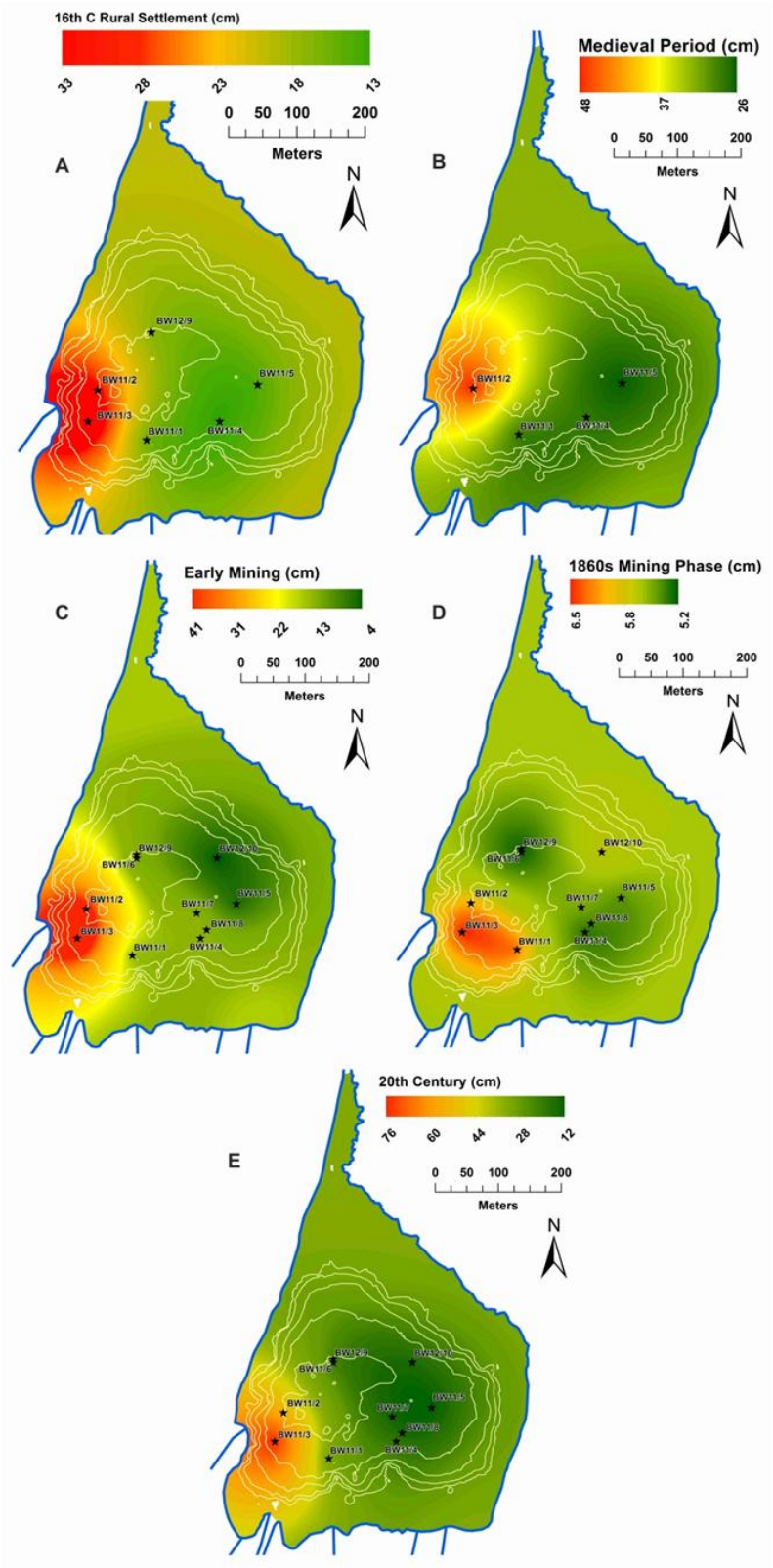

Figure 4-7 Interpolated depths of accumulated sediment during distinct phases of elevated sediment flux to Brotherswater. Due to variable core depth, the locations of cores used for each phase are plotted on each map.

throughout the lake (Grayson and Plater, 2008). Likewise, smaller waterbodies upstream of Windermere act as pollutant sinks, reducing the quantity of heavy metals reaching Windermere and modifying the expected down-lake depositional gradient (Miller *et al.,* 2014). These results suggest small, first-order lakes like Brotherswater are the primary sink for mining-derived material and offer the best location for understanding past mining activity and its long-term environmental impacts.

Strong correlation in the stratigraphy between core sites allows interpolation of sediment accumulation rates to generate maps by krigging in ARCGIS and volumetric estimates of total sediment accumulation for the five zones (Figure 4.7). Total estimate sediment flux to the lake rose from 0.2 to 0.3 $m^3\ yr^{-1}$ across the Medieval population expansion (zones 5/4). The most substantial increases occur during peak mining phase (0.6 $m^3\ yr^{-1}$) and with 20th agricultural activity (0.5 $m^3\ yr^{-1}$). Relating these sediment accumulation data to equivalent interpolation of Pb concentrations indicates that circa 6 kg of particulate Pb was delivered to Brotherswater and the delivery rate remains around 0.023 $kg\ yr^{-1}$ (peak Pb 0.17 $kg\ yr^{-1}$).

4.4.4 Post-mining trajectory

The transformation of Earth's surface by human activity has garnered increasing interest from trans-disciplinary researchers framed within the Anthropocene concept (Crutzen, 2002; Steffen et al., 2007). Chemically-distinctive alluvial sediments heavily contaminated by mining waste have been proposed as potential stratigraphic markers for the Anthropocene (Foulds et al., 2013; Stinchcomb et al., 2013; Macklin et al., 2014). As lakes act as very efficient sinks for catchment sediment flux, historical pollution records extracted from lake sediments operate as event markers (Meybeck & Vörösmarty, 2005; Oldfield, 2014) and proxy records for metal production at historic mining locations. Furthermore, intensive human activity leading to increased eutrophication (Wang et al., 2012) or the release of artificial chemical compounds (e.g., Sayer et al., 2006) have led some lakes to undergo regime shifts, preventing a return to their natural (pre-human modification) state. At Brotherswater, the sediment record clearly portrays mining-derived pollution as an important driver of sediment flux during the past 300 years. For core BW11-2, the mean Pb concentration below 125 cm is 62 ppm, compared to 351 ppm between 62 cm and 82 cm depth and 806 ppm above 34 cm. A slight negative trajectory is observed since AD 1942 (the year of mine closure) however present-day concentrations exceed the pre-mining baseline by more than one

order of magnitude. The increase is even greater in magnitude when Pb flux is considered: the mean pre-mining flux is 0.07 g m^{-2} yr^{-1}, but the mean flux since AD 1942 is 1.95 g m^{-2} yr^{-1} (for BW11-2).

Elsewhere, some heavily polluted lakes have displayed a marked recovery after progressive emission reductions or closures of industry, such as near Wawa, Canada (Greenaway et al., 2012) and Lake Malären, Sweden (Renberg et al., 2001). Intensive remediation efforts have had more limited impact at other lakes, such as near Sudbury, Canada (Tropea et al., 2010), Falun, Sweden (Ek and Renberg, 2001) and Goldenville, Nova Scotia, Canada (Wong et al., 1999). The current trajectory of Pb concentrations in the profundal sediments at Brotherswater suggests a recovery to pre-mining levels is unlikely and points towards the adaptation to a new 'Anthropocene' contaminated baseline at Brotherswater. Analysis of soils, hillslope, alluvial and deltaic sediment stores down-system of the mine and smelter (Pb > 100 ppm, in some instances >1000 ppm) show that mining waste has been incorporated widely in the catchment sedimentary system.

Remediation work at Hartsop Hall Mine is not a UK Environment Agency priority (Environment Agency, 2008) thus a prolonged period of Pb-enriched sediment flux, contaminated soils and associated risk to human, livestock and aquatic ecosystems will persist. Recent sediment budget studies have shown it can take more than 5000 years for mining-derived Pb stored in floodplains, soils and alluvial sediments to be naturally removed from a UK catchment (Dennis et al., 2009). Management strategies remediating of mining spoil and ongoing efforts convert a channelized stream system into a multiple channel riparian (Salix and Alnus) deltaic swamp at Brotherswater are required to dampen particulate flux and reduce the movement of dangerous Pb levels. In addition, that lake sediment sequences can faithfully mimic the production and technological development histories of metal mines and the system adjustment post-industry shows the analysis of recent sediment cores can quantify the success level of strategies to implement remediation, an approach more cost effective and less labour-intensive than sediment trapping.

4.5 Conclusions

The Brotherswater sediments have clearly been heavily impacted by historical mining in the catchment, particularly at Hartsop Hall, with Pb concentrations recorded in the deposited sediments exceeding 10 000 ppm at certain depths. These exceptional levels

almost certainly reflect a contamination from a local point-source as opposed to atmospheric delivery.

The sedimentary record portrays mining activity as an important driver of sediment flux over the past 300 years, with known phases of ore extraction coinciding with episodic and substantial increases in sediment mass accumulation rate, in some cases up to two-fold within a few years. The supply of clastic material to Brotherswater also fluctuates throughout the earlier record, which extends to ~CE 600, most likely attributable to known phases of human occupation and more intensive agriculture.

Comparing the written history of Hartsop Hall Mine and the geochemical record of heavy metal contamination offers a number of chronological markers with variable certainty. The most reliable links peak Pb flux to the most intensive phase of mining during the CE 1860-70s, and is verified using ^{210}Pb dating. The inclusion of this date in the Bayesian age-depth model results in better constrained recent ^{14}C ages that have wide probability distributions as a result of atmospheric fossil fuel emissions. A more muted Pb spike dated to the CE 1930-40s mining episode is interpreted to reflect the more advanced ore extraction techniques used at that time which minimised waste, suggesting lake sediment records are sensitive to technological advances as well as the intensity of mining activity.

The Pb profile is well replicated in twelve cores extracted from different parts of the lake, and shows a strong decline in sediment accumulation rates away from the inflow, from ~80 cm in 150 years near the delta to ~17 cm in the depocentre.

Despite the cessation of mining in CE 1942, sediment trap data from 2012-13 show particulate Pb levels in the lake exceed pre-mining levels by more than one order of magnitude and the post-1942 trend has been only slightly negative. These data suggests a recovery in aquatic ecosystem health is unlikely, especially given remediation work at Hartsop Hall is not a priority, and may reflect a regime shift to a new contaminant baseline at Brotherswater, essentially representing an Anthropocene marker.

5 Developing a late-Holocene palaeoflood record from lake sediments: Brotherswater, northwest England

Abstract

Recent severe floods in the UK (Winter 2013-14, November 2009 in northwest England) have raised questions pertaining to the role of anthropogenic climate change in increasing the frequency and magnitude of these extremes. Lake sediment sequences have recently been recognised as a potentially valuable archive of reconstruct the recurrence of floods on centennial or millennial times scales. This paper presents the first attempt to develop a lacustrine palaeoflood record for the UK through high-resolution (0.5 cm) particle size and geochemistry measurements on three sediment

cores (length 1.38 – 3.52 m) extracted along a delta-proximal to distal transect from Brotherswater, a small, deep lake in the English Lake District. The cores were chronologically constrained through integrating two ^{210}Pb profiles, a Pb contamination marker of historical mining and thirteen radiocarbon dates obtained from terrestrial plant macrofossils; prominent geochemical markers enabled the age-depth model to be confidently transferred between cores. Core lithologies exhibit numerous coarser-grained lenses that punctuate a silt-dominated matrix and have been interpreted to reflect deposition by historical high flow events, characterised by peaks in the P90 grain size metric and higher contribution of the coarsest end-member (EM3 or EM4). A normalisation procedure applied to the P90 metric to account for longer-time fluctuations in catchment-derived sediment flux showed good success after temporally testing against historical and instrumental flood records. The process-response link between increased discharge and the delivery of coarser grains has been explicitly demonstrated in two ways: i) using the sedimentological signature of the December 1964 flood as an analogue to discriminate deeper palaeoflood units and ii) the capture of the coarsest material during an 18 month sediment trapping programme in response to high rainfall and discharge in December 2012. The palaeoflood reconstruction is characterised by flood-rich (CE 675 – 775, 1100 – 1300, 1400 – 1500 and since 1850) and generally shorter flood-poor (CE 850 – 900, 950 – 1000, 1300 – 1375, 1500 – 1550, 1625 – 1675 and 1775 – 1825) phases that are most likely attributable to climatic drivers, especially the NAO, but its different seasonal modes makes drawing direct temporal comparisons more challenging. Finally, the possibility that the November 2009 event was among the and potentially the, highest-magnitude flood of the last 1500 years is also shown.

5.1 Introduction

The severe flooding in southern England during the winter of 2013-2014 reiterated the profound socio-economic impacts of prolonged, intense precipitation in the UK (Huntingford *et al.,* 2014). The floods of summer 2007 culminated in £3.2 billion in damages and 15 fatalities (Chatterton *et al.,* 2010). The recent spate of major floods and more regional events (e.g., northwest England, November 2009, J. D. Miller *et al.,* 2013) has fuelled discussion regarding the likelihood for the frequency and intensity of extreme floods to increase during the 21st century conditioned by the sensitivity of the hydrological cycle to a projected warming climate (Knox, 2000; Huntington, 2006).

Probabilistic simulations showed that 20th Century anthropogenic global warming very likely (90%) increased the likelihood of the summer 2000 floods occurring by 20% (Pall *et al.,* 2011). Subsequent climate modelling projects more intensive summer and winter rainfall in the UK through the 21st Century (Kendon *et al.,* 2014). Difficulties disentangling the respective contributions of natural climatic fluctuations, human factors (e.g., removal of riparian woodland, urbanisation of floodplains) or local antecedent hydrometeorological conditions in controlling the trends in flood frequency and magnitude means detecting a significant increase in precipitation-driven floods in the UK resulting from atmospheric warming remains uncertain (Huntingford *et al.,* 2014).

Research in Europe (e.g., Moreno *et al.,* 2008; Swierczynski *et al.,* 2012; Czymzik *et al.,* 2013; Simmonneau *et al.,* 2013; Wirth *et al.,* 2013a; Wilhelm *et al.,* 2013; Corella *et al.,* 2014; Kämpf *et al.,* 2014) and globally (e.g., Noren *et al.,* 2002; Kastner *et al.,* 2010; Schiefer *et al.,* 2011; Schlolaut *et al.,* 2014) has demonstrated that lake sediment sequences can record the distinct imprints of historic floods over centennial to millennial timescales (elaborated in Chapter 2). These sedimentary datasets often exceed the duration of river flow records monitored instrumentally or reconstructed from documentary archives and so offer considerable potential to more fully account for natural variability in patterns in flood frequency and intensity (Swierczynski *et al.,* 2013). This paper presents a finely-resolved palaeoflood reconstruction using lake sediments for the UK of unprecedented duration (~1500 years). The signature of floods preserved in the sediment record has been identified and characterised mainly using particle size data. Use of these data is underpinned by the hydrodynamic relationship between particle size carrying capacity and river discharge (Hjülström, 1939). The particle size metrics are supported by other proxy data, principally geochemistry.

Motivated by the large-scale flooding that affected northwest England in November 2009 (Sibley, 2009; Eden and Burt, 2010; Miller *et al.,* 2013b) and Winter 2005 (Environment Agency, 2006), the aim of this chapter is to contribute to on-going efforts to better understand the hydrometeorological drivers of floods in the River Eden catchment, northwest England (e.g., Lavers *et al.,* 2011; J. D. Miller *et al.,* 2013; Pattison and Lane, 2012), an area of biological and recreational importance and exploited for potable water supply. Record-breaking rainfall and the associated November 2009 flood led to substantial

revision of regional flood frequency estimations (Miller *et al.,* 2013). Placing that event within a longer sediment-based palaeoflood context may contribute further refinement of the flood risk understanding.

The Lake District has a north Atlantic maritime climate often affected by moisture-laden westerly zonal air masses, but the topography creates a highly spatially heterogeneous precipitation distribution (Malby *et al.,* 2007). Cyclonic systems originating from a westerly/south-westerly direction were the trigger for >80% of floods known to have affected the Eden catchment since CE 1976 (Pattison and Lane, 2012). The North Atlantic Oscillation (NAO) is a key control on the strength of atmospheric circulation systems and weather types moving towards Western Europe, including the western, upland UK (Rodwell *et al.,* 1999; Barker *et al.,* 2004; Malby *et al.,* 2007; Pattison and Lane, 2012; Burt and Howden, 2013). Positive phases of winter NAO tend to lead to greater precipitation in northwest England during winter months (Barker *et al.,* 2004), especially at higher-elevation, upland sites (Burt and Howden, 2013). It has been proposed that this mechanism strongly influences the timing and duration of recent flood-rich and flood-poor phases in northern England (Fowler & Kilsby, 2002) and intense precipitation events driven by winter westerly storm systems have increased over recent decades in the region (Malby *et al.,* 2007). Regional climate modelling suggests higher-magnitude flows may intensify by 25% in upland catchments through the 21st Century, with more muted trends in lowland regions (Fowler & Kilsby, 2007).The negative summer NAO mode also delivers cyclonic storm tracks from the Atlantic across the UK (Folland *et al.,* 2009) and thus is coincident with recent severe summer floods. Ascertaining whether the NAO exerted a similar influence on flood frequency and intensity through the past two millennia may improve model projections of future flood risks conditioned by changing NAO and other circulation patterns.

5.2 Study site

Brotherswater is a small, oligo- to mesotrophic upland lake (Maberly *et al.,* 2011) and a Site of Special Scientific Interest (SSSI) located in the eastern Lake District National Park, Cumbria, northwest England. The lake is in the Eamont sub-catchment of the River Eden drainage basin (54.5066°N, 2.9249°W, 158 m above sea level (asl)) (Figure 5.1a and 5.1b). Kirkstone Beck enters the lake at the southeast corner, and is fed by five tributaries draining the upper hills (Figure 5.1c). The lake has a surface area of 0.18

km² and catchment area of 13.01 km² providing a high catchment to lake area ratio (72:1). The deep, bowl-like basin with a flat, central abyssal zone has a maximum water depth of 16 m (Figure 5.1d), limiting the potential for wind or wave-induced remobilisation of profundal sediments for a water-body of these dimensions (Dearing, 1997). Moderate thermal stratification occurs in the lake during the summer months (Maberly *et al.,* 2011). The southern shore is lined by an alder-willow fen woodland, but forest cover in the catchment has been almost entirely replaced by open hill grazing and some pasture.

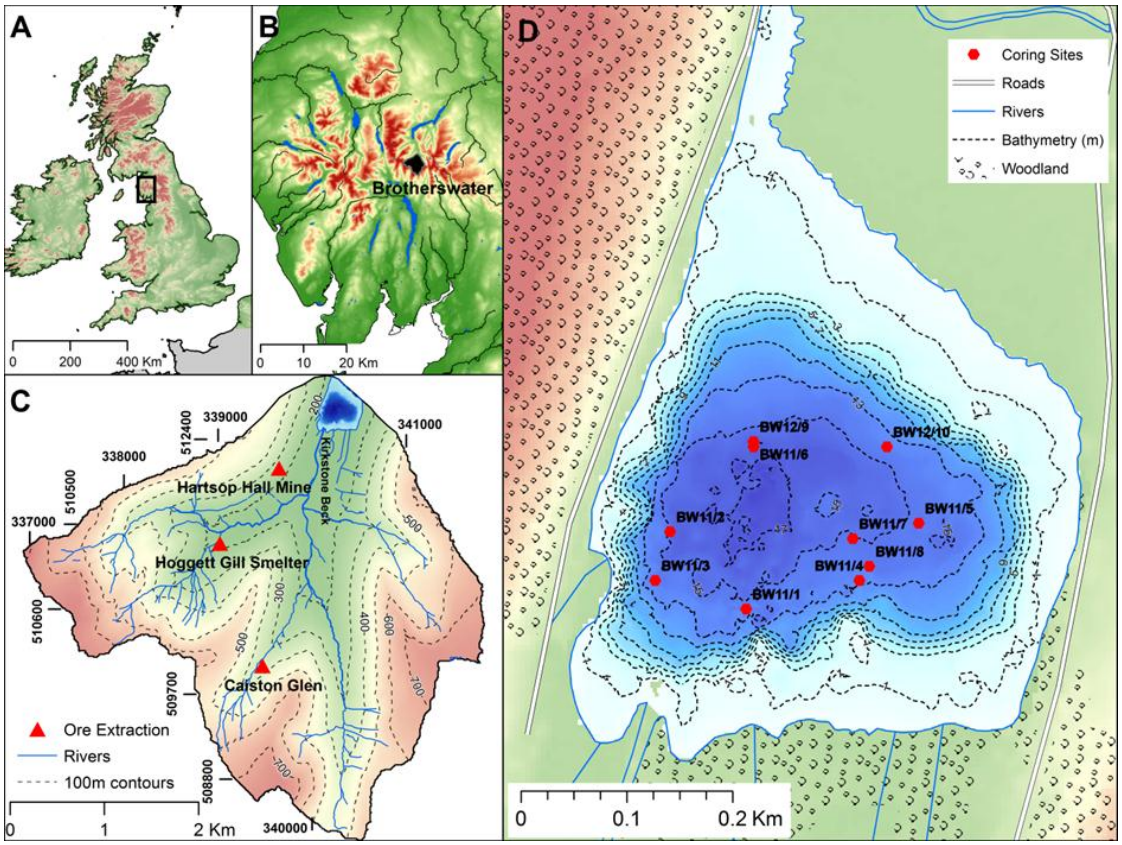

Figure 5-1 A) Location of the English Lake District within the UK. B) Topography and waterbodies within the English Lake District. The extent of the Brotherswater catchment is highlighted. C) Catchment DEM, fluvial system and local ore extraction sites. D) Bathymetric map of Brotherswater showing the location of ten coring locations.

Brotherswater lies in a glacially sculpted trough with steep catchment slopes (total relief within the catchment is approximately 600 m) formed by ice movement during multiple cold stages of the Pleistocene. Catchment geology is dominated by andesitic tufts (96%), interspersed with occasional andesitic and rhyolitic flows (4%), of the

Borrowdale Volcanic Series of Ordovician age, remnants of caldera collapse (Chambers, 1978). The glacial sediments and landforms reflect the most recent Devensian (80-14.7 kya) glaciation and the Younger Dryas (12.9-11.7 kya) ice re-advance (McDougall, 2013). Significant glacial diamict and slope deposits blanket the lower slopes and valley floor (McDougall, 2013), offering substantial sediment availability throughout the Holocene (Ballantyne, 2002). Soils are generally shallow and minerogenic (<30 cm thick), with podzolic brown earth and gleyed soils on lower gradient slopes, thicker peaty deposits on higher ridges and skeletal soils on mid-slopes, often alongside substantial scree deposits (Oldfield and Wu, 2000). Site selection was guided by the physical characteristics of the lake basin and its catchment being potentially conducive to the preservation of palaeoflood laminations (see Chapter 2; Schillereff *et al.,* 2014).

Annual maximum precipitation at Brotherswater is approximately 2400 mm, but varies substantially with altitude across the catchment (Eakins *et al*, 1984). Precipitation gradients across the Lake District means only 800 mm falls annually at Carlisle further downstream in the Eden catchment (Pattison and Lane, 2012). Carlisle has a long history of flooding (Black & Law, 2004; Pattison & Lane, 2012), but the distance between the city and flood generating upland sectors of the catchment should be considered when comparing headwater sedimentary and lowland historical archives.

5.3 Methods

5.3.1 Field and laboratory

Bathymetry was determined using a Garmin dual frequency echo-sounder, with multiple transects across the lake generating >500 points interpolated to produce a bathymetric grid in ARCGIS. Comparison of the bathymetric grid and sounded depths at core location provide a validation and correction for the echo-sound survey. A suite of sediment cores were extracted from ten abyssal locations at Brotherswater between March 2011 and October 2012 (Figure 5.1d). The coring sites form delta-proximal to distal transects from the present-day inflow as well as retrieval of materials from the more sheltered eastern basin. Short gravity cores (0.16 – 0.25 m length, 0.08 m diameter; Boyle, 1995) were obtained at most sites to capture the sediment-water interface while the longer record was sampled as overlapping 1 or 1.5 m drives using a Russian-type corer (0.075 m diameter). Total sediment profiles varied in length between 1.35 – 5 m. Short cores were immediately sliced at 0.5-1 cm intervals. Longer

cores were sealed tightly in polythene sleeves and stored at 4°C in plastic guttering before target cores were sliced at 5 mm intervals and freeze dried. Sub-samples were weighed before and after drying to calculate moisture content. Where multiple drives were recovered, overlaps were verified using water content, particle size, magnetic susceptibility and geochemical profiles. Based on their position within the lake, cores BW11-3, BW11-2 and BW12-9 were sub-sampled at 0.5 cm resolution, weighed, freeze-dried and re-weighed after drying to estimate moisture content. Dry bulk densities were calculated using a value of 2.65 g cm^{-3}, assuming mineral composition is dominated by quartz and feldspar.

The elemental composition of the sediments was measured using X-ray fluorescence (XRF). Wet cores (BW11-3 and BW12-9) were analysed on the Geotek MSCL-XZ bench-top core scanning system at the University of Liverpool which houses an Olympus Delta hand-held energy-dispersive XRF analyser with a Rh X-ray tube. Cores were scanned under Soil mode (40 keV, 40 keV (filtered) and 15 keV beam intensities were applied successively for 20 seconds) for heavier elements and MiningPlus mode (40 keV and 15 keV) for lighter elements. The Olympus Delta completes a daily calibration check against a known standard (Alloy 316 Stainless Steel). Elemental concentrations for the wet sediment cores were converted to a dry-mass equivalent values using a subsample training set (BW12-9) of correlations between wet sediment element concentrations and dry sediment mass specific element concentrations (see Chapter 3.3).

Dried sediment analysis on BW11-2 and the calibration set for BW12-9 was performed using a Bruker S2 Ranger energy-dispersive instrument (Geography, University of Liverpool). Homogenised loose powders were pressed into sample cups lined with 6 µm polypropylene film and were measured under a helium atmosphere at three x-ray intensity settings. Measurements were corrected for variable organic matter concentrations, calculated thermogravimetrically (PerkinElmer S6000) as the mass loss between burn intervals of 230° and 530°C under a nitrogen atmosphere. Both the Bruker and Olympus XRF undergo laboratory consistency checks using a set of up to eight certified reference materials (Table 3.1, Chapter 3.3).

High-resolution particle size measurements were performed on cores BW11-2, 11-3 and 12-9 using a Beckman Coulter™ LS200 laser granulometer (Geography, University of Liverpool). This instrument is capable of determining the dimensions of individual grain sizes within discrete classes from 0.375 to 2000 µm computed using a combined Fraunhofer and Mie optical model. Reference materials of known distribution were

measured before and after each sample set and the standard error of all repeat measurements is 2.03%. Prior to analysis, organic matter was digested with a 30% H_2O_2 solution for a period of 24 h to 96 h dependant on organic content and evaporated to a moist paste on a hot place. Samples were then mixed with a deflocculating solution of 1% sodium hexametaphosphate ($(NaPO_3)_6$) and dispersed ultrasonically to minimise the risk of adhesion between individual grains. Final results were the averages of three successive runs after the three particle size distributions were compared manually to verify complete dispersion.

Particle size parameters were calculated using the geometric measurement formulae of Folk and Ward (1957) within the GRADISTAT 8.0 software (Blott & Pye, 2001). The Folk and Ward (1957) graphical procedures, which are sensitive to the presence of coarse tails in the distributions due to variable sand content (Folk, 1966), are most suitable for describing the broad size composition of the Brotherswater sediments. Furthermore, the majority of particle size distributions are uni- or bi-modal and thus employing conventional frequency statistics is appropriate (Beierle *et al.,* 2002), including presenting log-normal particle size distributions (Blott and Pye, 2001). The measured particle size distributions are considered robust because modal values consistently lie in silt-sized classes and laser diffraction instruments are most effective at differentiating between silt-dominated sediment samples (Roberson and Weltje, 2014). Furthermore, the patterns that emerge between mean, sorting and skewness, depicted in Figures 5.2a-d, approach the sinusoidal (5.2a and 5.2b), circular (5.2c) and helical (5.2d) relationships common in natural settings (Folk, 1966).

5.3.2 Geochronology

The age model for Brotherswater was produced by integrating artificial radioisotopic dating (^{210}Pb, ^{137}Cs, ^{241}Am) using gamma spectroscopy (Appleby *et al.,* 1986) of a delta-proximal and more distal core (BW11-2 and BW12-9s) with 13 radiocarbon ages from BW11-2 and the reconstructed pollution history of local lead mining within the sediments (Chapter 4). Accelerator mass spectrometry (AMS) ^{14}C measurements of 14 terrestrial plant macrofossil samples were performed at the Natural Environmental Research Council Radiocarbon Laboratory at East Kilbride. Sample preparation followed their standard method of an Acid-Alkali-Acid wash to remove dissolved humic acids, the conversion to carbon dioxide by combustion in quartz tubes and graphitisation by iron-zinc reduction. An age model was produced for BW11-2 using

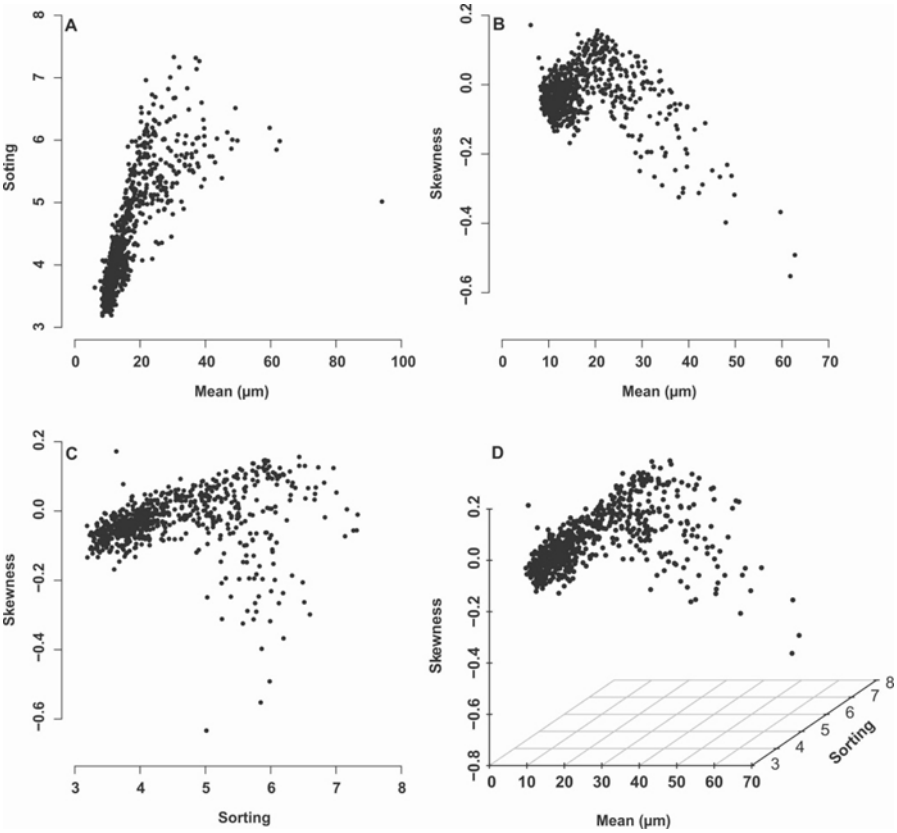

Figure 5-2 Relationships between particle size frequency statistics for BW11-2. A) A sinusoidal relationship is hinted at between mean and sorting; B) A similar relationship is identified between mean and skewness. C) The relationship between sorting and skewness D) To some extent, a helical relationship is observed within the 3D scatter plot comparing mean, sorting and skewness values.

the Bayesian routine 'Bacon' (Blaauw and Christen, 2011) operating in the R environment (v 3.0.1, R Development Team). The MCMC repetitions were constrained by a gamma distribution with mean 5 yr cm^{-1} and shape 2 and a beta distribution with mean 0.5 and shape 20. All ^{14}C measurements were calibrated using the IntCal13 curve (Reimer *et al.,* 2013). The BW12-9s ^{210}Pb chronology was transferred to the BW11-2 master chronology by tightly correlating multiple geochemical profiles (Chapter 4).

5.4 Results

5.4.1 Geochronology

A coherent chronology and age-depth model was generated with five outlying radiocarbon ages for BW11-2 (Figure 5.3). In this model, four 14C measurements appear too old, likely the result of eroded soils delivering 'old carbon' into the lake (cf. Pennington, 1981) and one appears to be too young, potentially due to contamination during sample preparation. Using CE 2011 as the surface age, the Bacon output established a chronology back to CE 519 (weighted mean; CE 593 minimum; CE 417 maximum), although the depths 335 – 351 cm are extrapolated below the deepest ^{14}C age. Two well-defined ^{137}Cs peaks were revealed at 11-13 and 22-23 cm depth in the BW11-2 sequence and 4-5.5 and 9.5-11 cm in BW12-9s. The presence of a ^{241}Am peak coinciding with the earlier ^{137}Cs maxima links it to the 1963 fallout from atmospheric testing of nuclear weapons. The more recent spike therefore relates to emissions from the 1986 Chernobyl event. Comparison of the stable Pb profile with the documented history of Hartsop Hall Mine allows an age of CE 1860 to be assigned to Pb concentrations (>10 000 ppm) at 58 cm, which almost certainly relate to the period of most intensive mining. Distinct geochemical markers in mining related elements (Pb, Zn and Cu) and those associated with the catchment erosion history (e.g. Zr, K and Ti) conditioned by agriculture and reductions in woodland cover facilitate correlation of the age-depth model from BW11-2 to other core sites across the basin (see Chapter 4). Correlation of cores based on mining and lower frequency erosive episodes avoids reliance on matches between more noisy grain size markers.

5.4.2 Sedimentology

Lithology of BW11-2 (Figure 5.4) is relatively homogenous, dominated by silt with variable sand and organic matter content that is reflected in variations between darker and lighter brown units. The sediments turn black towards the top of all cores. The delta-proximal cores (BW11-2 and BW11-3) are more mineral-rich with sporadic light-gray sand lenses visible throughout the sequence and there is no visible evidence of bioturbation or mixing of the laminations. Sediment has accumulated in Brotherswater fairly rapidly throughout the record (typically >0.2 cm yr^{-1}), and the highest sediment accumulation rate (SAR) appears to have occurred during the last 150 years, exceeding 0.4 cm yr^{-1}, while SAR exceeded 0.3 cm yr^{-1} at 160 – 260 cm depth (~CE 1200 – 1500)

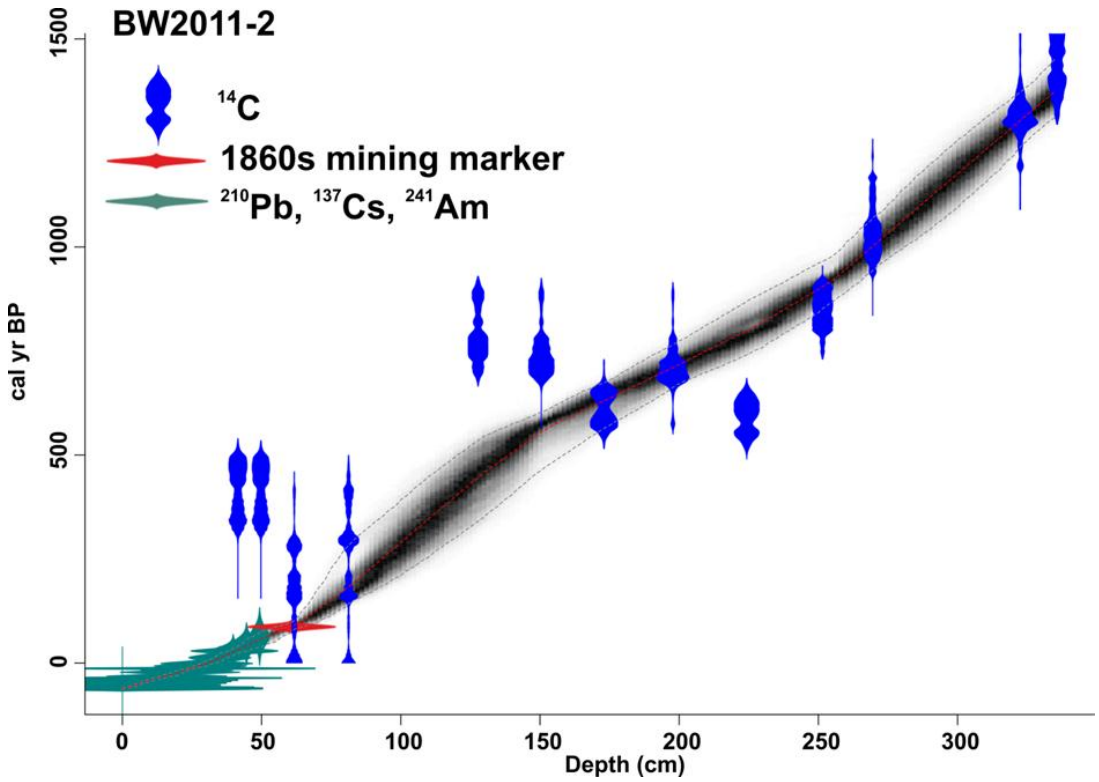

Figure 5-3 Age-depth model for core BW11-2 incorporating thirteen radiocarbon ages (blue symbols), ^{210}Pb and ^{137}Cs radionuclide dating for recent sediments (teal) and the 1860s mining marker in red.

(Chapter 4). Co-variance between the sediment matrix and other proxies is evident, with lighter sediments at 250 – 310 cm and 75 – 175 cm depths characterised by higher bulk density values, coarser grain sizes and higher Ti and Zr concentrations.Conversely, elevated organic carbon content occurs across the darker brown segment at 175 – 250 cm. Phases of particularly coarse grain size are observed at the double-peak between 250 and 280 cm where the P90 values exceed 300 µm, 60 – 110 cm with P90 values higher than 400 µm and similar values reached at 25 – 50 cm. The significant colour change to near-black sediments in surface sediments of all cores was dated by Chambers (1978) using ^{210}Pb to ~CE 1830, and this is confirmed by our chronology and corresponds with an upturn in sediment accumulation rate attributed by the author to drainage of the valley floor and anthropogenic soil disturbance (Chambers, 1978).

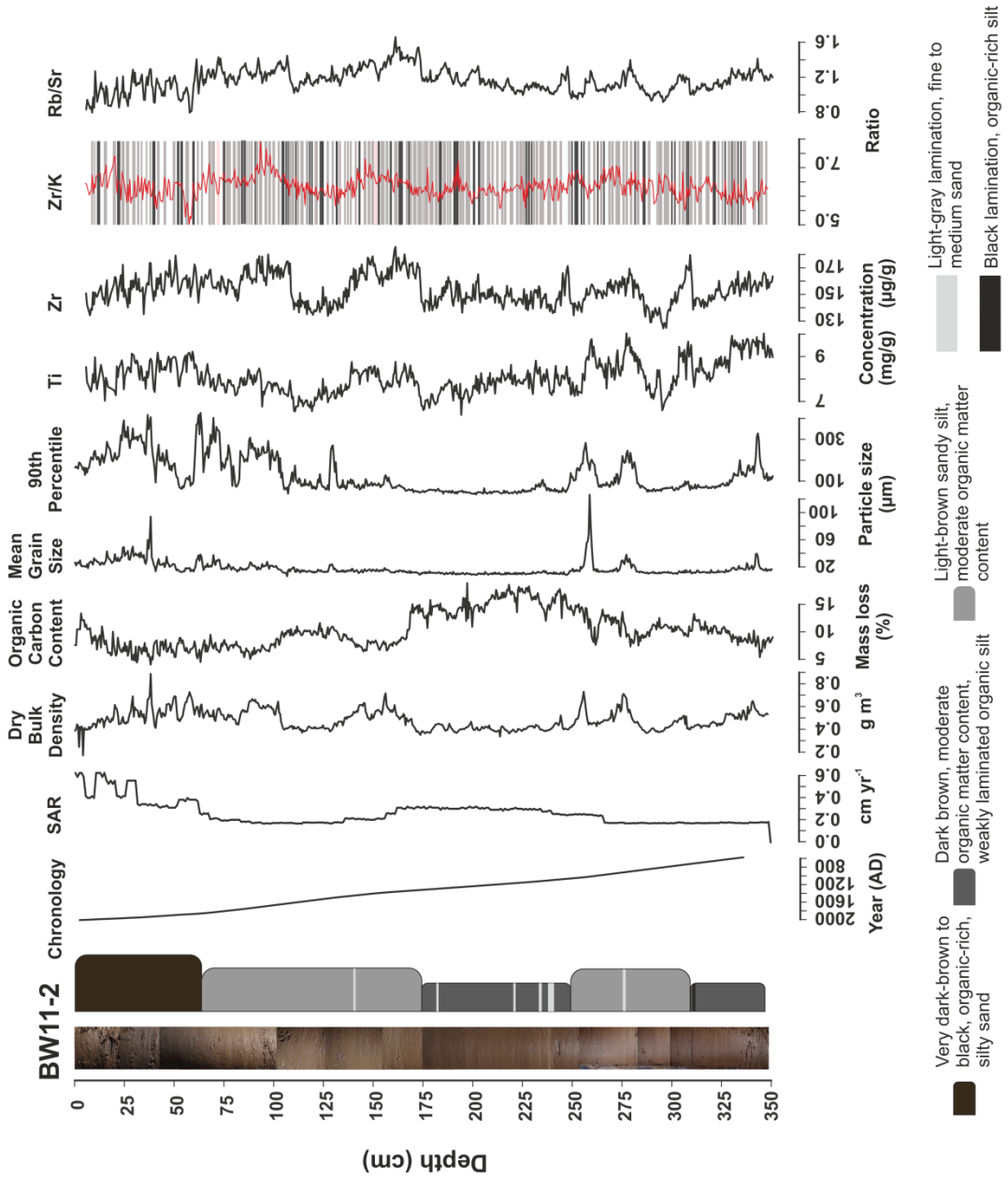

Figure 5-4 Digital photograph and lithostratigraphy of core BW11-2 plotted alongside the chronology, sediment accumulation rate (SAR), dry bulk density, organic matter content estimated via thermogravimetry, mean and 90th percentile particle size data, Ti and Zr concentrations and the Zr/K and Rb/Sr ratios. Light grey layers indicate a correspondence between high Zr/K values and P90$_{normalised}$ exceeding 0.5 σ (see text for explanation). Dark grey bands represent Zr/K peaks that are not concurrent with a change in P90$_{norm}$ and black bands indicate a correspondence between higher P90$_{norm}$ and low Zr/K.

5.4.3 Grain size frequency statistics

For palaeoflood reconstruction, discriminating the coarse layers punctuating the finer-grained sediment matrix is key, which suggests variations in the coarser fraction (e.g., 90th percentile) may be a useful indicator. All the cores depict a silt-dominated sediment matrix punctuated by repeated thin layers or laminations with coarser-grained materials. The profiles of P90, sorting and skewness for BW11-2, BW11-3 and BW12-9 (Figure 5.5a) exhibit down-core variability but with considerable reproducibility of this pattern between cores. The stratigraphical match between BW11-3 and BW11-2 is particularly strong and marked coarse layers occur towards the tops of both BW11-3 and BW11-2. A trend towards finer, better sorted and less negatively skewed sediments is present moving from delta-proximal to distal sites, with P90 values exceeding 600 μm near the delta, but reducing to less than 170 μm in the central basin (Figure 5.5a). BW12-9 from the central basin exhibits some similar features, including the coarser P90 values above the 1860's Pb peak, but a phase of coarser particle size between the Pb peak and the earlier Pb rise is less clear. Below a well-defined marker for enhanced mineral supply (Figure 5.5a), there are greater variations in particle size in BW12-9 relative to the other cores. A selection of particle size distributions (PSD) from BW11-2 mostly display uni- or bi-modal distributions dominated by two groupings, interpreted as reflecting flood and non-flood deposition (Figure 5.5b). The first, a silt-sized fraction with modal particle size of 10-20 μm and typically consisting of 60-85% silt), is present in all distributions, while a second sand-dominated fraction (typically 45-70% sand) with a modal particle size 150-250 μm appears in selected samples. Contour plots of full-core PSDs (Figure 5.7) show this bi-modal behaviour punctuates both the BW11-3 and BW11-2 sequences. The fine silt mode is also present in BW12-9, but the secondary coarser mode is in the silt domain, probably a finer-grained distal equivalent of the now-absent sand component.

5.4.4 End-member modelling of particle size data

End-member modelling of the BW11-2 particle size data using the R package EMMAgeo (Dietze & Dietze, 2013) (v.3.0.1, R Core Team, 2014) partitions datasets into statistically meaningful signals or end members that potentially correspond to sediment delivery processes (Dietze *et al.,* 2012). The modelling process includes a preliminary assessment to delimit the likely number of end-members (q). In order to identify the appropriate weighting transformation (L_w), the variance explained by a

range of L_w values (0 - 0.04; Figure 56a) were assessed. Based on the point of inflection of each q on Figure 5.6b, setting q = three using a low weight transformation (Klovan & Imbrie, 1971) of 0.005 (R^2 = 0.86) appears appropriate due to the large dataset under investigation. Tests confirm that the optimum number of end-members capable of explaining more than 95% of the variance in the dataset (Figure 5.6b) is 3. Modal limits are derived by identifying the most frequent distributions within the entire particle size dataset assimilated from 92 possible grain size classes (0.375 – 2000 μm) collected by the Coulter LM210 (Figure 5.6c). Distinct groupings are visible amongst the modal histograms, lying in the clay, fine silt, coarse silt and fine to coarse sand fractions, although the coarse-silt grouping occurs somewhat less frequently than the others. Running the EMMA algorithm using these limits, q = 3 and L_w = 0.015, un-mixes the grain size distributions into three end-members groupings with dominant modes at 3.21 μm (clay domain), 15.65 μm (fine silt fraction) and 213.22 μm (medium sand). BW11-3 is also partitioned into three end-members (Figure 5.6c), with a coarser sand fraction (EM3 modal value = 282 μm). Four end-members are required to model the

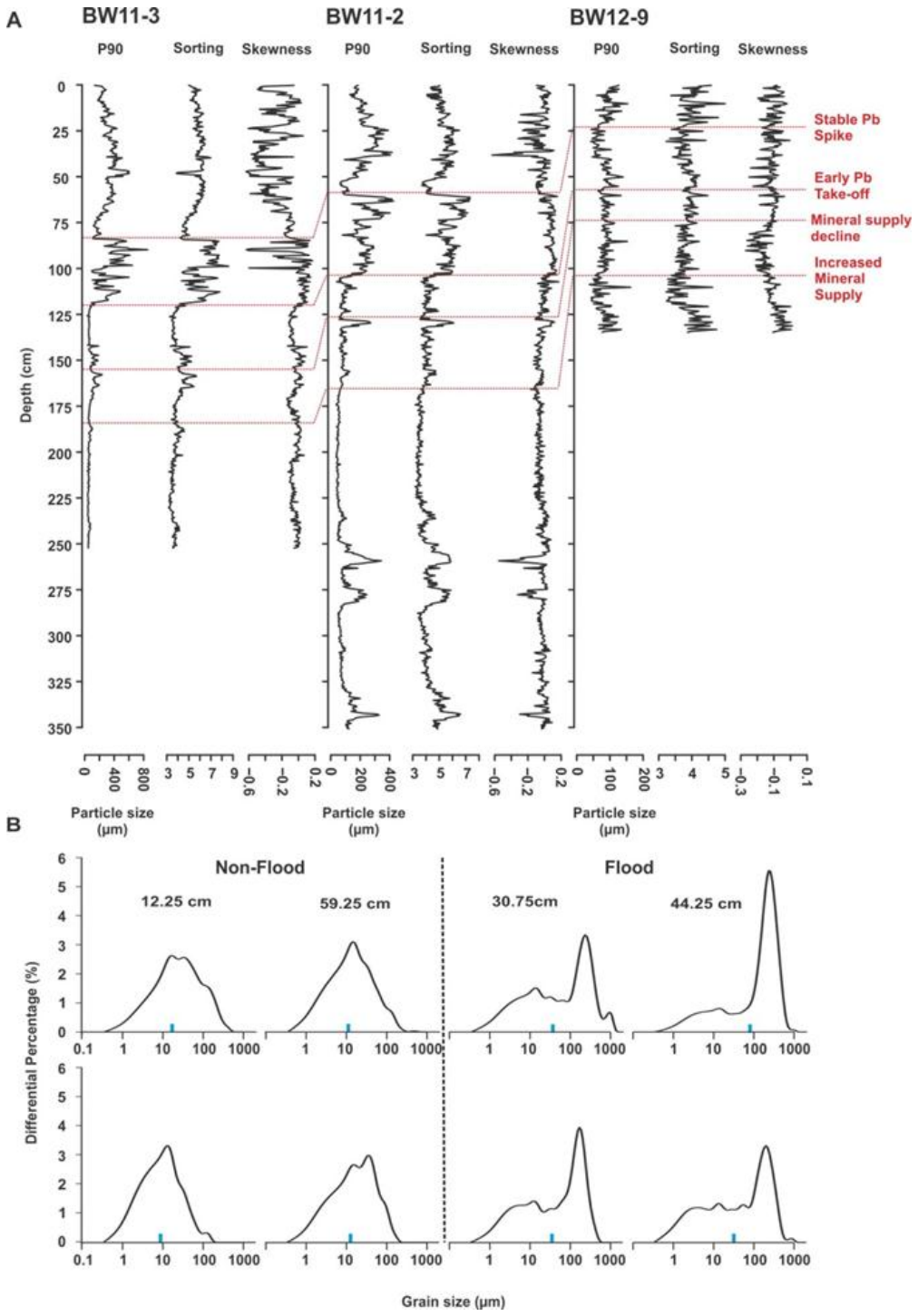

Figure 5-5 A) Down-core P90 (90th percentile), Sorting and Skewness profiles for BW11-3, BW11-2 and BW12-9. Independent stratigraphic markers that correlate across all cores are highlighted by red dashed lines (Discussed in Chapter 4). B) Selected particle size distributions from core BW11-2 interpreted to reflect flood and non-flood conditions. Mean particle size is marked by a blue vertical dash.

BW12-9 dataset (explaining 86% of the variance) including an additional coarse-silt component (EM3) and a significantly finer sand class (EM4 mode = 146.82 μm).While EM3, representing the sand fraction (EM3+4 for BW12-9), declines both in its modal grain size and contribution to overall composition with distance from the inflow (Figure 5.7), its dominant contribution above 120 cm in BW11-3 and 100 cm in BW11-2 suggests a possible flood signal is overprinted by enhanced supply from the catchment (detailed in Chapter 4). The central core (BW12-9) is less influenced by fluctuations in supply, however, and the punctuated appearance of EM4 appears more diagnostic of palaeofloods.

5.4.5 Indirect proxies for grain-size in geochemistry

Preliminary analysis in Chapter 2.1 suggested the Zr/K ratio may be a useful proxy for particle size at Brotherswater. The element Zr is primarily sourced from the resistant mineral zircon and is commonly linked to the abundance of the coarser-grained siliciclastic sediments (Dypvik and Harris, 2001). K and Rb tend to co-vary and represent the fine-grained detrital clay fraction (Dypvik and Harris, 2001; Chawchai *et al.,* 2013; Croudace *et al.,* 2006). Figure 5.4 shows that, for BW11-2, coarser layers most often exhibit elevated Zr/K ratios (light grey bands), but there are occasions where Zr/K peaks do not correspond with coarser units (dark grey). There are also occasional coarse laminations that correspond with a trough in Zr/K. Furthermore, there is no clear relationship in terms of magnitude of peaks in particle size and Zr/K values and commonly used data transformations (e.g., Log_e: Jones *et al.,* 2012) do not improve or alter the relationship. Phases where the relationship is not as strong may be due to periodic shifts between parent material and soil being the dominant catchment-to-lake sediment source (Oldfield and Wu, 2000).

5.4.6 Adjusting palaeoflood proxies for changes in catchment state

Migration of the inflow channel and delta progradation influences the dispersion of fluvially-delivered material into the basin. Historical maps (Ordnance Survey, 1899; Figure 5.8a) show that, prior to CE 1897, the Kirkstone Beck entered the lake on the western margin of the valley floor constructing a delta along the lake shore. Canalisation of the channel sometime after CE 1897 straightened the course of

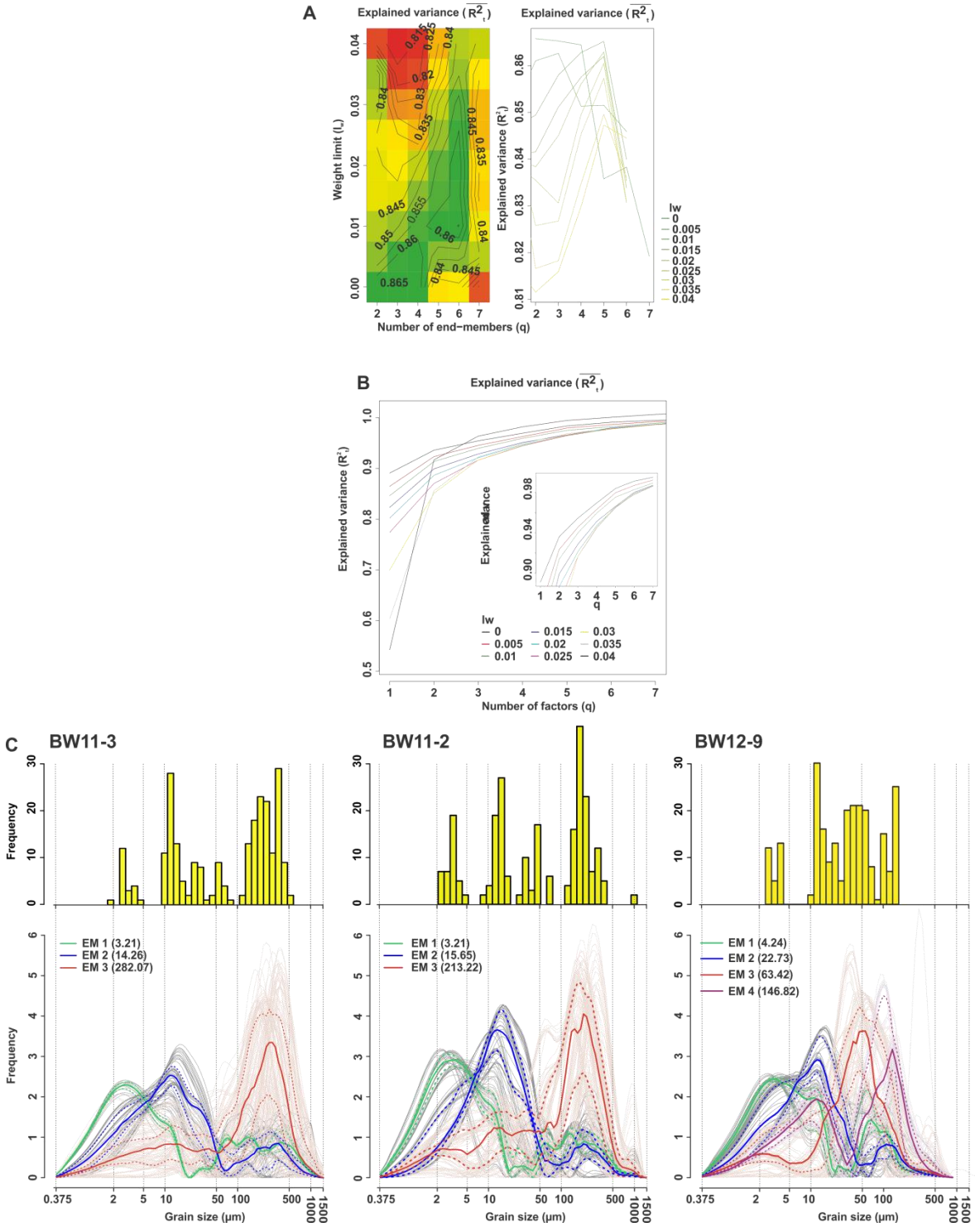

Figure 5-6 A) Variance explained using different q (# of end-members); B) Weighting transformation required when using 3 end-members to explain 95% of the variance; C) Modal histograms and end-member models for BW11-3, BW11-2 and BW12-9, plotted from left to right in order to distance from the inflow.

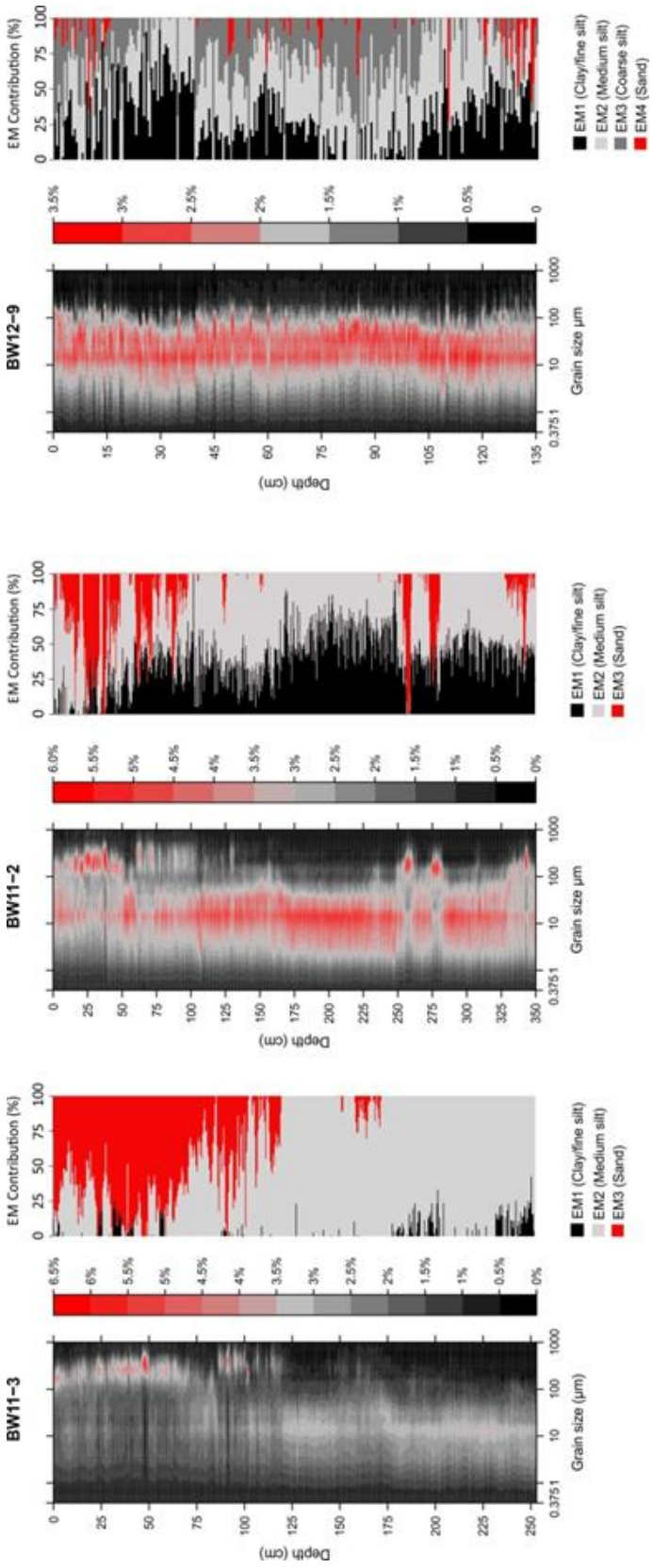

Figure 5-7 Particle size data for cores BW11-3, BW11-2 and BW12-9 expressed as contour plots and according to their down-core end-member contribution.

Kirkstone Beck moving the inflow and producing a prograding gravel delta 30 m to the east (Figure 5.8b). Modification to the channel could impact the sediment load into Brotherswater and could explain the problems with the ^{210}Pb measurements on BW11-2. Implications for the palaeoflood record are limited as the core sites are sufficiently central that the proximal-distal fining trend is consistent throughout and it appears the lateral shift of the delta had little impact on the profundal deposition of coarser materials. A sketch of the Ullswater Valley from ~CE 1595 (Figure 5.9) and a diagram of agricultural land adjacent to Brotherswater from CE 1764 (Figure 5.10) shows the inflow entering Brotherswater (then Broader Water) from the southwestern corner. Over longer timescales, there are two further features on the southern shoreline that appear to relict deltas inactive today. Profundal sediments in the eastern cores (BW11-4, 11-5) show phases of high concentrations of terrigenous elements at depth that likely reflect the distal toes of deltas operating during the mid- to early-Holocene. Uniformity of grain size behaviour through time presented here indicates that the flow has continuously entered the south-western corner of Brotherswater.

A B

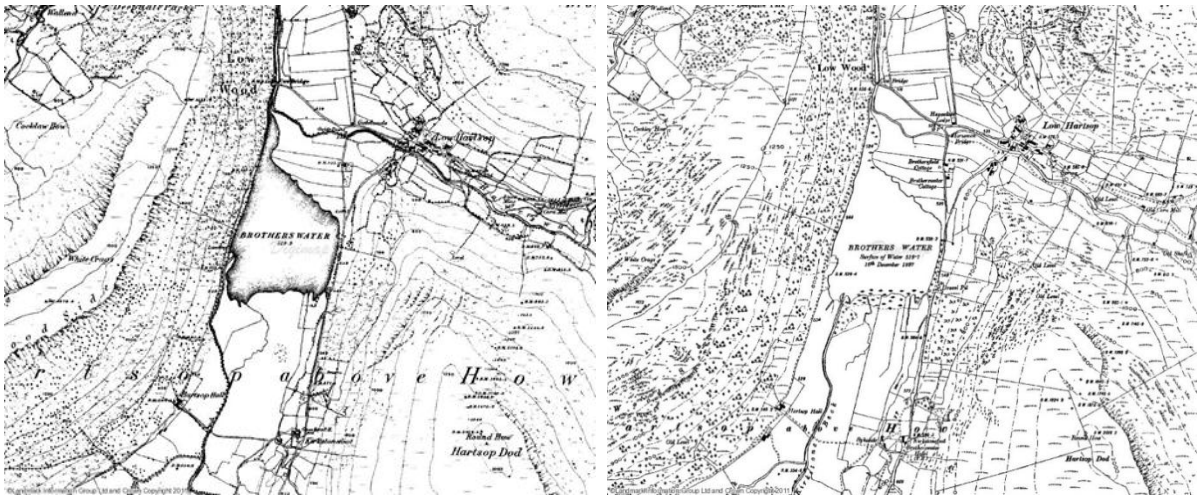

Figure 5-8 Historical Ordnance Survey maps of Brotherswater dating to A) AD 1860;B) AD 1897.

Figure 5-9 Sketch of the Patterdale Valley dated to CE 1595. The study site is labelled 'Broader Water'.

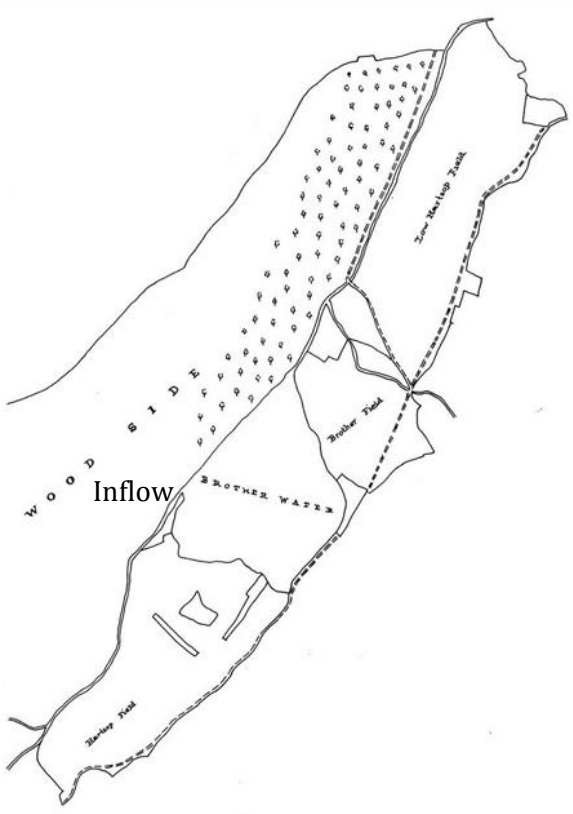

Figure 5-10 Depiction of Brother Field, Low Hartsop Field and (High) Hartsop Field in 1764.

Changes in the provenance and character of material supplied from the catchment also affect the clarity of palaeoflood records preserved in the lake sediments. Cumbria, and northwest England in general, has experienced expansion and contraction of the population and economy (agriculture and industry) throughout the past 200 years, with significant impacts on the geomorphological system driving variations in longer-term or non-event sediment supply (c.f. Pennington, 1991; Chiverrell, 2006; Chiverrell *et al.,* 2007; 2008). Mineral magnetic data for Brotherswater (Oldfield and Wu, 2000) showed variation in relative contributions from eroded soil versus parent material over a 200 year timescale and these are signals manifested over millennia (Chapter 4). In essence, the palaeoflood record has developed in a geomorphological regime that is non-stationary, with phases more and less conducive to rapid flux of materials from the catchment, a plausible explanation for the major contribution of EM3 at the top of BW11-2 and BW11-3.

Correcting for variations in stationarity can be accomplished by plotting the data as residuals of longer terms averages and ranges calculated over the timescales of variation in sediment supply or provenence. Essentially this involves subtracting the mean (μ) and dividing by the standard deviation (σ) (Eq 1) as a moving band-pass window or filter, which discriminate the extremes in grain size metrics (e.g., P90, EM3) within their time domain so positive $P90_{norm}$ excursions will be diagnostic of palaeoflood deposits.

$$P90_{normalised} = \frac{(P90 - P90\mu)}{P90\sigma} \qquad \text{(Equation 1)}$$

5.4.7 Signature of a known event

Underpinning this research is a process-response linking delivery of coarser materials with increases in river discharge, specifically floods and explicit demonstration of the mechanisms on a site-specific basis is critical. At Brotherswater, the distinctive sedimentary fingerprint at 14.75 -18.75 cm was initially linked to the March 1968 flood (Chapter 2) but subsequent analysis based on the second ^{210}Pb series for BW12-9 suggests it is more likely to be December 1964. Discharge data obtained from Pooley Bridge (outflow of Ullswater) subsequent to the formal publication of Chapter 2 (Schillereff *et al.,* 2014) show the CE 1964 event was regionally much larger so this unit

is more likely to represent deposition during this flood. The contour plot (Figure 5.11a) illustrates a shift to a bi-modal particle size distribution with the dominant modal grain size lying in the medium sand domain, similar to the P90 and EM3 full-core profile (Figure 5.7). The potential flood-indicator particle size parameters (P90, P50) show a gradual coarsening upwards gradient and fining from peak grain size across the sedimentary unit (Figure 5.11a), a pattern identified in deeper possible palaeoflood laminations (Figure 5.11b). The flood layer also becomes progressively more poorly sorted and negatively skewed, reflecting an abundance of fine grains towards the top of the unit. The flood unit is also characterised by increasing dry bulk density values mirroring the coarsening grain size (0.51 g cm^{-3} at 16.25 cm depth) and by lower organic matter content. Two geochemical ratios, Rb/Sr (Vasskog *et al.,* 2011) and Zr/K (Chapter 2; Schillereff *et al.,* 2014) commonly used to discern variations in particle size also portray a similar profile peaking at 16.25 cm.

This association is also visible when Brotherswater sediment trap data are compared with local meteorological and hydrological records. Persistent rainfall through December 2012 led to the highest discharge of the sampling interval (Oct 2012 – Jan 2013) in Goldrill Beck (outflow of Brotherswater) between Dec 29 and Jan 1 (Figure 5.11c), a temporary lake level rise of ~60 cm and short pulses of elevated water

temperature in Brotherswater, most likely reflecting a warm river water plume (Figure 5.11c). The PSDs (Figure 5.11d) of trapped material are exceptional compared to the rest of year, heavily skewed towards the sand fraction. Mean particle size declines with water depth (top trap = 62 μm; middle trap mean = 50 μm, bottom = 43 μm), suggesting Kirkstone Beck under flood conditions delivered coarse suspended material that diffused across the upper lake as a hypopycnal flow, exiting suspension according to particle diameter (Stokes, 1851).

In summary, metrics for coarse particle size peaks across flood events discerned from monitored data and the recent stratigraphy in Brotherswater provide a framework for assessing the longer stratigraphical record.

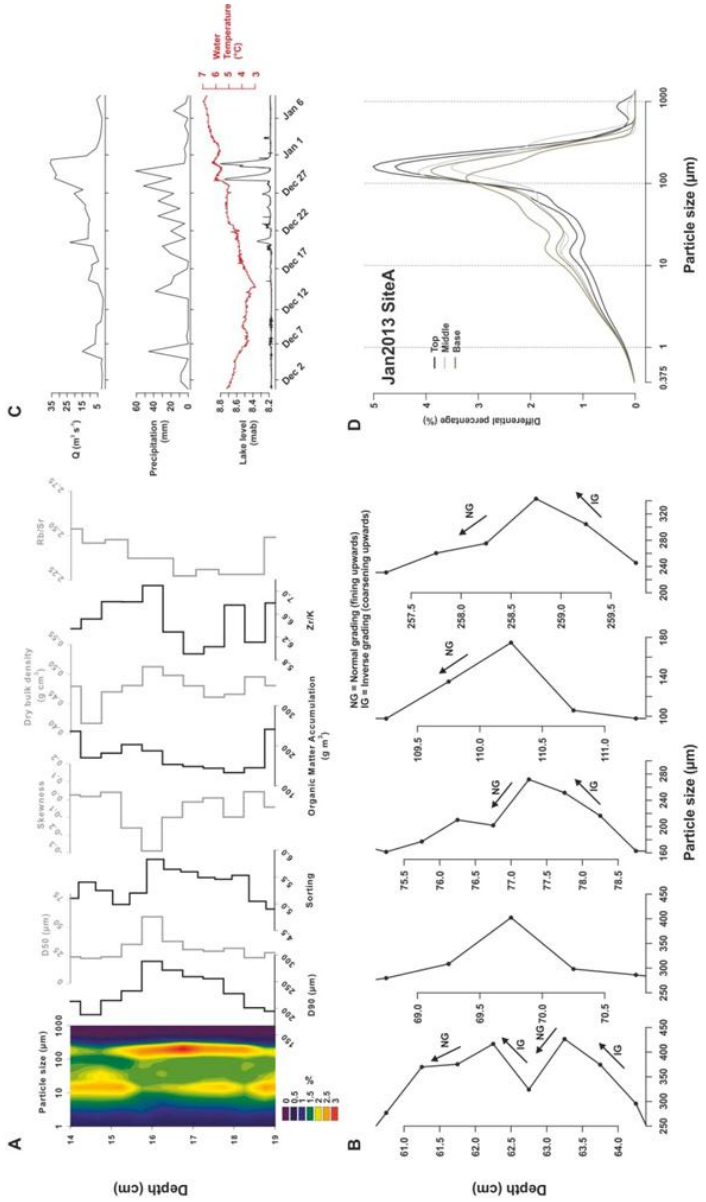

Figure 5-11 A) Multi-proxy information across the likely December 1964 flood. B) Sedimentary units in core BW11-2 that exhibit an inverse underlying fining-upwards grading sequence. C) Local hydrological and meteorological data for Brotherswater measured between 01/12/2012 and 07/01/2013. Daily maximum discharges measured at Patterdale Side Farm, Goldrill Beck (the outflow of Brotherswater), daily rainfall recorded at Hartsop Hall and lake level and water temperature recorded at ten-minute intervals using barometric pressure loggers installed at 4 m water depth on a delta-proximal sediment trap. Lake level expressed as metres above lake bed. D) Particle size distributions for material recovered in Jan 2013 from the top, middle and bottom delta-proximal sediment traps installed in Brotherswater.

5.5 Discussion

5.5.1 Lake sediment evidence for past floods

The aim in characterising flood laminations in sediment sequences is primarily to discern the frequency and/or absolute/relative magnitude of these events. Declining grain size (P90: Figure 5.4), Pb concentrations in sediment profiles (Chapter 4) and EM3 contribution (Figure 5.7) with distance from the inflow delta show that Brotherswater receives sediment primarily as fluvial delivery from the catchment. Dominance of terrigenous sediment supply over autochthonous materials is conducive to the deposition and preservation of a palaeoflood record in lakes (Chapter 2; Schillereff *et al.,* 2014).

Decomposition of the particle size data for three cores (delta proximal to distal) highlights two dominant fractions interpreted to reflect key depositional processes (Figures 5.6 and 5.7). Fine material accumulates throughout the record, probably a combination of autochthonous organic or silicaceous material along with fine silts and clays (End-members 1 and 2; modal grain sizes ~3 and ~15 μm) carried in suspension into the lake under normal or low flow conditions. Samples characterised by the coarser mode (EM3 and EM4, modal values 146 - 282 μm) occur in all three cores although lower frequency phases of enhanced mineral supply masks a clear signal of discrete palaeoflood laminations near the inflow (BW11-2 and BW11-3). The punctuated nature of EM4 in BW11-9 and its tight match to the $P90_{normalised}$ metric is interpreted here as reflecting more substantial floods. The deposition of such material in the central basin (maximum P90 in BW12-9 is 150 μm) requires powerful river plumes capable of transporting coarse particles considerable distances from the inflow. Sediment trap data (above and Chapter 6) and fluvial bedload measurements (Chambers, 1978) confirm only higher magnitude flows transport coarser calibre particles (fine to very fine sand) into Brotherswater.

Discrete units at least two times thicker than the sampling interval in some cases contain internal structure that record the depositional mechanisms controlling the dispersal of sediment-laden river plume within the lake. The 1964/8 flood deposit (5.7a) as well as deeper palaeoflood layers (5.7b) display the inverse-grading (coarsening-upwards) followed by normal-grading (fining-upwards) characteristic of deposition from a hyperpycnal turbidity current (Sturm and Matter, 1978; Mulder and Alexander, 2001; Schillereff *et al.,* 2014; Chapter 2). These occur when the inflow

suspended sediment concentration exceeds the density of the water column, causing the plume to rapidly plunge to depth and disperse across the lake bed, keeping particles entrained due to turbulent momentum (Mulder *et al.,* 2003). Such deposits have been identified in a number of lacustrine palaeoflood records (e.g., Hofmann and Hendrix, 2010; Stewart *et al.,* 2011; Czymzik *et al.,* 2013). The 0.5 cm sampling interval prevents the microstructure of thinner layers from being determined, such as 69.25-70.25 cm depth in BW11-2 (Figure 5.11b). Where grading is absent (or unobserved), a hypopycnal flow is more likely, where the plume remains buoyant and spreads across the upper water column. Particles thus settle out of suspension at a rate mostly determined by their diameter, density and shape (Stokes, 1851). Brotherswater develops a moderately thermal stratification in summer (Maberly *et al.,* 2011) thus summer flood events are more likely to generate hypopycnal flows. Limnological and sediment trap (Chapter 6) data indicate both hypopycnal and hyperpycnal flows can occur at Brotherswater (Chambers, 1978).

5.5.2 Late-Holocene palaeofloods in NW England

Sediment depths characterised by peaks in the $P90_{normalised}$ profiles are interpreted as reflecting significant high-magnitude discharges if they exceed a 1.5 sigma (σ) threshold (set at 1 σ for BW12-9 due to slower sediment accumulation) (Figure 5.12). The filtering procedure is assumed to also account for possible shifts in the exceedance threshold through time. This produces a palaeoflood record for northwest England that spans nearly one millennia in cores BW11-3 and BW12-9 and ~1500 years in BW11-2. The frequency of events is not consistent through the record; instead, intervals of 50-200 years can be classed as flood-rich or flood-poor (≤1 in ≥50 years). High flood recurrence is highlighted in all three cores at CE 1100-1300 (BW12-9 ends at CE 1200), CE1400-1550 and through the 20th Century, highlighted in light grey in Figure 5.12. A flood-rich phase present in two of the cores dates to CE 1575-1700 and a link may be drawn between two 18th Century flood deposits in BW11-3 and BW12-9. The BW11-2 chronology was transferred to the other cores using non-particle size metrics (primarily geochemistry) so there is not an issue of circular reasoning in the stratigraphical correlation.

Comparising the number of events in each flood-rich band (light grey shading) reveals that the BW11-3 CE 1100-1300 period contains 11 peaks, although the proximity of double-peaks at CE 1110 and CE 1310 means they could represent multiple sediment

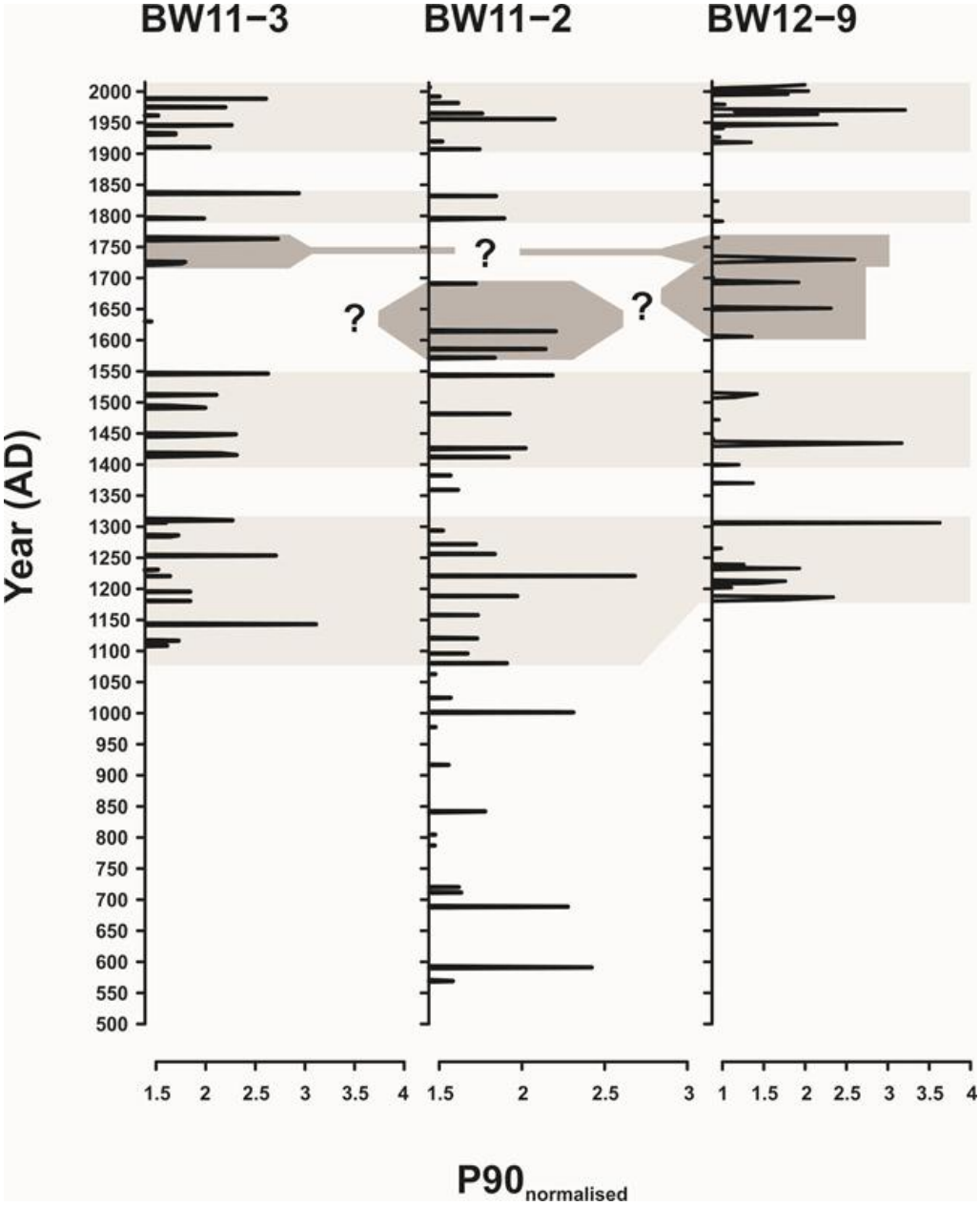

Figure 5-12 Normalised 90th percentile ($P90_{normalised}$) profiles for three cores plotted along a delta-proximal to distal transect. A 20 point moving filter was applied to the BW11-3 data and a 10 point step size to BW11-2. Light grey regions highlight flood-rich phases identified in all cores. Dark grey blocks represent flood-rich phases that can be tentatively linked across two of the three cores.

pulses during a single event, equalling the nine peaks in BW11-2. Five events appear in BW11-3 during the CE 1400-1550 interval compared to four in BW11-2 and BW12-9, although one additional peak is present slightly earlier in both cores. Limited

relationship is observed between the calculated $P90_{normalised}$ values of individual units traced across the three cores, although the exceedance values of the two 19th Century events decline with distance from the inflow, perhaps reflecting deceleration of the flood plume (Kämpf *et al.,* 2014a).

Historical data (since ~CE 1770) compiled for the River Eden and Carlisle in particular (Black and Law, 2004; Pattison and Lane, 2012) identify 137 floods, which exceeds the number recorded in the Brotherswater sediments. Discrepancies with the Brotherswater palaeoflood record are attributable to three possible factors: firstly, it is highly likely that fewer floods than recorded in the historical record are of sufficient magnitude to leave a sedimentary imprint. Secondly, event sequencing may condition the regime unable to produce a signature for successive floods, whereby a large event depletes catchment sediment stores and subsequent flood(s) deliver insufficient material to overprint natural lacustrine sedimentation. Thirdly, the flood generating mechanisms may differ between the small, upland catchment of Brotherswater (probably short, intense events) compared to the larger watershed of the River Eden. Northwest England, and the Lake District in particular, has a spatially heterogeneous distribution of rainfall (Lean & Browning, 2013) and Carlisle lies in the lowland coastal floodplain. Brotherswater is only part of the River Eden headwaters, with further east headwaters in the Pennines lying in the rain shadow of the Lake District fells (Mayes, 1996).

As a result, directly integrating the dates of documented floods into the Brotherswater chronology is unwise and could lead to circular reasoning when correlating the records. Instead, temporal links are tested by comparing the timing of the most severe historically documented floods for the River Eden (British Chronology of Hydrological Events (BCHE); Black and Law, 2004) with the probability distributions yielded by the age-depth model for each detected palaeoflood unit (Figure 5.13). Age probability distributions for the 13 layers in core BW11-2 where $P90_{normalised} > 1\ \sigma$, and thus are interpreted as flood deposits, were generated using the Bacon.hist() function in the BACON software (Blaauw and Andrés Christen, 2011) and the weighted mean age and 95% age range were calculated for each flood deposit.

Comparing the dates of the fourteen severe floods noted for the local area in the BCHE plus the CE 1953 heavy rainfall event recorded near Grisedale Beck (outflow of Brotherswater) (vertical lines) with the weighted mean ages for flood laminations at Brotherswater reveals strong matches with the deposition of a flood layer at CE 1710,

1822, 1856, 1933 and 1953 (Figure 5.13). Less strong, but reasonably convincing cases can be made for CE 1696 (96.75 cm), 1763 (83.25 cm) and 1925 (42.25 cm). Some noted historical floods cannot be confidently tied to sediment units; intriguingly some of these coincide with floods that occurred in rapid succession e.g., CE 1809 and 1815, and CE 1903 and 1914 floods. Perhaps sediment stores were flushed from the catchment during the earlier event leaving limited material was available for later floods (Kämpf *et al.,* 2012). Recovery time between floods may also condition the completeness of the lacustrine palaeoflood record. The flood in CE 1868 occurred during the most intensive phase of mining, which encouraged considerable flux of sediment to Brotherswater (Chapter 4), possibly masking the flood event stratigraphy. Conversely, one coarse layer assumed to have been lain down by a flood (88.75 cm) does not correlate with a historically documented event.

Comparison between the sedimentary record and instrumental river flow data for Grisedale Beck (the outflow of Brotherswater) also reveals some degree of correspondence (Figure 5.14). Temporal uncertainty remains the greatest challenge because the coherent ^{210}Pb record including prominent ^{137}Cs peaks in BW12-9 and to a lesser degree in BW11-2 are based on sediment slices of at least 1 cm thick. As a result, age uncertainties of ±3 years for a single sample are propagated into larger errors for a sediment core sampled at higher resolution (i.e., 0.5 cm). Furthermore, river discharge exceeded 35 m^3 s^{-1} on more occasions than palaeoflood deposits were identified, so either event sequencing or the 0.5 cm sampling interval prevented thinner laminations from being discriminated. Nevertheless, some links between high discharge and flood deposits can be made with reasonable confidence: The 1960s peak present in all cores probably relates to the 1964 flood and the 1968 event has been captured in BW12-9. The post-1990 record matches well in BW11-2 and BW12-9: high discharges in 1995, 1997, 2004 and 2005. Examining the cores immediately post-extraction suggested some sediment loss at the top of BW11-3 so the absence of these deposits is reasonable. The 1980s are most difficult to explain: the feature dated to 1975 in BW11-3 and 1985 in BW11-2 is probably the same event but chronological transferral at cm-scale resolution was inaccurate; the same signal may be present in BW12-9 as three more muted peaks. It seems most reasonable to tie these layers to the successive floods of high magnitude in 1985 and 1989.

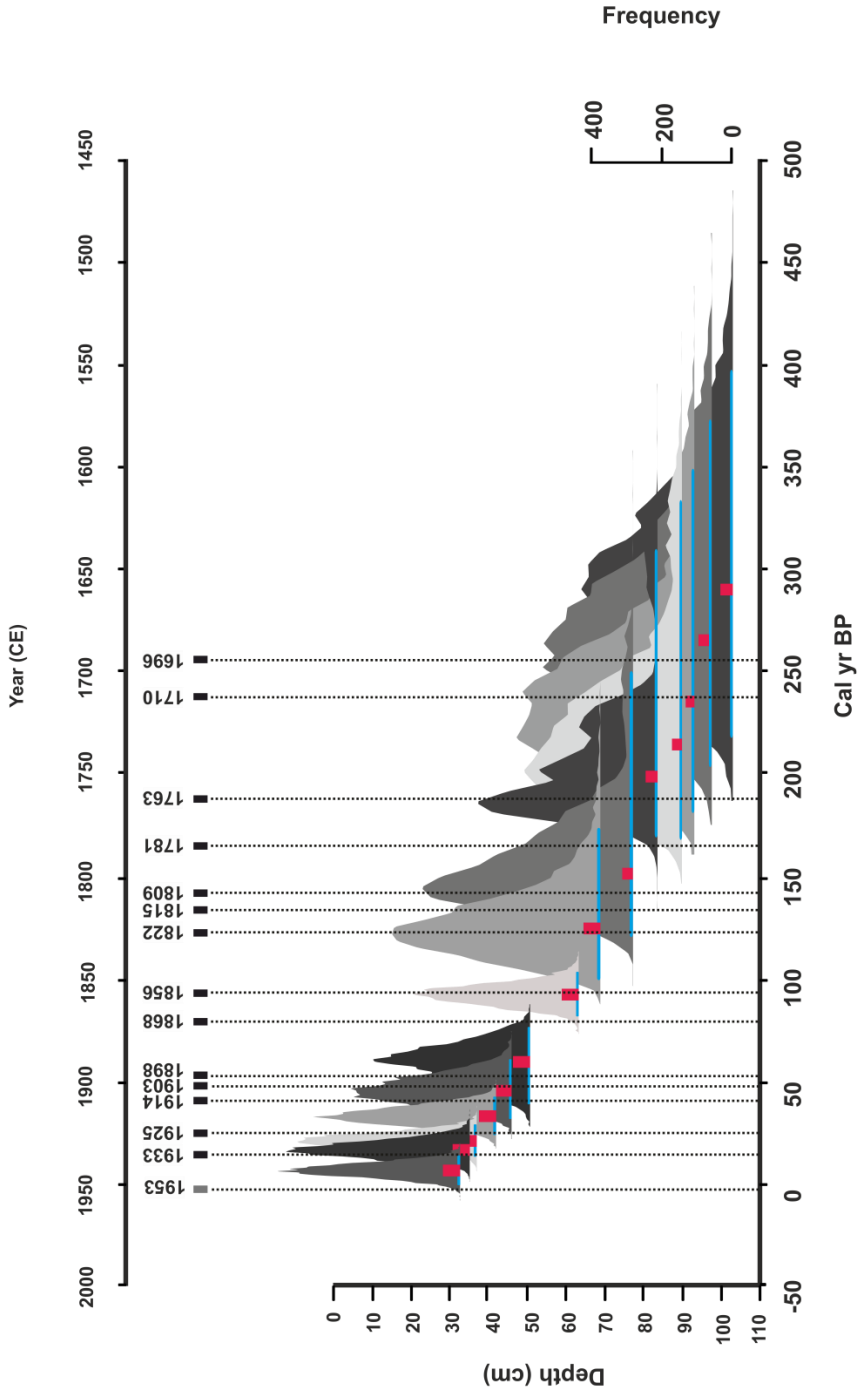

Figure 5-13 Age probability distributions for each sedimentary unit interpreted to reflect a palaeoflood deposit. The probability distributions are plotted so that their bases correspond with the basal depth of each unit and they are scaled proportionally using the right-hand y-axis. The red marks reflect the weighted mean age for each distribution and the blue horizontal line reflects the 95% age range. Vertical black dashes highlight known historical floods and the dark grey dash represents a recorded high rainfall event.

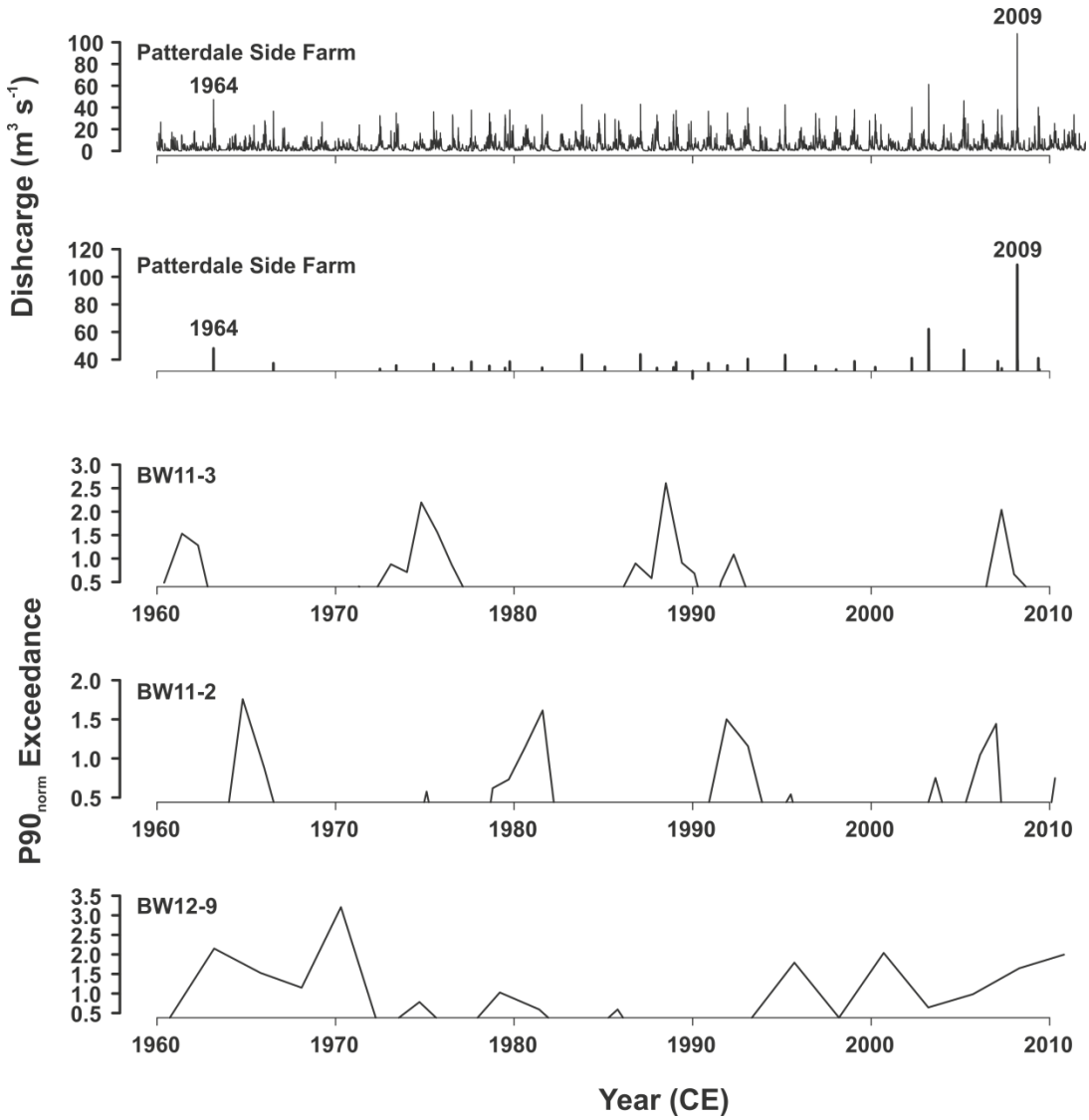

Figure 5-14 Comparison between Grisedale Beck discharge, recorded at Patterdale Side Farm since CE 1960, and normalised P90 values exceeding 0.5 σ for BW11-3, BW11-2 and BW12-9. The lower discharge graph displays those flows that exceeded a threshold of 35 m^3 s^{-1}.

5.5.3 Flood-rich periods and climate forcing

Assimilating the occurrence of flood laminations (henceforth) in core BW11-2 using a 50-year moving window (Figure 5.15) highlights those periods rich with $floods_{P90}$: CE 675 – 775, 1100 – 1300, 1400 – 1500 and since 1850. More short-lived episodes flood-rich episodes occurred at CE 1550 – 1600 and 1700 – 1750. The hydrological regime was characterised by fewer floods at CE 850 – 900, 950 – 1000, 1300 – 1375, 1500 – 1550, 1625 – 1675 and 1775 – 1825, periods that are generally shorter in duration

than the flood-rich intervals. Periods characterised by more frequent flooding correspond in part with those previously identified at Brotherswater (Chambers, 1978), but there were significant problems with age reversals in the radiocarbon chronology of this earlier work. The flood-rich periods spanning CE 1200-1300 and 1550-1600 corroborate well with a national synthesis of historical high-magnitude floods (Macdonald, 2014) but the paucity of floods recorded from CE 1775-1825 is a localised signal.

Extreme rainfall capable of generating floods does not always correlate with longer-term precipitations trends. In the case of the wider River Eden catchment, however, Malby *et al.,* (2007) showed southwesterly and westerly air masses make the principal contribution to decadal-scale precipitation and are the most important regional flood-triggering weather type (Pattison and Lane, 2012). A 250-year annual rainfall reconstruction for Carlisle (Todd *et al.*, 2014) shows higher rainfall in the mid-18th and early- to mid-19th Centuries, corresponding to more frequency $P90_{flood}$ but at the monthly scale, limited temporal correlation is observed with a 200-year monthly-resolved precipitation record reconstructed from documentary sources for Grasmere, central Cumbria (Barker *et al.,* 2004).

Looking at the entire record, visual assessment of the timing of P90 flood-rich/flood-poor phases and variability in precipitation reconstructions for the UK based on multiple proxies suggests an in-phase relationship (Figure 5.15), although both intra-proxy agreement and their temporal match to the palaeoflood record are variable. Flood-rich phases and shorter flood-poor episodes tend to coincide with higher and lower annual precipitation, respectively, in southern England reconstructed from *Quercus* tree-rings (Wilson *et al*, 2013) over the last 1000 years, except at CE 1400-1500. This interval is characterised by higher bog surface wetness levels in northern Britain (Charman *et al.,* 2006), however the period of increased flood frequency during the Medieval Climate Anomaly (CE 1100 – 1300) is represented by drier conditions in the peat-based reconstruction. We also observe phased agreement between our record and a reconstruction of annual precipitation derived from the growth rate of a stalagmite from northwest Scotland (Proctor *et al.,* 2002), especially at CE 600 – 775, 1400 – 1500, 1550 – 1600 and 1700 – 1750 but the CE 1100 – 1300 episode is absent. Importantly, the fairly short-term nature of the flood-poor phases points towards a climatic control on flooding; known phases of human occupation in northwest England tend to occur over longer time spans (Chiverrell, 2006). Furthermore, the onset of

more frequent flooding after CE 1100 appears too late to associate with the increased sediment flux linked to Medieval land pressure (see Chapter 4).

The link between sedimentary-based flooding and precipitation is assessed in a quantitative manner through comparing whether the number of $P90_{flood}$ laminations at Brotherswater detected in the 50-year phases corresponds to patterns of rainfall across the equivalent periods (Figure 5.16). A statistically significant relationship ($p \leq 0.01$) is observed for all three precipitation proxies, with moderately high, positive correlation ($r^2 = 0.309$, $r^2 = 0.554$) with the Lamb (1965) and Wilson et al. (2013) records, respectively. A negative relationship is observed with the Proctor et al. (2002) dataset, but as slower annual growth rates of speleothem layers are driven by increased precipitation, the P90flooding-rainfall link is consistent, although the strength of the regression is substantially lower ($r^2 = 0.109$). The Charman et al. (2006) record could not be used in the comparison due to the variable temporal resolution of the data points.

The build-up of westerly airflows from the North Atlantic, linked to the NAO, is generally considered the most important storm generating mechanisms for the region (Pattison and Lane, 2012; Burt and Howden, 2013). NAO appears to intensify rainfall events at higher elevations in particular (Burt & Howden, 2013); sites such as Brotherswater with heavily grazed, steep catchment slopes are thus at greatest risk from localized flooding (Orr and Carling, 2006; Malby *et al.,* 2007). However, the different seasonal NAO modes make it difficult to diagnose the principal forcings. Positive shifts in the winter NAO (wNOA) have been proposed as a driver of extreme floods in northwest England (Wilby *et al*, 997; Pattison & Lane, 2012), and wNAO entered a persistent positive phase from CE 1049- 1450 and CE 1550 – 1600 (Trouet *et al.,* 2009), during which floods were common at Brotherswater. The inverse relationship holds during the early 17th century (low flood frequency concurrent with negative wNAO anomaly) but breaks down during the moderately flood-rich CE 1700s when wNAO weakened through the Little Ice Age (Trouet *et al.,* 2009). Conversely, Macklin and Rumsby (2007) attributed extreme flood occurrence in upland Britain to *negativ*e wNAO, which would explain the latter finding but decouples elsewhere in the record. The summer NAO (sNAO) is a muted companion of the winter mode that influences the UK summer flood regime (Folland *et al.,* 2009) but shows limited connection to the Brotherswater record; in particular a paucity of floods during the CE 1800s despite the strongly negative sNAO. Furthermore, contemporary data show

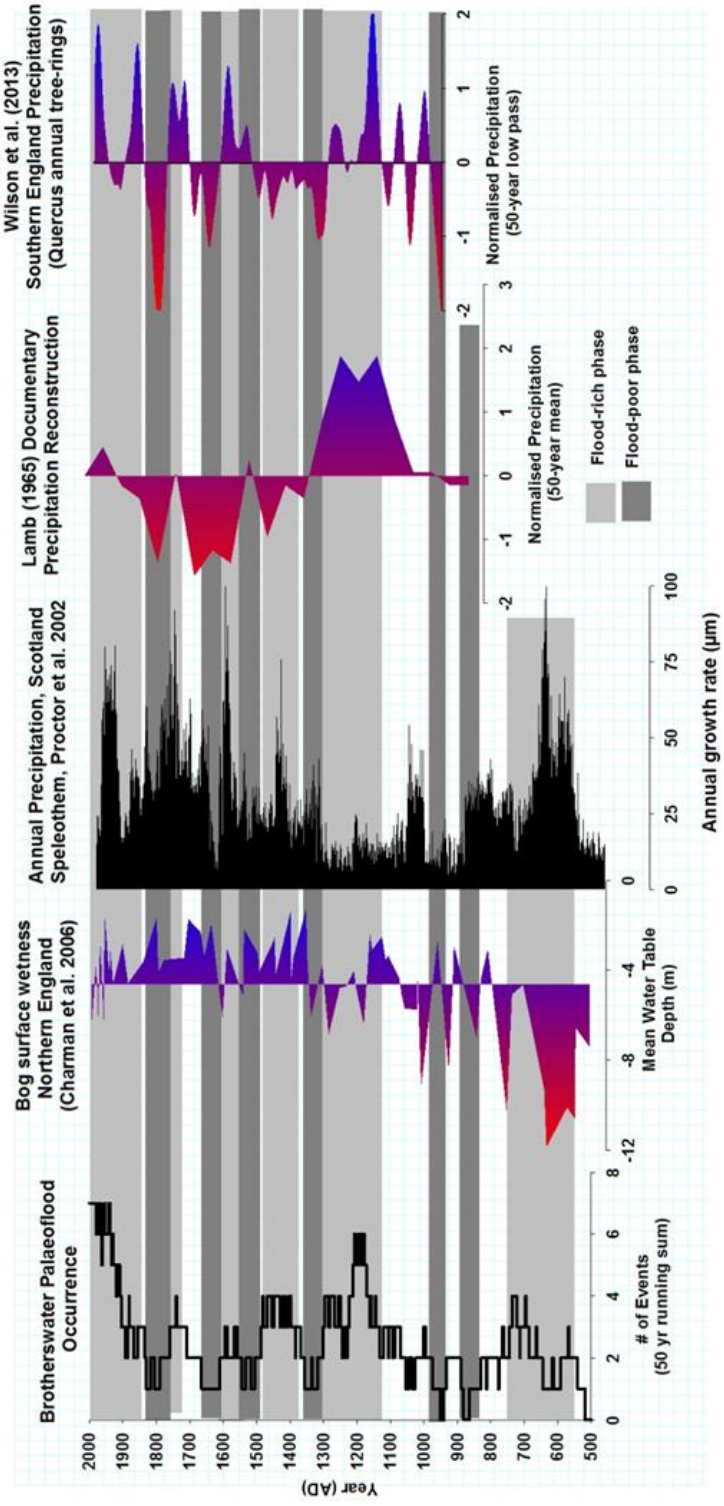

Figure 5-15 Comparison of the Brotherswater palaeoflood time-series with regional precipitation reconstructions based on multiple UK palaeoclimate proxies. These include testate-amoebae reconstructions of bog surface wetness, annually-resolved speleothem and *Quercus* tree-ring records and documentary sources.

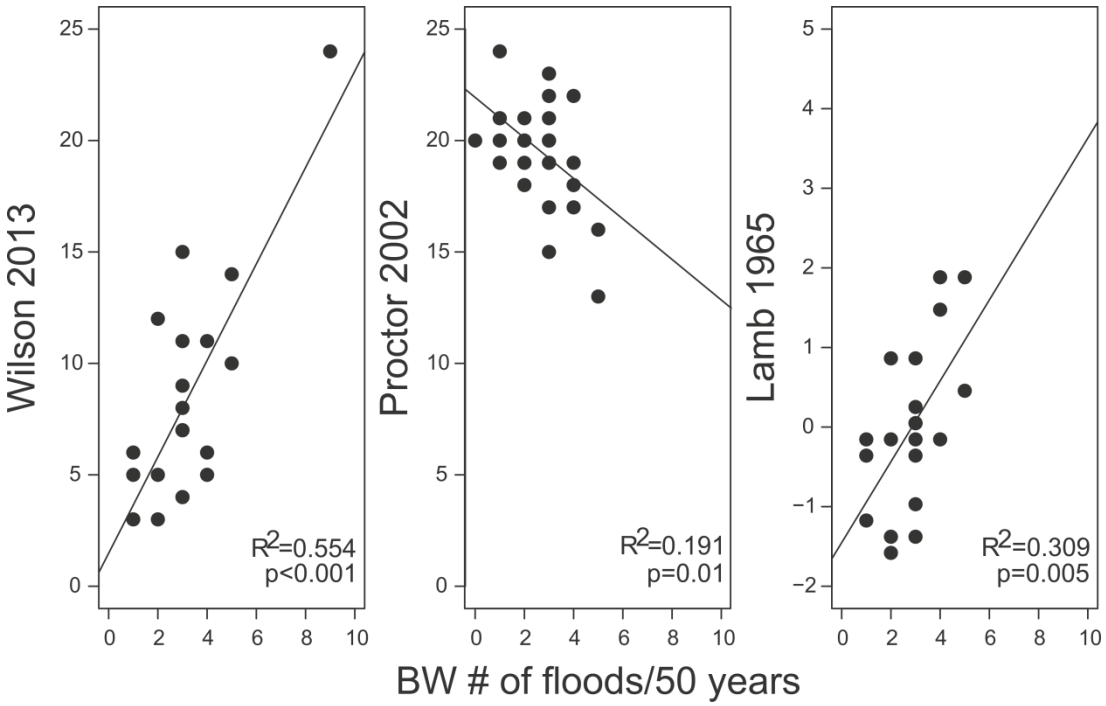

Figure 5-16 Testing the temporal correlation between palaeoflood laminations in Brotherswater against three precipitation reconstructions for the UK. Flood frequency at Brotherswater is portrayed as the number of flood laminations in BW11-2 summed into 50 year bins. The Wilson et al. (2013) annual tree-ring precipitation record and the Proctor et al. (2002) annual growth-rate of speleothems have been standardized and values greater than 1 summed into 50 year bins. The Lamb (1965) data has been compared in its original format. The Proctor and Lamb records do not span the most recent period CE 1950-2000 and thus are not included.

winter floods are most notable in the region (e.g., December 1964; March 1968, November 2005; November 2009).

5.5.4 20th century flood frequency trends

Palaeoflood laminations have been most frequently recorded in Brotherswater since CE 1850 (Figures 5.12 and 5.15); demonstrating a persistent link between this trend and climate has significant implications for future flood projections. On one hand, confidence in the palaeoflood reconstruction has been fostered by temporally correlating the sediment record with historical and instrumental hydrological datasets. Furthermore, flood-generated boulder berms became more frequent in the Lake District at CE 1850-1900 (Macklin and Rumsby, 2007), but explaining the sustained

trend through the 20th Century is more difficult to explain. Plausible non-climatic drivers must thus also be considered, including the increased sediment supply at this time (Chapter 4) due to intensive mining in the CE 1860s, channelization of Kirkstone Beck that triggered movement and probably delta progradation. This is one explanation for the greater deposition of coarse material (increased EM3 contribution) at delta-proximal core sites (BW11-3 and BW11-2), although we have attempted to account for this using the $P90_{normalised}$ profile. Compaction of the lake sediments potentially facilitates the identification of more flood units at 0.5 cm sampling resolution near the tops of cores than the lower sediment. However, the faster sediment accumulation in the upper sediments appears to be independent of compaction as it's matched by higher density-corrected mass accumulation rates. Furthermore, the ^{210}Pb dates of BW12-9 indicate relatively uniform sediment accumulation rates since the late 19th Century in the basin centre, suggesting little sediment compaction over the timescale of more frequent flooding. Disentangling these signals is a major challenge and, as a result, attributing the appearance of more palaeoflood laminations during the 20th Century to climatic factors remains difficult, especially as long instrumental datasets have not found a similar trend (Robson, 2002), although prominent region-specific signals have been found elsewhere (Macklin and Rumsby, 2007).

The reasonable correlation between the Brotherswater palaeoflood record and the 1960 – present river flow record from Grisedale Beck (Figure 5.14) suggests the lacustrine sediments do record imprints of the highest-magnitude events but more moderate events are missed, either due to a lack of sedimentary imprint or during the sub-sampling process. While the Brotherswater sequence is not sufficiently resolved to consider decadal trends during the 20th century and insight cannot be acquired into long-term trends of lower magnitude floods, our data indicates that the 20th Century has experienced more exceptional floods than any other time period of equal length in the palaeoflood record.

A quantitative assessment of palaeoflood magnitude is difficult due to variable sediment supply to the near-delta region and the $P90_{normalised}$ particle size signature of individual flood layers fluctuating between the three analysed cores (Figure 5.12). If the BW11-3 and BW11-2 P90 normalisation procedure has accounted for variable sediment supply, then five events of equal or slightly greater magnitude than a 20th Century flood are identified. The BW12-9 record could be considered more robust as

fluctuations in sediment supply are less prominent; in this sequence, two events of similar or slightly greater discharge in 800 years are identified around CE 1300 and CE 1450.

The Cumbrian floods of 2009 and 2005 were both exceptional in terms of discharge and rainfall for the region and the UK (Miller *et al.,* 2009) as well as at Grisedale Beck (Figure 5.14). Although a discharge reconstruction has not been attempted, a qualitative comparison of flood magnitude can be performed though comparing the 2009 event to the full late-Holocene record. The highest $P90_{normalised}$ value during the 20th century (pre-2009) in all cores is exceeded marginally when compared to the full-core P90 profiles (Figure 5.12), suggesting few late-Holocene floods exceeded those of the 20th Century in terms of magnitude. The exceptional discharge of the 2009 flood was 2.3 times greater than any flow recorded instrumentally during CE 1960 – 2005, however. It is thus reasonable to assert that the November 2009 flood was among, and potentially the, greatest in the region during the last 1500 years. The January 2005 event was probably of a similar magnitude to historical floods represented by particle size peaks exceeding a 20th century signature.

5.6 Conclusions

High-resolution particle size and geochemical analysis of three sediment profiles extracted from Brotherswater along a delta-proximal to distal transect have led to the generation of the first lacustrine palaeoflood record in the UK. The development of a robust age-depth model and its transferral between cores using independent geochemical markers indicates the record extends to approximately 1000, 1500 and 800 yr BP for BW11-3, 11-2 and 12-9, respectively. Particle size data decomposed using an end-member algorithm yielded three (BW11-3 and 11-2) and four (BW12-9) end-members linked to specific depositional processes. The periodic appearance of a coarser mode, represented by peaks in the P90 grain size metric and EM3 (EM4 in BW12-9), was attributed to high flow conditions. These peaks in P90 and EM3 occur throughout the cores and overprint longer-time fluctuations in catchment-derived sediment flux (examined in detailed in Chapter 4); a normalisation procedure aimed at accounting for non-stationary sediment supply ($P90_{norm}$) generated a sequence of palaeoflood laminations that can be correlated across multiple cores and shows consistent temporal matches to historical and instrumental flood records, improving confidence in the final reconstruction. The link between high river discharge and the

delivery of coarse calibre material to Brotherswater has been demonstrated through using the sedimentary signature of the December 1964 flood as an analogue to identify further palaeoflood units deeper in the cores and based on the particle size distributions of material captured in a sediment trap after a period of high rainfall and discharge in December 2012. The palaeoflood record is characterised by a sequence of flood-rich (CE 675 – 775, 1100 – 1300, 1400 – 1500 and since 1850) and generally shorter flood-poor (CE 850 – 900, 950 – 1000, 1300 – 1375, 1500 – 1550, 1625 – 1675 and 1775 – 1825) phases, probably the result of climatic variability but identifying a trigger was difficult. Some temporal matches to the winter NAO were found but the different seasonal NAO modes means the relationship is complex. Furthermore, identifying correspondence between flood occurrence at Brotherswater and rainfall or other palaeoflood proxies is also hampered by the geographical distribution of the records, elevation changes and differences in temporal resolution. A possible region-specific trend towards more frequent floods during the 20th century is observed but disentangling a signal from non-climatic drivers is imperfect. The November 2009 regional flood appears exceptional within the duration of the $P90_{norm}$ record although chronological uncertainly and the non-stationary sediment and hydrometeorological regime mean this is a highly uncertain conclusion.

6 CONTEMPORARY SEDIMENTATION DYNAMICS AND PROVENANCE AT BROTHERSWATER, NORTHWEST ENGLAND

6.1 Introduction

Studies of lacustrine sediments have yielded a wealth of palaeoenvironmental data using core-based approaches from a wide range of settings (Last & Smol, 2001). Nevertheless, evaluating the dynamics of contemporary sediment delivery to specific lakes and its relationship with local meteorological and hydrological processes has been shown to lead to a better understanding of the mechanics of within-lake sediment deposition and varve formation (e.g., Chu *et al.,* 2005; Francus *et al.,* 2008; Roop *et al.,* 2014), more robust palaeoclimate reconstructions (Raubitschek *et al.,* 1999; Blass *et al.,* 2007) and insight into temporal and spatial patterns of sediment yield (e.g., Cockburn and Lamoureux, 2008; Lewis and Lamoureux, 2010). Sediment traps provide a direct measurement of total flux of the various components of material accumulating at the lake bed including allochthonous siliciclastic material, biogenic and siliceous

matter, humic substances and planktonic or benthic microbes (Håkanson and Jansson, 1983). To this end, sediment traps have been an important tool for both limnologists and palaeolimnologists since the 1950s (Bloesch and Burns, 1980). Sediment traps have been installed in the North American Great Lakes to understand contamination and nutrient cycling (Eadie, 1997; Urban *et al.,* 2004) as well as lakes where re-suspension of sediments tied to wind-stress can be a significant issue (Evans, 1994; Douglas & Rippey, 2000). Sediment trapping coupled with long-term monitoring has been undertaken at lakes and reservoirs in environments across the globe (e.g., Cockburn and Lamoureux, 2008; Effler *et al.,* 2006; Fortino *et al.,* 2008; Orwin *et al.,* 2010, Roop *et al.,* 2014).

Establishing a programme of sediment trapping to assess the dispersal dynamics of a river plume entering a lake under high-discharge conditions potentially forms a key stage in the development of palaeoflood research using lake sediment archives (Kämpf *et al.,* 2014b). Incoming plumes can diffuse across the lake surface (hypopycnal flow), at the thermocline (interflow) or at depth (hyperpycnal flow), generally controlled by temperature or density differences between the inflow and the ambient lake water or within the water column (Chapter 2; Sturm and Matter, 1978). Brotherswater complies with physical characteristics identified as desirable for preserving palaeoflood laminations (Chapter 2; Schillereff *et al.,* 2014). Building on previous sediment trap surveys at Brotherswater in the 1970s (Chambers, 1978; Chambers & Parker, 1979), our programme was aimed at better understanding the association between the sedimentary record and flood events, facilitating linkages to be made between hydrometeorological behaviour and sediment characteristics. Identifying any associations between different flow conditions and sediment metrics including volume of material delivered to the lake, grain size, geochemical signatures and organic matter content was of particular interest. Traps were installed at multiple water depths and locations within the basin to address the patterns of river plume diffusion and potential dynamics of re-suspension of sediment within the lake. Trapped materials were collected at approaching monthly intervals to explore the intra-annual pattern of allo- and authigenic sediment delivery/production in the lake.

6.2 Study site

Trapping of sediment deposition was carried out at Brotherswater in the eastern Lake District, a small but comparatively deep lake (area 0.18 km^2, mean depth 7.2 m,

maximum depth 16 m) (northwest England; Figure 6.1a). The catchment is dominated by a Lower Palaeozoic bedrock of volcani-clastic sandstones mantled with glacial and hillslope sediments and podzolic - brown earth soils beneath a largely upland pasture and rough grazing vegetation cover. Woodland is limited to oak and hazel on the western slopes and a willow-alder wetland fringing the southern shoreline. Historically extraction of metal ores has affected the catchment with Hartsop Hall Mine (CE 1696-1941) and Caiston Copper Mine (CE 1860-1870) (Tyler, 1992) generating significant flux of both metals and sediment to the lake (Chapter 4). The lake was classified on the oligotrophic/mesotrophic boundary (Maberly *et al.,* 2011) based on quarterly measurements in 2010 of total phosphorus (annual mean 9.5 mg m^{-3}), phytoplankton chlorophyll *a* (max 4.5 mg m^{-3}) and Secchi disk depth (annual mean 6.1 m). The lake has a pH around 7.0; there is some oxygen depletion at depth in the central basin (minimum 0.1 mg m^{-3}) and high silica content in the water column (annual mean 1475 mg m^{-3}). The water column develops moderate thermal stratification during summer and autumn (temperatures recorded in July and Oct 2010), with the metalimnion forming at between four and eight metres water depth in July. The deeper central basin is flanked by steep sides (Figure 6.1b) with limited littoral areas, and wind or wave re-suspension of sediment to the profundal areas is unlikely (*sensu* Dearing, 1997). Two sediment trap sites were chosen on a gradient away from the river inflow (Figure 6.1b); site A was installed proximal to the present-day delta (75 m north) in 12 m water depths and site B was installed in the deep central basin (max. 16 m) 225 m north of the inflow (Figure 6.1b).

6.3 Methods

6.3.1 Field techniques

Cylindrical sediment traps (designed following the recommendations of Blomqvist and Håkanson (1981), Håkanson and Jansson (1983) and Ohlendorf and Sturm (2001) were built to collect material settling out of suspension in the lake. Each of the traps consisted of opaque PVC pipes (11 cm diameter, 75 cm length) and they were fitted with removable 500 mL beakers at the base. The 6.8:1 aspect ratio ensures the

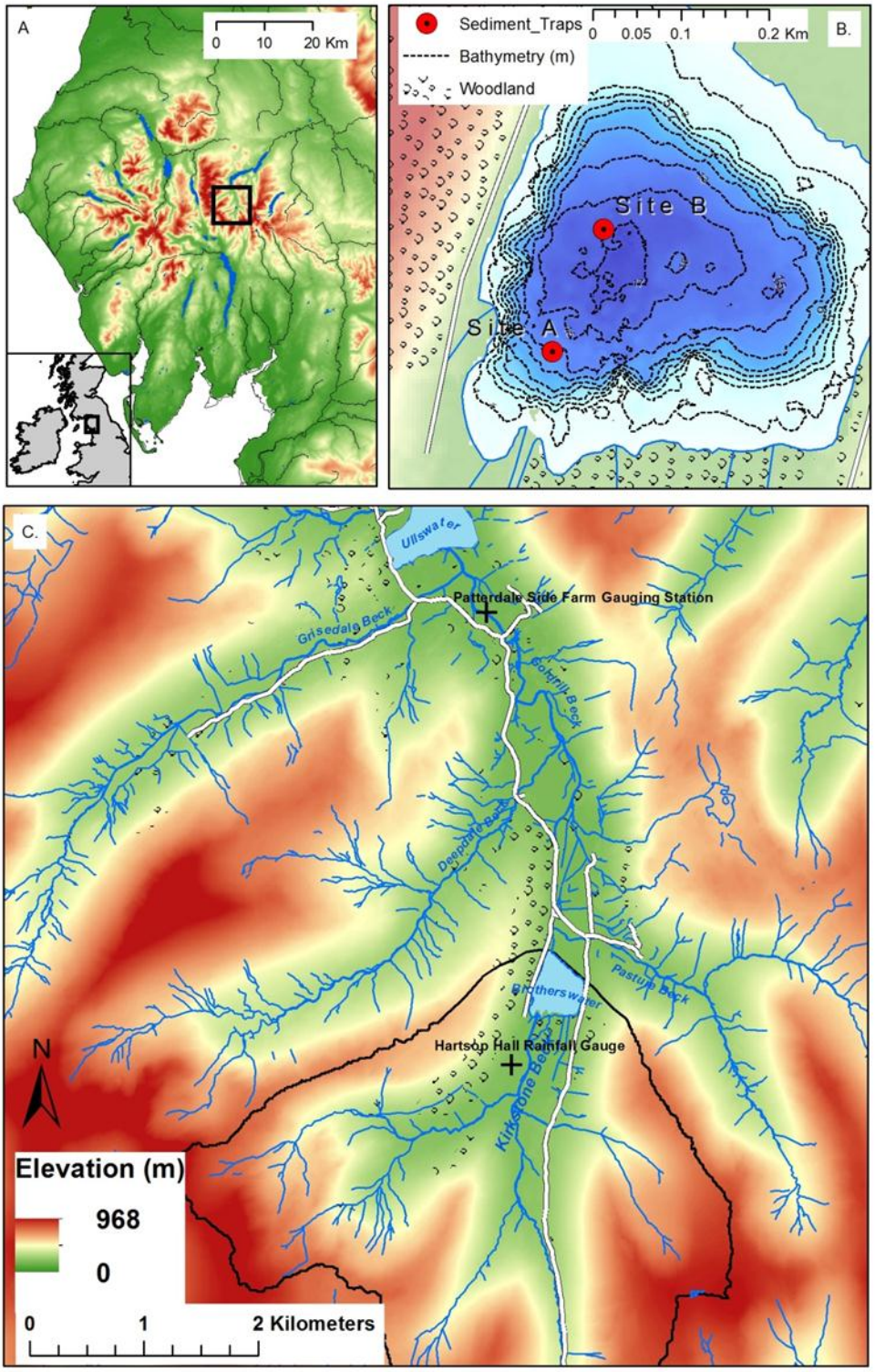

Figure 6-1 A) Location of Patterdale Valley within northwest England. B) Sediment trap locations within Brotherswater. C) Topography of the Patterdale Valley and location of the rainfall and river flow gauging stations. The catchment of Brotherswater is outlined in black.

representative capture of sediment within the water column (after Bloesch and Burns, 1980). Both configurations consisted of a 20 kg flat plastic-coated dumbbell anchor, 8 mm diameter stainless steel cabling held taut by a surface buoy to avoid trap tilt (Gardner, 1985), and three sediment trap stations were fixed: i) basally above the sediment/water interface (mouth of the trap was 1 m above lake bed) in order to assess re-suspension and track hyperpycnal flows; ii) middle water column (6 and 8 m, respectively) broadly at the seasonal metalimnion, setup to capture deposition from interflows following the epilimnion/hypolimnion thermal boundary and iii) upper station at 4 m water depth to trap sediments diffusing as hypopycnal flows. Two replicate traps were placed side-by-side at each station to maximise the volumes of sediment collected. Trap collection was broadly monthly in part regulated by logistical difficulties and inclement weather. Sampling intervals thus varied between 31 and 121 days (Table 6.1; 6.2). The replacement of traps was carried out carefully to minimise disturbance of the unconsolidated surface sediments. There was no evidence of disturbance of collected particulate material during retrieval of the trap samples with relatively clear water overlying the deposited material (Effler *et al.,* 2006).

6.3.2 Laboratory methods

Processing of samples involved upright storage for 24 h and then sieving through a coarse mesh (100 μm) to identify and remove leaves, copepods, and, during spring, Caddisfly and Mayfly nymphs, while retaining this sediment fraction. Samples were centrifuged to remove the nascent water, freeze-dried to remove the last moisture and weighed to obtain the dry mass sediment accumulation. Laboratory analyses were performed as follows.

Elemental composition was measured via X-ray fluorescence (XRF) after homogenisation of the sediment to a loose powder using a mortar and pestle on a Bruker S2 Ranger energy-dispersive instrument housed at the Department of Geography, University of Liverpool. Sample cups lined with 6 μm polypropylene film were measured under a helium atmosphere at three x-ray intensity settings. The Buffalo River certified reference sample (NIST-RM 8704) was used to ensure instrument consistency. Organic carbon content was calculated as the mass loss or thermal decomposition between as each sample was heated at 20°C per minute across the interval 150°-530°C under a nitrogen atmosphere using a PerkinElmer STA6000 thermogravimeter / differential scanning calorimeter (further methodological detail is

given in Chapter 3.2.2) and XRF measurements were corrected for organic matter content. Particle size distributions for each trap sample were measured using a Beckman Coulter™ LS320 laser granulometer at the University of Liverpool after the removal of the organic fraction using a 30% H_2O_2 solution (in some cases for up to 144 h to ensure complete dissolution).

Sediment weights were divided by the trap surface area (95 cm^2) and the time between consecutive trap replacement to provide estimates of gross sedimentation fluxes (g dry mass m^{-2} day^{-1}).

The sequential fluxes of total dry mass (MAR; mg cm^{-2} d^{-1}) for sites A and B are presented in Figure 6.4, calculated as:

$$MAR = W_D / d / (\pi * r^2)$$

where W_D = dry sample mass, d = number of days between sampling and r = radius of the trap tube.

6.3.3 Meteorological and hydrological data

Daily maximum river flow data (Aug 1997 – Feb 2014) were obtained from the UK Environment Agency for Goldrill Beck (the outflow of Brotherswater) recorded at the Patterdale Side Farm gauging station (station ID 761511, NY339664 516020, 54.535°N 2.933°W; Figure 6.1c). This is the closest monitoring station to Brotherswater and represents flow exiting the lake as well as the addition of flows from two downstream tributaries, Pasture Beck and Deepdale Beck (Figure 6.1c). The landscape throughout Patterdale is largely deforested so a consistent fluvial response is likely, along with high overland flow during heavy rainfall. Data were double-checked to avoid duplicates and 99.91% of data-points were classified "Good" (i.e., high data quality). Local precipitation data were acquired from the UK Environment Agency as daily totals recorded in a Tipping Bucket gauge at Hartsop Hall (NY 339884 512059, 54.500°N 2.930°W Figure 6.1c). 100% of the data-points are considered 'Good' over the timespan of analysis, Aug 2012 – Aug 2014. A pressure-transducer-based water level and temperature logger (HOBO U20-001-04) was installed at the upper trap at both sites (maximum operating depth of 4 m) to record water level (maximum error ±0.1% FS, 0.6 cm), barometric pressure (±0.3% FS, 0.43 kPa) and temperature (estimated accuracy ±0.44°C) throughout the survey period. Data-points were recorded at ten minute intervals throughout the survey period and lake levels were calculated by

correcting the trap-mounted absolute pressure to atmospheric pressure measured at equal intervals by a sensor positioned at the lake edge.

6.4 Results and Discussion

6.4.1 Trends in discharge and precipitation

Rainfall events were generally short-lived (1-3 days), with the highest daily rainfall (98 mm) on 24/09/2012, and some extended periods of heavy rainfall occurred, most notably 386 mm on 14-31 Dec 2012 (Figure 6.2a). Base flows exiting Brotherswater tend to be low (<2 m^3 s^{-1} during autumn and winter, <1 m^3 s^{-1} during spring and summer) with rapid increases lagging rainfall events by generally less than one day (Figure 6.2b). Discharges exceeded 35 m^3 s^{-1} at 07:30 on 25/09/2014 at Patterdale Side Farm following the brief, major rainfall event. Discharges exceeded 25 m^3 s^{-1} on ten occasions through the survey period although between February 17th and July 28th, river discharge exceeded 10 m^3 s^{-1} on only one occasion, in mid-April 2013 (Q_{max} = 29.4 m^3 s^{-1}).

The majority of the rainfall and high discharge events during the survey period occurred during the autumn and especially winter, fitting the longer-term trend (1997 – present) (Figure 6.2c and 6.2d). The discharge record can be extended to 1960 by calibration on to the Pooley Bridge (Ullswater outflow) record on the river Eamont. The April 2013 event timing and magnitude is thus historically unusual. Discharge exceeded 35 m^3 s^{-1} twice during the trapping programme, generated by differing rainfall patterns: 98.8 mm fell within a 24 hour period on 24 Sept 2012 and led to a muted particle size response (described later) whereas prolonged, moderate rainfall (more than 20 mm on 7 of 11 days 19-30 Dec 2012 delivered the coarsest calibre material of the survey period. From mid-April through late-July river discharges were <10 m^3 s^{-1}, including the subdued response to 35.8 mm of rainfall on 27 May 2013. In autumn and winter of both years, flow events of moderate magnitude on six occasions generated discharges >15 m^3 s^{-1}, despite comparatively low rainfall; in each case, however, a major rainfall event had occurred within the preceding 2 weeks. High flows on 14 and 18 Apr 2013 (29.2 and 29.4 m^3 s^{-1}) were generated by rainfall exceeding 43 mm on both preceding days, only slightly higher than May 27 but insignificant rainfall during the preceding February-March likely conditioned the system to respond rapidly to heavy downpours.

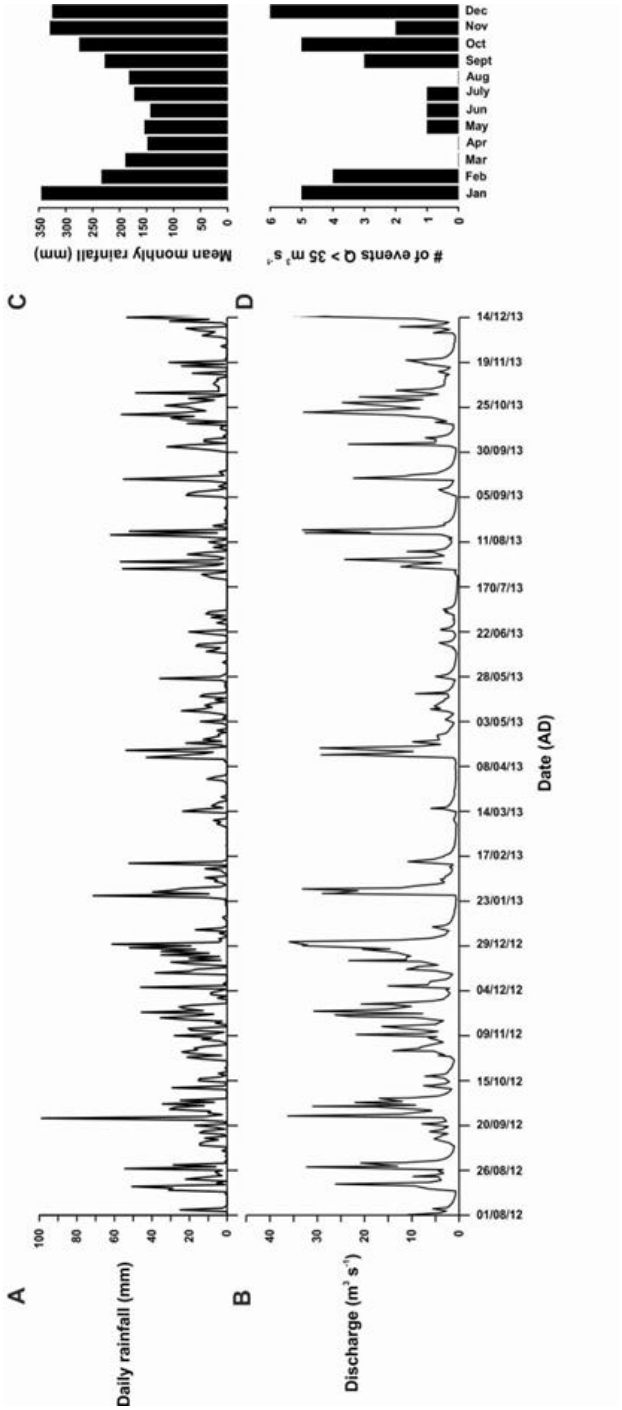

Figure 6-2 A) Daily total rainfall at Hartsop Hall spanning 01/08/2012 – 14/12/2013. B) Daily maximum discharge at Patterdale Side Farm spanning the equivalent time period. C) Mean total monthly rainfall for the period of tipping tucket operation at Hartsop Hall (08/02/1997 – 31/12/2013). D) The frequency of floods (Q > 35 m^3 s^{-1}) in monthly bins for the period of measurement at Patterdale Side Farm (19/03/1997 – 31/12/2013).

6.4.2 Variations in sediment flux

Total dry weight accumulation varied substantially between sampling intervals, water depth and trap location (Table 6.1; Figure 6.3a). More material (total dry weight) was captured overall in the top and middle water depths at Site A (0.26 – 6.03 g and 0.33 – 4.85 g, respectively) compared to the lake centre (Site B; 0.31 – 2.93 g and 0.43 – 3.67 g) during the survey period. More material was found in the basal traps than higher in the water column at both sites, although the increase in sediment accumulation with depth was much larger at site B. Strong evidence exists that water depth affects the volume of material deposition (2-way ANOVA, $F(1, 48)=6.629$, $p=0.003$), however, there is no evidence of interaction between site and depth ($F(1, 48)=1.131$, $p=0.331$) or trap location having a significant influence ($F(1, 48)=0.002$, $p=0.963$). A significant, positive relationship (ANOVA, $p<0.001$) is observed between sediment accumulation in upper and mid water depths at both stations as well as between Site A Top and Site B Top (Figure 3c).

Total dry mass fluxes (MAR; mg cm^{-2} d^{-1}) (Figure 6.4) entering the top and middle traps near the inflow show a distinct seasonal signal, with higher accumulation during autumn (0.85 and 0.70 mg cm^{-2} d^{-1}) and winter (1.07 and 1.40 mg cm^{-2} d^{-1}) than in summer (0.20 and 0.16 mg cm^{-2} d^{-1}). This pattern is less visible at Site B, with relatively stable values Aug 2012 – May 2013, declining slightly through June and July before rising during the autumn and winter of 2013. MAR is higher in the basal traps at both sites throughout the year, exceeding 1.25 mg cm^{-2} d^{-1} during all months, except Jan and July 2013 at Site A. Exceptional accumulation took place at Site B Base during June and July 2013 (6.17 and 4.57 mg cm^{-2} d^{-1}) and the accumulating material is fine-grained (P90 = 118 μm and 34 μm), organic matter content is slightly lower than other spring and summer months (13-14%) and no clear excursions in elemental composition. The mechanism is difficult to explain but a couple of processes could account for these unusual patterns. Given the absence of high flows in the two months, autogenic sediments must be responsible, either the result of sediment focusing under moderately stratified summer conditions (Larsen and Macdonald, 1993) or sub-aqueous slumping of material from littoral areas of the lake due to its steep basin sides (the fine grain size negates the likelihood of a delta collapse). The flow of sediment subsequently bypasses Site A and is deposited at Site B, either after descending to the thermocline and diffusing in the water column (there are peaks in the upper trap at site A; Figure 6.4)

Table 6-1 Dry weight (DW) for each trap pair (Tube 1 and 2) and summed for each water depth (Total) and sediment accumulation rate (SAR) measured at Sites A and B during the collection intervals. "____" indicates trap was unable to be located. All values rounded to 3 decimal places. *Fish trapped in beaker.

Site A		**Top**				**Middle**				**Base**			
Deployed	Collected	Tube 1 DW (g)	Tube 2 DW (g)	Total DW (g)	SAR	Tube 1 DW (g)	Tube 2 DW (g)	Total DW (g)	SAR	Tube 1 DW (g)	Tube 2 DW (g)	Total DW (g)	SAR
7 Jul 12	15 Aug 12			0.260	0.007			0.323	0.008			0.212	0.005
15 Aug 12	10 Oct 12	2.444	2.405	4.849	0.851	1.865	2.137	4.002	0.702	3.462	4.024	7.486	1.313
10 Oct 12	9 Jan 13	2.965	3.065	6.030	0.700	2.075	2.774	4.850	0.561	2.780	2.441	5.222	0.604
9 Jan 13	15 Feb 13	____	____	____	____	1.630	1.338	2.969	0.844	3.192	1.279*	4.473	1.272
15 Feb 13	24 Apr 13	____	____	____	____	1.040	____	1.040	0.161	3.304	5.161	8.466	1.310
24 Apr 13	6 Jun 13	0.386	0.470	0.855	0.204	____	____	____	____	2.971	2.873	5.846	1.398
6 Jun 13	10 July 13	0.153	0.116	0.269	0.083	0.182	0.189	0.539	0.167	1.573	1.174	2.748	0.850
10 July 13	10 Aug 13	1.630	1.528	3.158	1.072	2.117	1.995	4.112	1.396	2.499	2.705	5.205	1.767
10 Aug 13	10 Dec 13	1.684	1.737	3.421	0.295	1.615	2.217	3.832	0.331	2.661	____	2.661	0.230

Site B		Top				Middle				Base			
Deployed	Collected	Tube 1 DW (g)	Tube 2 DW (g)	Total DW (g)	SAR	Tube 1 DW (g)	Tube 2 DW (g)	Total DW (g)	SAR	Tube 1 DW (g)	Tube 2 DW (g)	Total DW (g)	SAR
7 Jul 12	15 Aug 12	____	____	____	____	____	____	____	____	____	____	____	____
15 Aug 12	10 Oct 12	0.373	1.020	1.394	0.244	1.195	____	1.195	0.210	5.544	3.443	8.987	1.576
10 Oct 12	9 Jan 13	____	____	____	____	____	____	____	____	____	____	____	____
9 Jan 13	15 Feb 13	0.527	0.565	1.092	0.311	0.684	0.556	1.240	0.353	1.073	1.058	2.131	0.606
15 Feb 13	24 Apr 13	0.741	0.773	1.514	0.234	0.769	0.921	1.690	0.262	1.300	1.186	2.485	0.385
24 Apr 13	6 Jun 13	0.406	0.340	0.746	0.178	0.309	0.430	0.738	0.177	3.049	22.757	25.805	6.171
6 Jun 13	10 July 13	0.155	0.154	0.309	0.096	0.266	0.163	0.429	0.133	1.452	13.329	14.781	4.575
10 July 13	10 Aug 13	1.086	1.215	2.301	0.781	0.746	0.800	1.546	0.525	____	____	____	____
12 Aug 13	10 Dec 13	1.570	1.358	2.928	0.253	1.766	1.902	3.669	0.316	2.460	6.755	9.214	0.795

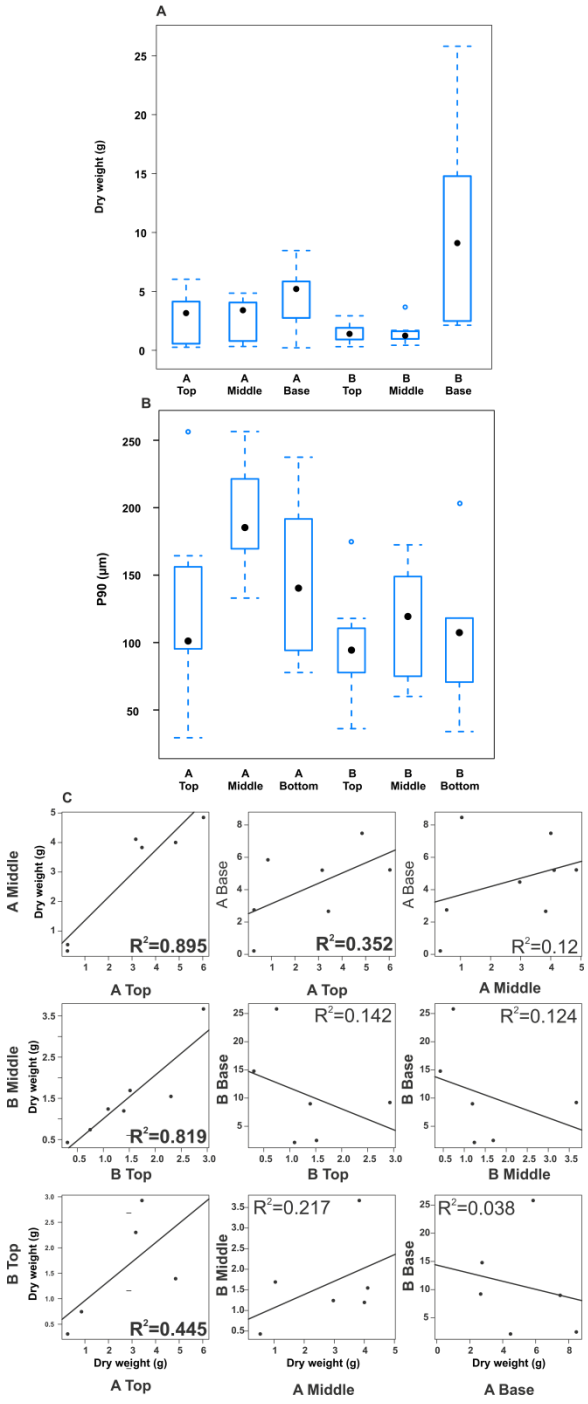

Figure 6-3 A) Variation in total dry weight captured during each sampling interval by trap station. B) Distribution of monthly P90 values for each trap station C) Relationship between dry weight accumulation during each sampling interval at each water depth and between trap stations. R^2 value is highlighted in bold where the relationship is statistically significant ($p<0.001$).

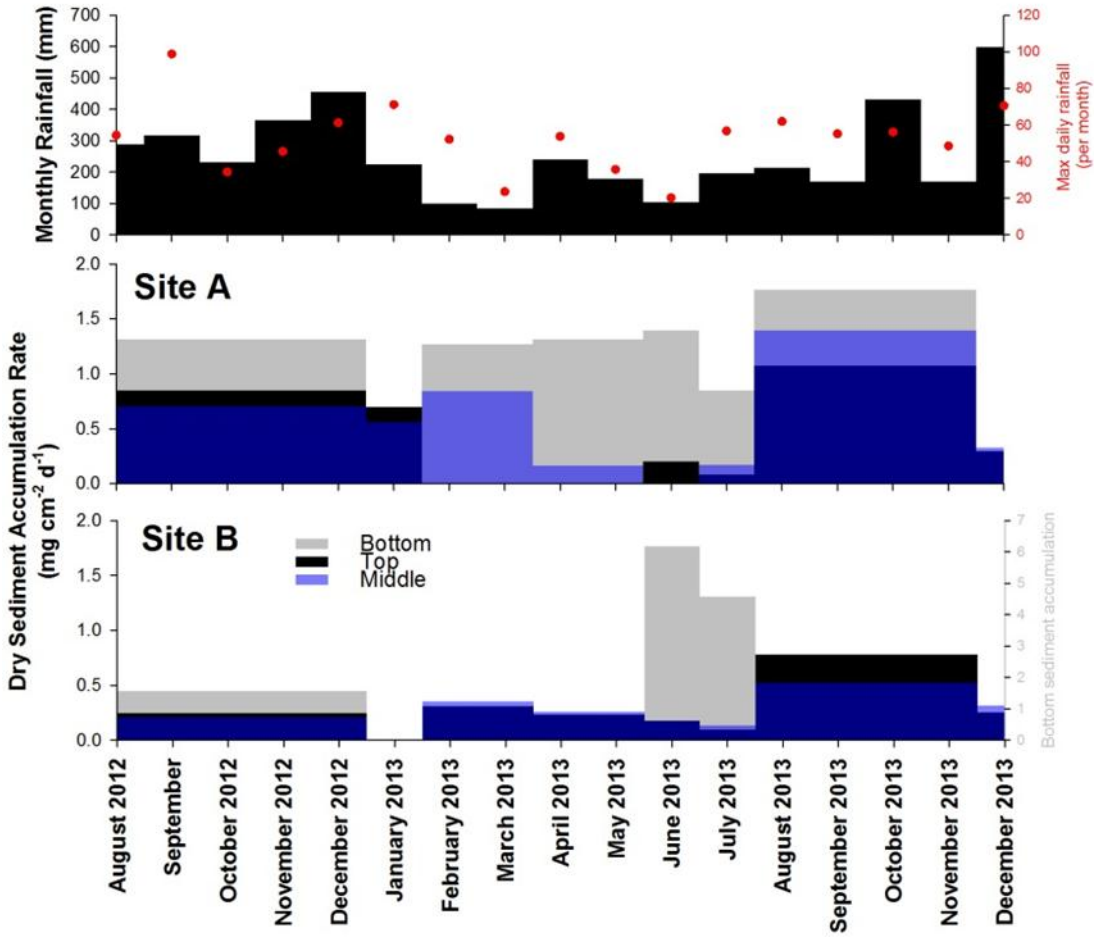

Figure 6-4 Total monthly dry mass flux to each station compared to monthly total and daily maximum (per month) rainfall. Sediment flux values are constant between sampling intervals. Note the secondary *y*-axis for Site B Base sediment accumulation due to exceptional high values.

or a turbidity current is formed and particles are maintained in suspension until the Reynolds number threshold is reached and the turbulent flow collapses (Mulder & Alexander, 2001).

6.4.3 Contemporary sediment provenance

Integrating geochemical data from all traps reveals associations as well as decoupling between the inter-month concentrations of certain elements (Figure 6.5). Particularly

strong positive correlations ($R > 0.85$) are observed between lithogenic elements (Ti, V, Y and Zr), including those commonly associated with clay minerals (Al, Ba, K, Rb). This co-variation suggests catchment-derived eroded material has been an important sediment source during the survey period (Engstrom and Wright, 1984; Boyle, 2001b), matching the longer-term trend (Chapter 4 and Oldfield and Wu, 2000). Si behaviour is inversely correlated with almost all elements, in particular Fe (R = -0.86), pointing towards a biogenic Si source such as diatom frustules (Kylander *et al.,* 2011). Normalising Si against detrital Al (c.f. Peinerud, 2000) reveals maximum Si/Al occur in April and June, the result of elevated Si concentrations (Figure 6.6a), indicative of a late-spring diatom bloom (Peinerud, 2000).

Fe and Mn exhibit a moderate, positive relationship (R = 0.44), possibly indicating an influence from redox conditions in the lake (Davison, 1993), but Fe and Mn are also related to the trace metals (Fe: Cu, R = 0.58), material with considerably different solution phases (Boyle *et al.,* 2004). Plotting the Mn/Fe ratio, which should reflect the state of redox conditioning (Peinerud, 2000), reveals no seasonal trend, despite moderate thermal stratification and bottom water anoxia of the summer water column (Maberly *et al.,* 2011).

The pattern of seasonal organic matter (OM) content variability is consistent between trap stations (Figure 6.6b), higher during spring and summer (13-22 %) and lowest in Oct 12 – Jan 13 (5-12 %). The Dec 13 material includes some late-Summer accumulation (affected by late emptying of the traps), which probably explains the higher than expected OM content (14-16%). A moderately strong correlation between OM content and Br (0.64) is observed, a function of the tendency of Br to associate with detrital organic matter (Ziegler *et al.,* 2008). Br is inversely correlated with the minerogenic fraction (Br:Zr, R = -0.62) but somewhat related to the trace metals (Br:Pb, R = 0.47). Based on their high concentrations (63, 548, 793 ppm, respectively), Cu, Pb and Zn are almost certainly sourced from Hartsop Hall Mine, either through the oxidisation of surface spoil or seepage of contaminated water from leats or mine shafts (Hudson-Edwards *et al.,* 2011), possibly through sub-surface soil piping (*sensu* Jones, 1977). One hypothesis is that the trace metals and organic matter are flocculating together in the fluvial system before transmission to the lake (Hudson-Edwards, 2003).

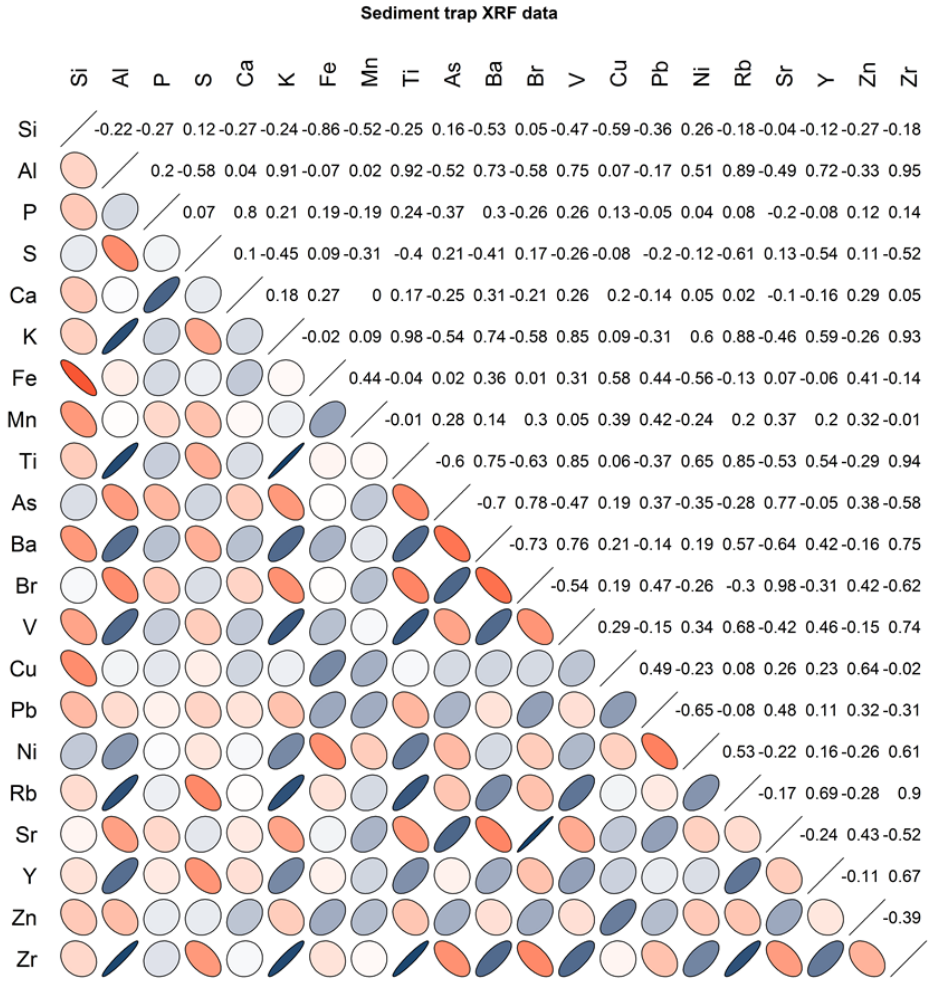

Figure 6-5 Correlations between concentrations of 21 major and trace elements found within the full sediment trapping dataset expressed as coloured ellipses and the corresponding *R* value. Red and blue represent negative and positive correlations, respectively, and the narrowness of each ellipse corresponds to the strength of the relationship (thin = higher *R*).

While some elements have a tendency to be enriched in particle size fractions (Dypvik and Harris, 2001; Taboada *et al.,* 2006), the strongest relationships in the sediment trap data are between the terrigenous elements and the coarse silt/fine sand fraction. An inverse correlation is observed with finer silts and a limited relationship with clay. This suggests that periods of intensive erosion will be recorded as peaks in lithogenic elemental concentrations in the Brotherswater sediments but discriminating a grain- size signal will be more problematic, most likely due the grain sizes inherent in catchment bedrock geology (J.

Boyle, personal communication). The suitability of Zr/K as an event-specific grain size proxy is demonstrated in Chapter 2.1, but the relationship frequently breaks down in the core profiles (Chapter 5), and this disconnection is further supported by the sediment trapping data as Jan 2013 samples are not significantly higher than non-flood months.

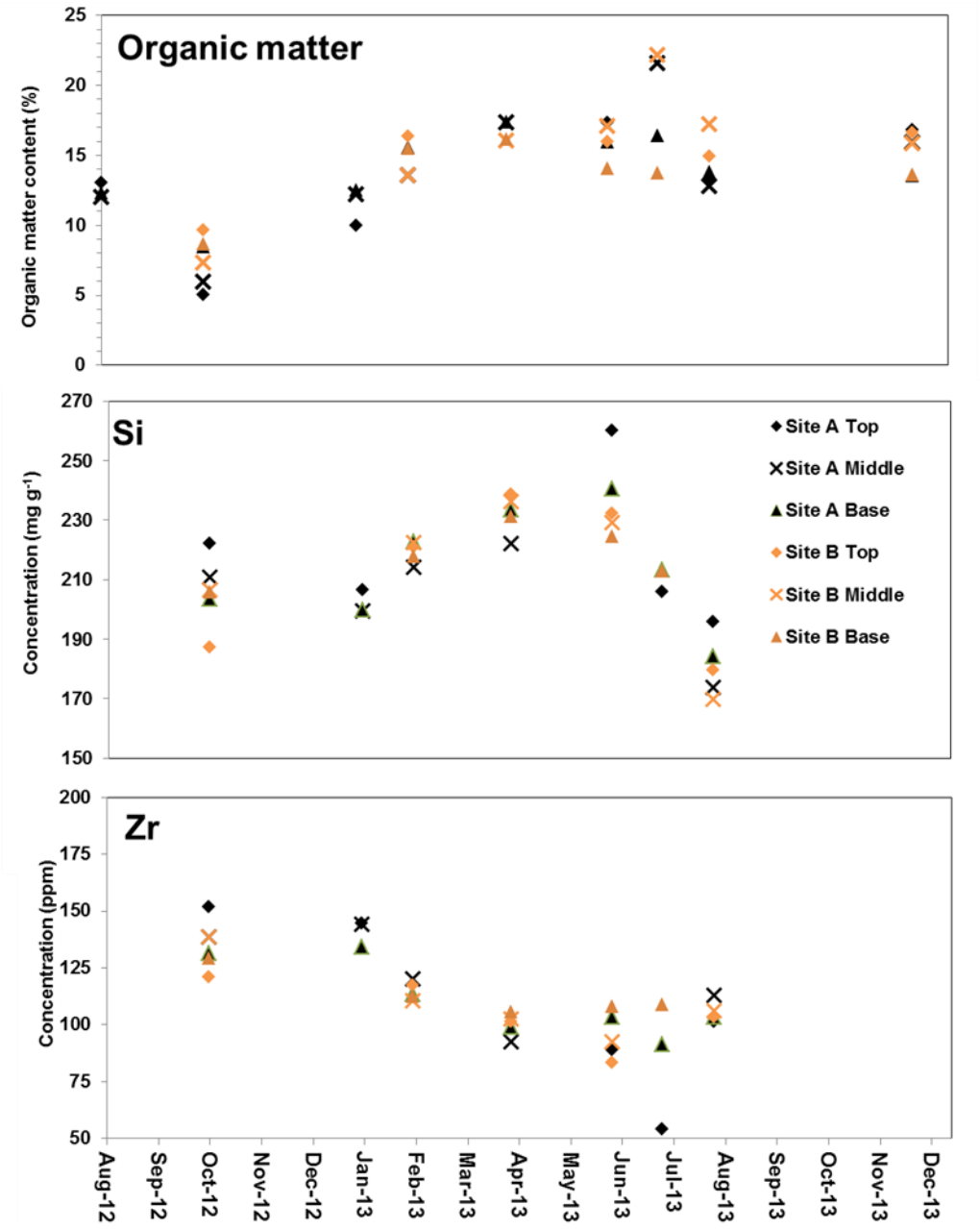

Figure 6-6 A) Organic matter content measured via thermogravimetry (150-530 °C burn interval) for all traps B) Monthly Si concentrations for all traps C) Monthly Zr concentrations for all traps.

6.4.4 Assessing linkages between process and particle size

Comparison between Site A and Site B

Some associations between particles size, within-lake processes and the hydrological data can be distinguished, although the modest number of completed sampling intervals must be firmly kept in mind, especially in the case of the process-specific sediment signatures that are described that feature in only one trap interval. Overall, finer particles were captured at the distal Site B than A during almost all months (Figure 6.3c; Figure 6.7), the sole exception being the top traps collected in June 2013 (Figure 6.5), while the highest P90 values were recorded at mid water depths at both stations throughout the survey period (Figure 6.3c). This supports long core data that show the rate and calibre of sedimentation across Brotherswater is strongly controlled by fluvial delivery and dissipation of flow energy leading to settling of coarse to finer particles with distance from the inflow (Chapter 4 and 5).

Comparing sediment trap and lake sediment data

Undertaking paired end-member (EM) analysis of the particle size data for both trap (Site A) and adjacent sediment core (BW11-2) materials reveals that sediment trap material is composed of three particle size groupings (EM1 = clay/fine silt, EM2 = medium silt, EM3 = fine sand) equivalent to those found in the lake sediment record (Figure 6.8; the end-member analysis methodology is described fully in Chapter 5). Monthly contributions from each EM are of similar magnitude to the variability within the lake sediment core, especially the top 35 cm (representing the last ~100 years). EM3 (coarse fraction) dominated the Jan 2013 samples (93% in the Top trap) but is absent from the July 2013 material, which has the highest EM1 (fine) contribution.

Some variability with water depth is also evident (Figure 6.8). The contribution of EM1 to Oct 2012 increases with depth, and this trend of progressively less coarse material with depth is also identified in sand-rich Jan 2013 trap samples. EM3 does not appear in Jun 13 Top but makes a minor contribution at middle and basal depths. Jul 2013 has more clay/fine silt in the upper water depths and Aug 2013 traps increase in EM3 contribution with water depth. The relationship between trap and lake bed sediments is in part less clear comparing Site B and core BW12-9. The dataset is partitioned into the equivalent four end-members, but EM4 (sand) appears to be over-represented in

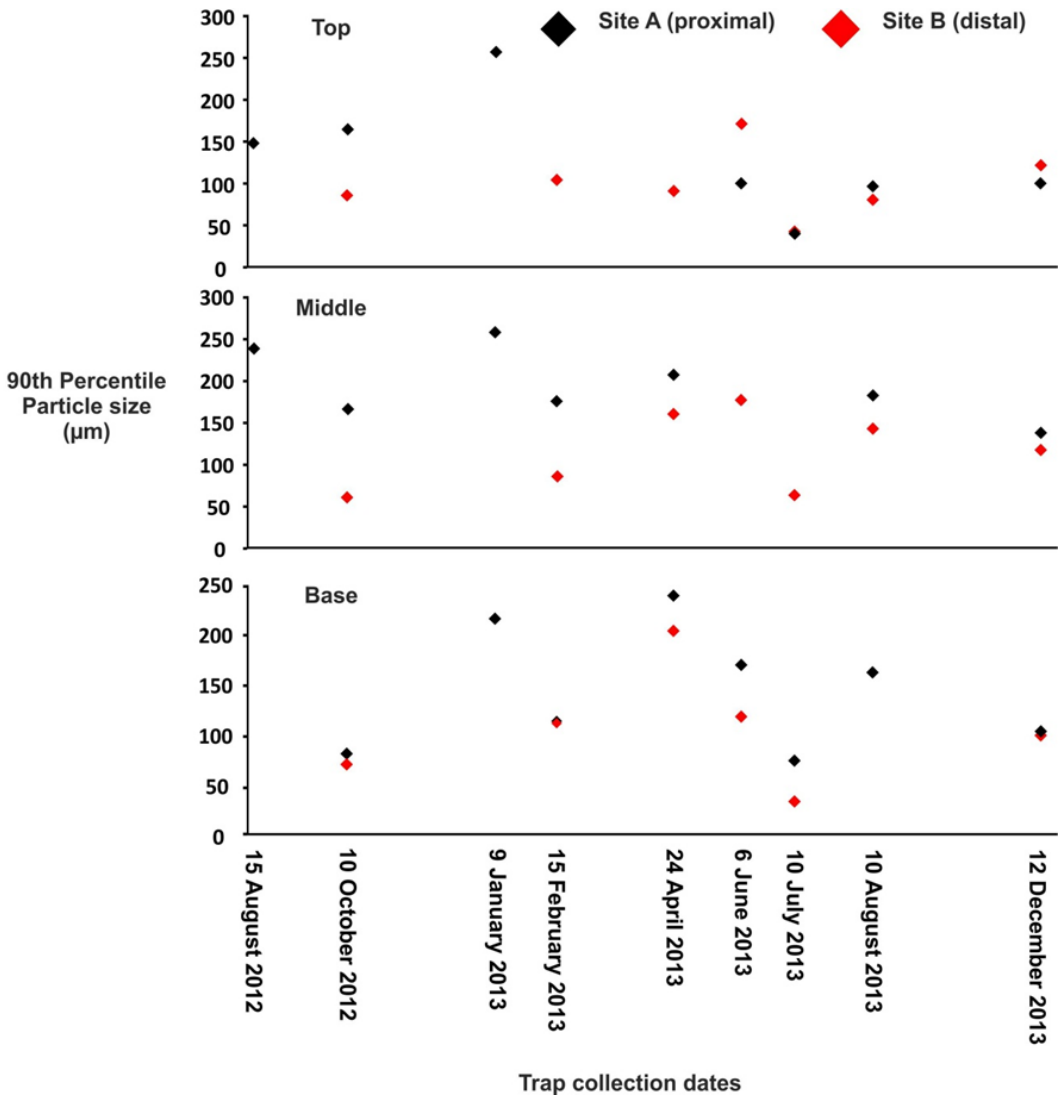

Figure 6-7 Particle size data plotted as their 90th percentile values for each collected trap data, organised by site and depth within the water column. Daily maximum discharges for the duration of the survey period are also presented.

the sediment trap material, especially during April and June 2013, and EM3 (coarse silt) occurs only in July and August 2013. That said the record from the sediment core shows a trend towards coarser materials and increased occurrence of EM4 in the upper 20 cm. Using three end-members yields greater similarity between trapped material and core composition but the flood-diagnostic end-member loading is lost. This is most likely attributable to the presence of secondary modes in some of the end-member distributions, especially a fine tail in EM4 straddling the medium silt fraction.

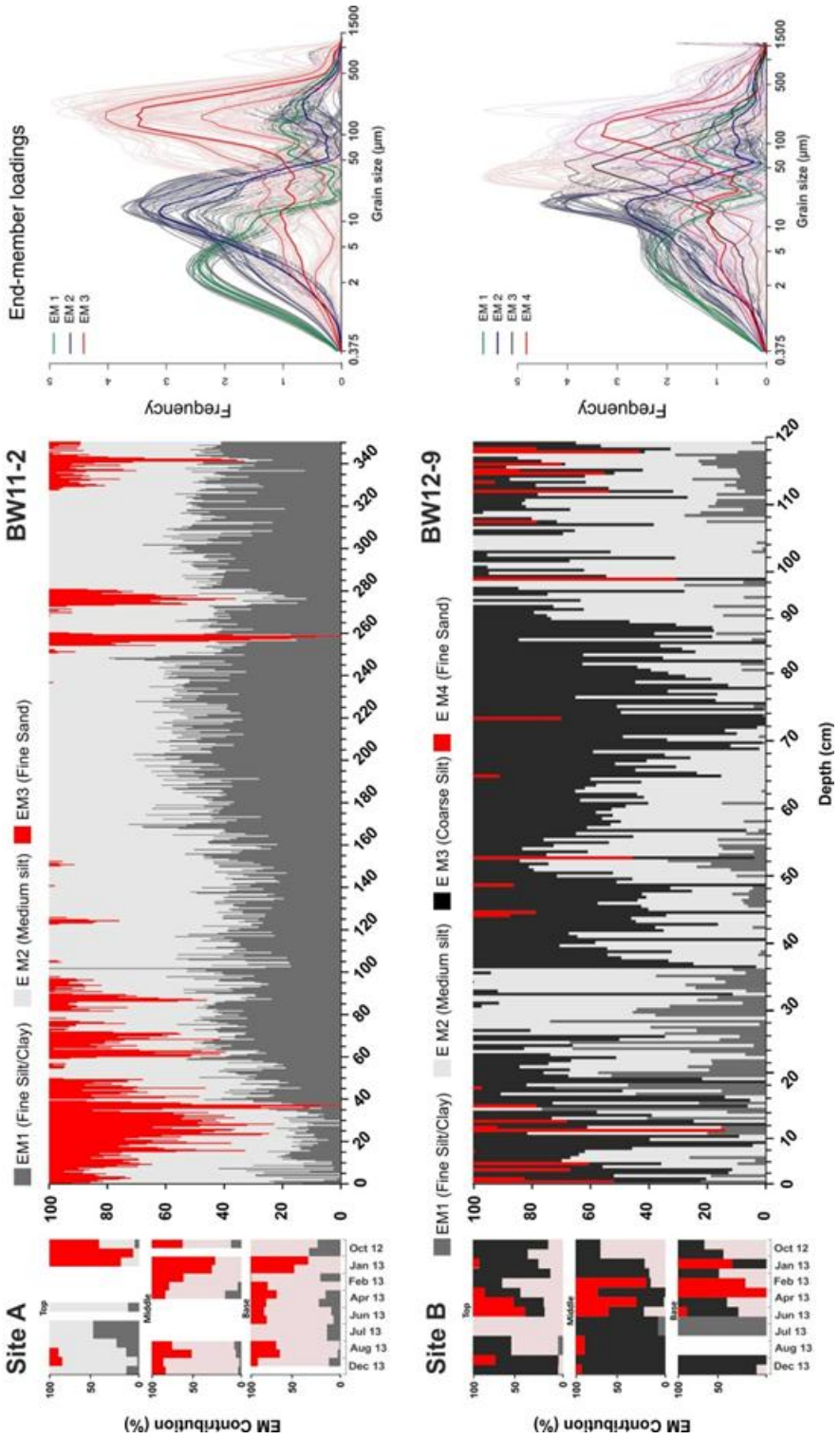

Figure 6-8 End-member loadings from the particle size distributions of the trap samples (left) and adjacent long cores. The modelled end-member distributions are shown at the right.

The EM dataset for site A appears more appropriate for deciphering process-based particle size signatures within the trap material. This lends weight to assertions in Chapter 2 (Schillereff *et al.,* 2014) and for the sites selected in this thesis that delta-proximal sites should be targeted for flood reconstruction, although other palaeolimnological studies suggest alternative optimal coring locations. A solid understanding of the depositional mechanics at a site-specific scale is clearly required (Kämpf *et al.,* 2012; 2014).

Significant winter flood

Jan 2013 material was dominated by EM3 (coarse) and yielded the highest P90 values (P90 > 250 μm at top and middle, 225 μm at base; Figure 6.8) and generated heavily right-skewed particle-size distributions (PSD) (Figure 6.9a), probably reflecting the notable rainfall and discharge pattern over the trapping interval (Figure 6.2a and 6.2b). Although a higher 24 hour rainfall volume was recorded 24 Sept 2012, Jan 2013 captures a period of prolonged, elevated but unexceptional rainfall over a two-week period from 19 to 30 Dec 2012. This suggests the area under the hydrograph curve as opposed to short-lived peaks may govern sediment supply under flood conditions and the absence of a relationship between grain size and the volume of fluvially-delivered sediment (Cockburn and Lamoureux, 2008). The EM3 behaviour of Jan 2013 material matches the most significant coarse-grained laminations preserved in long core BW11-2 (Figure 6.8), and reflects that the late-Dec 2012 discharges are analogous in their sedimentary response to historical major floods at Brotherswater. This has significant implications for palaeoflood interpretation as it suggests intense, short-lived rainfall events can leave a subdued sedimentary imprint compared with multiple days of moderate rainfall, at least for autumn and winter events. This presents a challenge when correlating the timing of a single palaeoflood lamination with the documentary or epigraphic record, which are more likely to record short-lived downpours (Macdonald, 2006). The declining EM3 contribution with trap depth (>90 % in the top, 50% at the lake bed) indicates material was delivered under hypopycnal flow conditions, diffusing across the upper water column under strong horizontal forces and settling out of suspension at a rate controlled largely by particle size (also mineral density and shape) (*sensu* Stokes, 1851).

Regime conditioning/successive flood events

Despite a significant flood on 27-29 Jan 2013 (Q_{max} = 33.1 m^3 s^{-1}), Feb 2013 trap samples are characterised by unimodal PSDs (predominantly medium-coarse silt), low P90 values (180 μm at Site A Middle, < 150 μm in all others) and lower EM3 contribution than Jan 2013, declining from 45% in the Top trap to <20% at the basal station. A plausible explanation is that the high flow conditions in Dec 2012 flushed the fluvial system of larger particles, reducing their availability in the subsequent late-January event. This potentially highlights the role of antecedent sediment availability or build-up and system conditioning of flood-driven sediment delivery. Foster *et al.,* (2003) noted similar results using magnetic measurements of sediment trap samples at Annecy. Coarse-silt sized particles were delivered during this event, possibly indicating this is the calibre of soil particles loosened by intense rainfall and transported into the fluvial system via overland flow during a storm. An alternative explanation is that the 27-29 Jan 2013 flows followed a different trajectory or flow path within the lake (Girardclos *et al.,* 2012), but this seems unlikely given the basin configuration and location of the traps in front of the inflow delta.

Summer flood conditions

The samples retrieved on 10 Aug 2013 are moderately coarse, especially in the Middle trap (P90 = 190 μm) and EM3 also makes the greatest contribution (45%) at middle water depth, reflecting higher flows 28 Jul – 1 Aug 2013 in response to two intense rainfall events. Their abrupt nature after a prolonged absence of rainfall appears to have mobilised significant large calibre particles despite maximum discharges being modest (Qmax = 24.2 m^3 s^{-1}). The trapping by the middle water depth station of the coarsest particles suggests the flood plume of warmer, sediment-laden water entered the moderately stratified (summer) water column, descended to the thermocline and dispersed as an interflow, potentially highlighting seasonal effects on the depositional mechanisms in the lake (Desloges and Gilbert, 1994; Schiefer *et al.,* 2006b; Hodder *et al.,* 2007; Kämpf *et al.,* 2014a).

Summer low-flow conditions

River discharge did not exceed 10 m^3 s^{-1} between 20 Apr and 10 July 2013, and the sediments delivered to the lake during this timeframe display uni-modal particle size distributions dominated by fine silt and contain the lowest P90 values in all traps through the survey period (July 2013). EM3 is a minor component in Jun 2013 basal traps and absent from July 2013 while EM1 (fine silt) makes its most significant

contribution during the survey period, especially in the July 13 upper trap. The materials collected during this period are typical of the background fine silt or gyttja accumulating in the lake, and have a higher organic content with reduced concentrations of lithogenic elements (Figure 6.6c).

Autumn/winter normal flow conditions

The Oct 2012 and Dec 2013 samples exhibit similar particle size signatures, with moderate to low P90 values and EM3 contribution, despite both trapping periods experiencing episodes of high rainfall and elevated discharges. A key hydrological difference that may explain the finer calibre of material than measured in the Jan 2013 samples is the lack of sustained high discharge, compared to 20 – 31 Dec 2012 when discharge was above 10 m^3 s^{-1} for eleven consecutive days (Figure 6.2a). Flood hydrographs rose and fell much more steeply through the high flow events that occurred during the Oct 2012 and Dec 2013 sampling intervals. These results suggest the Kirkstone Beck delta is an effective sediment trap with a high threshold for sediment retention, confirmed by significant accumulation of medium to fine gravel on the delta top-set, and this threshold appears only exceeded by sustained high flows producing sediment-rich plumes that are capable of delivering coarser material across the lake basin.

6.4.5 Reconstructing an annual amalgamated PSD

Sediment accumulation rates (SAR) during the 20th century reconstructed from BW11-2 are 0.4 - 0.7 cm yr^{-1} (Chapter 4), which is an SAR approximately equal to the sampling resolution for particle size analysis on the long cores. The likelihood that flood laminations thinner than 0.5 cm will be missed was highlighted in Chapter 5 and the comparison between the peaks in $P90_{norm}$ and instrumental discharge since CE 1960 showed Q exceeded 35 m^3 s^{-1} on many more occasions than the number of flood units identified in the sediment cores. Here, we use the trap data to explore whether this could reflect the proportionally greater contribution to total annual sedimentation from fine calibre material (EM1 and 2), which could mask the sedimentary imprint of palaeofloods.

The monthly trap PSDs were integrated to reconstruct the longer-term (18 month) particle size signature at both trap sites, thus reflecting the annual load transferred from suspension to the lake bed and potentially preserved in the accumulating sediments. The sediment trap grain size data were summed to represent annual

accumulation on a proportional basis, accounting for the amount of material captured and the time span of each sampling period (Figure 6.9a and 6.9b).

Keeping in mind that material was not collected from all traps in all months (Tables 6.1 and 6.2), the particle size distributions for individual traps exhibit some variability with depth and location. In particular, the coarser modes (sand fraction) are prominent in the middle and upper traps than at depth at Site A and a sand mode is largely absent at Site B (no sample was obtained in January 2013). The primary mode at both trap locations lies in the medium silt domain, which is the typical PSD signature of background sedimentation. The sand mode is much less conspicuous at Site A when the trap-specific monthly data are converted to an annual PSD, which is a significant finding. The annual integrated PSDs exhibit decreasing sand contribution with water depth (Figure 6.9a), but the sand fraction is not represented by a primary mode at any station. The prominent tail of the Jan 2013 distributions lies in the sand domain and comprises a relatively minor contribution to the annual PSD, which reflects the low total dry weight sedimentation during this timeframe (Table 6.1).

The PSDs generated by combining the three depths at each station are regarded as representing the total composition of material reaching the lake bed. At Site A, a secondary mode in the very coarse silt domain is visible, but the sand fraction is represented as a subtle inflection or shoulder in the PSD curve. Essentially, the coarse material delivered to Brotherswater through the survey period, especially during Dec 2012, is masked by the much more regular deposition of silt-sized material. Cockburn and Lamoureux (2008) highlight a similar mechanism in Canadian Arctic lakes. The majority of the combined PSD lies in the silt domain at Site B, with the mode consistent with the sediment core sequences (Chapter 5). These amalgamated PSDs are actually more similar to EM2 than EM3 (Chapter 5; Figure 5.5), which also incorporates a subdued tail in the sand domain.

These results suggest that, despite periods of elevated river discharge delivering coarse material to the lake (especially at Site A), the eventual sedimentary signature preserved in the lake sediment record would not be regarded as indicative of the occurrence of a high-flow event. The implications for the longer palaeoflood record at Brotherswater (Chapter 5) are that events preserved in the PSD palaeoflood record as a discrete coarse-grained lamination (≥0.5 cm thick) dominated by the sand-sized mode must represent the rare, highest-magnitude events. Moderate, more frequent

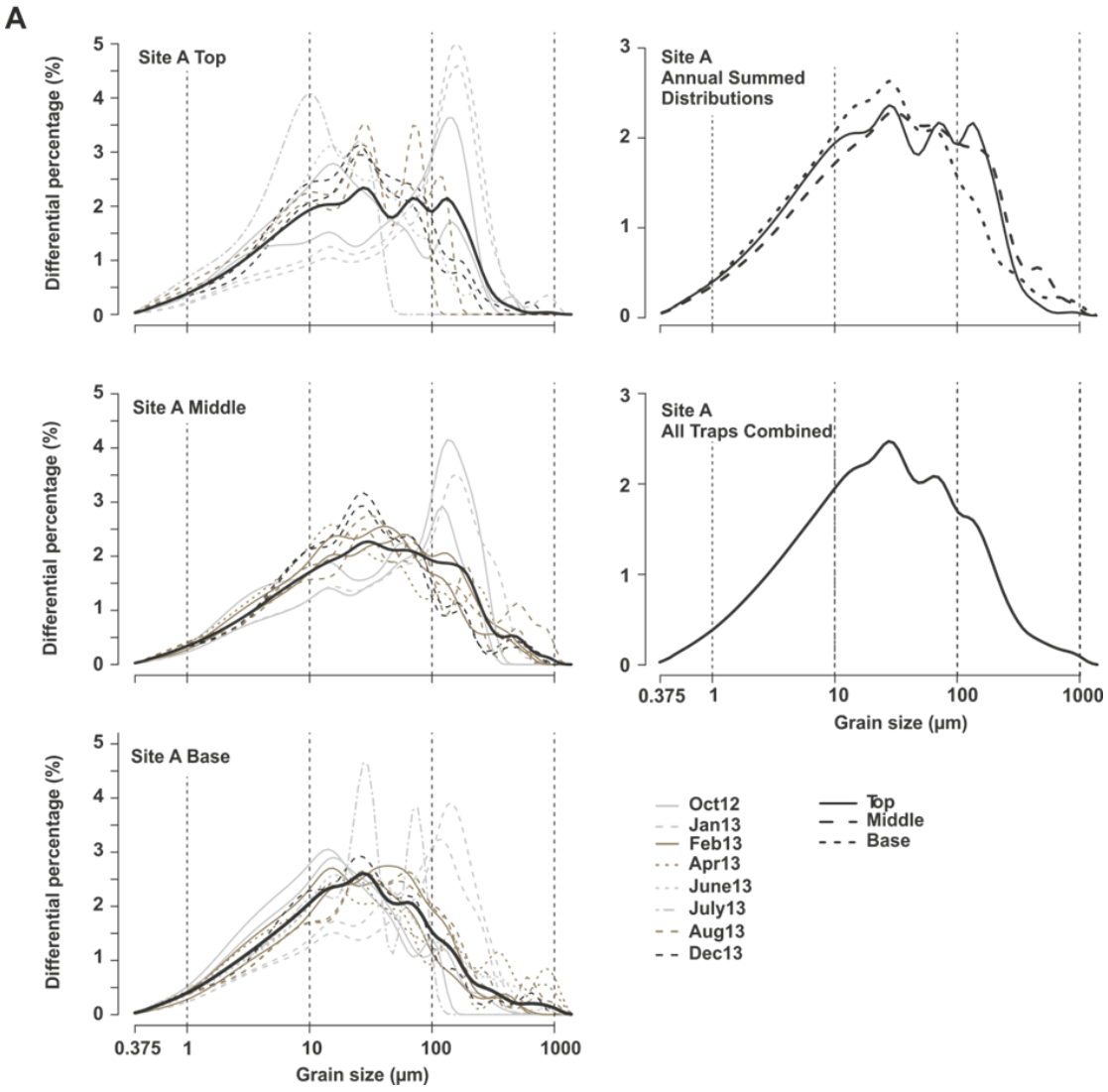

(Figure 6.9 continued overleaf)

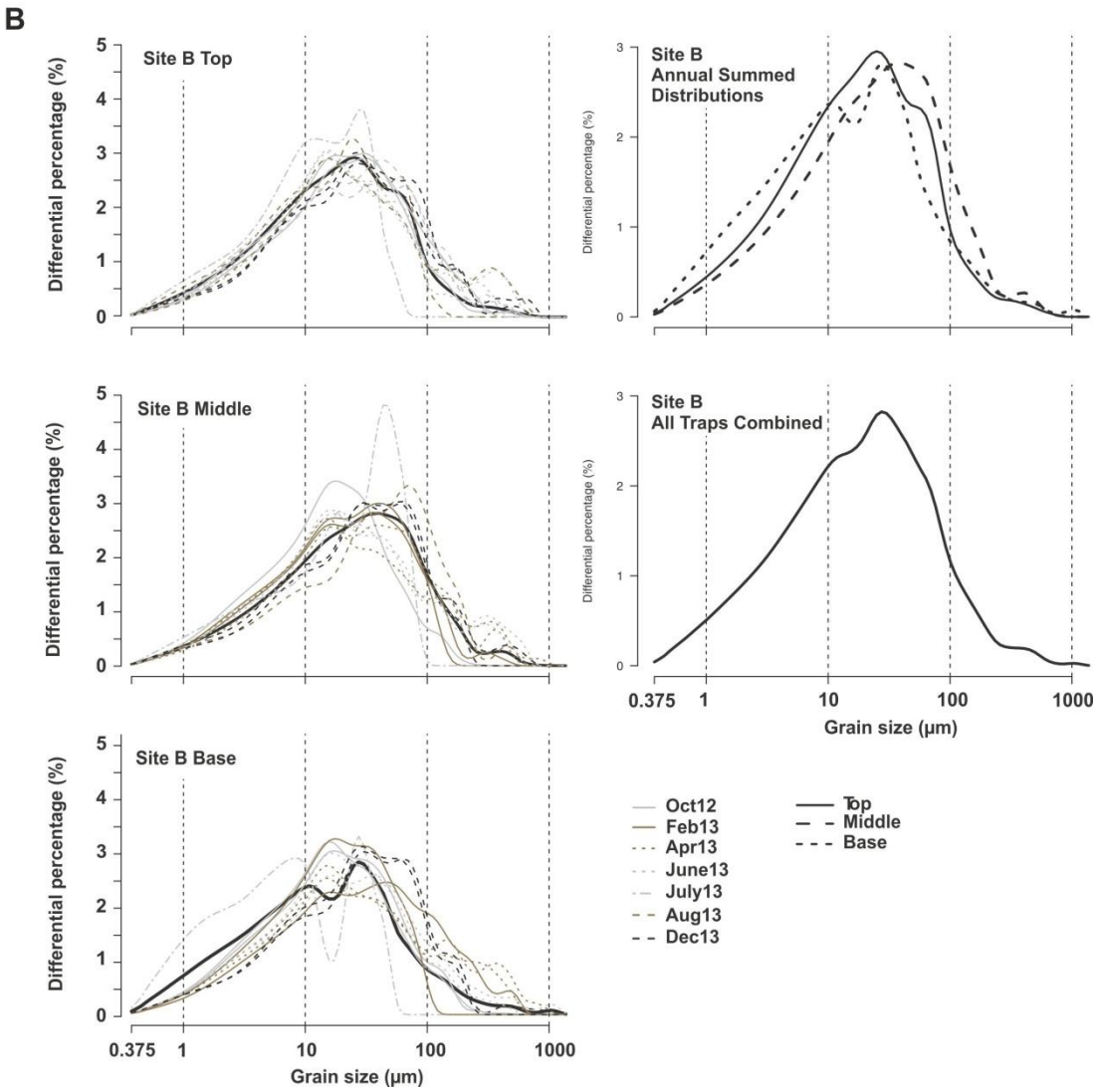

Figure 6-9 A) Annual summed particle size distributions for trap site A. B) Annual summed particle size distributions for trap site B.

events are less likely to leave a sedimentological imprint detectable by our analyses of the long sediment record. It is important to keep in mind, however, that these results reflect a low number of sampling intervals over an 18 month period that may not be representative of long-term hydro-meteorological conditions in the catchment-lake system; extending this programme could be greatly beneficial for verifying these findings. This is probably less of an issue at other lake-catchment configurations, but this will be regulated by composition of the sediments and the mechanics of deposition at that site. Annually-laminated alpine lakes in the European Alps, for example, have unique seasonal laminations that are clearly distinguishable from detrital flood laminations (e.g., Swiercynski *et al.,* 2012; Czymzik *et al.,* 2013). This is not the case for

lakes with a homogenous silt-dominated sediment matrix like Brotherswater and many other British lakes (c.f. Pennington 1991).

6.5 Conclusions

An 18 month sediment trapping programme was undertaken at Brotherswater to shed light on contemporary within-lake sediment dynamics and depositional mechanisms, sediment provenance and the response of the system to high discharge events. Despite the moderate number of data points, particle size signatures of prolonged elevated discharge during winter, low flow during summer months, normal flow conditions during autumn and winter and the influence of successive flood events on grain size transport have all been classified. Interestingly, delivery of the coarsest particles appears to require persistent elevated flow as opposed to 24 hours of exceptional rainfall and discharge. Total sediment volume captured by the traps responds to discharge to a certain degree but this is overprinted by a seasonal signal of spring/summer diatom bloom and increased organic productivity. The installation of sediment traps at three different water depths and at delta-proximal and distal sites provided data that hints at summer stratification influencing whether hypopcynal or hyperpycnal flows occur. Probably the most significant result revolves around the estimation of the time-averaged particle size distribution representing the full survey period. The particle size distributions of all traps were amalgamated and adjusted for variable sediment accumulation. Sediments deposited under low or normal flow conditions generally lie in the silt domain, matching the adjacent long cores, and this is the dominant signal within the annual PSD. Months during which coarse material was captured make a limited contribution to the annual PSD, suggesting the material that accumulates at the lake bed reflecting this 18 month period will not preserve a signal of elevated flow. This has large implications for palaeoflood research as floods of moderate magnitude may be missed, but it also indicates that coarse palaeoflood laminations identified within the Brotherswater cores must reflect floods of exceptional magnitude.

Acknowledgements

This work contains Environment Agency information © Environment Agency and database right (rainfall and river flow data).

7 LOCH OF THE LOWES

7.1 Introduction

Palaeoflood research has gained impetus in recent decades driven by concerns over impacts of extreme river flows and the potential for more frequent extreme climatic events under Intergovernmental Panel for Climate Change (IPCC) scenarios for the next 100 years (IPCC, 2013). In the context of palaeolimnological research this has seen a deluge of sites targeted and papers published, mostly focused in Europe but also elsewhere across the globe (see detailed review in Chapter 2; Schillereff *et al.,* 2014). This thesis has extended that research through reviewing the basin characteristics conducive to reconstructing flood histories (Chapter 2), and using Brotherswater, a small lake in the Eden catchment of northwest England, as a site for refining and developing methodological approaches for grain size (Chapter 5) and geochemical (Chapter 3) analyses to discern flood records. Comprehensive assessment of the lake sediments in the Brotherswater basin produced a consistent flood stratigraphy from multiple cores spanning the last 1500 years and an investigation of contemporary sedimentation dynamics, using 18 months of sediment trap data, characterised the catchment-to-lake sediment signatures of variable river flow.

As a test of the approach and methodology adapted and developed in this thesis, attention switches to another catchment and lake basin in the north of the British Isles. Loch of the Lowes lies in the headwaters of the eastwards-draining River Tweed catchment in southern Scotland (Figure 7.1). The basin geometry and physical setting of the loch and catchment meet many of the traits conducive to the effective recording

of distinct signatures of historic floods in the profundal sediments (Chapter 2; Schillereff *et al.,* 2014). Previous investigations of the recent sediment record at Loch of the Lowes identified an association between the winter mode of the North Atlantic Oscillation (NAO), an important driver of inter-annual to decadal precipitation, and cyclical variations in coarser grained sediment parameters (% sand and HIRM/χLF) in the profundal lake sediment record of the last 400 years (Foster *et al.,* 2008).

Extreme floods in Scotland during the AD 1990s and AD 2000 generated considerable public interest and re-assessment of the flood risks (McEwen, 2006). Data on historical flood occurrence obtained from documentary and epigraphic sources (e.g., Macdonald *et al.,* 2006; McEwen, 1990) as well as preserved in sedimentary sequences from alluvial settings (e.g., Werritty *et al.,* 2006) have in fact shown south-eastern Scotland has experienced repeated severe floods over the past several centuries. The most sustained flood-rich period on the River Tay dates to the mid-19th Century (McEwen, 2006; Werritty *et al.,* 2006), while both the early and mid-20th Century were also characterised by high flood frequency (Macdonald *et al.,* 2006), with flood events most often associated with westerly airflows (McEwen, 2006). Acquiring a better understanding of historical severe flood occurrence is particularly important for regional rivers, including the River Tweed, that are biologically rich (Clayton, 1997) and heavily exploited for water supply (Fox & Johnson, 1997). Investigating whether sediments of Loch of the Lowes, a small loch in the Southern Uplands of Scotland, have preserved a palaeoflood stratigraphy may offer valuable data to complement the existing historical flood research. Palaeoenvironmental data (Tipping & Halliday, 1994; Tipping, 1998; Campbell *et al*, 2002; Chiverrell *et al*, 2007; Foster *et al*, 2008) for the region reveal a landscape heavily modified by human activity for several millennia, with the pulsed development of a deforested, agricultural landscape at CE 100–400 and CE 600–900 and during population expansions at CE 1200–1400 and after CE 1500 (Foster *et al.,* 2008). This landscape context is conducive to high rates of erosion and the efficient delivery of soils and sediments from the catchment under both low and high flow regime, shown in environmental magnetic and geochemical sediment provenance investigations at Loch of the Lowes (Foster *et al.,* 2008).

A similar methodological approach will be adapted as the Brotherswater research, specifically using particle size and geochemical metrics to discriminate potential palaeoflood laminations from a sequence of cores extracted along a delta-proximal to distal transect. Accounting for non-flood related shifts in sediment supply or calibre

and, provided suitable chronological control can be established, the palaeolimnological record of the timing and magnitude of floods will be explored in the context of historical and fluvial information for the Tweed and southwest Scotland.

7.2 Loch of the Lowes and the Tweed catchment

Loch of the Lowes lies in the Tweedsmuir Hills, in the central Southern Uplands of Scotland (55.2756°N, 3.1226°W), and occupies a headwater of the large River Tweed watershed, the second largest in Scotland (total area ~5000 km^2). The small loch (area 0.47 km^2) receives flows from five sub-catchments (total area 27 km^2, C:L ratio ~57) with a maximum elevation 610 m. Most drainage enters the southern shore along with two smaller inflows at the northeast and northwest. The loch is adjoined to the downstream larger St Mary's Loch by a small stream. An alluvial fan that probably developed during the early-Holocene (Murray & Pullar, 1910) separates the two water-bodies. Yarrow Water is the outflow of St Mary's Loch and its confluence with the Tweed is 20 km downstream. The lake is oligotrophic and has an elongated basin dominated by a single, flat central basin 12 – 15 m depth and with limited littoral area (Murray and Pullar, 1910). Catchment bedrock geology is dominated by Lower Palaeozoic greywacke sand/silt/mud-stones, which have been sculpted by Quaternary glacial erosion into an upland terrain comprising U-shaped valleys and more rounded summits.

Geomorphic investigations of the catchment (Foster *et al.,* 2008) noted alluvial fan deposits (dated using ^{14}C) associated with relict gully and cone systems as well as multiple late-Holocene river terraces, reflecting past episodes of fluvial invision and hillslope erosion. Several phases of increased hillslope to valley-floor sediment transmission were identified during the Bronze to Iron Ages (2000–0 BCE), and more intensive region-wide phases around CE 700–900, 1100–1300 and after CE 1450–1550 (Foster *et al.,* 2008). These correspond strongly with phases identified for the wider region across northwest England and southwest Scotland (Tipping, 1994; Chiverrell *et al.,* 2007, 2008). Increased regional precipitation during the Little Ice Age has been proposed as a driver of accelerated channel migration, fluvial erosion and sediment deposition along the River Tweed (Tipping, 1994). Alongside climatic variability, natural or anthropogenic landscape evolution may alter the supply of sediment within the system, thus modifying the hydrodynamic relationship between river flow and

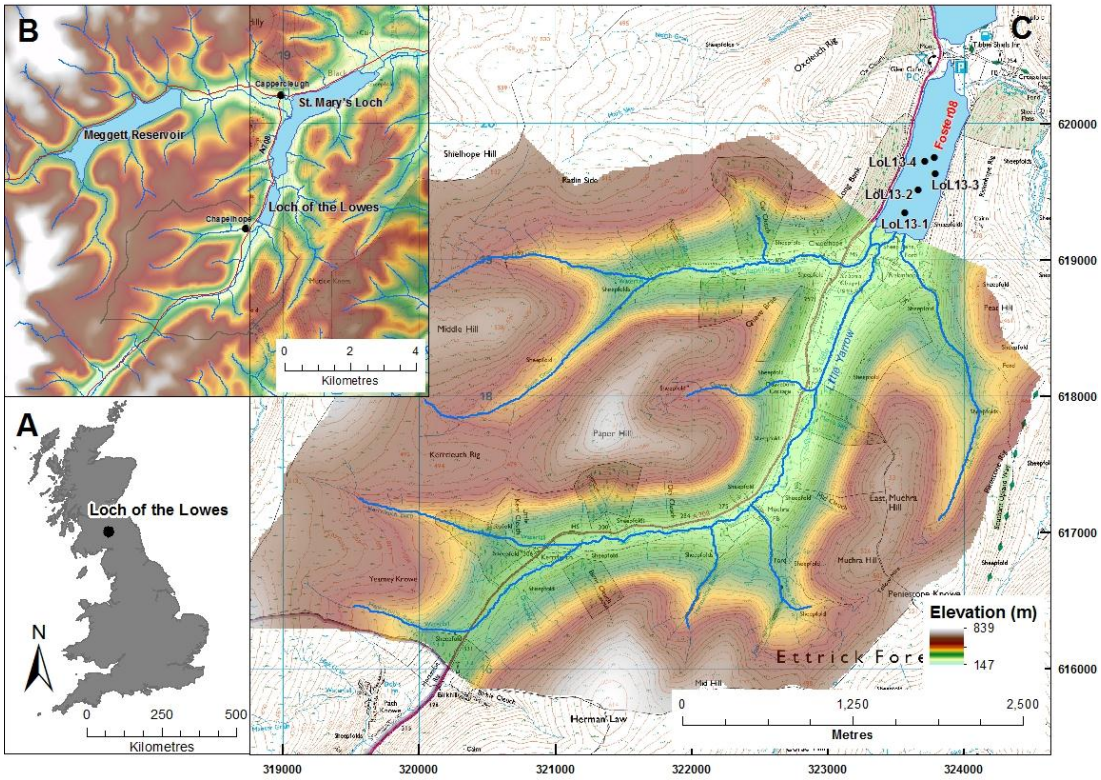

Figure 7-1 A) Location of the study site within the UK. B) The topography of the catchment and wider area around Loch of the Lowes. C) Core locations, catchment morphology and the main, southern drainage system of Loch of the Lowes.

sediment transport to the lake. Land cover today is a mixture of managed blanket moorland on hill tops and grazing pasture growing on podzolic soils that have developed on hillslopes artificially drained through the 18th and 19th centuries (Tipping, 1994; McEwen, 1990). Forest cover is largely absent except for small conifer plantations, and palaeoecological records indicate widespread woodland clearance in the nearby Cheviot Hills (~50 km east) in the late Iron Age (Tipping, 1998) and negligible forest cover by ~CE 300 (Campbell *et al.,* 2002) that largely persisted through to the present day, but there is some indication of *Betula* and *Corylus* re-growth at nearby Talla Moss from ~CE 400 – 650 (Chambers *et al.,* 1997).

The catchment climate is generally cool and temperate (mean annual temperature of ~9 °C, mean annual precipitation at Eskdalemuir is ~2000 mm). While the winter mode of the North Atlantic Oscillation (NAO) appears an important driver of inter-annual to decadal precipitation (Foster *et al.,* 2008), highly regionalised precipitation is

also an important hydro-meteorological feature, generally controlled by easterly longitude and elevation (reduced precipitation in the low-lying easterly region) across the Tweed catchment (Fox and Johnson, 1997), leading to flow regime in the River Tweed that exhibits pronounced annual and seasonal variability (Fox and Johnson, 1997). Historical data point towards summer (July-October) frontal convection systems triggering intense rainfall and severe floods (Mcewen, 1989), but gauged river flow data from the River Tweed are more characterised by winter flooding (November through January, moderate frequency in October, February, March; McEwen, 1990). Snowmelt is also known to make a contribution to regional flooding, including the February 1831 event (McEwen, 1990) and the recent severe CE 1993 flood (McEwen, 2006).

7.3 Methods

7.3.1 Field sampling

Overlapping sediment cores were extracted at four sites across Loch of the Lowes in April 2013 following a delta-proximal to distal transect (Figure 7.1) using a 1.5 m length Russian-type corer (diameter 70 mm). Water depths ranged between 12 and 13 metres. Cores were tightly wrapped to prevent drying, and stored in darkness at 4 °C at the University of Liverpool. Short gravity cores (Boyle, 1995) were obtained at LoL13-2 (sediment length 24 cm) and LoL13-3 (30 cm), recovering an intact sediment-water interface in both cases. A short core was not recovered at core site 1 because of the high sand content. The gravity cores were extruded and subsampled at 0.5 cm contiguous intervals. All four long cores were analysed on a wet sediment basis using an ITRAX μXRF scanner for major element chemistry and X-ray density. Scans were also completed using a Geotek XZ desktop MSCL for major element chemistry (XRF), magnetic susceptibility (Bartington MS-2), colour (diffuse UV/Visual light reflectance spectroscopy) and by high resolution photography. Two cores were selected for detailed particle size analysis, the most proximal and distal to the southern delta, where the sediment lengths recovered were 178 cm (LoL13-1) and 262 cm (LoL13-4).

7.3.2 Visual analysis

The cores were cleaned and the depths of visually distinguishable light and dark laminations carefully noted before being photographed at 100 μm image pixel

resolution using a Canon EOS 600D Line-scan (LS) camera on the Geotek XZ MSCL instrument, after calibration to 18% grey and white plates. Colour separation into red, green and blue channels is performed during the photographing process and converted into RGB values at 100 μm resolution. Quantitative colour measurements were also performed at 0.5 cm intervals using a Konica Minolta CM-2600d diffuse reflectance spectrophotometer (DRS) mounted on the Geotek which records reflectance spectra in the near UV through to near IR range (wavelengths 360-740 nm). Dark and light laminations were delimited using both techniques with a strong correspondence between the two approaches; in later sections Line-scan RGB values are used given their higher resolution.

7.3.3 Density and organic matter content

Dry bulk density was measured on the contiguous gravity core samples as well as at 5 cm intervals along LoL13-4-1. These were weighed, freeze-dried and reweighed after drying to calculate moisture content and dry masses were calculated using mineral density of 2.65 g cm^{-3}. The organic matter (OM) content of the LoL13-4-1 sample set was estimated using thermogravimetry (TGA) / differential scanning calorimetry (DSC) (Perkin Elmer STA6000), following the procedures outlined in Section 3.2. Thermal decomposition between 150° and 530°C was regarded as representing OM content.

7.3.4 Geochemistry

Geochemical profiles were obtained on a wet sediment basis for all cores via X-ray fluorescence using both Geotek MSCL and ITRAX core scanners. The Geotek μXRF measurements were performed at 5 mm and 1 mm resolutions using an Olympus Delta Energy-Dispersive XRF (ED-XRF) analyser fitted to a robotic arm while the ITRAX scans were carried out using a step size of 300 μm and occupation time of 30 seconds. A detailed inter-comparison of both core scanning devices (Chapter 3.4), tested after correcting raw elemental concentrations to dry mass equivalent using the methodology outlined in Chapter 3.3) highlights a broadly consistent signal is obtained for most elements and that the ITRAX and Geotek/Olympus 5 mm and 1 mm data are broadly comparable (Chapter 3.4).

7.3.5 Particle size

Core LoL13-1 was sub-sampled at 0.5 cm intervals for particle size analysis. The upper drive of core LoL13-4 was sliced at variable thickness guided by the visual stratigraphy to capture and analyse particle size changes across rhythmic or event layering. Sampling intervals ranged from 1 mm to 5 mm and the thicker light and dark bands were subdivided into multiple samples to assess grain size changes within layers. Samples were treated with 30% H_2O_2 to remove the organic fraction, sonicated to disperse the samples and measured via laser granulometry on a Beckman Coulter™ LS320. Collected particle size distributions (1-2000µm) are the average of two successive runs and frequency statistics were calculated using the geometric measurement formulae of Folk and Ward (1957) within the GRADISTAT 8.0 software (Blott and Pye, 2001). Where differences between successive run occurred typically this reflects aggregates or poor dispersion in the earlier run, further sonication and measurement cycles ensured the two runs were virtually identical in all cases.

7.4 Results

7.4.1 Geochronology

Radiocarbon dating is still in progress for the Loch of the Lowes cores, with preliminary determinations failing due to insufficient carbon in the plant macrofossil samples. Previous geochronological analysis of a 70 cm sediment core extracted from a central location (Foster *et al.,* 2008) yielded a reliable ^{210}Pb record, with a prominent 137Cs peak that most likely reflects maximum atmospheric fallout during CE 1963 nuclear weapons testing. The basal ^{210}Pb age is CE 1882 ± 27 at a depth of 18 cm. Foster et al. (2008) identified a take-off in Zn and stable Pb from 24 cm depth that continues to present day, most likely reflecting atmospheric deposition. The onset of increasing Zn and Pb concentrations also occurs at 22 cm in the new core LoL13-4, extracted in close proximity to LL5 (Foster *et al.,* 2008). These geochemical profiles match the general up-core trace metal pollution patterns seen at other lakes in Scotland (Yang and Rose, 2005; Farmer et al., 1997b) and northern Europe (Renberg *et al.,* 2001), attributed to emissions to the atmosphere during industrialisation. In most cases the onset is dated to the AD 1860s, and so provides a chronological marker that is also present in the other three cores (Figure 7.2). Assuming a constant linear sedimentation rate (SAR), accumulation rates of 0.42 and 0.14 cm yr^{-1} are calculated,

although the Foster et al. (2008) ^{210}Pb measurements indicated some variability in 20th Century SAR.

7.4.2 Sedimentology, down-core trends and core correlation

All cores are heavily laminated throughout (Figure 7.2), with sub-mm as well as thicker (up to 1-2 cm) light and dark bands. The laminations are generally thinner in the lake centre (LoL13-3 and 13-4), although some light laminations (e.g., 6.5, 20 and 73 cm in LoL13-4) and the thick organic unit at 124 and 136 cm in LoL13-3 and 13-4, respectively, are particularly prominent. Variation in unit thickness and occurrence means annual layering is unlikely. Instead, coarse sand lenses are distinguishable throughout core 1, normally in the dark brown to black layers. The punctuated nature of these coarser laminations points towards the preservation of discrete flood units. The extent of overlap between successive drives at each core site was determined on the basis of down core lithological markers, sediment colour metrics and element profiles. Geochemical behaviour appears to be dominated by co-variance amongst the lithogenic elements, likely to be indicators of mineral supply (e.g., Si, Al, Ti, K, Rb, Zr), with light-coloured laminations yielding higher concentrations. Mineral indicators also fluctuate with colour changes over more moderate depth scales, with generally higher concentrations in the lighter sediments below 130 cm in LoL13-1 and the thick, very light sections around 220 – 230cm in LoL13-3 and 13-4. Ca is enriched in some light laminations, but in general shows inverse behaviour to the lithogenic fraction.

Correlation of the stratigraphy between core locations across the lake basin was based on atmospheric fallout Zn, detrital elemental indicators (K, Rb, Ti, Sr and Zr) as well as Ca and Fe, which all exhibit somewhat different down-core behaviour (Figure 7.2). For example, the sections designated 'Higher Ca' are characterised by increased Ca content while the detrital elements decline in concentration. The signal of atmospheric Zn deposition (atmospheric Pb signals are less clear) is present at the top of all cores, although the take-off occurs at shallower depths with distance from the inflow reflect reducing sediment accumulation away from the southern delta: ~65 cm in LoL13-1 decreasing to ~28 cm in 13-3 and 13-4. These depths are considered robust as gravity cores extracted nearby (LoL13-2s and 13-3s) recovered intact sediment-water interfaces that show rising Zn from similar depths (Figure 7.3). As well as the atmospheric pollution story, the gravity core geochemical data also reveal elevated Fe and Mn concentrations in the uppermost sediments of LoL13-2s and LoL13-3s (Figure

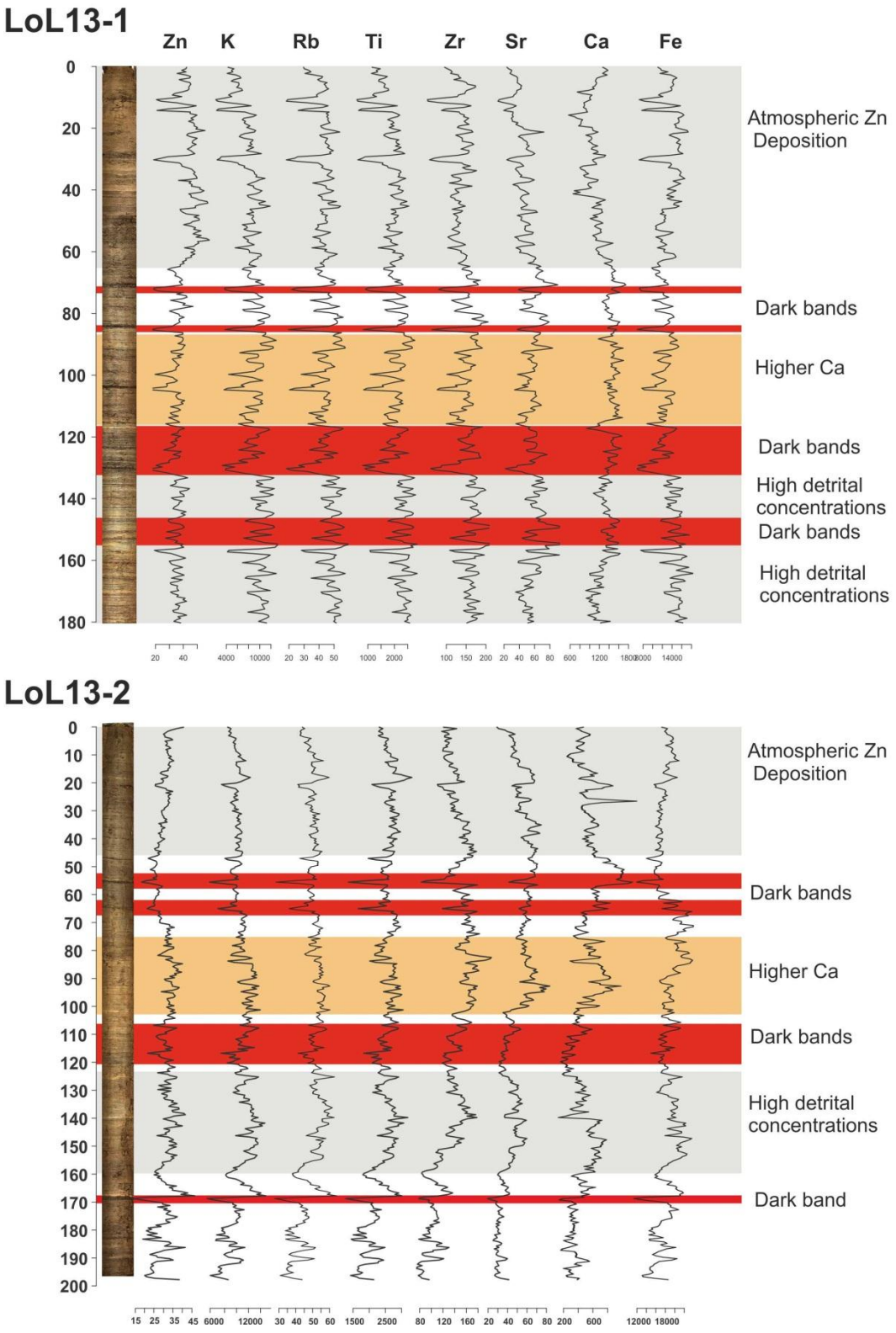

(Figure 7.2 continued overleaf)

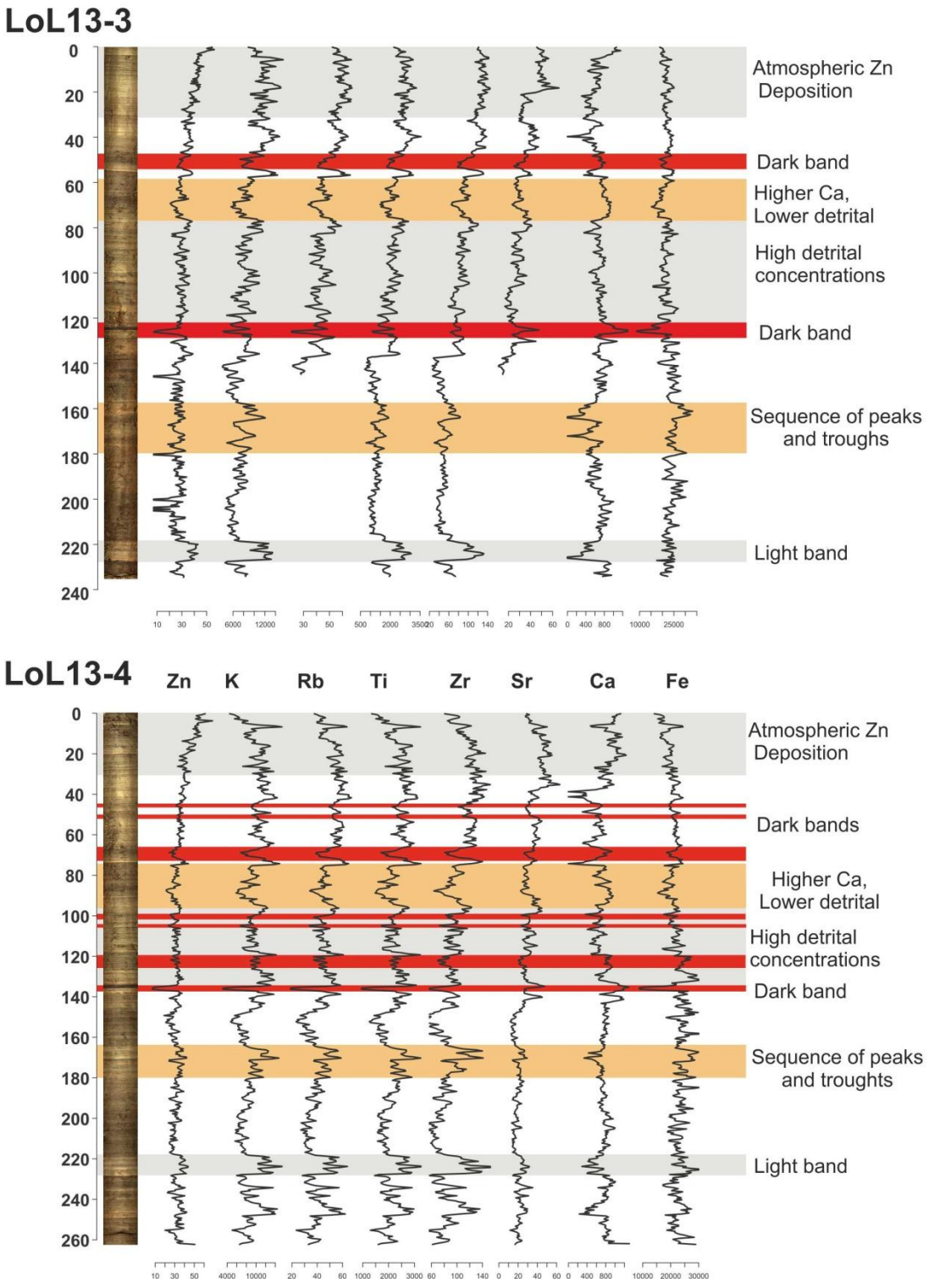

Figure 7-2 Core photographs and down-core geochemical profiles of the four long cores extracted from Loch of the Lowes. Correlation points are highlighted and labelled.

7.3), indications of redox conditions (Boyle, 2001b). This trend is not picked up in any scanned long core datasets, probably due to either the uppermost wet sediment being lost during the coring process or the lower count rates on the core scanners due to non-compacted sediment with higher water content at the top of the cores. Sporadic peaks in Mn occur through the long cores with a spike of especially high concentrations corresponding to the thick black band at 135 cm depth in LoL13-4.

Conspicuous features in the stratigraphy and geochemical profiles Cores LoL13-1 and 13-2 can be used to correlate both cores, especially two dark bands at 70 and 84 cm in LoL13-1 and 55 and 65 cm in LoL13-2, and in particular the couplet of a light band with high lithogenic element concentrations immediately above a dark section containing lower lithogenic element concentrations at 115-132 cm in 13-1 and 105-120 cm in 13-2 (Figure 7.2).

The thick dark/light couplet at 168 cm depth in LoL13-2 is probably the same feature as 122 cm in 13-3 and 136 cm in 13-4. Broader geochemical features present in all cores include a phase of higher Ca concentrations and a deeper phase of higher lithogenic element concentrations (Figure 7.2). A broadly opposing trend is observed between lower-resolution (5 cm) estimates of sediment bulk density and organic matter (OM) content derived from TGA data for LoL13-4 (Figure 7.5). OM content is highest around 66 and 86 cm depth, occurring within thicker intervals of dark sediments that extent from 64 – 72 cm and 84 – 90 cm depth. Both sections also have low bulk densities: 0.81 and 0.61 g cm^{-3}, respectively. The black band at 135 cm depth was not measured thermogravimetrically, but microscopic investigations showed abundant fragments of terrestrial macrofossils including *Sphagnum* leaves, reflecting the erosion and transmission of peat eroded from the catchment.

7.4.3 Direct and indirect particle size data

Material in core LoL13-1 is consistently coarser than LoL13-4, with background mean values consistently around 25 μm (Figure 7.4) compared to ~10 μm in the central basin (Figure 7.5). Coarse laminations in LoL13-1 are characterised by mean and P90 values reaching 200 μm and 1100 μm, whereas maximum mean and P90 values in LoL13-4-1 are 40 μm and 160 μm, respectively. Material in both cores is poorly to very poorly sorted (>3 in LoL13-1, >2.5 in LoL13-4), most likely due to the broad sediment calibre range, from clays to coarse sands. A weak sinusoidal relationship is observed between sorting and mean grain sizes as well as between sorting and P90 (Figure 7.6).

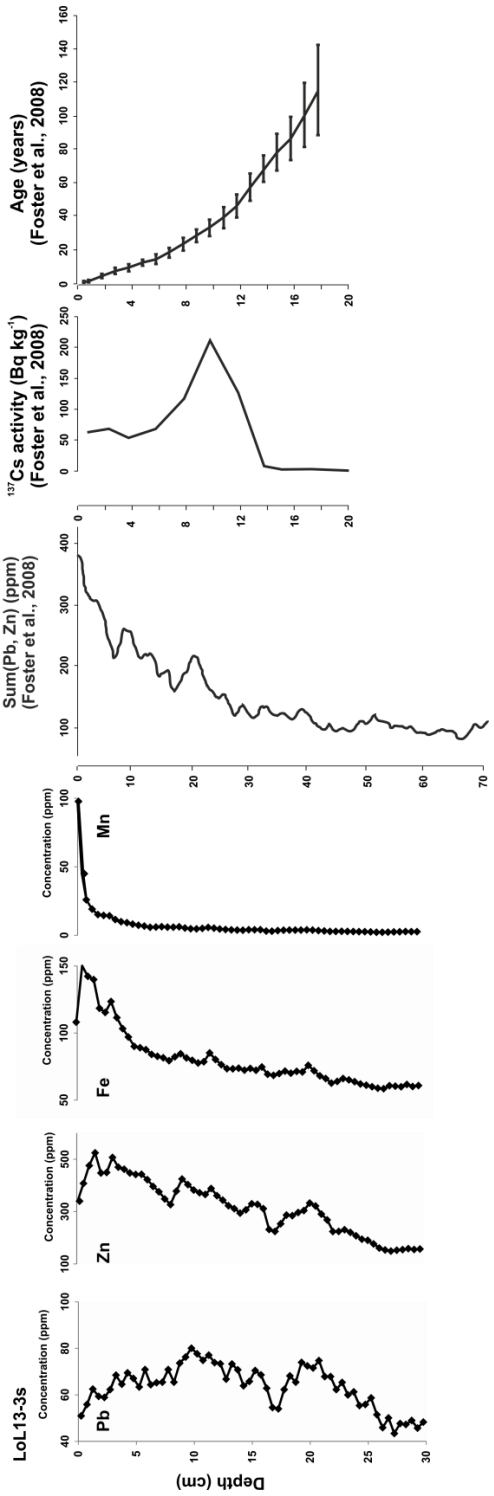

Figure 7-3 Selected geochemical profiles for the gravity core LoL13-3s in which an intact sediment-water interface was recovered. A signal of post-CE 1850 atmospheric pollution is reflected in the Zn and Pb profiles that matches the Foster et al. (2008) record. Their age-depth model for a core extracted from the lake-centre is also presented.

Skewness plotted as a function of mean grain size yields a modest trend towards positive skewness with decreasing grain size, somewhat less apparent in LoL13-4. The darker intervals at 84 – 90 cm and 99 – 105 cm in LoL13-4 correspond with the coarsest grain size measurements (mean = 21 and 35 μm, P90 = 160 and 155 μm). This relationship extends to darker laminations in both cores and, in general, these coarser layers are also more negatively skewed. Lighter bands generally exhibit lower mean and P90 grain sizes and are dominated by fine silts and clays. Most of these laminations are much less negatively skewed than the dark layers (in some cases weakly positive) and are often less poorly sorted.

The similar overall trend between the Zr/Rb ratio and sediment colour emerges when cores LoL13-1 and 13-4 are visually examine (Figures 7.4 and 7.5). The Zr/Rb ratio has been normalised and plotted against the stratigraphy and, in many cases, darker layers have positive Zr/Rb ratios while negative values occur where light bands are present, although the differing analytical resolution means a direct comparison is not performed (Figures 7.4 and 7.5). This relationship is particularly evident across the black laminations at 30, 70, 80, 100 and 130 cm depth in LoL13-1 and the light layers at 6, 20 and 75 cm depth in LoL13-4. This relationship is particularly evident across the black laminations at 30, 70, 80, 100 and 130 cm depth in LoL13-1 and the light layers at 6, 20 and 75 cm depth in LoL13-4. As dark laminations are characterised by peaks in mean and P90 grain size, this appears to reflect a positive relationship between higher Zr/Rb_{norm} and grain size with Zr a coarse indicator and Rb finer grained. This pattern has been tested with the calibrated ITRAX data employed in the μXRF intercomparison (Chapter 3.4; Schillereff *et al.,* 2014) and the same peaks and troughs appear, but the dataset is noisier so the raw data have been plotted here (Figure 7.4 and 7.5). Laminations that exhibit a sedimentological signature comprising high P90, negative skewness and positive

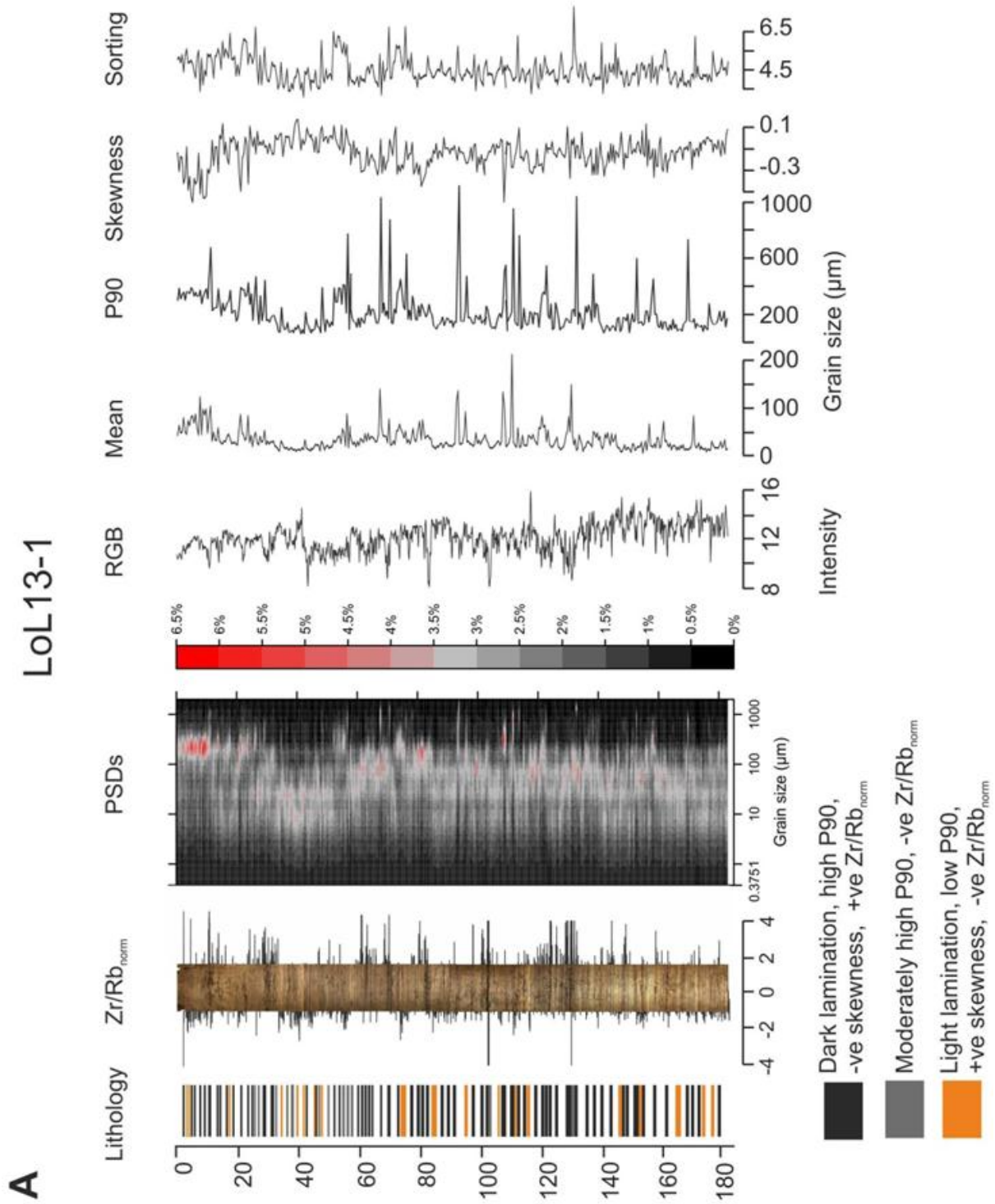

Figure 7-4 Core lithology, particle size and the Zr/Rb$_{normalised}$ data for LoL13-1.

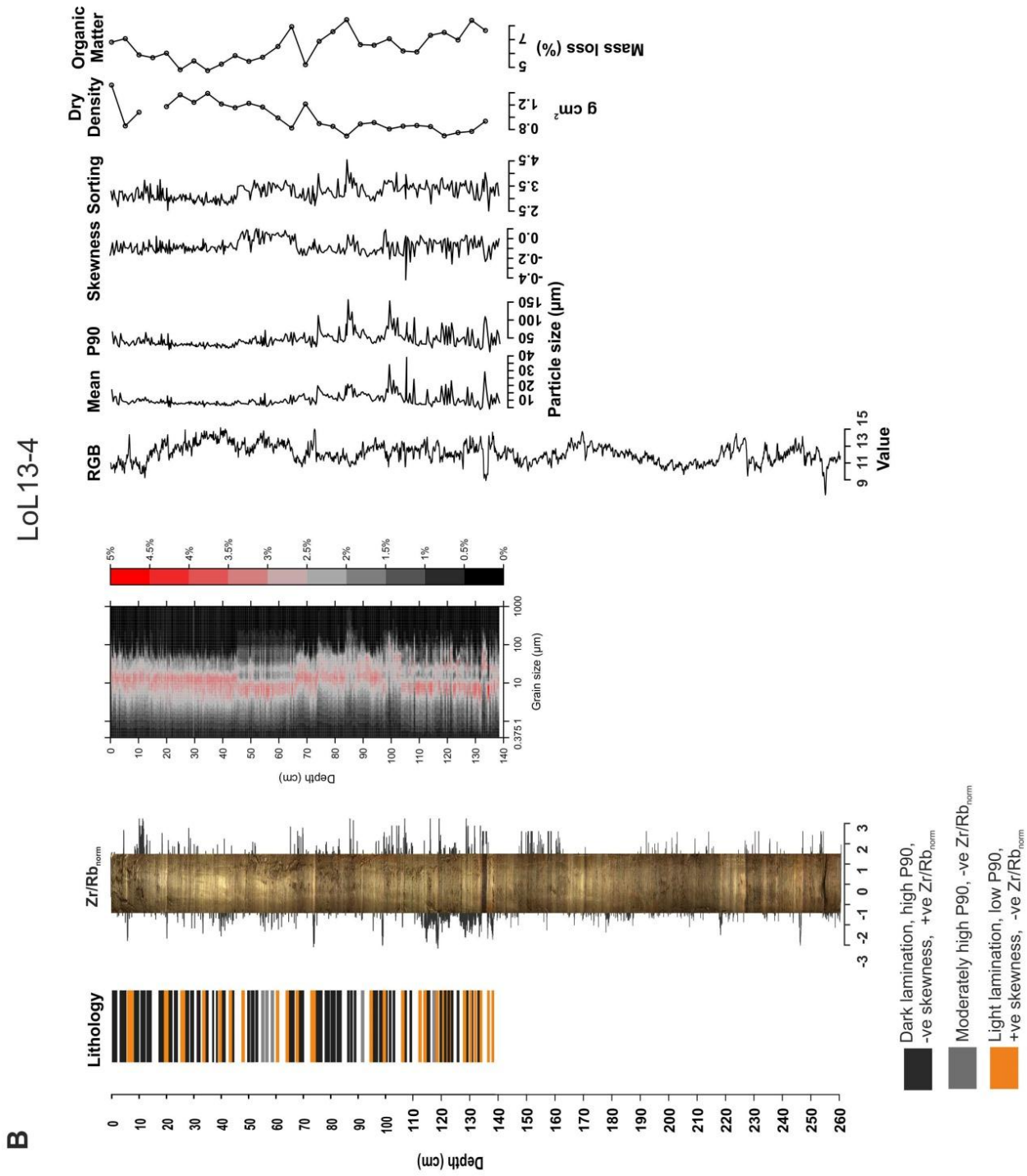

Figure 7-5 Core lithology, particle size, dry density, LOI and $Zr/Rb_{normalised}$ data for LoL13-4.

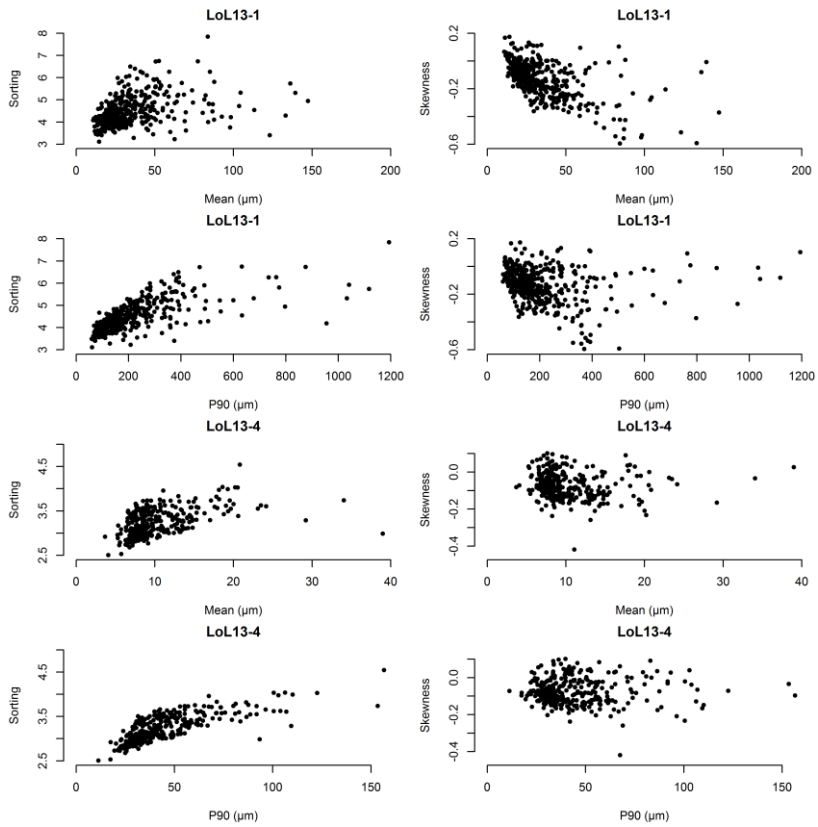

Figure 7-6 Relationship between selected particle size frequency statistics for cores LoL13-1 and LoL13-4.

The four cores exhibit heavily laminated sequences that can be tightly correlated by conspicuous shifts in elemental profiles as well as marker layers, in particular thick (1-3 cm) black units. Characterising the light and dark laminations in terms of their particle size behaviour and elemental concentrations reveals the dark layers that punctuate the sequence are much coarser-grained (P90 > 1000 µm), containing lenses of sand that are often visually distinguishable, and return more positive $Zr/Rb_{normalised}$ values. These layers have been classified as Type 1 and almost certainly reflect deposition under high-energy conditions capable of delivering grains >1000 µm diameter. Their sporadic occurrence throughout the sequence provides strong evidence that this is the signature of past floods.

7.4.4 Micro-scale characterization of discrete laminations

Visual inspection of the cores indicates the laminations were recovered horizontally and the slicing was as parallel as possible. Therefore, the tendency for minerogenic elemental indicators (Zr, Rb, Ti) to increase in concentration across light bands with

lower concentrations across dark laminations can be verified by examining four short vertical sections from LoL13-1 and 13-4 in greater detail (Figure 7.7). This pattern in the minerogenic elements generally occurs over vertical scales exceeding 0.5 cm. These fluctuations are overprinted by a finer structure within the Zr data that behaves in an opposing manner to Rb. As a result, positive and negative excursions in the normalised Zr/Rb curve using μXRF ITRAX data correspond to dark and light laminations, respectively, that are visible at mm and in some cases sub-mm scales (Figure 7.7). The positive Zr/Rb_{norm} peaks almost always exceed 2, reaching nearly 4 at 20-30 cm in LoL13-1. The negative features are somewhat less distinctive, in some cases reaching less than -2 but the two thin laminations at 74.4 and 74.9 cm depth in LoL13 -4 associate the light bands with values of only -0.75 to -1. Peaks in grain size coinciding with darker bands and positive Zr/Rb_{norm} values are also observed across the sub-sections, most visible at 21, 23.5, 27-29, 80.75 and 81.75 cm depth in LoL13-1. The relationship also holds for minor grain size peaks at 26, 83.25 and 84.25 cm depths. Each peak also corresponds with more negative skewness values, particularly prominent at 21 and 23 cm depth.

Microfacies analysis indicates a fairly consistent palaeoflood signal emerges where high P90 and positive Zr/Rb_{norm} values coincidence with dark laminations. The limitations on sub-sampling intervals means many thinner dark layers are characterised by high Zr/Rb_{norm} values and no clear variation in particle size. To ensure consistency, the palaeoflood record will be developed based on Type 1 layers where sediment colour, XRF and particle size data record a palaeoflood signature.

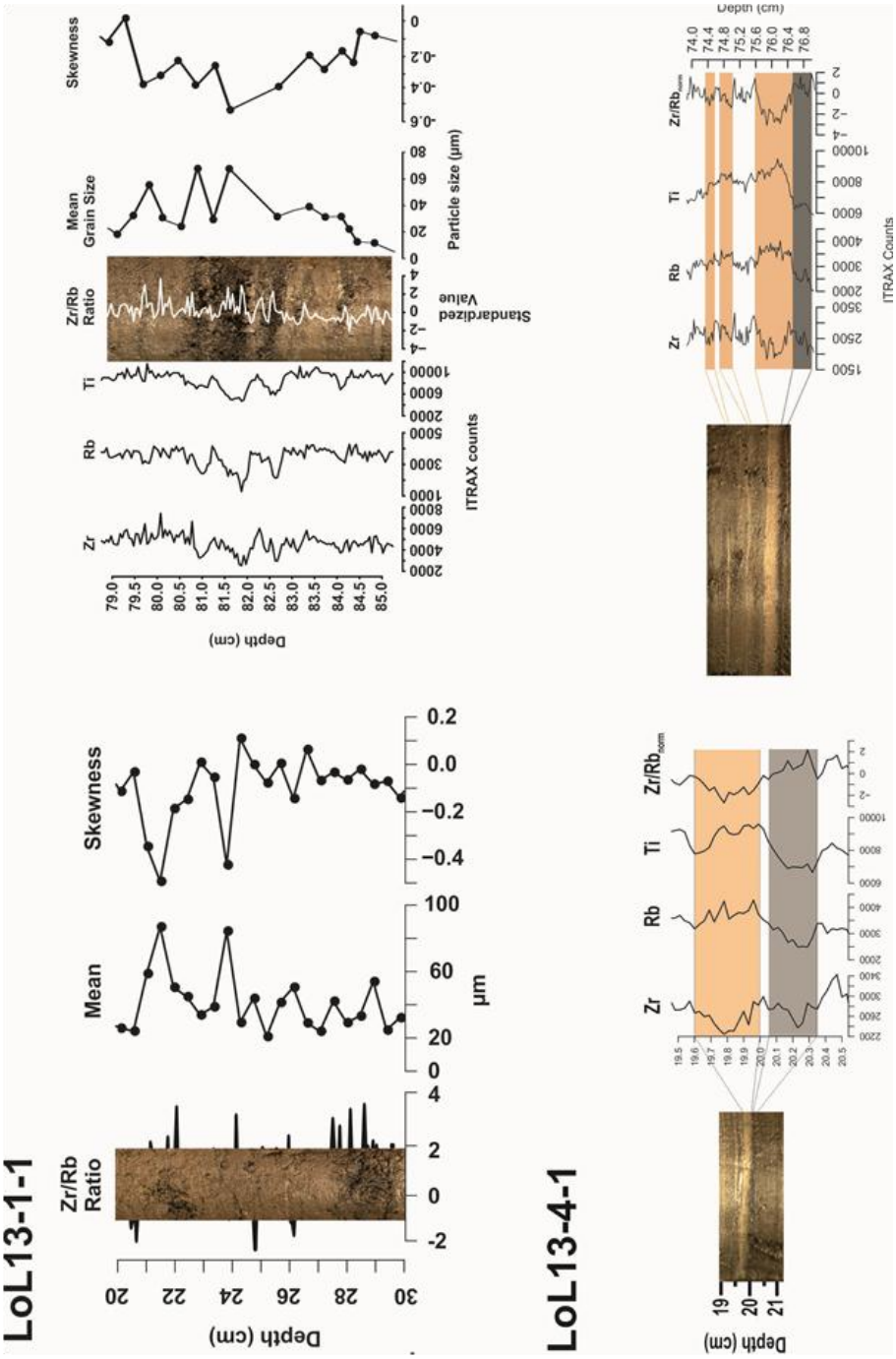

Figure 7-7 Selected sub-sections from LoL13-1 and LoL13-4 illustrating the relationship between Zr/Rb_{norm}, grain size and lamination colour. Darker layers tend to be characterised by positive Zr/Rb (>2), higher mean grain size and more negative skew.

7.5 Discussion

7.5.1 Testing an indirect particle size proxy

Particle size measurements along cores LoL13-1 and LoL13-4 reveal repeated spikes in coarser values interpreted here as reflecting palaeoflood deposits. The Loch of the Lowes sediment sequence contains many laminations thinner than the 0.5 cm sub-sampling interval for particle size measurements. Ratios between specific elements provide data at much higher resolution than was possible for the particle size analysis, and appear to include a signal that reflects changes in grain size (reviewed in Chapter 2.1; Schillereff *et al.,* 2014). The long cores (Figures 7.4 and 7.5) and selected sub-sections (Figure 7.7) highlight a co-variance between Zr/Rb_{norm}, changes in sediment colour and grain size. In particular, positive (>2) Zr/Rb_{norm} values correlate well with dark laminations and are characterised by the coarsest particles. This geochemical ratio has been successfully employed to discriminate fluctuations in grain size elsewhere (e.g., Jones *et al.,* 2012), and critically here we have confirmed the association and application for this site (Chapter 2.1; Schillereff *et al.,* 2014). Both elements are broadly controlled at the multi-cm scale by the supply of minerogenic material to the lake (co-varying with K, Ti; Figure 7.2). However, Zr and Rb show opposing behaviour at very fine scales. As Zr is often associated with the coarse silt fraction while Rb tends to be linked with clay particles, it appears that this application of the Zr/Rb ratio functions well because although sediment supply has varied on longer (centennial to decadal) timescales, perhaps in conjunction with the intensity of soil erosion in the catchment, the deposition of layers enriched in either Zr or Rb over short timescales (hours to day) depends on river flow.

In general, Zr/Rb_{norm} varies in tandem with sediment colour and grain size, but the relationship breaks down at times or exhibits mismatches in the depth correlation. On one hand, the contiguous 0.5 cm sub-sampling of LoL13-1 may have resulted in some loss of congruence and blurring between the resolution of the grain size and μXRF analyses. The peak in grain size at 21.5 cm depth (LoL13-1) probably corresponds with the elevated Zr/Rb_{norm} value at 22 cm, for example. The finer resolution of the μXRF data means all Zr/Rb_{norm} peaks or troughs would not be expected to appear in the P90 profiles. The inter-comparison (Chapter 3.4) illustrated a section with a homogenous stratigraphy where oscillations in minerogenic element ITRAX counts (Ti, Rb, Zr) were of a similar magnitude to their variability across distinct layers. Furthermore, there are

instances where multiple Zr/Rb_{norm} peaks and troughs at sub-mm scales occur within a single dark or light band (81.5-82 cm in LoL13-1). These could reflect repeated high-flow pulses within a single event, but equally they could be a function noise in the ITRAX counts given the 300 μm step-size. However, instances where Zr/Rb_{norm} and colour do not shift in tandem present a challenge, such as the peaks at 80.25 and 82.25 cm that do not correspond with a darker layer. Ascribing this is difficult, but it is possible that the darkness of the Type 1 layers reflects eroded peat carried during floods and so the lighter but coarse layers could simply reflect a flood not carrying as much eroded peat. That the sediment colour and the geochemical mineral supply story also fluctuate over longer intervals (>5 cm) is probably conditioned by changes in catchment sediment supply driven by agriculture or population change as opposed to short-term events in the hydrological regime (Foster *et al.,* 2008). These oscillations in catchment stability may modify or negate the usefulness of the Zr/Rb_{norm} proxy at times. Due to these uncertainties, the palaeoflood record developed here will be determined using laminations classified as Type 1 or Type 2 using the proxies: colour, Zr/Rb_{norm}, P90 and skewness.

7.5.2 A palaeoflood record for the Loch of the Lowes

Sand-rich lenses punctuating the finer-grained sediment matrix at Loch of the Lowes are characteristic of the delivery of coarser material from high-energy plumes sporadically entering the lake. These deposits of low frequency or extreme events could represent high river discharge (e.g., Brown *et al.,* 2000) or sub-aqueous turbidity currents within the lake (Sletten *et al.,* 2003). The increasing sediment accumulation rates away from the southern delta and the declining grain size with distance from these inflows suggests episodic high fluvial discharge from Little Yarrow, Chapelhope Burn or Riskinhope Burn are dominant sources of sediment delivery (Figures 7.4 and 7.5). The eastern shoreline of Loch of the Lowes slopes steeply to the lake edge and comprises rough grazing dissected by a small number of minor gullies that connect directly with the lake edge. It is possible that debris flows could plunge directly into the loch and disperse sediment across the lake bed. However, the gully features are small and rare and are regarded as unlikely to generate the heavily stratified sediment sequences traceable across the whole basin (Figure 7.2).

Palaeoflood units at Brotherswater (Chapter 5) contrast with the background sediments through being lighter in colour due to the higher content of clastic material.

At Loch of the Lowes, however, the darker-brown to black laminations are interpreted as geologically instant events layers and contain coarser grain sizes. Dark-coloured event layers have been attributed elsewhere to historical floods (e.g., Vasskog *et al.,* 2011; Simonneau *et al.,* 2013) reflecting eroded soil combined with organic particles and vegetation debris flushed from agricultural catchment landscape. There is significant peat cover in the catchment with gullied peat-bogs in the catchment headwaters. Zr, Rb and Ti concentrations decline across the dark units (Figures 7.4, 7.5 and 7.7), but the presence of sand and coarse silt verify increases in coarser mineral input. It appears likely that the terrestrial organic fraction delivered during the flood has diluted the overall inorganic geochemical concentrations. These flood laminations are also characterised by more negatively skewed particle size distributions. The packing of fine grains within the pore spaces remaining in a matrix of coarser particles has been identified in other lacustrine palaeoflood reconstructions (Bøe *et al.,* 2006), reflecting the faster settling rate of the coarser grains and the subsequent deposition of fines.

Attributing the light coloured laminations to a single depositional mechanism is more difficult. Some clastic palaeoflood layers exhibit multiple microfacies, possibly reflecting multiple waxing and waning phases within a single flood (Saitoh & Masuda, 2013) or the formation of a clay cap of the finest material that settles out of suspension most slowly (e.g., Wilhelm *et al.,* 2013). While this is plausible at Loch of the Lowes, and some dark underlying light couplets are visible in the long cores (Figure 7.7), more often they appear as distinctive layers. Furthermore, where dark-light couplets are observed, the lighter sediments are generally thicker (e.g., 75.6-76.8 cm in LoL13-4), which does not correspond to the typical clay cap signature (Wilhelm *et al.,* 2013). The light laminations are typically characterised by finer grains and more positive skew, similar to the deposition of the winter layer of a clastic varve that occurs during seasonal ice-cover (Ojala *et al.,* 2012). While there is evidence of winter ice formation on Scottish lochs (Bright, 1975), it is unclear whether this is a possibility at Loch of the Lowes during its recent history.

7.5.3 Historical flood frequency on the River Tweed

Core correlation across the basin was undertaken using multiple elements that reveal the onset of atmospheric pollution deposition, short and longer-term fluctuations in mineral supply to the lake (K, Rb, Ti, Zr) and traceable shifts in Ca and Fe (Figure 7.2).

To directly compare the potential palaeoflood records, LoL13-4 depths are re-calculated to match LoL13-1 based on these tie points (Figure 7.8) for the P90 core profile. Importantly, the frequency of peaks does correlate between both cores (r2 = 0.518, p = 0.001), offering confidence in the consistency of the reconstruction. The magnitude of corresponding peaks do not appear to fit on a one-to-one basis and linking discrete units is avoided as the depths are interpolated between correlation markers but these data do suggest peaks in grain size reflect pulses of sediment delivered under high-energy flood conditions that disperse across the basin and have been preserved within the abyssal sediments.

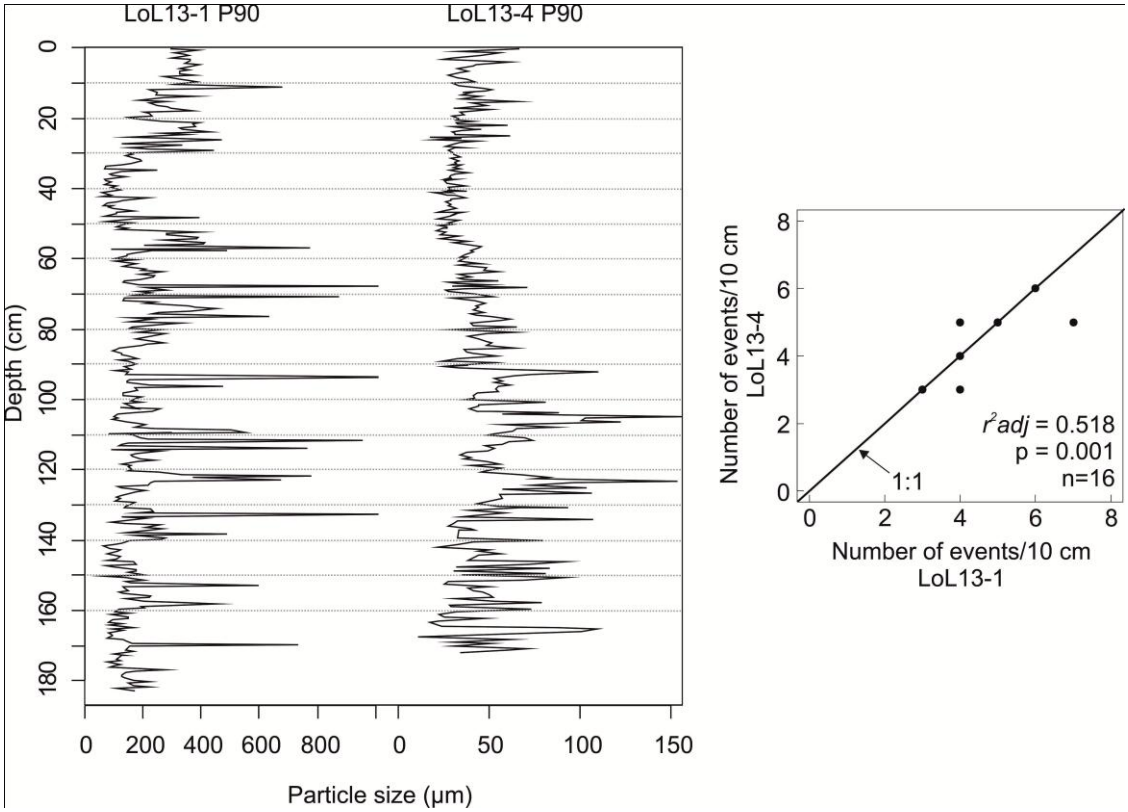

Figure 7-8 P90 particle size profiles for LoL13-1 and LoL13-4. The depths of LoL13-4 have been adjusted to match the delta-proximal core on the basis of the correlation markers in Figure 7.2. The consistency between both sedimentary records is tested by correlating the peak counts per 10 cm interval for both cores.

The lack of chronological control minimises the possibility of comparison with other regional palaeoflood data. An attempt at reconstructing variations in flood frequency for recent centuries was undertaken by calculating the number of Type 1 laminations

identified in each 10 cm interval in LoL13-1, due to its more consistent sedimentary record (Figure 7.9). This temporally-tentative palaeoflood record shows encouraging temporal similarity with the Foster et al. (2008) record of NAO-driven sediment mass accumulation rate (MAR) (Figure 7.9a and 7.9b) and discharge estimates reconstructed for severe floods on the River Tweed (Figure 7.9c, N. Macdonald, unpublished data). Foster et al. (2008) hypothesise that NAO is a major control on flood frequency at Loch of the Lowes. The atmospheric pollution marker places 60 cm at ~CE 1860 (Yang and Rose, 2005); assuming constant subsequent rate of sedimentation, floods have been fairly frequent since CE 1950 (above 20 cm), matching the Foster et al. (2008) MAR reconstruction. The resolution of the sedimentary record is too low to draw direct comparison with the post-CE 1960 discharge record. The MAR spike dated to ~ CE 1850 fits well with the most frequent flooding falling in the 60 – 70 cm window, immediately below the onset of elevated Zn, as well as major floods on the Tweed in the mid-19th Century. Other features that can be tentatively correlated between the LoL13-1 and Foster et al. (2008) records include the flood-poor phase at 30-40 cm (early-mid 20th Century) and less frequent floods below 140 cm, dating to pre CE 1700 assuming a constant sedimentation rate, corresponding with relatively low MAR at a similar time. The major floods on the Tweed in mid-late 18th Century correspond with higher MAR and a flood-rich interval at 110-130 cm.

While this record is entirely tentative, an attempt at placing the LoL13-1 record in a regional flooding context is presented. Debate exists between geomorphic records of fluvial incision reflecting increased or decreasing flood frequencies for the Tweed and other catchments in southwest Scotland/northeast England (Mcewen, 1989; Tipping & Halliday, 1994). However, the mid-19th Century is highlighted as particularly flood-rich (Foster *et al.,* 2008; Werrity *et al.,* 2006; Macdonald *et al.,* 2006; McEwen, 1990; McEwen, 2006) and the pollution chronological marker does offer some temporal constraint for the high number of floods around 60-70 cm depth, which is a promising fit. Likewise, McEwen (2006) suggested CE 1789-1794 experienced a high number of moderate to extreme floods on the River Tay, which would fit with 80-90 cm depth assuming constant sedimentation rate. Rumsby (1991) suggested low flood frequency in the 17th Century in northern England, which would fit the low numbers of palaeoflood laminations identified below 140 cm, shifting to a higher frequency of large floods at 110-140 cm which is more difficult to temporally match with documentary

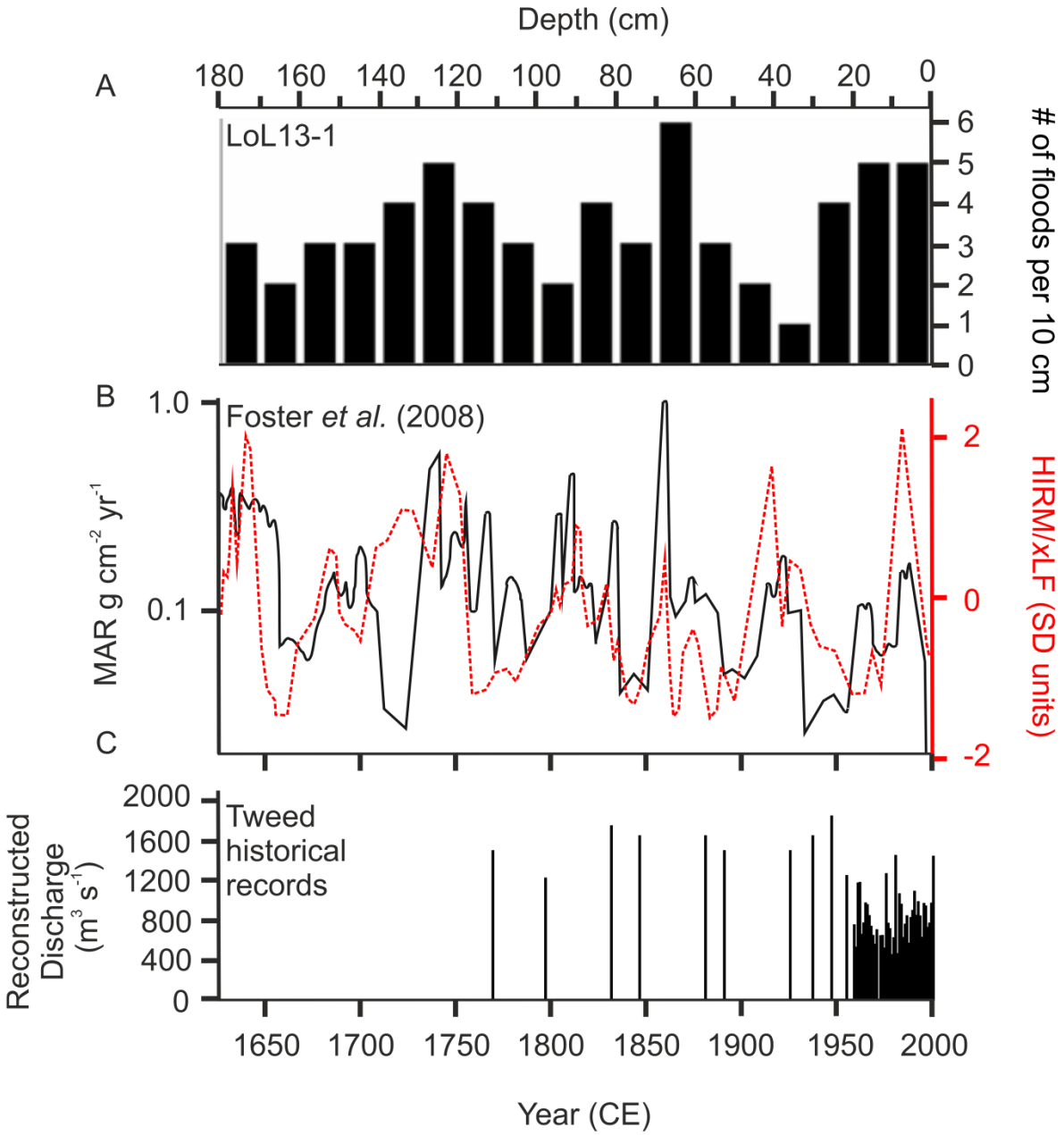

Figure 7-9 A) The total number of Type 1 river flood laminations discerned in 10 cm intervals from LoL13-1. B) Reconstructed sediment mass accumulation rate at Loch of the Lowes (Foster08) (solid black) and inferred NAO strength (dashed red) for CE 1627 – 1997 (from Foster *et al.,* 2008). C) Reconstructed discharges for historically-documented floods on the River Tweed (N. Macdonald, unpublished data.

and geomorphic records, but does correspond with a wet shift recorded in regional bog stratigraphies and dated to ~ CE 1700 (Chambers *et al.,* 1997).

7.6 Conclusions

The methodology for extracting palaeoflood information from lake sediments developed at Brotherswater has been tested at a second site in southern Scotland. Four sediment cores were extracted from Loch of the Lowes (180 – 260 cm length) that were heavily laminated with light and dark units and the cores were tightly correlated based on the stratigraphy and multiple elemental profiles. The silt-rich sediment matrix is frequently punctuated by spikes in the P90 particle size metric, corresponding with dark laminations rich in terrestrial plant macrofossils and visible sand particles. Usefully, the Zr/Rb ratio clearly discriminates between the dark, flood units and fine-grained lighter units at this site. Coupled with down-lake decreases in sediment accumulation rates and grain size, this strongly suggests these sand lenses were delivered by high-energy fluvial events that also brought eroded peat from catchment, resulting in the dark units. Limited chronological control is available at present but a clear marker of atmospherically derived Zn, probably reflecting industrialisation after ~CE 1850, enables some tentative comments on flood frequency trends to be made. The mid-19th century appears to have been particularly flood-rich and possibly the early 18th Century, consistent with regional trends. There was a paucity of floods in the early-20th Century.

8 SYNTHESIS AND WIDER IMPLICATIONS

8.1 Extended Discussion

The investigations of the sediment record at Brotherswater (NW England) and Loch of the Lowes (Southern Scotland) set out to test the hypothesis that lakes in the temperate northwest of the United Kingdom, typically characterised by a uniformly brown stratigraphy and often having experienced accelerated flux of soils from their catchments in the last 2-3000 years, also contain information on flooding over centennial or millennial timescales. The data and discussions in chapters 4-7 provide a resounding positive outcome, with sequences of discrete laminations interpreted to reflect historical floods identified in the late-Holocene lake sediments of Brotherswater and Loch of the Lowes. Applying a series of analytical methods to the sediment records reveals stratigraphic signatures indicative of repeated high-magnitude floods in both the River Eden and Tweed catchments. In addition eighteen months of process monitoring at Brotherswater using sediment traps confirms the mechanics of sediment delivery for this system and a strong continuity to the late-Holocene sediment record. Opportunities arose during the research to rigorously test and contribute to improving the use of micro-XRF scanning technologies in the analysis of lake and other soft sediment sequences. The comprehensive investigations for the Brotherswater sediments, principally to assess the performance of commonly used grain-size indicators in the geochemistry, revealed a complex history related to mining of metals,

perhaps the mostly tightly resolved record of such for a UK lake. This chapter revisits and draws together the key findings of chapters 3-7, assesses the extent to which the key research questions (chapter 1) have been addressed and explores wider implications that extend beyond the scope of the individual papers.

I) Basin-catchment controls and methods of accessing the flood archive from lake sediments

Investigations of lake sediments have been on-going for decades, especially in the English Lake District (Pennington, 1991), and have contributed important palaeoenvironmental and palaeoclimate data to global climate syntheses (e.g., IPCC, 2013). The virtual absence of any significant focus on their potential as recorders of floods was both intriguing and challenging. The motivation for the comprehensive review of lake-based flood research came from this paucity in the UK. The review of the growing body of lacustrine palaeoflood literature for a wide geographical spread of case studies elsewhere in the world and their site physical characteristics (Chapter 2.2) shows that flood evidence is well preserved for a set of ideal lake basin characteristics and sediment delivery processes. Building on the recommendations of Gilli et al. (2013), a conceptual model was devised to guide both the selection of the lake, but also locations within lakes for future palaeoflood research (Figure 2.5). The catchment-lake configurations of Brotherswater and Loch of the Lowes meet many of these criteria and are a partial test of those selection criteria. Key characteristics were their high catchment-lake area ratio, ample sediment availability and a well-connected fluvial system enabling efficient sediment transfer to the lake during floods. Essentially, Brotherswater and Loch of the Lowes were formal tests of the recommendations defined in Chapter 2.1.

Brotherswater does appear to be moderately thermally stratified in summer (Maberly *et al.,* 2011) and the formation of a thermocline can affect river plume migration and alter the likelihood for over-, inter- or underflows to form. While this may complicate the annual pattern of sediment dispersion, Kampf et al. (2014a) were able to extract a seasonal palaeoflood signal because the within-lake depositional mechanisms were season-specific due to summer stratification. A non-stratified water column is thus not essential provided limnological processes are closely monitored (as done by Kampf *et al.,* 2014a) or sediment traps are installed (i.e., Chapter 5). The field site choice for this thesis was further prompted by indications in previous data that sediment deposition at Brotherswater and Loch of the Lowes responded strongly to hydrometeorological

conditions (Chambers, 1978; Foster *et al.,* 2008). The availability of these data was critical as many of the criteria set out in the conceptual model require detailed field measurements if published data is unavailable, such as basin bathymetry and limnological conditions (Figure 2.5). The availability of extended river flow, rainfall and documentary records of hydrometeorological extremes for the Eden and Tweed basins also means they are good candidates to assess how consistently and how well sedimentological signatures of known floods are preserved.

One aspect that was not explicitly highlighted in Figure 2.5 pertains to the type of soil and surficial sediments most likely to be eroded during a flood and whether this may vary through time. This is particularly relevant for comparing the proposed Loch of the Lowes and Brotherswater palaeoflood units; coarse laminations with a significant sand contribution in Loch of the Lowes are mostly very dark brown to black, with significant volumes of terrestrial macrofossils probably from peat deposits in the watershed that are absent around Brotherswater.

The role of fluvial delivery as the primary control on sedimentation patterns across the lake was demonstrated using multiple lines of evidence at both sites. At Brotherswater, the depth of sediment above the CE 1860s Pb marker (Chapter 4, Figure 4.4), mass accumulation rates, minerogenic sediment flux (Figure 4.5) and heavy metal flux (Figure 4.4) all declined with distance from the inflow. The calibre of background and flood-derived sediments followed a similar fining trend in both lakes (Chapters 5 and 7, Figures 5.4 and 7.4) and correlating discrete light and dark laminations across Loch of the Lowes shows less sediment accumulating in the lake centre than nearer the inflow. This increases the potential recovery of a palaeoflood signal and illustrates that extracting multiple cores from a single basin is critical. Delta-proximal regions tend to be avoided by palaeoflood researchers (e.g., Czymzik *et al.,* 2013) but the tighter match between the PSDs of captured material in sediment trap A and its adjacent core BW11-2 than the centre of the lake means this is not always a valid approach.

II) A sediment-based record of palaeofloods in UK lakes

At both Brotherswater and Loch of the Lowes, the main premise that down-core particle sizes fluctuate in a punctuated manner holds true, with the sediment matrix generally dominated by silt-sized material with periodic overprinting by thin (generally 0.5 – 2 cm) coarser intervals (Chapters 5 and 7, Figures 5.6 and 7.4). This patterning in grain size data has previously been characterised as reflecting past flood

events (e.g., Bøe *et al.,* 2006; Vasskog *et al.,* 2011) and the behaviour of the individual particle distributions confirms this interpretation. The particle size distributions at Brotherswater are generally unimodal, with the bulk of material lying in the silt fraction (mode = ~16 μm), but a second mode is identified in the sand domain in some PSDs (Figure 5.4), and in some instances becomes the dominant mode. Whole-core contour plots clearly illustrate this bi-modal behaviour occurs periodically throughout the cores (Figure 5.6). Decomposing the particle size through end-member analysis (Dietze *et al.,* 2012) reveals similar patterning among the 3 or 4 discrete end-members that appear to reflect two key depositional processes. The fine material accumulates throughout the record, probably a combination of autochthonous organic or silicaceous material along with fine silts and clays (End-members 1 and 2; modal grain sizes ~3 and ~15 μm) carried in suspension into the lake under normal or low flow conditions. Samples characterised by the coarser mode (EM3 and EM4, modal values 146 - 282 μm) require powerful plumes capable of transporting coarse particles considerable distances from the inflow. This behaviour is consistent with delivery and deposition under conditions that can be classified as irregular but of a high-magnitude. An analogue deposit probably deposited by the CE 1964 flood but possibly the 1968 event was also identified. Peaks in the P90 profile are also observed in the Loch of the Lowes sequence, interpreted to reflect palaeoflood units. However, the core lithologies are considerably different between the two sites and thus their signature using other proxy data, especially the visual stratigraphy and geochemistry, does diverge between both lakes. The Brotherswater cores are fairly homogenous and light brown in colour and light bands that visually appear coarser are occasionally present. The Loch of the Lowes stratigraphy is much more heavily laminated and lenses of sand are repeatedly observed, especially at the delta-proximal LoL13-1 core site. Interestingly, these correspond with very dark laminations that contain considerable terrestrial plant macrofossils within a light-brown sediment matrix. The opposing association of organic matter content in palaeoflood units in Brotherswater (low OM) and Loch of the Lowes (high OM) probably relates to different sediment sources. A combination of parent material, eroded soil and riverbank erosion all contribute at Brotherswater (Oldfield and Wu, 2000; Chambers, 1978; Rae and Parker, 1996) and catchment soils are mineral-rich, and peat deposits are only present on the summits and unconnected with the fluvial system, leading to a mineral-rich palaeoflood signature. Widespread peatlands around Loch of the Lowes (e.g., Chambers *et al.,* 1997), on the other hand,

make a substantial contribution, especially during periods of flood, leading to the formation of a palaeoflood deposit that is rich in organic matter as well as sand. This shows the importance of direct high-resolution measurements of particle size as the most dependable means of discriminating palaeoflood signatures.

III) A sediment-based history of mining activity at Hartsop Hall Lead Mine

There are numerous applications of using geochemical approaches to investigate heavy metal records preserved in lake sediments (Chapter 2.2). Lake sediment sequences have been reported to contain either a signal of regional atmospheric deposition (e.g., Renberg, 1994) or a much more local signal of ore exploitation or industry in the watershed (e.g., Grayson and Plater, 2008). Brotherswater appears to be a clear example of the latter case (Chapter 4), with mining activity primarily at Hartsop Hall Mine alongside smaller-scale initiatives elsewhere in the catchment acting as a point-source for heavy metals deposition in the lake since the late-17th Century (Tyler, 1992) while the uppermost Loch of the Lowes sediments exhibit rising Zn and to some extent Pb concentrations (Chapter 7), probably reflecting atmospheric deposition (Yang and Rose, 2005; Foster *et al.,* 2008). The long cores extracted from Brotherwater allow the background or 'natural' baseline Pb concentration to be established (<100 ppm) which illustrates the significance of the recent peaks in Pb concentration (>10 000 ppm Pb, >1000 ppm Zn) and flux (>40 g m^{-2} yr^{-1} Pb)(Figure 4.4 and 4.6). These exceptional values can only be plausibly explained by direct input from the mine during its most intensive phase of operation, known to have occurred during the CE 1860s based on historical documents, and supported by ^{210}Pb dating (Figure 4.2). This further illustrates the tight link that can exist between lake sediments and local industrialisation (e.g., Ek and Renberg, 2001).

Furthermore, the lake sediment record is sufficiently well-resolved for a signal of technological development to be extracted, from inefficient early smelting techniques, open-cast mining during the CE 1860s and mechanised operations in the 20th Century limiting effluent release. On the other hand, annual ore extraction figures published for larger Cumbrian mines (e.g., Force Crag; Tyler, 2005) that enable multiple chronological markers to be identified within the Bassenthwaite sediment record (R. Chiverrell *et al.,* unpublished data) are unavailable at Hartsop Hall. Nevertheless, the Brotherswater record has been able to quantify the hitherto unknown metal flux from the mine and its persistent impacts on the aquatic ecosystem and establish a baseline from which system recovery can be judged; based on these data, a regime shift appears

more likely than full recovery. A national strategy to manage contamination from non-coal mines is being developed in the UK (Mayes *et al.,* 2009), building on the European Water Framework Directive (Environment Agency, 2008). However, Hartsop Hall Mine and Brotherswater are not listed as a prioritisation site for remediation and a water quality monitoring station (Mayes *et al*, 2009) is not installed on Kirkstone Beck, presumably due to its small size. A recent limnological survey indicated Pb levels in filtered water samples were surprisingly below the limit of detection (Maberly *et al.,* 2011) although moderate levels of Zn were detected. Neither Windermere nor Ullswater yielded detectable metal concentrations from water samples while their sediments are heavily contaminated (Grayson and Plater, 2008; Miller *et al.,* 2014). Thus there appears to be extensive scope and arguably a necessity to integrate data from sediment cores and traps into future remediation plans (*sensu* Bindler *et al.,* 2011a).

IV) The hydrodynamic relationship between river flow and lake sediments

While sedimentological signatures of palaeofloods have been proposed based on multiple independent proxies (e.g., Noren *et al.,* 2002), demonstrating a direct link between the process (flooding) and the response (preservation of distinctive material) on a site-specific basis is important because de-coupling between hydrometeorological conditions and the resultant sedimentary behaviour has been shown (e.g., Cockburn and Lamoureux, 2008). The process-response is often inferred from microfacies structure and composition (e.g., Czymzik *et al.,* 2013), while comparisons between well-dated individual flood deposits and instrumental discharge data have been undertaken here (Chapter 5.5.2; Figure 5.9) and elsewhere (Schiefer *et al.,* 2011; Kampf *et al.,* 2012; 2014; Jenny *et al.,* 2013); establishing physical links via sediment trapping or monitoring is rare (Kämpf *et al.,* 2014b).

The sediment trapping programme undertaken at Brotherswater produced notable findings on the hydrodynamic relationship between grain size and river discharge. The process of amalgamating broadly monthly particle size data into an annual distribution is particularly interesting and not previously reported. Sediment captured in the traps during the eighteen month survey was dominated by silt and some clay. Although the January 2013 material was dominated by the sand domain, the sand fraction is only represented in the aggregated 'annual' particle size distribution as a subtle secondary mode (Figure 6.9). Essentially, it appears the coarse material delivered to Brotherswater throughout the survey period is masked by the much more regular

deposition of silt-sized material. Such decoupling has been noted elsewhere (e.g., Cockburn and Lamoureux, 2008), but its implications for palaeoflood research have not previously been highlighted. Because the total volume of material captured in the sediment traps equates to 0.5 cm sub-sampling interval, the PSD of a single core sample would not exhibit the bi-modal behaviour or high EM3 contribution considered typical of palaeoflood deposits in Brotherswater (Chapter 5; Figures 5.4 and 5.6). On the other hand, these data do suggest that particle size distributions from sediment core samples that are dominated by the sand domain (high contribution from EM3) must reflect events of a much higher magnitude than occurred during the sediment trapping programme

The process-response of particle size data to high flows recorded in individual trap samples is also intriguing because the coarsest material was deposited after a sustained period (ten days) in late December 2012 of moderately high flow, as opposed to during short-lived (~24 hours) intense rainfall events (e.g., September 2012). This suggests it is the volume of water within a timeframe as opposed to maximum discharge that is most important. The sedimentological signatures of non-flood summer months, normal autumn and winter hydrological conditions and the influence of flood event sequence have also been described and seasonal variability in sediment provenance is also observed, including a late-Spring diatom bloom and increased organic productivity during the summer. It must be kept in mind that these data represent a comparatively short timeframe and may not adequately reflect inter-annual or decadal variability in rainfall, discharge and/or sediment transport.

V) µXRF scanning and the utility of geochemical proxies for grain size

The recent proliferation of µXRF scanning within palaeoenvironmental research (Croudace *et al.,* 2006) has carried over to palaeoflood investigations of alluvial (Jones *et al.,* 2012) and lacustrine sequences (e.g., Vasskog *et al.,* 2011; Czymzik *et al.,* 2013). However, the typical acquisition of data from wet sediment cores can introduce issues of data quality and concentrations or counts output are affected by water content (Hannekam and Lange, 2012). The two methodological chapters (3.3 and 3.4) explicitly addressed some of these concerns. Two methods are proposed that should be applied to µXRF data in the first instance to evaluate whether fluctuations in down-core water content may significantly alter the apparent elemental concentrations obtained on a wet-sediment basis. This is particularly true where the composition of core material and water content changes dramatically, such as from late-Glacial/Younger Dryas

minerogenic material to more organic sediment lain down during the Holocene, as shown in Chapter 3.3.

The first calibration method involves estimating water content for the full core using the coherent and incoherent backscattering data obtained during scanning, and shows great success at Lilla Öresjön. The second method is a more simple regression to convert geochemical data obtained from wet cores into the dry-sediment equivalent and is particularly successful at Brotherswater (Chapter 3.3) and Loch of the Lowes (Chapter 3.4) where sediment composition is fairly homogenous. Several different core scanners are currently in use but different instrument configurations prevent direct comparison between datasets (provided all other conditions were equal). A first inter-comparison between an ITRAX and a Geotek core scanner concluded that each instrument has certain research questions to which it is more appropriate (Chapter 3.4). The ITRAX core scanner can perform measurements at a higher step-size (200 μm) than the Geotek scanner (minimum 1 mm), enabling thin palaeoflood laminations to be described in greater detail. However, the ITRAX were generally noiser, especially after calibration to dry-weight equivalent, potentially resulting in misleading interpretations where peaks or troughs in a certain element are more likely to be data artefacts, potentially resulting in palaeoflood laminations being misclassified, for example, if on μXRF data acquired using an ITRAX device is the only data source. These results suggest a multi-proxy approach is most appropriate.

Both of these methodological considerations should be first steps during palaeoflood research, especially if geochemical ratios are being employed (e.g., Wilhelm *et al.,* 2013). With this in mind, the viability of indirect grain-size proxies has been tested at Brotherswater and Loch of the Lowes. The likely CE 1964 deposit was clearly discriminated by its particle size structure but commonly employed grain size proxies (e.g., Zr/Rb; Jones *et al.,* 2012) showed a limited trend across the unit (Chapter 2.1). The Zr/K ratio did exhibit a peak corresponding with the maximum P90 (Figure 2.8) and, based on the respective geochemical behaviours of Zr (tends to associate with the coarse-silt fraction) and K (clays), has the potential to reflect fluctuations in grain size but the relationship in the long cores often breaks down (Figure 5.3b). On the other hand, microfacies analysis of the Loch of the Lowes cores showed a consistent co-variance between the Zr/Rb and changes in grain size. Closer examination of the data showed that Zr and Rb (along with other lithogenic elements) co-vary in tandem with fluctuations in catchment-derived mineral supply but this is overprinted by a higher-

resolution opposing response that must reflect stream power and its carrying capacity. The mechanics underpinning the use of a certain geochemical ratio must be explicitly demonstrated in this manner on a site-specific scale as local factors are critical: the absent or blurred signal at Brotherswater can be attributed to the fractionation of bedrock geology at grain sizes inherent to its volcanic provenance (Chapter 5 and 6). This can be accomplished either through direct correlation between grain size and geochemistry (e.g., r=0.93 between Zr/Fe and grain-size at Lac Blanc (Wilhelm *et al.,* 2013)) or monitoring the contemporary fluvial and limnological dynamics.

Overall, this thesis highlights that, if appropriate calibration techniques are applied, data obtained using μXRF techniques can be of tremendous value due to their fine resolution, enabling palaeoflood laminations thinner than manual sub-sampling permits to be discriminated, but site-specific testing is critical.

VI) Developing late-Holocene sedimentary records of flood frequency and magnitude in northern Britain

Chronologically constraining the sediment cores is vital to establish the timing and thus the recurrence intervals of past floods (reviewed in Chapter 2.1; Gilli *et al.,* 2013). Neither Brotherswater nor Loch of the Lowes contains an annually laminated sequence (e.g., Czymik *et al.,* 2013; Schlolaut *et al.,* 2014); instead, age control was established at Brotherswater through integrating multiple independent techniques (described in Chapter 4) while the Loch of the Lowes chronology is dated relative to known markers that were correlated across the basin.

The recent sediments (post late-19th Century) of two Brotherswater cores were dated using ^{210}Pb. In both cases, ^{137}Cs peaks associated with maximum emissions from weapons testing around CE 1963 and the 1986 Chernobyl disaster, with the depth of the former being confirmed by a peak in ^{241}Am. The more coherent BW12-9 was transferred to BW11-2 to calibrate the older (pre-1963 ^{137}Cs peak) dates. The deeper Brotherswater record is underpinned by thirteen radiocarbon dates modelled within a BACON framework (Blaauw and Andrés Christen, 2013) (Figure 4.3). Despite challenges associated with fluctuating atmospheric ^{14}C concentrations (Hua, 2009), reasonable chronological control was established for the past 300 years through integrating a heavy metal (Pb) chronological marker into the BACON model which tightened the ^{14}C age distribution significantly. Applying the recommendations contained in Chapter 2.2, peak Pb flux can be attributed to intensive mining during the

CE 1860/70s with high confidence, offering an invaluable chronological marker. While mining markers have been used to calibrate chronologies at other lakes (e.g., Hammarlund *et al.,* 2008), the Brotherswater record is exceptional in the prominence of the CE 1860/70s heavy metal signal and tight temporal constraint it provides (±8 years). Where mines exist in a watershed, a similar approach coupling geochemical measurements of lake sediment sequences with mine production data or lease dates should be systematically conducted following the recommendations outlined in Chapter 2.2.

The integration of historical flood dates identified from documents or epigraphic records into chronological models (e.g., Wilhelm *et al.,* 2012) was intentionally avoided in this thesis due to potential circular reasoning. Instead, the timing of floods based on the independent BW11-2 chronology (Figure 4.3) was compared with historical information on the basis of their full probability distributions (Figure 5.9a). The importance of this inter-comparison approach underpinned by independent datasets cannot be overstated.

Flood occurrence at both lakes appears to be characterised by flood-rich and flood-poor periods, consistent with regional and national trends (McEwen, 2006; Pattison and Lane, 2012; Macdonald, 2014). Further verification of the well-dated Brotherswater sequence through direct correlation with documentary flood records illustrated some tight matches (Figure 5.9a) for the most severe events but the chronological uncertainties means comparing the full age probability distributions is preferable to embedding the historical dates directly into the age-depth model (e.g., Wilhelm *et al.,* 2012). The Brotherswater record spans ~1500 years, a period characterised by climatic fluctuations and rural population expansion and contraction in northern Britain (Charman *et al.,* 2006; Winchester, 1987). Some temporal correlation between flood-rich phases and proposed climatic drivers of severe floods (e.g., NAO; Pattison and Lane, 2012) are observed (Figure 5.10), but there were no clear matches between periods of human occupation and frequent flooding. Overall, it remains challenging to discriminate a single driver of trends in late-Holocene flood frequency as highly variable precipitation patterns, upland and lowland environments, orographic rainfall, wind direction and catchment size may all condition the likelihood of flood occurrence in individual catchments (e.g., Malby *et al.,* 2007).

The November 2009 flood in Cumbria led to substantial revisions of regional flood frequency curves due to its apparent exceptional severity within the timeframe of

exisiting record. The ultimate goal of palaeoflood research is to offer longer-term context to contemporary flood patterning. In the case of Brotherswater, the normalised sedimentary record contains more distinct palaeoflood laminations during the past 150 years than any other period. Removing the non-climatic signal is difficult, however, as the sediment regime within the watershed is known to have shifted during this timeframe, so concluding floods have been more frequent during the 20th Century is a highly uncertain conclusion. Nevertheless, there is some indication from the particle size data that the November 2009 event should be considered historically unusual, with only four deposits that possibly represent floods of an equivalent magnitude identified within the 1500 year record.

VII) To what extent are catchments affected by changes in land-use or vegetation cover perturbing or influencing palaeoflood reconstructions?

The prospect of human-induced destabilisation of a catchment leading to enhanced sediment supply, and thus masking or altering the characteristics of palaeoflood units through time is a significant concern for palaeoflood researchers (Giguet-Covex *et al.,* 2011; Simmonneau *et al.,* 2013). This appears to be the case at Brotherswater, where the supply of catchment-derived minerogenic material to the lake has varied substantially over the past 1500 years (Chapter 4). The timing of these phases of elevated sediment flux suggests a human trigger because of their temporal correspondence with known periods of human occupation in the region (Chiverrell, 2006). The delivery of coarse material to the delta-proximal zones has significantly increased over the past ~300 years with other similar phases lasting ~100 years also visible in the sedimentary record (Figures 5.3, 5.4, 5.5). As a result, the values of certain particle size metrics (P90 and EM3) interpreted to characterise paleoflood deposits vary through time. The potential for human interference to modify palaeoflood records is generally recognised but rarely explicitly addressed (e.g., Lauterbach *et al.,* 2012). However, this research has indeed attempted to address these shifts in catchment state through the application of a normalisation procedure to the P90 data that uses a moving filter to identify extreme values within the particle size metrics within a shorter timeframe of consistent sediment supply (Section 5.4.6; Figure 5.8). Comparison of the resultant $P90_{normalised}$ palaeoflood record shows a reasonable temporal match with historically documented floods in the broader River Eden catchment (Pattison and Lane, 2012) and local discharge data available since CE 1960,

and is used to assess long-term flood frequency with some confidence, indicating the success of this data processing technique.

The Loch of the Lowes sequence appears to be less influenced by background fluctuations in sediment supply. The peaks in particle size interpreted to reflect flood units increase from mean and P90 values that are more or less constant throughout the record (Figure 7.4). The sediments do fine above ~70 cm in core LoL13-4, and the peaks in particular are much more subdued, although this pattern is not matched at the delta-proximal site (LoL13-1). This is the reverse of behaviour within Brotherswater, where the core from central basin (BW12-9) exhibits the least response to increased sediment supply. These findings further demonstrate the site-specific nature of palaeoflood deposit and emphasises that multiple cores are always essential. Sediment colour in the Loch of the Lowes cores does fluctuate over ~5 – 10 cm intervals, reflecting a greater or smaller contribution of mineral or organic material (Figures 7.4 and 7.6), and this is picked up in the geochemical composition. While certain elements are clearly tuned to respond to short-lived events, as depicted by the Zr/Rb profiles, these curves shift to overall more negative or more positive values at the wider scale (5-10 cm). This may lead to misidentification of palaeoflood laminations at certain depths based solely on the Zr/Rb_{norm} measurements.

8.2 Limitations and further work

A palaeoflood record has been successfully extracted from both study sites and a method for assessing the palaeoflood record demonstrated. However, a number of limitations related to the sediments, chronological development and process-response interpretations do exist.

- The variable sediment supply at Brotherswater poses some challenges, and while the detailed interrogation of the particle size data provided a palaeoflood record, it was necessary to disentangle this signal of increased flood magnitude and frequency during the 20th Century from the higher sediment accumulation rates. On one hand, seeking palaeoflood record from lakes less influenced by human activity seems sensible. However, the increased sediment availability typical of human-perturbed catchments may be a positive characteristic in some instances to maximise the likelihood of sediment mobilisation during a flood. Testing the methodology at other sites to verify the conceptual model of site selection seems wise.

- The programme of sediment trapping at Brotherswater contributed important data in terms of understanding limnological (within-lake) processes, sediment provenance and the role of seasonal processes. However, only a moderate number of discrete trapping intervals were accomplished and increased confidence in the data would be fostered by more frequent collections over a longer timeframe, with sampling intervals ideally spanning discrete river discharge events. Tracking the preservation of sediments captured in traps during a flood of exceptional magnitude through gravity core surveys in subsequent years will enable the mechanics of palaeoflood deposition to be explicitly investigated for the first time. A better understanding of whether hyperpycnal flows are generated at Brotherswater due to suspended sediment loading or thermal differentiation, and whether this is a seasonal phenomenon, will also be valuable.
- Palaeoflood laminations can be discriminated at a high-resolution within the Loch of the Lowes stratigraphy, but producing an extended palaeoflood record is hampered by the lack of chronological control, particularly at depth. Successful acquisition of radiocarbon dates and tightening the Loch of the Lowes chronology is thus a priority. There is also scope to improve the Brotherswater chronology through undertaking SCP counts or the identification of exotic pollen species.
- At present the poor level of understanding of the relationship between contemporary climatic drivers of flood generation and flooding patterns hampers the ability to associate the observed flood histories extracted from the sedimentary sequences with reconstructed palaeoclimatic signals of potential flood drivers (e.g., NAO). Integrating lacustrine sequences with other palaeoflood archives both regionally and nationally may shed further light on potential flood drivers.
- The November 2009 flood in Cumbria led to substantial revisions of regional flood frequency curves due to its apparent exceptional severity within the timeframe of exisiting record. Testing approaches to integrate palaeoflood data extracted from sedimentary archives into flood frequency analysis in a quantitative manner is an important follow-up but independent verification of the lacustrine record is essential.

8.3 Concluding statements

- The physical characteristics of a catchment and lake system most conducive to preserving sedimentary signatures of historic flood events have been embedded into a conceptual model to guide site selection for palaeoflood research.
- A sequence of sediment cores extracted from Brotherswater (northwest England) and Loch of the Lowes (southern Scotland), chosen based on these rigorous criteria, reveal systems dominated by fluvial delivery and sediment matrices punctuated by repeated coarser-grained laminations.
- A coherent chronology was developed for Brotherswater that integrates short-lived radionuclide dating (^{137}Cs, ^{241}Am, ^{210}Pb), ^{14}C ages and contaminant markers reveals long-term variability in sediment supply over the last 1500 years, probably driven by human activity. In particular, a highly-resolved record of persistent and exceptional heavy metal flux into the aquatic environment and increased sedimentation within the lake due to mining activity at Hartsop Hall (~0.5 km from Brotherswater) has been reconstructed.
- High-resolution particle size analysis and its decomposition into process-driven end-members has successfully discriminated a signature of coarse calibre material deposited during high-energy events from the background, silt-dominated matrix. An analogue palaeoflood unit deposited by the CE 1964 flood has also been identified. A normalisation procedure applied to explicitly deal with variations in catchment stability and sediment supply yields good temporal coherence with local and regional flood information (historical records and instrumental data), using the full age probability distribution of flood deposits to ensure independent comparability.
- Flood occurrence over the past millennium is characterised by flood-rich and flood-poor phases generally 50 – 100 years in duration. In some cases, the pattern can be directly linked to changes in the North Atlantic Oscillation, particularly its persistent positive phase from ~CE 1100 – 1400. The relationship is no longer in phase at other times, however, preventing the identification of a dominant climatic driver of extreme flooding in upland Britain.

- An 18 month sediment trapping programme at Brotherswater captured the hydrodynamic relationship between rainfall, discharge and the calibre of fluvial-delivered material. Unique particle size signatures were identified for a major winter flood, low-flow conditions and successive flood events flushing the fluvial system. The potential for coarse material delivered during short-lived events to be masked by near-constant, fine-grained sedimentation over annual timescales is a previously unreported finding with significant implications for palaeoflood research.
- Rigorous testing of μXRF data quality obtained from wet sediment cores using core scanners and inter-instrument comparability led to the development of robust and rapid calibration procedures. Building on these experiments, the performance of commonly-used geochemical ratios acting as indirect proxies of particle size was tested at both study sites. Their suitability at Brotherswater is generally poor, most likely because of bedrock geology, but down-core Zr/Rb fluctuations appear to mirror changes in grain size at Loch of the Lowes. The process mechanism underpinning its functionality has been verified through microfacies analysis. These results confirm the need to explicitly demonstrate the suitability of specific elemental ratios as grain size proxies on a site-specific basis.

9 REFERENCES

Aalto R, Nittrouer C (2012) 210Pb geochronology of flood events in large tropical river systems. *Philosophical Transactions of the Royal Society A: Mathematical, Physical and Engineering Sciences* **370**: 2040–2074 doi:10.1098/rsta.2011.0607.

Abbott MB, Finney BP, Edwards ME, Kelts KR (2000) Lake-Level Reconstruction and Paleohydrology of Birch Lake, Central Alaska, Based on Seismic Reflection Profiles and Core Transects. *Quaternary Research* **53**: 154–166 doi:10.1006/qres.1999.2112.

Adams J (1988) Mines of the Lake District Fells (Dalesman).

Ahmed F., Bibi M.H., Monsur M.H., Ishiga H. (2005) Present environment and historic changes from the record of lake sediments, Dhaka City, Bangladesh. *Environmental Geology* **48**: 25-36.

Allen S.E., Grimshaw H.M., Parkinson J.A., Quarmby C. (1974) Chemical analysis of ecological materials. Blackwell Scientific, Oxford, 565 pp.

Anderton J, Haworth E, Horne D, Wray D (1998) Environmental impacts of lead mining in the Ullswater catchment (English Lake District): dam failures and flooding. In Issues in Environmental Geology: A British Perspective, M. Bennett, and P. Doyle, eds. (The Geological Society, London), pp. 226–242.

Appleby PG (2001) Chronostratigraphic techniques in recent sediments. In Tracking Environmental Change Using Lake Sediments. Volume 1: Basin Analysis, Coring and Chronological Techniques., W.M. Last, and J.P. Smol, eds. (Kluwer Academic Publishers, The Netherlands), pp. 171–203.

Appleby PG (2013) 210Pb dating: thirty-five years on. *Journal of Paleolimnology* **49**: 697–702 doi:10.1007/s10933-013-9685-y.

Appleby PG, Nolan PJ, Gifford DW, Godfrey MJ, Oldfield F, Anderson NJ, Batterbee RW (1986) 210Pb dating by low background gamma counting. *Hydrobiologia* **143**: 21–27.

Appleby PG, Oldfield F (1978) The calculation of Lead-210 dates assuming a constant rate of supply of Unsupported 210Pb to the sediment. *Catena* **5**: 1–8.

Appleby PG, Richardson N, Nolan PJ (1991) 241Am dating of lake sediments. *Hydrobiologia* **214**: 35–42.

Arain M.B., Kazi T.G., Jamali M.K., Afridi H.I., Jalbani N., Sarfraz R.A., Baig J.A., Kandhro G.A., Memon M.A. (2008) Time saving modified BCR sequential extraction procedure for the fraction of Cd, Cr, Cu, Ni, Pb and Zn in sediment samples of polluted lake. *Journal of Hazardous Materials* **160**: 235-239.

Arnaud F, Lignier V, Revel M, Desmet M, Beck C, Pourchet M, Charlet F, Trentesaux A, Tribovillard N (2002) Flood and earthquake disturbance of 210Pb geochronology (Lake Anterne , NW Alps). *Terra Nova* **14**: 225–232.

Aston S.R., Bruty D., Chester R., Padgham R.C. (1973) Mercury in Lake Sediments - Possible Indicator of Technological Growth. *Nature* **241**: 450-451.

Audry S, Schäfer J, Blanc G, Jouanneau J-M (2004) Fifty-year sedimentary record of heavy metal pollution (Cd, Zn, Cu, Pb) in the Lot River reservoirs (France). *Environmental Pollution* **132**: 413–426.

Ayuso R.A., Kelley K.D., Eppinger R.G., Forni F. (2013) Pb-Sr-Nd Isotopes in Surficial Materials at the Pebble Porphyry Cu-Au-Mo Deposit, Southwestern Alaska: Can the Mineralizing Fingerprint be Detected Through Cover? *Economic Geology* **108**: 543-563.

Bäckstrom M., Bohlin H., Karlsson S., Holm N.G. (2006) Element (Ag, Cd, Cu, Pb, Sb, Tl and Zn), element ratio and lead isotope profiles in a sediment affected by a mining operation episode during the late 19th century. *Water Air and Soil Pollution* **177**: 285-311.

Baker VR (1973) Paleohydrology and sedimentology of Lake Missoula flooding in eastern Washington. *Geological Society of America Special Publication* **144**: 1–73.

Baker VR (1987) Paleoflood hydrology and extraordinary flood events. *Journal of Hydrology* **96**: 79–99 doi:10.1016/0022-1694(87)90145-4.

Baker VR (2002) The study of superfloods. *Science* **295**: 2379–2380.

Baker VR (2008) Paleoflood hydrology: Origin, progress, prospects. *Geomorphology* **101**: 1–13 doi:10.1016/j.geomorph.2008.05.016.

Ballantyne CK (2002) A general model of paraglacial landscape response. *The Holocene* **12**: 371–376 doi:10.1191/0959683602hl553fa.

Baltzer F (1991) Late Pleistocene and Recent detrital sedimentation in the deep parts of northern Lake Tanganyika (East African rift). *Lacustrine Facies Analysis: Special Publication 13 of the International Association of Sedimentologists* **13**: 147–173.

Barker PA, Wilby RL, Borrows J (2004) A 200-year precipitation index for the central English Lake District / Un indice de précipitation de 200 ans pour la Région des Lacs en Angleterre. *Hydrological Sciences Journal* **49**: 769–785.

Battarbee R.W. 1997. Freshwater quality, naturalness and palaeolimnology. In Boon, PJ and Howell, DL. (Eds.) Freshwater Quality: Defining the Indefinable? SNH The Stationary Office, Edinrbugh, pp. 155-171.

Battarbee R.W., Allott T.E.H., Juggins S., Kreiser A.M., Curtis C., Harriman R. (1996) Critical loads of acidity to surface waters: An empirical diatom-based palaeolimnological model. *Ambio* **25**: 366-369.

Battarbee R.W., Anderson N.J., Jeppesen E., Leavitt P.R. (2005) Combining palaeolimnological and limnological approaches in assessing lake ecosystem response to nutrient reduction. *Freshwater Biology* **50**: 1772-1780.

Bayliss AC, Reed DW (2001) The use of historical data in flood frequency estimation (Wallingford, UK: Centre for Ecology and Hydrology, UK).

Beck C (2009) Late Quaternary lacustrine paleo-seismic archives in north-western Alps: Examples of earthquake-origin assessment of sedimentary disturbances. *Earth-Science Reviews* **96**: 327–344 doi:10.1016/j.earscirev.2009.07.005.

Beierle BD, Lamoureux SF, Cockburn JMH, Spooner I (2002) A new method for visualizing sediment particle size distributions. *Journal of Paleolimnology* **27**: 279–283.

Benito G, Lang M, Barriendos M, Llasat C, Francés F, Ouarda T, Varyl R, Enzel Y, Bardossy A (2004) Use of Systematic, Palaeoflood and Historical Data for the Improvement of Flood Risk Estimation. Review of Scientific Methods. *Natural Hazards* **31**: 623–643.

Bennion H., Battarbee R.W., Sayer C.D., Simpson G.L., Davidson T.A. (2011) Defining reference conditions and restoration targets for lake ecosystems using palaeolimnology: a synthesis. *Journal of Paleolimnology* **45**: 533-544.

Bennion H., Fluin J. ,Simpson G.L. (2004) Assessing eutrophication and reference conditions for Scottish freshwater lochs using subfossil diatoms. *Journal of Applied Ecology* **41**: 124-138.

Bennion H, Winchester A (2010) Linking historical land-use change with palaeolimnological records of nutrient changes in Loweswater, Cumbria. Loweswater Care Project Short Project Report.

Benson BMA, Carter RW (1973) A National Study of the Streamflow Data-Collection Program. Geological Survey Water-Supply Paper 2028 (United States Government Printing Office, Washington).

Besonen MR, Bradley RS, Mudelsee M, Abbott MB, Francus P (2008) A 1,000-year, annually-resolved record of hurricane activity from Boston, Massachusetts. *Geophysical Research Letters* **35**: L14705 doi:10.1029/2008GL033950.

Best JL, Kostaschuk RA, Peakall J, Villard P V., Franklin M (2005) Whole flow field dynamics and velocity pulsing within natural sediment-laden underflows. *Geology* **33**: 765–768 doi:10.1130/G21516.1.

Bindler R, Renberg I, Klaminder J. (2008) Bridging the gap between ancient metal pollution and contemporary biogeochemistry. *Journal of Paleolimnology* **40**: 755-770.

Bindler R, Renberg I, Rydberg J, Andren T (2009) Widespread waterborne pollution in central Swedish lakes and the Baltic Sea from pre-industrial mining and metallurgy. *Environmental Pollution* **157**: 2132-2141.

Bindler R, Rydberg J, Renberg I (2011a) Establishing natural sediment reference conditions for metals and the legacy of long-range and local pollution on lakes in Europe. *Journal of Paleolimnology* **45**: 519–531 doi:10.1007/s10933-010-9425-5.

Bindler R., Segerstrom U., Pettersson-Jensen I.M., Berg A., Hansson S., Holmstrom H., Olsson K. and Renberg I. (2011b). Early medieval origins of iron mining and settlement in central Sweden: multiproxy analysis of sediment and peat records from the Norberg mining district. *Journal of Archaeological Science* **38**: 291-300.

Björck S, Wohlfarth B (2001) 14C chronostratigraphic techniques in paleolimnology. In Tracking Environmental Change Using Lake Sediments. Volume 1: Basin Analysis, Coring and Chronological Techniques., W.. Last, and J.P. Smol, eds. (Kluwer Academic Publishers, The Netherlands), pp. 205–245.

Blaauw M, Andrés Christen J (2011) Flexible Paleoclimate Age-Depth Models Using an Autoregressive Gamma Process. *Bayesian Analysis* **6**: 457–474 doi:10.1214/11-BA618.

Black AR, Law FM (2004) Development and utilization of a national web-based chronology of hydrological events. *Hydrological Sciences Journal* **49**: 237–246.

Blass A, Grosjean M, Troxler A, Sturm M (2007) How stable are twentieth-century calibration models? A high-resolution summer temperature reconstruction for the

eastern Swiss Alps back to AD 1580 derived from proglacial varved sediments. *The Holocene* **17**: 51–63 doi:10.1177/0959683607073278.

Bloemsma MR, Zabel M, Stuut JBW, Tjallingii R, Collins J, Weltje GJ (2012) Modelling the joint variability of grain size and chemical composition in sediments. *Sedimentary Geology* **280**: 135–148 doi:10.1016/j.sedgeo.2012.04.009.

Bloesch J, Burns N (1980) A critical review of sedimentation trap technique. *Schweizerische Zeitschrift für Hydrologie* **42**: 15–55.

Blomqvist S, Håkanson L (1981) A review on sediment traps in aquatic environments. *Archiv für Hydrobiologie* **91**: 101–132.

Bloom N, Fitzgerald WF (1988) Determination of Volatile Mercury Species at the Picogram Level by Low-Temperature Gas-Chromatography with Cold-Vapor Atomic Fluorescence Detection. *Analytica Chimica Acta* **208**: 151-161.

Blott SJ, Pye K (2001) GRADISTAT: a grain size distribution and statistics package for the analysis of unconsolidated sediments. *Earth Surface Processes and Landforms* **26**: 1237–1248 doi:10.1002/esp.261.

Bøe A-G, Dahl SO, Lie Ø, Nesje A (2006) Holocene river floods in the upper Glomma catchment, southern Norway: a high-resolution multiproxy record from lacustrine sediments. *The Holocene* **16**: 445–455 doi:10.1191/0959683606hl940rp.

Boehrer B, Schultze M (2008) Stratification of lakes. *Reviews of Geophysics* **46**: 1–27 doi:10.1029/2006RG000210.

Boes X., Rydberg J., Martinez-Cortizas A., Bindler R., Renberg I. (2011) Evaluation of conservative lithogenic elements (Ti, Zr, Al, and Rb) to study anthropogenic element enrichments in lake sediments. *Journal of Paleolimnology* **46**: 75-87.

Bouma A (1962) Sedimentology of some Flysch Deposits: a Graphic Approach to Facies Interpretation (Elsevier, Amsterdam).

Boyle J, Chiverrell R, Plater A, Thrasher I, Bradshaw E, Birks H, Birks J (2013) Soil mineral depletion drives early Holocene lake acidification. *Geology* **41**: 415–418 doi:10.1130/G33907.1.

Boyle JF (1995) A simple closure mechanism for a compact, large-diameter, gravity corer. *Journal of Paleolimnology* **13**: 85–87.

Boyle J.F. and Birks H.J.B. (1999). Predicting heavy metal concentrations in the surface sediments of Norwegian headwater lakes from atmospheric deposition: An application of a simple sediment-water partitioning model. *Water Air and Soil Pollution* **114**: 27-51.

Boyle JF (2000) Rapid elemental analysis of sediment samples by isotope source XRF. *Journal of Paleolimnology* **23**: 213–221.

Boyle JF (2001) Inorganic geochemical methods in palaeolimnology. In Tracking Environmental Change Using Lake Sediments. Volume 2: Physical and Geochemical Methods, W.M. Last, and J.P. Smol, eds. (Kluwer Academic Publishers, The Netherlands), pp. 83–142.

Boyle JF, Chiverrell RC, Schillereff DN (2015a) Approaches to water content correction and calibration for µXRF core scanning: comparing x-ray scatter with simple regression of elemental concentrations. In Developments in Palaeoenvironmental Research: Micro-XRF Studies of Sediment Cores, R.G. Rothwell, and I.W. Croudace, eds. (Dordrecht: Springer),.

Boyle JF, Chiverrell RC, Schillereff DN (2015b) Lacustrine archives of metals from mining and other industrial activities - a geochemical approach. In Environmental Contaminants: Using Natural Archives to Track Sources and Long-Term Trends of Pollution, J. Blais, M. Rosen, and J. Smol, eds. (Springer, Dordrecht),.

Boyle JF, Mackay AW, Rose NL, Flower RJ, Appleby PG (1998) Sediment heavy metal record in Lake Baikal: natural and anthropogenic sources. *Journal of Paleolimnology* **20**: 135–150.

Boyle JF, Rose NL, Appleby PG, Birks HJB (2004) Recent Environmental Change and Human Impact on Svalbard: The Lake-Sediment Geochemical Record. *Journal of Paleolimnology* **31**: 515–530 doi:10.1023/B:JOPL.0000022549.07298.6e.

Brännvall M.L., Bindler R., Emteryd O., Nilsson M, Renberg I. (1997) Stable isotope and concentration records of atmospheric lead pollution in peat and lake sediments in Sweden. *Water Air and Soil Pollution* **100**: 243-252.

Brännvall M, Bindler R, Emteryd O, Renberg I (2001) Four thousand years of atmospheric lead pollution in northern Europe : a summary from Swedish lake sediments. *Journal of Paleolimnology* **25**: 421–435.

Brázdil R, Glaser R, Pfister C, Dobrovolný P, Antoine J-M, Barriendos M, Camuffo D, Deutsch M, Enzi S, Guidoboni E, Kotyza O, Rodrigo FS (1999) Flood events of selected European rivers in the Sixteenth Century. *Climatic Change* **43**: 239–285.

Brázdil R, Kundzewicz ZW, Benito G (2006) Historical hydrology for studying flood risk in Europe. *Hydrological Sciences Journal* **51**: 739–764.

Bronk Ramsey C (2008) Deposition models for chronological records. *Quaternary Science Reviews* **27**: 42–60 doi:10.1016/j.quascirev.2007.01.019.

Bronk Ramsey C (2009) Bayesian analysis of radiocarbon dates. *Radiocarbon* **51**: 337–360.

Bronk Ramsey C, Staff RA, Bryant CL, Brock F, Kitagawa H, van der Plicht J, Schlolaut G, Marshall MH, Brauer A, Lamb HF, Payne RL, Tarasov PE, Haraguchi T, Gotanda K, Yonenobu H, Yokoyama Y, Tada R, Nakagawa T (2012) A complete terrestrial radiocarbon record for 11.2 to 52.8 kyr B.P. *Science (New York, NY)* **338**: 370–374 doi:10.1126/science.1226660.

Brown SL, Bierman PR, Lini A, Southon J (2000) 10 000 Yr Record of Extreme Hydrologic Events. *Geology* **28**: 335 doi:10.1130/0091-7613(2000)28Y.

Brugam R.B., Ketterer M., Maines L., Lin Z.Q, Retzlaff W.A. (2012) Application of a simple binary mixing model to the reconstruction of lead pollution sources in two Mississippi River floodplain lakes. *Journal of Paleolimnology* **47**: 101-112.

Bruland K.W., Bertine K., Koide M, Goldberg E.D. (1974) History of Metal Pollution in Southern-California Coastal Zone. *Environment Science and Technology* **8**: 425-432.

Burt TP, Howden NJK (2013) North Atlantic Oscillation amplifies orographic precipitation and river flow in upland Britain. *Water Resources Research* **49**: 3504–3515 doi:10.1002/wrcr.20297.

Byrne P, Reid I, Wood PJ (2010) Sediment geochemistry of streams draining abandoned lead/zinc mines in central Wales: the Afon Twymyn. *Journal of Soils and Sediments* **10**: 683–697 doi:10.1007/s11368-009-0183-9.

Camarero L., Botev I., Muri G., Psenner R., Rose N, Stuchlik E. (2009) Trace elements in alpine and arctic lake sediments as a record of diffuse atmospheric contamination across Europe. *Freshwater Biology* **54**: 2518-2532.

Campbell C (1998) Late Holocene Lake Sedimentology and Climate Change in Southern Alberta, Canada. *Quaternary Research* **49**: 96–101 doi:10.1006/qres.1997.1946.

Campbell C, Tipping R, Cowley D (2002) Continuity and stability in past upland land uses in the western Cheviot Hills, southern Scotland. *Landscape History* **24**: 111–120 doi:10.1080/01433768.2002.10594542.

Carignan R., Tessier A. (1985) Zinc Deposition in Acid Lakes - the Role of Diffusion. *Science* **228**: 1524-1526.

Carling PA, Villanueva I, Herget J, Wright N, Borodavko P, Morvan H (2010) Unsteady 1D and 2D hydraulic models with ice dam break for Quaternary megaflood, Altai Mountains, southern Siberia. *Global and Planetary Change* **70**: 24–34.

Catalan J., Pla-Rabés S., Wolfe A.P., Smol J.P., Rühland K.M., Anderson N.J., Kopáček J., Stuchlík E., Schmidt R., Koinig K.A., Camarero L., Flower R.J., Heiri O., Kamenik C., Korhola A., Leavitt P.R., Psenner R, Renberg I. (2013) Global change revealed by palaeolimnological records from remote lakes: a review. *Journal of Paleolimnology* **49**: 513-535.

Cesare G De, Schleiss A, Hermann F (2001) Impact of Turbidity Currents on Reservoir Sedimentation. *Journal of Hydraulic Engineering* **127**: 6–16.

Chambers FM, Barber KE, Maddy D, Brew J (1997) A 5500-year proxy-climate and vegetation record from blanket mire at Talla Moss, Borders, Scotland. *The Holocene* **7**: 391–399 doi:10.1177/095968369700700402.

Chambers K, Parker A (1979) A modified design for lake-sestion traps and a simple method for relocating them. *Earth Surface Processes and Landforms* **4**: 73–76.

Chambers KC (1978) Source-sediment relationship in Cumbrian Lakes. Unpublished PhD Thesis, University of Reading.

Chapron E, Juvigné E, Mulsow S, Ariztegui D, Magand O, Bertrand S, Pino M, Chapron O (2007) Recent clastic sedimentation processes in Lake Puyehue (Chilean Lake District, 40.5°S). *Sedimentary Geology* **201**: 365–385 doi:10.1016/j.sedgeo.2007.07.006.

Charman DJ, Blundell A, Chiverrell RC, Hendon D, Langdon PG (2006) Compilation of non-annually resolved Holocene proxy climate records: stacked Holocene peatland palaeo-water table reconstructions from northern Britain. *Quaternary Science Reviews* **25**: 336–350 doi:10.1016/j.quascirev.2005.05.005.

Chatterton J, Vivattene C, Morris J, Penning-Rosweel E, Tapsell S (2010) The Costs of the Summer 2007 Floods in England. Project Report (SC070039/R1), Environment Agency, Bristol.

Chawchai S, Chabangborn A, Kylander M, Löwemark L, Mörth C-M, Blaauw M, Klubseang W, Reimer PJ, Fritz SC, Wohlfarth B (2013) Lake Kumphawapi – an archive of Holocene palaeoenvironmental and palaeoclimatic changes in northeast Thailand. *Quaternary Science Reviews* **68**: 59–75 doi:10.1016/j.quascirev.2013.01.030.

Cheng N-S (1997) Simplified settling velocity formula for sediment particle. *Journal of Hydraulic Engineering* **123**: 149–152.

Chiverrell RC (2006) Past and future perspectives upon landscape instability in Cumbria, northwest England. *Regional Environmental Change* **6**: 101–114 doi:10.1007/s10113-005-0005-6.

Chiverrell RC, Foster GC, Thomas GSP, Marshall P (2010) Sediment transmission and storage: the implications for reconstructing landforms. *Earth Surface Processes and Landforms* **15**: 4–15 doi:10.1002/esp.

Chiverrell RC, Foster GC, Thomas GSP, Marshall P, Hamilton D (2009) Robust chronologies for landform development. *Earth Surface Processes and Landforms* **34**: 319–328 doi:10.1002/esp.

Chiverrell RC, Harvey A. M, Foster GC (2007) Hillslope gullying in the Solway Firth — Morecambe Bay region, Great Britain: Responses to human impact and/or climatic deterioration? *Geomorphology* **84**: 317–343 doi:10.1016/j.geomorph.2005.12.014.

Chiverrell RC, Oldfield F, Appleby PG, Barlow D, Fisher E, Thompson R, Wolff G (2008) Evidence for changes in Holocene sediment flux in Semer Water and Raydale, North Yorkshire, UK. *Geomorphology* **100**: 70–82 doi:10.1016/j.geomorph.2007.04.035.

Chiverrell RC, Thorndycraft VR, Hoffmann TO (2011) Cumulative probability functions and their role in evaluating the chronology of geomorphological events during the Holocene. *Journal of Quaternary Science* **26**: 76–85 doi:10.1002/jqs.1428.

Christen JA, Pérez S (2009) A new robust statistical model for radiocarbon data. *Radiocarbon* **51**: 1047–1059.

Chu G, Liu J, Schettler G, Li J, Sun Q, Gu Z, Lu H, Liu Q, Liu T (2005) Sediment Fluxes and Varve Formation in Sihailongwan, a Maar Lake from Northeastern China. *Journal of Paleolimnology* **34**: 311–324 doi:10.1007/s10933-005-4694-0.

Clayton JW (1997) The biology of the River Tweed. *Science of the Total Environment* **194-195**: 155–162 doi:10.1016/S0048-9697(96)05361-2.

Cockburn JMH, Lamoureux SF (2008) Inflow and lake controls on short-term mass accumulation and sedimentary particle size in a High Arctic lake: implications for interpreting varved lacustrine sedimentary records. *Journal of Paleolimnology* **40**: 923–942 doi:10.1007/s10933-008-9207-5.

Coombes PM V, Chiverrell RC, Barber KE (2009) A high-resolution pollen and geochemical analysis of late Holocene human impact and vegetation history in

southern Cumbria, England. *Journal of Quaternary Science* **24**: 224–236 doi:10.1002/jqs.

Couillard Y, Cattaneo A, Gallon C, Courcelles M (2007) Sources and chronology of fifteen elements in the sediments of lakes affected by metal deposition in a mining area. *Journal of Paleolimnology* **40**: 97–114 doi:10.1007/s10933-007-9146-6.

Couillard Y, Courcelles M, Cattaneo A, Wunsam S (2004) A test of the integrity of metal records in sediment cores based on the documented history of metal contamination in Lac Dufault (Québec, Canada). *Journal of Paleolimnology* **32**: 149–162.

Coumou D, Rahmstorf S (2012) A decade of weather extremes. *Nature Climate Change* **2**: 1–6 doi:10.1038/nclimate1452.

Croudace IW, Rindby A, Rothwell RG (2006) ITRAX: description and evalutation of a new multi-function X-ray core scanner. In New Techniques in Sediment Core Analysis, R.G. Rothwell, ed. (Geological Society of London Special Publications), pp. 51–63.

Croudace I.W., Warwick P.E, Greenwood R (2006) A novel approach for the rapid decomposition of Actinide (TM) resin and its application to measurement of uranium and plutonium in natural waters. *Analytica Chimica Acta* **577**: 111-118.

Crutzen PJ (2002) Geology of mankind. *Nature* **415**: 23 doi:10.1038/415023a.

Cuven S, Francus P, Lamoureux S (2011) Mid to Late Holocene hydroclimatic and geochemical records from the varved sediments of East Lake, Cape Bounty, Canadian High Arctic. *Quaternary Science Reviews* **30**: 2651–2665 doi:10.1016/j.quascirev.2011.05.019.

Cuven S, Francus P, Lamoureux SF (2010) Estimation of grain size variability with micro X-ray fluorescence in laminated lacustrine sediments, Cape Bounty, Canadian High Arctic. *Journal of Paleolimnology* **44**: 803–817 doi:10.1007/s10933-010-9453-1.

Cuven S, Paris R, Falvard S, Miot-Noirault E, Benbakkar M, Schneider J-L, Billy I (2013) High-resolution analysis of a tsunami deposit: Case-study from the 1755 Lisbon tsunami in southwestern Spain. *Marine Geology* **337**: 98–111 doi:10.1016/j.margeo.2013.02.002.

Czymzik M, Brauer A, Dulski P, Plessen B, Naumann R, von Grafenstein U, Scheffler R (2013) Orbital and solar forcing of shifts in Mid- to Late Holocene flood intensity from varved sediments of pre-alpine Lake Ammersee (southern Germany). *Quaternary Science Reviews* **61**: 96–110 doi:10.1016/j.quascirev.2012.11.010.

Czymzik M, Dulski P, Plessen B, von Grafenstein U, Naumann R, Brauer A (2010) A 450 year record of spring-summer flood layers in annually laminated sediments from Lake Ammersee (southern Germany). *Water Resources Research* **46**: W11528 doi:10.1029/2009WR008360.

Das S.K., Routh J., Roychoudhury A.N, Klump J.V. (2008) Major and trace element geochemistry in Zeekoevlei, South Africa: A lacustrine record of present and past processes. *Applied Geochemistry* **23**: 2496-2511.

Davis RB (1974) Stratigraphic effects of tubificids in profundal lake sediments. *Limnology and Oceanography* **19**: 466–488.

Davison W (1993) Iron and manganese in lakes. *Earth-Science Reviews* **34**: 119–163 doi:10.1016/0012-8252(93)90029-7.

Davison W, Hilton J, Lishman JP, Tutin WP (1985) Contemporary lake transport processes determined from sedimentary records of copper mining activity. *Environmental Science & Technology* **19**: 356–360 doi:10.1021/es00134a009.

Dearing JA (1983) Changing patterns of sediment accumulation in a small lake in Scania, southern Sweden. *Hydrobiologia* **103**: 59–64 doi:10.1007/BF00028428.

Dearing JA (1991) Lake sediment records of erosional processes. *Hydrobiologia* **214**: 99–106.

Dearing JA (1997) Sedimentary indicators of lake-level changes in the humid temperate zone: a critical review. *Journal of Paleolimnology* **18**: 1–14.

Dearing JA (1999) Holocene environmental change from magnetic proxies in lake sediments. In Quaternary Climates and Magnetism, B.A. Maher, and R. Thompson, eds. (Cambridge University Press, UK), pp. 231–278.

Dearing JA, Jones RT (2003) Coupling temporal and spatial dimensions of global sediment flux through lake and marine sediment records. *Global and Planetary Change* **39**: 147–168 doi:10.1016/S0921-8181(03)00022-5.

Debret M, Chapron E, Desmet M, Rolland-Revel M, Magand O, Trentesaux a., Bout-Roumazeille V, Nomade J, Arnaud F (2010) North western Alps Holocene paleohydrology recorded by flooding activity in Lake Le Bourget, France. *Quaternary Science Reviews* **29**: 2185–2200 doi:10.1016/j.quascirev.2010.05.016.

Dennis IA, Coulthard TJ, Brewer P, Macklin MG (2009) The role of floodplains in attenuating contaminated sediment fluxes in formerly mined drainage basins. *Earth Surface Processes and Landforms* **34**: 453–466 doi:10.1002/esp.1762.

Desloges JR, Gilbert R (1994) Sediment source and hydroclimatic inferences from glacial lake sediments: the postglacial sedimentary record of Lillooet Lake, British Columbia. *Journal of Hydrology* **159**: 375–393 doi:10.1016/0022-1694(94)90268-2.

Dietze E, Hartmann K, Diekmann B, IJmker J, Lehmkuhl F, Opitz S, Stauch G, Wünnemann B, Borchers A (2012) An end-member algorithm for deciphering modern detrital processes from lake sediments of Lake Donggi Cona, NE Tibetan Plateau, China. *Sedimentary Geology* **243-244**: 169–180 doi:10.1016/j.sedgeo.2011.09.014.

Dietze M, Dietze E (2013) End-member modelling algorithm and supporting functions for grain-size analysis. 27.

Dong X, Bennion H, Battarbee RW, Sayer CD (2011) A multiproxy palaeolimnological study of climate and nutrient impacts on Esthwaite Water, England over the past 1200 years. *The Holocene* **22**: 107–118 doi:10.1177/0959683611409780.

Douglas RW, Rippey B (2000) The random redistribution of sediment by wind in a lake. *Limnology and Oceanography* **45**: 686–694.

Droppo IG (2001) Rethinking what constitutes suspended sediment. *Hydrological Processes* **15**: 1551–1564 doi:10.1002/hyp.228.

Droppo IG, Leppard GG, Flannigan DT, Liss SN (1997) The freshwater floc: a functional relationship of water and organic and inorganic floc constituents affecting suspended sediment properties. *Water, Air, and Soil Pollution* **99**: 43–54.

Duvauchelle P, Peix G, Babot D (1999) Effective atomic number in the Rayleigh to Compton scattering ratio. *Nuclear Instruments and Methods in Physics Research B* **155**: 221–228.

Dypvik H, Harris NB (2001) Geochemical facies analysis of fine-grained siliciclastics using Th/U , Zr/Rb and (Zr + Rb) / Sr ratios. *Chemical Geology* **181**: 131–146.

Eades L.J., Farmer J.G., MacKenzie A.B., Kirika A, Bailey-Watts A.E. (2002) Stable lead isotopic characterisation of the historical record of environmental lead contamination in dated freshwater lake sediment cores from northern and central Scotland. *Science of the Total Environment* **292**: 55-67.

Eadie BJ (1997) Probing particle processes in Lake Michigan using sediment traps. *Water, Air and Soil Pollution* **99**: 133–139.

Eakins JD, Cambray RS, Lally AE, Chambers KC (1984) The transfer of natural and artificial radionuclides to Brotherswater from its catchment. In Lake Sediments and Environmental History, E. Haworth, and W. Lund, eds. (Leicester University Press, UK), pp. 125–144.

Eden P, Burt S (2010) Extreme Rainfall in Cumbria. *Weather* **65**: 14.

Edwards KJ, Whittington G (2001) Lake sediments, erosion and landscape change during the Holocene in Britain and Ireland. *Catena* **42**: 143–173 doi:10.1016/S0341-8162(00)00136-3.

Effler SW, Matthews DA, Kaser JW, Prestigiacomo AR, Smith DG, Prestigiacomo R (2006) Runoff event impacts on a water supply reservoir: suspended sediment loading, turbid plume behavior, and sediment deposition. *Journal of the American Water Resoures Association* **10595**: 1697–1710.

Ek AS, Renberg I (2001) Heavy metal pollution and lake acidity changes caused by one thousand years of copper mining at Falun, central Sweden. *Journal of Paleolimnology* **26**: 89–107.

Engstrom DR, Rose NL (2013) A whole-basin, mass-balance approach to paleolimnology. *Journal of Paleolimnology* **49**: 333–347 doi:10.1007/s10933-012-9675-5.

Engstrom DR, Wright HE (1984) Chemical stratigraph of lake sediments as a record of environmental change. In Lake Sediments and Environmental History,.

Environment Agency (2006) Cumbria floods technical report: factual report on the meteorology, hydrology and impacts of the January 2005 flooding in Cumbria.

Evans RD (1994) Empirical evidence of the importance of sediment resuspension in lakes. *Hydrobiologia* **284**: 5–12 doi:10.1007/BF00005727.

Everard N (2010) The 2009 Cumbrian floods : using acoustic Doppler technology to rebuild a monitoring capability. In BHS Third International Symposium, Managing Consequences of a Changing Global Environment, pp. 1–8.

Farmer JG, MacKenzie AE, Eades LJ, Kirika A, Bailey-Watts AE (1997a) Influences on the extent and record of heavy metal pollution in sediment cores from Loch Tay in a mineralised area of Scotland. *Journal of Geochemical Exploration* **58**: 195–202.

Farmer JG, MacKenzie AE, Sugen, CL, Edgar, PJ, Eades LJ (1997b) A comparison of the historical lead pollution records in peat and freshwater lake sediments from central Scotland. *Water, Soil and Air Pollution* 100: 253-270.

Finkelshtein A. L, Brjansky N (2009) Estimating particle size effects in X-ray fluorescence spectrometry. *Nuclear Instruments and Methods in Physics Research Section B: Beam Interactions with Materials and Atoms* **267**: 2437–2439 doi:10.1016/j.nimb.2009.05.005.

Folk RL (1966) A review of grain-size parameters. *Sedimentology* **6**: 73–93.

Folland CK, Knight J, Linderholm HW, Fereday D, Ineson S, Hurrell JW (2009) The Summer North Atlantic Oscillation: Past, Present, and Future. *Journal of Climate* **22**: 1082–1103 doi:10.1175/2008JCLI2459.1.

Forel FA (1885) Les ravins sous-lacustres des fleuves glaciaires. *Compte Rendus de l'Académie des Sciences de Paris* **101**: 1–3.

Förstner U (1976) Lake sediments as indicators of heavy-metal pollution. *Die Naturwissenschaften* **63**: 465–470.

Fortino K, Hershey AE, Keyse MD, Whalen SC (2009) Summer sedimentation in six shallow arctic lakes. *Hydrobiologia* **621**: 75–84 doi:10.1007/s10750-008-9633-4.

Foster GC, Chiverrell RC, Harvey AM, Dearing J., Dunsford H (2008) Catchment hydro-geomorphological responses to environmental change in the Southern Uplands of Scotland. *The Holocene* **18**: 935–950 doi:10.1177/0959683608091799.

Foster GC, Dearing JA, Jones RT, Crook DS, Siddle DJ, Harvey AM, James PA, Appleby PG, Thompson R, Nicholson J, Loizeau J-L (2003) Meteorological and land use controls on past and present hydro-geomorphic processes in the pre-alpine environment: an integrated lake-catchment study at the Petit Lac d'Annecy, France. *Hydrological Processes* **17**: 3287–3305 doi:10.1002/hyp.1387.

Foster I.D.L, Charlesworth S.M. (1996) Heavy metals in the hydrological cycle: Trends and explanation. *Hydrological Processes* **10**: 227-261.

Foulds SA, Macklin MG, Brewer PA (2013) Agro-industrial alluvium in the Swale catchment, northern England, as an event marker for the Anthropocene. *The Holocene* **23**: 587–602 doi:10.1177/0959683612465445.

Fowler H, Kilsby CG (2002) Precipitation and the North Atlantic Oscillation. *International Journal of Climatology2* **22**: 843–866.

Fowler HJ, Kilsby CG (2007) Using regional climate model data to simulate historical and future river flows in northwest England. *Climatic Change* **80**: 337–367 doi:10.1007/s10584-006-9117-3.

Fox IA, Johnson RC (1997) The hydrology of the River Tweed. *The Science of the Total Environment* **194-195**: 163–172.

Francus P, Bradley RS, Lewis T, Abbott M, Retelle M, Stoner JS (2008) Limnological and sedimentary processes at Sawtooth Lake, Canadian High Arctic, and their influence on varve formation. *Journal of Paleolimnology* **40**: 963–985 doi:10.1007/s10933-008-9210-x.

Francus P, von Suchodoletz H, Dietze M, Donner R V., Bouchard F, Roy A-J, Fagot M, Verschuren D, Kröpelin S (2013) Varved sediments of Lake Yoa (Ounianga Kebir, Chad) reveal progressive drying of the Sahara during the last 6100 years. *Sedimentology* **60**: 911–934 doi:10.1111/j.1365-3091.2012.01370.x.

Friedman GM, Sanders JE (1978) Principles of Sedimentology (John Wiley & Sons, Inc.).

Fryirs K (2012) (Dis)Connectivity in catchment sediment cascades: a fresh look at the sediment delivery problem. *Earth Surface Processes and Landforms* **State of S**: 1–17 doi:10.1002/esp.3242.

Fryirs K, Brierley GJ, Preston NJ, Kasai M (2007) Buffers, barriers and blankets: The (dis)connectivity of catchment-scale sediment cascades. *Catena* **70**: 49–67 doi:10.1016/j.catena.2006.07.007.

Gallagher L., Macdonald R.W, Paton D.W. (2004) The historical record of metals in sediments from six lakes in the Fraser River Basin, British Columbia. *Water Air and Soil Pollution* **152**: 257-278.

Garçon M., Chauvel C., Chapron E., Faïn X., Lin M.F., Campillo S., Bureau S., Desmet M., Bailly-Maître M.C, Charlet L. (2012) Silver and lead in high-altitude lake sediments: Proxies for climate changes and human activities. *Applied Geochemistry* **27**: 760-773.

Gardner J V, Mayer LA (2000) Morphology and processes in Lake Tahoe (California-Nevada). *Geological Society of America Bulletin* **112**: 736–746 doi:10.1130/0016-7606(2000)112.

Gardner WD (1985) The effect of tilt on sediment trap efficiency. *Deep-Sea Research* **32**: 349–361.

Garnett MH, Stevenson AC (2004) Testing the use of bomb radiocarbon to date the surface layers of blanket peat. *Radiocarbon* **46**: 841–851.

Garrels R.M, Mackenzie F.T. (1971) Evolution of sedimentary rocks. W.W. Norton and Co., Ltd., New York, 397 pp.

Garzanti E, Andò S, Vezzoli G (2008) Settling equivalence of detrital minerals and grain-size dependence of sediment composition. *Earth and Planetary Science Letters* **273**: 138–151 doi:10.1016/j.epsl.2008.06.020.

Gibbs RJ, Matthews MD, Link DA (1971) The relationship between sphere size and settling velocity. *Journal of Sedimentary Research* **41**: 7–18.

Giguet-Covex C, Arnaud F, Poulenard J, Disnar J-R, Delhon C, Francus P, David F, Enters D, Rey P-J, Delannoy J-J (2011) Changes in erosion patterns during the Holocene in a currently treeless subalpine catchment inferred from lake sediment geochemistry (Lake Anterne, 2063 m a.s.l., NW French Alps): The role of climate and human activities. *The Holocene* **21**: 651–665 doi:10.1177/0959683610391320.

Gilbert GK (1885) The topographic features of lake shores. *US Geological Survey 5th Annual Report* 69–123.

Gilli A, Anselmetti FS, Ariztegui D, McKenzie JA (2003) A 600-year sedimentary record of flood events from two sub-alpine lakes (Schwendiseen, Northeastern Switzerland). *Eclogae Geologica Helvetia* **96**: 49–58.

Gilli A, Anselmetti FS, Glur L, Wirth SB (2013) Lake Sediments as Archives of Recurrence Rates and Intensities of Past Flood Events. In Dating Torrential Processes on Fans and Cones, M. Schneuwly-Bollschweiler, M. Stoffel, and F. Rudolf-Miklau, eds. (Dordrecht: Springer Netherlands), pp. 225–242.

Girardclos S, Hilbe M, Corella JP, Kremer K, Delsontro T, Arantegui A, Moscariello A, Arlaud F, Akhtman Y, Flavio S, Lemmin U (2012) Searching the Rhone delta channel in Lake Geneva since François Alphonse Forel. *Archives des Sciences* **65**: 103–118.

Girardclos S, Schmidt OT, Sturm M, Ariztegui D, Pugin A, Anselmetti FS (2007) The 1996 AD delta collapse and large turbidite in Lake Brienz. *Marine Geology* **241**: 137–154 doi:10.1016/j.margeo.2007.03.011.

Glur L, Wirth SB, Büntgen U, Gilli A, Haug GH, Schär C, Beer J, Anselmetti FS (2013) Frequent floods in the European Alps coincide with cooler periods of the past 2500 years. *Scientific Reports* **3**: 2770 doi:10.1038/srep02770.

Gorham E, Boyce FM (1989) Influence of Lake Surface Area and Depth Upon Thermal Stratification and the Depth of the Summer Thermocline. *Journal of Great Lakes Research* **15**: 233–245 doi:10.1016/S0380-1330(89)71479-9.

Goring S, Williams JW, Blois JL, Jackson ST, Paciorek CJ, Booth RK, Marlon JR, Blaauw M, Christen JA (2012) Deposition times in the northeastern United States during the Holocene: establishing valid priors for Bayesian age models. *Quaternary Science Reviews* **48**: 54–60 doi:10.1016/j.quascirev.2012.05.019.

Gorman PAO, Schneider T (2009) The physical basis for increases in precipitation extremes in simulations of 21st-century climate change. *Proceedings of the National Academy of Sciences of the United States of America* **106**: 14733–14777.

Gray J.E., Fey D.L., Holmes C.W, Lasorsa B.K. (2005) Historical deposition and fluxes of mercury in Narraguinnep Reservoir, southwestern Colorado, USA. *Applied Geochemistry* **20**: 207-220.

Grayson RP, Plater AJ (2008) A lake sediment record of Pb mining from Ullswater, English Lake District, UK. *Journal of Paleolimnology* **42**: 183–197 doi:10.1007/s10933-008-9270-y.

Greenaway CM, Paterson AM, Keller BW, Smol JP (2012) Dramatic diatom species assemblage responses in lakes recovering from acidification and metal contamination near Wawa, Ontario, Canada: a paleolimnological perspective. *Canadian Journal of Fisheries and Aquatic Sciences* **669**: 656–669 doi:10.1139/F2012-003.

Von Gunten HR, Sturm M, Moser RN (1997) 200-Year Record of Metals in Lake Sediments and Natural Background Concentrations. *Environmental Science and Technology* **31**: 2193–2197.

Haberlah D, Mctainsh GH (2011) Quantifying particle aggregation in sediments. *Sedimentology* **58**: 1208–1216 doi:10.1111/j.1365-3091.2010.01201.x.

Håkanson L. (1977) Influence of Wind, Fetch, and Water Depth on Distribution of Sediments in Lake Vanern, Sweden. *Canadian Journal of Earth Science* **14**: 397-412.

Håkanson L. (1981) On Lake Bottom Dynamics - the Energy-Topography Factor. *Canadian Journal of Earth Science* **18**: 899-909.

Håkanson L, Jansson M (1983) Principles of Lake Sedimentology (Blackburn Press, USA).

Hamilton-Taylor J (1983) Heavy metal enrichments in the recent sediments of six lakes in northwest England. *Environmental Technology Letters* **4**: 115–122.

Hammarlund D, Mackay AW, Fallon DMJ, Pateman G, Tavio LC, Leng MJ, Rose NL (2007) A sedimentary record of the rise and fall of the metal industry in Bergslagen, south central Sweden. *Journal of Paleolimnology* **39**: 463–475 doi:10.1007/s10933-007-9124-z.

Hardy L (2013) A multi-proxy analysis to determine sediment-source linkage in Brotherswater, English Lake District. Unpublished BSc Dissertation, University of Liverpool.

Harvey AM (1992) Process interactions, temporal scales and the development of hillslope gully systems: Howgill Fells, northwest England. *Geomorphology* **5**: 323–344 doi:10.1016/0169-555X(92)90012-D.

Haschke M (2006) The Eagle III BKA system, a novel sediment core X-ray fluorescence analyser with very high spatial resolution. In New Techniques in Sediment Core Analysis, R.G. Rothwell, ed. (London: Geological Society of London Special Publications 267), pp. 21–37.

Hatfield RG, Maher BA (2009) Holocene sediment dynamics in an upland temperate lake catchment: climatic and land-use impacts in the English Lake District. *The Holocene* **19**: 427–438 doi:10.1177/0959683608101392.

Hatfield RG, Maher BA, Pates JM, Barker PA (2008) Sediment dynamics in an upland temperate catchment: changing sediment sources, rates and deposition. *Journal of Paleolimnology* 1143–1158 doi:10.1007/s10933-008-9221-7.

Hennekam R, de Lange G (2012) X-ray fluorescence core scanning of wet marine sediments: methods to improve quality and reproducibility of high-resolution paleoenvironmental records. *Limnology and Oceanography: Methods* **10**: 991–1003 doi:10.4319/lom.2012.10.991.

Herget J (2005) Reconstruction of Pleistocene Ice-Dammed Lake Outburst Floods in the Altai Mountains, Siberia. *Geological Society of America Special Publication* **386**: 118.

Hilton J (1985) A conceptual framework for predicting the occurrence of sediment focusing and sediment redistribution in small lakes. *Limnology and Oceanography* **30**: 1131–1143.

Hilton J., Davison W, Ochsenbein U. (1985) A Mathematical-Model for Analysis of Sediment Core Data - Implications for Enrichment Factor Calculations and Trace-Metal Transport Mechanisms. *Chemical Geology* **48**: 281-291.

Hirabayashi Y, Mahendran R, Koirala S, Konoshima L, Yamazaki D, Watanabe S, Kim H, Kanae S (2013) Global flood risk under climate change. *Nature Climate Change* **3**: 1–6 doi:10.1038/nclimate1911.

Hjülström F (1939) Transportation of detritus by moving water. In Recent Marine Sediments, P. Trask, ed. (American Association of Petroleum Geologists, Tulsa), pp. 5–31.

Hodder KR (2009) Flocculation : a key process in the sediment flux of a large , glacier-fed lake. *Earth Surface Processes and Landforms* **34**: 1151–1163 doi:10.1002/esp.

Hodder KR, Gilbert R (2007) Evidence for flocculation in glacier-fed Lillooet Lake, British Columbia. *Water Research* **41**: 2748–2762 doi:10.1016/j.watres.2007.02.058.

Hodder KR, Gilbert R, Desloges JR (2007) Glaciolacustrine varved sediment as an alpine hydroclimatic proxy. *Journal of Paleolimnology* **38**: 365–394 doi:10.1007/s10933-006-9083-9.

Hofmann MH, Hendrix MS (2010) Depositional processes and the inferred history of ice-margin retreat associated with the deglaciation of the Cordilleran Ice Sheet: The sedimentary record from Flathead Lake, northwest Montana, USA. *Sedimentary Geology* **223**: 61–74 doi:10.1016/j.sedgeo.2009.10.004.

Hooke J (2003) Coarse sediment connectivity in river channel systems: a conceptual framework and methodology. *Geomorphology* **56**: 79–94 doi:10.1016/S0169-555X(03)00047-3.

Hooke JM, Kain RJP (1982) Historical Change in the Physical Environment: A Guide to Sources and Techniques (Butterworth Scientific, London).

Hostetler SW (1995) Hydrological and Thermal Response of Lakes to Climate: Description and Modeling. In Physics and Chemistry of Lakes, A. Lerman, D. Imboden, and J. Gat, eds. (Springer-Verlag, Berlin), pp. 63–82.

Hua Q (2009) Radiocarbon: A chronological tool for the recent past. *Quaternary Geochronology* **4**: 378–390 doi:10.1016/j.quageo.2009.03.006.

Hudson-Edwards K A., Jamieson HE, Lottermoser BG (2011) Mine Wastes: Past, Present, Future. *Elements* **7**: 375–380 doi:10.2113/gselements.7.6.375.

Hudson-Edwards KA (2003) Sources, mineralogy, chemistry and fate of heavy metal-bearing particles in mining-affected river systems. *Mineralogical Magazine* **67**: 205–217 doi:10.1180/0026461036720095.

Humphries MS, Kindness A, Ellery WN, Hughes JC, Benitez-Nelson CR (2010) 137Cs and 210Pb derived sediment accumulation rates and their role in the long-term development of the Mkuze River floodplain, South Africa. *Geomorphology* **119**: 88–96 doi:10.1016/j.geomorph.2010.03.003.

Huntingford C, Marsh T, Scaife AA, Kendon EJ, Hannaford J, Kay AL, Lockwood M, Prudhomme C, Reynard NS, Parry S, Lowe JA, Screen JA, Ward HC, Roberts M, Stott PA, Bell VA, Bailey M, Jenkins A, Legg T, Otto FEL, Massey N, Schaller N, Slingo J, Allen MR (2014) Potential influences on the United Kingdom's floods of winter 2013/14. *Nature Climate Change* **4**: 769–777 doi:10.1038/nclimate2314.

Huntington TG (2006) Evidence for intensification of the global water cycle: Review and synthesis. *Journal of Hydrology* **319**: 83–95 doi:10.1016/j.jhydrol.2005.07.003.

Imboden DM, Wüest A (1995) Mixing Mechanisms in Lakes. In Physics and Chemistry of Lakes, A. Lerman, D. Imboden, and J. Gat, eds. (Springer-Verlag, Berlin), pp. 83–138.

Intergovernmental Panel on Climate Change (2012) Managing the risks of extreme events and disasters to advance climate change adaptation. A Special Report of Working Groups I and II of the Intergovernmental Panel on Climate Change (Cambridge: Cambridge University Press, UK).

IPCC (2013) Climate Change 2013: The physical science basis. Contribution of Working Group I to the Fifth Assessment Report of the Intergovernmental Panel on Climate Change. (Stocker TF, Qin D, Plattner G, Tignor M, Allen S, Boschung J, Nauels Y, Xia B, Bex B, Midgley B (Eds.)) Cambridge University Press, Cambridge, pp. 1535. doi:10.1017/CBO9781107415324

Ito T, Iwamoto H, Kamiya K, Fukushima T, Kumon F (2009) Use of flood chronology for detailed environmental analysis: a case study of Lake Kizaki in the northern Japanese Alps, central Japan. *Environmental Earth Sciences* **60**: 1607–1618 doi:10.1007/s12665-009-0295-y.

Jansen J, Van der Gaast S, Koster B, Vaars A (1998) CORTEX, a shipboard XRF-scanner for element analyses in split sediment cores. *Marine Geology* **151**: 143–153.

Jarrett RD, England JF (2002) Reliability of paleostage indicators for paleoflood studies. In Ancient Floods, Modern Hazards - Principles and Applications of Paleoflood Hydrology; Water Science and Application 5, P.K. House, R.H. Webb, V.R. Baker, and D.R. Levish, eds. (American Geophysical Union, Washington), pp. 91–109.

Jenny J, Arnaud F, Dorioz J, Covex CG, Frossard V, Sabatier P, Millet L, Reyss J, Tachikawa K, Bard E, Romeyer O, Perga M (2013) A spatiotemporal investigation of varved sediments highlights the dynamics of hypolimnetic hypoxia in a large hard-water lake over the last 150 years. *Limnology and Oceanography* **58**: 1395–1408 doi:10.4319/lo.2013.58.4.1395.

Jiménez J A, Madsen OS (2003) A Simple Formula to Estimate Settling Velocity of Natural Sediments. *Journal of Waterway, Port, Coastal and Ocean Engineering* **129**: 70–78 doi:10.1061/~ASCE!0733-950X~2003!129:2~70!

Johnson T (1980) Sediment redistribution by waves in lakes, reservoirs and embayments. In Symposium on Surface Water Impoundments, ASCE, June 2 - 5 1980, Minneapolis, Minnesota, Paper 7 - 9, pp. 1307–1317.

Johnston D, Watson I, Potter H, Jones C, Rolley S, Pritchard J (2008) Abandoned mines and the water environment. Environment Agency Science project SC030136-41.

Jones A, Rogerson M, Greenway G, Potter H A B, Mayes WM (2013) Mine water geochemistry and metal flux in a major historic Pb-Zn-F orefield, the Yorkshire Pennines, UK. *Environmental science and pollution research international* **20**: 7570–7581 doi:10.1007/s11356-013-1513-4.

Jones AF, Macklin MG, Brewer PA (2012) A geochemical record of flooding on the upper River Severn, UK, during the last 3750 years. *Geomorphology* **179**: 89–105 doi:10.1016/j.geomorph.2012.08.003.

Kämpf L, Brauer A, Dulski P, Lami A, Marchetto A, Gerli S, Ambrosetti W, Guilizzoni P (2012) Detrital layers marking flood events in recent sediments of Lago Maggiore (N. Italy) and their comparison with instrumental data. *Freshwater Biology* **57**: 2076–2090 doi:10.1111/j.1365-2427.2012.02796.x.

Kämpf L, Brauer A, Swierczynski T, Czymzik M, Mueller P, Dulski P (2014a) Processes of flood-triggered detrital layer deposition in the varved Lake Mondsee sediment record revealed by a dual calibration approach. *Journal of Quaternary Science* **29**: 475–486 doi:10.1002/jqs.2721.

Kämpf L, Müller P, Swierczynski T, Naumann R, Güntner A (2014b) Variable flood-related sediment flux in Lake Mondsee: causes and effects for detrital layer formation. In EGU General Assembly 2014, (Vienna, Austria), p. 2298.

Kastner S, Enters D, Ohlendorf C, Haberzettl T, Kuhn G, Lücke A, Mayr C, Reyss J-L, Wastegård S, Zolitschka B (2010) Reconstructing 2000 years of hydrological variation derived from laminated proglacial sediments of Lago del Desierto at the eastern margin

of the South Patagonian Ice Field, Argentina. *Global and Planetary Change* **72**: 201–214 doi:10.1016/j.gloplacha.2010.04.007.

Kauppila T (2006) Sediment-based study of the effects of decreasing mine water pollution on a heavily modified, nutrient enriched lake. *Journal of Paleolimnology* **35**: 25-37.

Kemp A.L.W, Thomas R.L. (1976) Impact of Mans Activities on Chemical Composition in Sediments of Lakes Ontario, Erie and Huron. *Water Air and Soil Pollution* **5**: 469-490.

Kendon EJ, Roberts NM, Fowler HJ, Roberts MJ, Chan SC, Senior C a. (2014) Heavier summer downpours with climate change revealed by weather forecast resolution model. *Nature Climate Change* **4**: 570–576 doi:10.1038/nclimate2258.

Kerfoot W.C., Harting S., Rossmann R, Robbins J.A. (1999) Anthropogenic copper inventories and mercury profiles from Lake Superior: Evidence for mining impacts. *Journal of Great Lakes Research* **25**: 663-682.

Kerfoot W.C., Harting S.L., Jeong J., Robbins J.A, Rossmann R (2004) Local, regional, and global implications of elemental mercury in metal (copper, silver, gold, and zinc) ores: Insights from Lake Superior sediments. *Journal of Great Lakes Research* **30**: 162-184.

Kirchner WB, Dillon PJ (1975) Empirical Method of Estimating Retention of Phosphorus in Lakes. *Water Resources Research* **11**: 182-183.

Klovan JE, Imbrie J (1971) An algorithm and FORTRAN-IV program for large-scale Q-mode factor analysis and calculation of factor scores. *Mathematical Geology* **3**: 61–77.

Knox JC (2000) Sensitivity of modern and Holocene floods to climate change. *Quaternary Science Reviews* **19**: 439–457.

Koinig KA, Shotyk W, Ohlendorf C, Sturm M (2003) 9000 years of geochemical evolution of lithogenic major and trace elements in the sediment of an alpine lake – the role of climate , vegetation , and land-use history. *Journal of Paleolimnology* **4**: 307–320.

Komar PD, Baba J, Cui B (1984) Grain-size analyses of mica within sediments and the hydraulic equivalence of mica and quartz. *Journal of Sedimentary Research* **54**: 1379–1391.

Komar PD, Miller C (1975) The initiation of oscillatory ripple marks and the development of plane-bed at high shear stressed under waves. *Journal of Sedimentary Research* **45**: 697–703.

Komar PD, Reimers CE (1978) Grain shape effects on settling rates. *Journal of Geology* **86**: 193–209.

Krantzberg G (1985) The influence of bioturbation on physical, chemical and biological parameters in aquatic environments: a review. *Environmental Pollution (Series A)* **39**: 99–122.

Kulbe T, Livingstone DM, Guilizzoni P, Sturm M (2008) The use of long-term, high-frequency, automatic sampling data in a comparative study of the hypolimnia of two dissimilar Alpine lakes. *Verhandlungen des Internationalen Vereinigung für theoretische und angewandte Limnologie* **30**: 371–376.

Kylander ME, Ampel L, Wohlfarth B, Veres D (2011) High-resolution X-ray fluorescence core scanning analysis of Les Echets (France) sedimentary sequence: new insights from chemical proxies. *Journal of Quaternary Science* **26**: 109–117 doi:10.1002/jqs.1438.

Kylander ME, Klaminder J, Wohlfarth B, Löwemark L (2013) Geochemical responses to paleoclimatic changes in southern Sweden since the late glacial: the Hässeldala Port lake sediment record. *Journal of Paleolimnology* **50**: 57–70 doi:10.1007/s10933-013-9704-z.

Kylander ME, Lind EM, Wastegard S, Lowemark L (2012) Recommendations for using XRF core scanning as a tool in tephrochronology. *The Holocene* **22**: 371–375 doi:10.1177/0959683611423688.

Lamb HH (1977) Climate: Past, Present, Future (Metheun, London).

Lambert A, Giovanoli F (1988) Records of riverborne turbidity currents and indications of slope failures in the Rhone delta of Lake Geneva. *Limnology and Oceanography* **33**: 458–468.

Langdon PG, Barber KE, Lomas-Clarke (previously Morriss) SH (2004) Reconstructing climate and environmental change in northern England through chironomid and pollen analyses : evidence from Talkin Tarn , Cumbria. *Journal of Paleolimnology* **32**: 197–213.

Lapointe F, Francus P, Lamoureux SF, Saïd M, Cuven S (2012) 1750 years of large rainfall events inferred from particle size at East Lake, Cape Bounty, Melville Island, Canada. *Journal of Paleolimnology* **48**: 159–173 doi:10.1007/s10933-012-9611-8.

Larsen CES, Macdonald GM (1993) Lake morphometry, sediment mixing and the selection of sites for fine resolution palaeoecological studies. *Quaternary Science Reviews* **12**: 781–792.

Last WM, Smol JP (2001) Tracking Environmental Change using lake sediments Volume 2: Physical and geochemical methods (Kluwer Academic Publishers, The Netherlands).

Lauterbach S, Brauer A, Andersen N, Danielopol DL, Dulski P, Hüls M, Milecka K, Namiotko T, Obremska M, Von Grafenstein U (2011) Environmental responses to Lateglacial climatic fluctuations recorded in the sediments of pre-Alpine Lake Mondsee (northeastern Alps). *Journal of Quaternary Science* **26**: 253–267 doi:10.1002/jqs.1448.

Lauterbach S, Chapron E, Brauer A, Huls M, Gilli A, Arnaud F, Piccin A, Nomade J, Desmet M, von Grafenstein U, Participants D (2012) A sedimentary record of Holocene surface runoff events and earthquake activity from Lake Iseo (Southern Alps, Italy). *The Holocene* **22**: 749–760 doi:10.1177/0959683611430340.

Lavers DA, Allan RP, Wood EF, Villarini G, Brayshaw DJ, Wade AJ (2011) Winter floods in Britain are connected to atmospheric rivers. *Geophysical Research Letters* **38**: L23803 doi:10.1029/2011GL049783.

Lean HW, Browning KA (2013) Quantification of the importance of wind drift to the surface distribution of orographic rain on the occasion of the extreme Cockermouth flood in Cumbria. *Quarterly Journal of the Royal Meteorological Society* **139**: 1342–1353 doi:10.1002/qj.2024.

Leermakers M., Baeyens W., Quevauviller P, Horvat M. (2005) Mercury in environmental samples: Speciation, artifacts and validation. *TrAC Trends in Analytical Chemistry* **24**: 383-393.

Lemmin U, Mortimer CH, Ba E (2005) Internal seiche dynamics in Lake Geneva. *Limnology and Oceanography* **50**: 207–216.

Leng MJ, Marshall JD (2004) Palaeoclimate interpretation of stable isotope data from lake sediment archives. *Quaternary Science Reviews* **23**: 811–831 doi:10.1016/j.quascirev.2003.06.012.

Lenzi MA, Marchi L (2000) Suspended sediment load during floods in a small stream of the Dolomites (northeastern Italy). *Catena* **39**: 267–282.

Lewis T, Francus P, Bradley RS (2009) Recent occurrence of large jökulhlaups at Lake Tuborg, Ellesmere Island, Nunavut. *Journal of Paleolimnology* **41**: 491–506 doi:10.1007/s10933-008-9240-4.

Lewis T, Lamoureux SF (2010) Twenty-first century discharge and sediment yield predictions in a small high Arctic watershed. *Global and Planetary Change* **71**: 27–41 doi:10.1016/j.gloplacha.2009.12.006.

Li H.O.L., Guo Y.P, Chang J.S. (2012) Toxic Element Analyses of Summer and Winter Storm-Water Sediment by Neutron Activation Analyses. *Journal of Environmental Engineering* **138**: 588-593.

Li Y, Guo Y, Yu G (2013) An analysis of extreme flood events during the past 400 years at Taihu Lake, China. *Journal of Hydrology* **500**: 217–225 doi:10.1016/j.jhydrol.2013.02.028.

Lindeberg C., Bindler R., Renberg I., Emteryd O., Karlsson E, Anderson N.J.(2006) Natural fluctuations of mercury and lead in Greenland Lake sediments. *Environmental Science & Technology* **40**: 90-95.

Liu X, Colman SM, Brown ET, Minor EC, Li H (2013) Estimation of carbonate, total organic carbon, and biogenic silica content by FTIR and XRF techniques in lacustrine sediments. *Journal of Paleolimnology* **50**: 387–398 doi:10.1007/s10933-013-9733-7.

Lockhart W.L., Macdonald R.W., Outridge P.M., Wilkinson P., DeLaronde J.B, Rudd J.W.M. (2000) Tests of the fidelity of lake sediment core records of mercury deposition to known histories of mercury contamination. *Science of the Total Environment* **260**: 171-180.

Loizeau J-L, Girardclos S, Dominik J (2012) Taux d'accumulation de sédiments récents et bilan de la matière particulaire dans le Léman (Suisse-France). *Archives des Sciences* **65**: 81–92.

Lowe JJ, Walker MJC (1997) Reconstructing Quaternary Environments (Addison Wesley Longman Ltd, Essex).

Löwemark L, Chen H-F, Yang T-N, Kylander M, Yu E-F, Hsu Y-W, Lee T-Q, Song S-R, Jarvis S (2011) Normalizing XRF-scanner data: A cautionary note on the interpretation of high-resolution records from organic-rich lakes. *Journal of Asian Earth Sciences* **40**: 1250–1256 doi:10.1016/j.jseaes.2010.06.002.

Ma J., Hintelmann H., Kirk J.L, Muir D.C.G. (2013) Mercury concentrations and mercury isotope composition in lake sediment cores from the vicinity of a metal smelting facility in Flin Flon, Manitoba. *Chemical Geology* **336**: 96-102.

Maas GS, Macklin MG (2002) The impact of recent climate change on flooding and sediment supply within a Mediterranean mountain catchment, southwestern Crete, Greece. *Earth Surface Processes and Landforms* **27**: 1087–1105 doi:10.1002/esp.398.

Maberly S, De Ville M, Thackeray S, Feuchtmayr H, Fletcher JM, James JB, Kelly JL, Vincent CD, Winfield IJ, Newton A, Atkinson D, Croft A, Drew H, Saag M, Taylor S, Titterington H (2011) A survey of the lakes of the English Lake District: The Lakes Tour 2010.

Macdonald N (2006) An underutilized resource: historical flood chronologies. A valuable resource in determining periods of hydro-geomorphic change. *IAHS/ICCE International Symposium on Sediment Dynamics and the Hydromorphology of Fluvial Systems [IAHS Red Book]* **306**: 120–127.

Macdonald N (2007) Epigraphic records: a valuable resource in reassessing flood risk and long-term climate variability. *Environmental History* **12**: 136–140.

Macdonald N (2012) Trends in flood seasonality of the River Ouse (Northern England) from archive and instrumental sources since AD 1600. *Climatic Change* **110**: 901–923 doi:10.1007/s10584-011-0117-6.

Macdonald N (2014) Millennial scale variability in high magnitude flooding across Britain. *Hydrology and Earth System Sciences Discussions* **11**: 10157–10178 doi:10.5194/hessd-11-10157-2014.

Macdonald N, Black AR (2010) Reassessment of flood frequency using historical information for the River Ouse at York, UK (1200–2000). *Hydrological Sciences Journal* **55**: 1152–1162 doi:10.1080/02626667.2010.508873.

Macdonald N, Werritty A, Black A R, McEwen LJ (2006) Historical and pooled flood frequency analysis for the River Tay at Perth, Scotland. *Area* **38**: 34–46 doi:10.1111/j.1475-4762.2006.00673.x.

Mackereth FJH (1966) Some chemical observations on post-glacial lake sediments. *Philisophical Transactions of The Royal Society B: Biological Sciences* **250**: 165–213.

Macklin MG, Lewin J, Jones A (2014) Anthropogenic alluvium: An evidence-based meta-analysis for the UK Holocene. *Anthropocene* doi:10.1016/j.ancene.2014.03.003.

Macklin MG, Rumsby BT (2007) Changing climate and extreme floods in the British uplands. *Transactions of the Institute of British Geographers* **NS32**: 168–186.

Macklin MG, Rumsby BT, Heap T (1992) Flood alluviation and entrenchment: Holocene valley-floor development and transformation in the British uplands. *Geological Society of America Bulletin* **104**: 631–643.

Mader D, Koeberl C. (2009) Using Instrumental Neutron Activation Analysis for geochemical analyses of terrestrial impact structures: Current analytical procedures at the University of Vienna Geochemistry Activation Analysis Laboratory. *Applied Radiation and Isotopes* **67**: 2100-2103.

Malby A, Whyatt JD, Timmis RJ, Wilby RL, Orr HG (2007) Long-term variations in orographic rainfall: analysis and implications for upland catchments. *Hydrological Sciences Journal* **52**: 276–291 doi:10.1623/hysj.52.2.276.

Manhes G., Allegre C.J., Provost A. (1984) U-Th-Pb Systematics of the Eucrite Juvinas - Precise Age-Determination and Evidence for Exotic Lead. *Geochimica Cosmochimica Acta* **48**: 2247-2264.

Marsh T, Hannaford J (2007) The Summer 2007 floods in England and Wales - a hydrological appraisal. Environment Agency Report, Project SC070039/S1.

Marsh TJ (2001) The 2000/01 floods in the UK - a brief overview. *Weather* **56**: 343–345.

Marshall M, Schlolaut G, Nakagawa T, Lamb H, Brauer A, Staff R, Ramsey CB, Tarasov P, Gotanda K, Haraguchi T, Yokoyama Y, Yonenobu H, Tada R (2012) A novel approach to varve counting using μXRF and X-radiography in combination with thin-section microscopy, applied to the Late Glacial chronology from Lake Suigetsu, Japan. *Quaternary Geochronology* **13**: 70–80 doi:10.1016/j.quageo.2012.06.002.

Marshall WA, Gehrels WR, Garnett MH, Freeman SPHT, Maden C, Xu S (2007) The use of "bomb spike" calibration and high-precision AMS 14C analyses to date salt-marsh sediments deposited during the past three centuries. *Quaternary Research* **68**: 325–337 doi:10.1016/j.yqres.2007.07.005.

Martin J, Meybeck M (1979) Elemental mass-balance of material carried by major world rivers. *Marine Chemistry* **7**: 173–206.

Martínez Cortizas A, López-Merino L, Bindler R, Mighall T, Kylander M (2013) Atmospheric Pb pollution in N Iberia during the late Iron Age/Roman times reconstructed using the high-resolution record of La Molina mire (Asturias, Spain). *Journal of Paleolimnology* **50**: 71–86 doi:10.1007/s10933-013-9705-y.

Matsapaeva I.V., Osinskaya N.S, Danilova E.A. (2010) Concentrations of heavy metals in bottom sediments of Lake Dautkul as an indicator of anthropogenic impact in the area south of the Aral Sea. *Water Resources* **37**: 586-590.

Mayes J (1996) Spatial and temporal fluctuations of monthly rainfall in the British Isles and variations in the mid-latitude westerly circulation. *International Journal of Climatology* **16**: 585–596.

Mayes WM, Potter HAB, Jarvis AP (2010) Inventory of aquatic contaminant flux arising from historical metal mining in England and Wales. *The Science of the Total Environment* **408**: 3576–3583 doi:10.1016/j.scitotenv.2010.04.021.

Mcewen LJ (1989) Extreme rainfall and its implications for flood frequency: a case study of the middle River Tweed basin, Scotland. *Transactions of the Institute of British Geographers* **14**: 287–298.

McEwen LJ (1990) The establishment of a historical flood chronology for the River Tweed catchment, Berwickshire, Scotland. *Scottish Geographical Magazine* **106**: 37–48 doi:10.1080/00369229018736773.

McEwen LJ (2006) Flood seasonality and generating conditions in the Tay catchment, Scotland from 1200 to present. *Area* **38**: 47–64 doi:10.1111/j.1475-4762.2006.00659.x.

Meybeck M, Vörösmarty C (2005) Fluvial filtering of land-to-ocean fluxes: from natural Holocene variations to Anthropocene. *Comptes Rendus Geoscience* **337**: 107–123 doi:10.1016/j.crte.2004.09.016.

Meyers PA, Ishiwatari R (1993) Lacustrine organic geochemistry - an overview of indicators of organic matter sources and diagenesis in lake sediments. *Organic Geochemistry* **20**: 867–900.

Migeon S, Mulder T, Savoye B, Sage F (2012) Hydrodynamic processes, velocity structure and stratification in natural turbidity currents: Results inferred from field data in the Var Turbidite System. *Sedimentary Geology* **245-246**: 48–62 doi:10.1016/j.sedgeo.2011.12.007.

Mighall TM, Abrahams PW, Grattan JP, Hayes D, Timberlake S, Forsyth S (2002) Geochemical evidence for atmospheric pollution derived from prehistoric copper mining at Copa Hill, Cwmystwyth, mid-Wales, UK. *The Science of the total environment* **292**: 69–80.

Miller H, Bull JM, Cotterill CJ, Dix JK, Winfield IJ, Kemp AES, Pearce RB (2013a) Lake bed geomorphology and sedimentary processes in glacial lake Windermere, UK. *Journal of Maps* **9**: 299–312 doi:10.1080/17445647.2013.780986.

Miller H, Croudace IW, Bull JM, Cotterill CJ, Dix JK, Taylor RN (2014) A 500 year sediment lake record of anthropogenic and natural inputs to Windermere (English Lake District) using double-spike lead isotopes, radiochronology, and sediment microanalysis. *Environmental Science & Technology* **48**: 7254–7263 doi:10.1021/es5008998.

Miller JD, Kjeldsen TR, Hannaford J, Morris DG (2013b) A hydrological assessment of the November 2009 floods in Cumbria, UK. *Hydrology Research* **44**: 180–197 doi:10.2166/nh.2012.076.

Milly PCD, Wetherald RT, Dunne K a, Delworth TL (2002) Increasing risk of great floods in a changing climate. *Nature* **415**: 514–517 doi:10.1038/415514a.

Min S-K, Zhang X, Zwiers FW, Hegerl GC (2011) Human contribution to more-intense precipitation extremes. *Nature* **470**: 378–381 doi:10.1038/nature09763.

Mingram J, Negendank JFW, Brauer A, Berger D, Hendrich A, Köhler M, Usinger H (2006) Long cores from small lakes—recovering up to 100 m-long lake sediment sequences with a high-precision rod-operated piston corer (Usinger-corer). *Journal of Paleolimnology* **37**: 517–528 doi:10.1007/s10933-006-9035-4.

Monsen NE, Cloern JE, Lucas L V, Monismith SG (2002) A comment on the use of flushing time, residence time, and age as transport time scales. *Limnology and oceanography* **47**: 1545–1553.

Moreno A, Valero-Garcés BL, González-Sampériz P, Rico M (2008) Flood response to rainfall variability during the last 2000 years inferred from the Taravilla Lake record (Central Iberian Range, Spain). *Journal of Paleolimnology* **40**: 943–961 doi:10.1007/s10933-008-9209-3.

Mudelsee M (2006) CLIM-X-DETECT: A Fortran 90 program for robust detection of extremes against a time-dependent background in climate records. *Computers & Geosciences* **32**: 141–144.

Muir D.C.G., Rose N.L.(2004) Lake sediments as records of arctic and Antarctic pollution. In: R. Pienitz, M. S. V. Douglas and J. P. Smol (eds.), Long-term Environmental Change in Arctic and Antarctic Lakes. Springer, Netherlands, pp. 209-239.

Mulder T, Alexander J (2001) The physical character of subaqueous sedimentary density flows and their deposits. *Sedimentology* **48**: 269–299.

Mulder T, Migeon S, Savoye B, Faugères J (2001) Inversely graded turbidite sequences in the deep Mediterranean: a record of deposits from flood-generated turbidity currents? *Geo-Marine Letters* **21**: 86–93 doi:10.1007/s003670100071.

Mulder T, Syvitski JPM (1995) Turbidity Currents Generated at River Mouths during Exceptional Discharges to the World Oceans. *Journal of Geology* **103**: 285–299.

Mulder T, Syvitski JPM, Migeon S, Faugères J-C, Savoye B (2003) Marine hyperpycnal flows: initiation, behavior and related deposits. A review. *Marine and Petroleum Geology* **20**: 861–882 doi:10.1016/j.marpetgeo.2003.01.003.

Müller G. (1979) Schwermetalle in den Sedimenten des Rheins-Veränderungen seit. *Umschav* **79**: 133-149.

Murray J, Pullar L (1910) Lochs of the Tweed Basin. In Bathymetrical Survey of the Fresh-Water Lochs of Scotland, 1897-1909 Volume II, pp. 134–140.

Nahm W-H, Lee GH, Yang D-Y, Kim J-Y, Kashiwaya K, Yamamoto M, Sakaguchi A (2010) A 60-year record of rainfall from the sediments of Jinheung Pond, Jeongeup, Korea. *Journal of Paleolimnology* **43**: 489–498 doi:10.1007/s10933-009-9345-4.

Natural Environmental Research Council (Institute of Hydrology) (1975) Flood Studies Report (NERC, London).

Negi B.S., Meenakshy V, Krishnamoorthy T.M. (1997) K-o method of quantification in neutron activation analysis as applied to environmental samples. *Environmental Monitoring and Assessment* **47**: 303-313.

Nesje A, Dahl SO, Matthews JA, Berrisford MS (2001) A ~ 4500-yr record of river floods obtained from a sediment core in Lake Atnsjøen, eastern Norway. *Journal of Paleolimnology* **25**: 329–342.

Noren AJ, Bierman PR, Steig EJ, Lini A, Southon J (2002) Millennial-scale storminess variability in the northeastern United States during the Holocene epoch. *Nature* **419**: 821–824 doi:10.1038/nature01132.

Normark WR, Piper DJW (1991) Initiation processes and flow evolution of turbidity currents: implications for the depositional record. *SEPM Special Publication* **46**: 207–230.

Norrman J (1964) Lake Vättern. Investigations on shore and bottom morphology. *Geografiska Annaler* **1-2**: 1–238.

Norton S.A., Kahl J.S. (1987) A comparion of lake sediments and ombrotrophic peat deposits as long term monitors of atmopsheric pollution. In: T. P. Boyle (ed.), New Approaches to Monitoring Aquatic Ecosystems. American Society for Testing Materials, Philadelphia, pp. 40-57.

Nuttall CA, Younger PL (1999) Reconnaissance hydrogeochemical evaluation of an abandoned Pb - Zn orefield, Nent Valley, Cumbria, UK. *Proceedings of the Yorkshire Geological Society* **52**: 395–405 doi:10.1144/pygs.52.4.395.

Ochsenbein U., Davison W., Hilton J., Haworth E.Y. (1983) The Geochemical Record of Major Cations and Trace-Metals in a Productive Lake - Analysis of Thinly Sliced Sediment Samples Characterized by Diatom Stratigraphy. *Archiv für Hydrobiologie* **98**: 463-488.

Ohlendorf C, Sturm M (2001) Precipitation and dissolution of calcite in a Swiss High Alpine Lake. *Arctic, Antarctic, and Alpine Research* **33**: 410–417.

Ojala AEK, Francus P, Zolitschka B, Besonen M, Lamoureux SF (2012) Characteristics of sedimentary varve chronologies – A review. *Quaternary Science Reviews* **43**: 45–60 doi:10.1016/j.quascirev.2012.04.006.

Olariu C, Bhattacharya JP (2006) Terminal distributary channels and delta front architecture of river-dominated delta systems. *Journal of Sedimentary Research* **76**: 212–233 doi:10.2110/jsr.2006.026.

Olariu C, Bhattacharya JP, Leybourne MI, Boss SK, Stern RJ (2012) Interplay between river discharge and topography of the basin floor in a hyperpycnal lacustrine delta. *Sedimentology* **59**: 704–728 doi:10.1111/j.1365-3091.2011.01272.x.

Oldfield F (2005) Environmental Change: Key Issues and Alternative Approaches (Cambridge University Press, UK).

Oldfield F (2014) Can the magnetic signatures from inorganic fly ash be used to mark the onset of the Anthropocene? *The Anthropocene Review* doi:10.1177/2053019614534402.

Oldfield F, Appleby PG, Battarbee RW (1978) Alternative 210Pb dating: results from the New Guinea Highlands and Lough Erne. *Nature* **271**: 339–342.

Oldfield F, Wake R, Boyle J, Jones R, Nolan S, Gibbs Z, Appleby P, Fisher E, Wolff G (2003) The late-Holocene history of Gormire Lake (NE England) and its catchment: a multiproxy reconstruction of past human impact. *The Holocene* **13**: 677–690 doi:10.1191/0959683603hl654rp.

Oldfield F, Wu R (2000) The magnetic properties of the recent sediments of Brothers Water , N W England. *Journal of Paleolimnology* **23**: 165–174.

Ordnance Survey (1899) County Sheet Westmorland, 6 inch (2nd Edition).

Orpin A, Carter L, Page MJ, Cochran U a., Trustrum N, Gomez B, Palmer AS, Mildenhall DC, Rogers KM, Brackley HL, Northcote L (2010) Holocene sedimentary record from Lake Tutira: A template for upland watershed erosion proximal to the Waipaoa Sedimentary System, northeastern New Zealand. *Marine Geology* **270**: 11–29 doi:10.1016/j.margeo.2009.10.022.

Orr HG, Carling PA (2006) Hydro-climatic and land use changes in the River Lune catchment, northwest England: implications for catchment management. *River Resources Applications* **22**: 239–255.

Orton GJ, Reading HG (1993) Variability of deltaic processes in terms of sediment supply , with particular emphasis on grain size. *Sedimentology* **40**: 475–512.

Orwin, JF, Lamoureux, SF, Warburton, J, Beylich, A (2010) A framework for characterizing fluvial sediment fluxes from source to sink in cold environments. *Geografiska Annaler: Series A, Physical Geography* **92 A:** 155–176.

Osleger DA, Heyvaert AC, Stoner JS, Verosub KL (2009) Lacustrine turbidites as indicators of Holocene storminess and climate: Lake Tahoe, California and Nevada. *Journal of Paleolimnology* **42**: 103–122 doi:10.1007/s10933-008-9265-8.

Page MJ, Trustrum N a., Orpin a. R, Carter L, Gomez B, Cochran U a., Mildenhall DC, Rogers KM, Brackley HL, Palmer a. S, Northcote L (2010) Storm frequency and magnitude in response to Holocene climate variability, Lake Tutira, North-Eastern New Zealand. *Marine Geology* **270**: 30–44 doi:10.1016/j.margeo.2009.10.019.

Pall P, Aina T, Stone D a, Stott P a, Nozawa T, Hilberts AGJ, Lohmann D, Allen MR (2011) Anthropogenic greenhouse gas contribution to flood risk in England and Wales in autumn 2000. *Nature* **470**: 382–385 doi:10.1038/nature09762.

Parris AS, Bierman PR, Noren AJ, Prins MA, Lini A (2010) Holocene paleostorms identified by particle size signatures in lake sediments from the northeastern United States. *Journal of Paleolimnology* **43**: 29–49 doi:10.1007/s10933-009-9311-1.

Parviainen A., Kauppila T, Loukola-Ruskeeniemi K. (2012) Long-term lake sediment records and factors affecting the evolution of metal(loid) drainage from two mine sites (SW Finland). *Journal of Geochemical Exploration* **114**: 46-56.

Passega R (1964) Grain size representation by CM patterns as a geological tool. *SEPM Journal of Sedimentary Research* **34**: 830–847 doi:10.1306/74D711A4-2B21-11D7-8648000102C1865D.

Pattison I, Lane SN (2012) The relationship between Lamb weather types and long-term changes in flood frequency, River Eden, UK. *International Journal of Climatology* **32**: 1971–1989 doi:10.1002/joc.2415.

Peinerud EK (2000) Interpretation of Si concentrations in lake sediments: three case studies. *Environmental Geology* **40**: 64–72.

Peña-Icart M., Tagle M.E.V., Alonso-Hernández C., Hernández J.R., Behar M., Alfonso M.S.P. (2011) Comparative study of digestion methods EPA 3050B (HNO3-H2O2-HCl) and ISO 11466.3 (aqua regia) for Cu, Ni and Pb contamination assessment in marine sediments. *Marine Environmental Research* **72**: 60-66.

Pennington W (1997) Vegetation history of the Lake District. In Flora of Cumbria Comprising the Vice-Counties of Westmoreland with Barrow-in-Furness, G. Halliday, ed. (Lancaster University Press, Lancaster), pp. 20–35.

Pennington WTG (1981) Records of a lake's life in time: the sediments. *Hydrobiologia* **79**: 197–219.

Pennington WTG (1991) Palaeolimnology in the English Lakes - some questions and answers over fifty years. *Hydrobiologia* **214**: 9–24.

Pennington WTG, Lishman JP (1984) The post-glacial sediments of Blelham Tarn: geochemistry and palaeoecology. *Archaeology Hydrobiology Supplement* **69**: 1–54.

Pomar L, Morsilli M, Hallock P, Bádenas B (2012) Internal waves, an under-explored source of turbulence events in the sedimentary record. *Earth-Science Reviews* **111**: 56–81 doi:10.1016/j.earscirev.2011.12.005.

Prieto MDR, García Herrera R (2009) Documentary sources from South America: Potential for climate reconstruction. *Palaeogeography, Palaeoclimatology, Palaeoecology* **281**: 196–209 doi:10.1016/j.palaeo.2008.07.026.

Proctor C, Baker A, Barnes W (2002) A three thousand year record of North Atlantic climate. *Climate Dynamics* **19**: 449–454 doi:10.1007/s00382-002-0236-x.

Punning J.M., Boyle J.F., Alliksaar T., Tann R., Varvas M. (1997) Human impact on the history of Lake Nommejarv, NE Estonia: A geochemical and palaeobotanical study. *Holocene* **7**: 91-99.

Pyrce RS (2004) Review and Analysis of Stream Gauge Networks for the Ontario Stream Gauge Rehabilitation Project (Peterborough).

Rae J, Parker A (1993) Sources, solid-phase transport and geochemical associations of Co and Cu in a small upland catchment, English Lake District. *Applied Geochemistry* **2**: 263–268.

Rae J, Parker A (1996) Techniques for validating the historic record of lake Sediments. A demonstration of their use in the English Lake District. *Applied Geochemistry* **11**: 211–215.

Raubitschek S, Lücke A, Schleser GH (1999) Sedimentation patterns of diatoms in Lake Holzmaar, Germany - (on the transfer of climate signals to biogenic silica oxygen isotope proxies). *Journal of Paleolimnology* **21**: 437–448.

Rauch S., Hemond H.F, Brabander D.J. (2006) High spatial resolution analysis of lake sediment cores by laser ablation-inductively coupled plasma-mass spectrometry (LA-ICP-MS). *Limnology and Oceanography Methods* **4**: 268-274.

Reimer PJ, Bard E, Bayliss A, Beck JW, Blackwell PG, Bronk C, Caitlin R, Hai EB, Edwards RL (2013) Intcal13 and Marine13 radiocarbon age calibration curves 0 – 50,000 years cal BP. *Radiocarbon* **55**: 1869–1887.

Reinwarth B, Franz S, Baade J, Haberzettl T, Kasper T, Daut G, Helmschrot J, Kirsten KL, Quick LJ, Meadows ME, Mäusbacher R (2013) A 700-year record on the effects of climate and human impact on the southern Cape coast inferred from lake sediments of Eilandvlei, Wilderness Embayment, South Africa. *Geografiska Annaler: Series A, Physical Geography* **95**: 345–360 doi:10.1111/geoa.12015.

Renberg I. (1986) Concentration and Annual Accumulation Values of Heavy-Metals in Lake-Sediments - Their Significance in Studies of the History of Heavy-Metal Pollution. *Hydrobiologia* **143**: 379-385.

Renberg I, Bindler R, Brännvall M-L (2001) Using the historical atmospheric lead-desposition record as a chronological marker in sediment deposits in Europe. *The Holocene* **11**: 511–516 doi:10.1191/095968301680223468.

Renberg I., Brännvall M.L., Bindler R, Emteryd O. (2002) Stable lead isotopes and lake sediments - a useful combination for the study of atmospheric lead pollution history. *Science Total Environment* **292**: 45-54.

Renberg I, Persson MW, Emteryd O (1994) Pre-industrial atmopsheric lead contamination detected in Swedish lake sediments. *Nature* **368**: 323–326.

Richter TO, van der Gaast S, Koster B, Vaars a., Gieles R, de Stigter HC, De Haas H, van Weering TCE (2006) The Avaatech XRF Core Scanner: technical description and applications to NE Atlantic sediments. *Geological Society, London, Special Publications* **267**: 39–50 doi:10.1144/GSL.SP.2006.267.01.03.

Rippey B, Douglas RW (2004) Reconstructing regional-scale lead contamination of the atmosphere (1850-1980) in the United Kingdom and Ireland using lake sediments. *Global Biogeochemical Cycles* **18**: n/a – n/a doi:10.1029/2004GB002305.

Rippey B (2010) A model for the concentration of lead and polychlorinated biphenyls in lake sediment. *Journal of Paleolimnology* **43**: 565-576.

Roberson S, Weltje GJ (2014) Inter-instrument comparison of particle-size analysers. *Sedimentology* **61**: 1157–1174 doi:10.1111/sed.12093.

Robson AJ (2002) Evidence for trends in UK flooding. *Philosophical Transactions of The Royal Society A: Mathematical, Physical and Engineering Sciences* **360**: 1327–1343 doi:10.1098/rsta.2002.1003.

Rodbell DT, Seltzer GO, Anderson DM, Abbott MB, Enfield DB, Newman JH (1999) An 15,000-Year Record of El Niño-Driven Alluviation in Southwestern Ecuador. *Science* **283**: 516–520 doi:10.1126/science.283.5401.516.

Rodríguez-Barroso M.R., García-Morales J.L., Ramírez-del Solar M., Blanco E, Quiroga J.M. (2010) Thermal Analysis as a First Screening Method to Evaluate Potential Contamination. *Water Air and Soil Pollution* **208**: 173-182.

Rodríguez-Barroso M.R., Solar M.R.D., Blanco E., Quiroga J.M, García-Morales J.L. (2008) Qualitative estimation of heavy metals in marine sediment using thermal analysis. *Soil and Sediment Contamination* **17**: 107-120.

Rodwell MJ, Rowell DP, Folland CK (1999) Oceanic forcing of the wintertime North Atlantic Oscillation and European climate. *Nature* **398**: 320–323.

Roop HA, Dunbar GB, Levy R, Vandergoes MJ, Forrest AL, Walker SL, Purdie J, Upton P, Whinney J (2014) Seasonal controls on sediment transport and deposition in Lake Ohau, South Island, New Zealand: Implications for a high-resolution Holocene palaeoclimate reconstruction. *Sedimentology* n/a – n/a doi:10.1111/sed.12162.

Rose N.L., Boyle J.F., Du Y., Yi C., Dai X., Appleby P.G., Bennion H., Cai S, Yu L. (2004) Sedimentary evidence for changes in the pollution status of Taihu in the Jiangsu region of eastern China. *Journal of Paleolimnology* **32**: 41-51.

Rose NL, Appleby PG (2005) Regional Applications of Lake Sediment Dating by Spheroidal Carbonaceous Particle Analysis I: United Kingdom. *Journal of Paleolimnology* **34**: 349–361 doi:10.1007/s10933-005-4925-4.

Rose NL, Harlock S, Appleby PG (1999) The spatial and temporal distributions of spheroidal carbonaceous fly-ash particles (SCP) in the sediment records of european mountain lakes. *Water, Air, & Soil Pollution* **113**: 1–32.

Rose N.L., Yang H.D., Turner S.D, Simpson G.L. (2012) An assessment of the mechanisms for the transfer of lead and mercury from atmospherically contaminated organic soils to lake sediments with particular reference to Scotland, UK. *Geochimica Cosmochimica Acta* **82**: 113-135.

Rowan D.J., Cornett R.J., King K., Risto B. (1995a) Sediment Focusing and Pb-210 Dating - a New Approach. *Journal of Paleolimnology* **13**: 107-118.

Rowan D.J., Kalff J, Rasmussen J.B. 1992. Profundal Sediment Organic Content and Physical Character Do Not Reflect Lake Trophic Status, but Rather Reflect Inorganic Sedimentation and Exposure. *Canadian Journal of Fisheries and Aquatic Science* **49**: 1431-1438.

Rowan D.J., Rasmussen J.B, Kalff J. (1995b) Optimal allocation of sampling effort in lake sediment studies. *Canadian Journal of Fisheries and Aquatic Science* **52**: 2146-2158.

Rubey WW (1933) Settling velocities of gravel, sand and silt particles. *American Journal of Science* **25**: 325–338.

Rumsby BT (1991) Flood frequency and magnitude estimates based on valley flood morphology and floodplain sedimentary sequences. University of Newcastle-upon-Tyne.

Saitoh Y, Masuda F (2013) Spatial Change of Grading Pattern of Subaqueous Flood Deposits In Lake Shinji, Japan. *Journal of Sedimentary Research* **83**: 221–233 doi:10.2110/jsr.2013.14.

Salonen V.P., Tuovinen N, Valpola S. (2006) History of mine drainage impact on Lake Orijarvi algal communities, SW Finland. *Journal of Paleolimnology* **35**: 289-303.

Sastre V, Loizeau J-L, Greinert J, Naudts L, Arpagaus P, Anselmetti F, Wildi W (2010) Morphology and recent history of the Rhone River Delta in Lake Geneva (Switzerland). *Swiss Journal of Geosciences* **103**: 33–42 doi:10.1007/s00015-010-0006-4.

Sayer CD, Hoare DJ, Simpson GL, Henderson ACG, Liptrot ER, Jackson MJ, Appleby PG, Boyle JF, Jones II, Waldock MJ (2006) TBT causes regime shift in shallow lakes. *Environmental Science & Technology* **40**: 5269–5275.

Schiefer E (2006) Contemporary sedimentation rates and depositional structures in a montane lake basin, southern Coast Mountains, British Columbia, Canada. *Earth Surface Processes and Landforms* **31**: 1311–1324 doi:10.1002/esp.

Schiefer E, Gilbert R, Hassan MA (2011) A lake sediment-based proxy of floods in the Rocky Mountain Front Ranges, Canada. *Journal of Paleolimnology* **45**: 137–149 doi:10.1007/s10933-010-9485-6.

Schiefer E, Menounos B, Slaymaker O (2006) Extreme sediment delivery events recorded in the contemporary sediment record of a montane lake, southern Coast Mountains, British Columbia. *Canadian Journal of Earth Science* **43**: 1777–1790 doi:10.1139/E06-056.

Schillereff DN, Chiverrell RC, Macdonald N, Hooke JM (2014) Flood stratigraphies in lake sediments: A review. *Earth-Science Reviews* **135**: 17–37 doi:10.1016/j.earscirev.2014.03.011.

Schlolaut G, Brauer A, Marshall MH, Nakagawa T, Staff RA, Bronk Ramsey C, Lamb HF, Bryant CL, Naumann R, Dulski P, Brock F, Yokoyama Y, Tada R, Haraguchi T (2014) Event layers in the Japanese Lake Suigetsu "SG06" sediment core: description, interpretation and climatic implications. *Quaternary Science Reviews* **83**: 157–170 doi:10.1016/j.quascirev.2013.10.026.

Schmocker-Fackel P, Naef F (2010a) Changes in flood frequencies in Switzerland since 1500. *Hydrology and Earth System Sciences* **14**: 1581–1594 doi:10.5194/hess-14-1581-2010.

Schmocker-Fackel P, Naef F (2010b) More frequent flooding? Changes in flood frequency in Switzerland since 1850. *Journal of Hydrology* **381**: 1–8 doi:10.1016/j.jhydrol.2009.09.022.

Schnellmann M, Anselmetti FS, Giardini D, McKenzie JA, Ward SN (2002) Prehistoric earthquake history revealed by lacustrine slump deposits. *Geology* **30**: 1131–1134 doi:10.1130/0091-7613(2002)030<1131:PEHRBL>2.0.CO;2.

Schottler SP, Engstrom DR (2006) A chronological assessment of Lake Okeechobee (Florida) sediments using multiple dating markers. *Journal of Paleolimnology* **36**: 19–36 doi:10.1007/s10933-006-0007-5.

Schultze E, Niederreiter R (1990) Palaolimnologische Untersuchungen an einem Borhkern aus dem Profundal des Mondsees (Oberosterreich). *Linzer Biologische Beitrage* **22**: 231–235.

Sebag D, Debret M, M'voubou M, Mabicka Obame R, Ngomanda A, Oslisly R, Bentaleb I, Disnar J-R, Giresse P (2013) Coupled Rock-Eval pyrolysis and spectrophotometry for lacustrine sedimentary dynamics: Application for West Central African rainforests (Kamalete and Nguene lakes, Gabon). *The Holocene* **23**: 1173–1183 doi:10.1177/0959683613483622.

Shaheen M.E, Fryer B.J. (2011) A simple solution to expanding available reference materials for Laser Ablation Inductively Coupled Plasma Mass Spectrometry analysis: Applications to sedimentary materials. *Spectrochimica Acta B* **66**: 627-636.

Shaheen M.E., Gagnon J.E, Fryer B.J. (2012) Femtosecond (fs) lasers coupled with modern ICP-MS instruments provide new and improved potential for in situ elemental and isotopic analyses in the geosciences. *Chemical Geology* **330**: 260-273.

Shaw JB, Mohrig D, Whitman SK (2013) The morphology and evolution of channels on the Wax Lake Delta, Louisiana, USA. *Journal of Geophysical Research: Earth Surface* **118**: 1562–1584 doi:10.1002/jgrf.20123.

Shen Z, Bloemendal J, Mauz B, Chiverrell R, Dearing JA, Lang A, Liu Q (2008) Holocene environmental reconstruction of sediment-source linkages at Crummock Water , English Lake District, based on magnetic measurements. *Holocene* **18**: 129–140.

Sheppard D.S., Christie A.B., Goff J, Carver R. (2009) Stream sediment geochemical survey in an area of volcanic-hosted epithermal Au-Ag-Zn-Pb-Cu deposits and porphyry Cu prospects, Thames, Coromandel Peninsula, New Zealand. *Geochemistry: Exploration, Environment, Analysis* **9**: 279-296.

Shotbolt L., Hutchinson S, Thomas A. (2006) Sediment stratigraphy and heavy metal fluxes to reservoirs in the Southern Pennine Uplands, UK. *Journal of Paleolimnology* **35**: 305-322.

Shuttleworth EL, Evans MG, Hutchinson SM, Rothwell JJ (2014) Assessment of Lead Contamination in Peatlands Using Field Portable XRF. *Water, Air, & Soil Pollution* **225**: 1844 doi:10.1007/s11270-013-1844-2.

Sibley A (2009) Analysis of extreme rainfall and flooding in Cumbria. *Weather* **65**: 287–292.

Simonneau A, Chapron E, Vannière B, Wirth SB, Gilli A, Di Giovanni C, Anselmetti FS, Desmet M, Magny M (2013) Mass-movement and flood-induced deposits in Lake Ledro, southern Alps, Italy: implications for Holocene palaeohydrology and natural hazards. *Climate of the Past* **9**: 825–840 doi:10.5194/cp-9-825-2013.

Sinex S.A, Helz G.R. (1981) Regional Geochemistry of Trace-Elements in Chesapeake Bay Sediments. *Environmental Geology* **3**: 315-323.

Skierszkan E.K., Irvine G., Doyle J.R., Kimpe L.E., Blais J.M. (2013) Is there widespread metal contamination from in-situ bitumen extraction at Cold Lake, Alberta heavy oil field? *Science of the Total Environment* **447**: 337-344.

Sletten K, Blikra LH, Ballantyne CK, Nesje A, Dahl SO (2003) Holocene debris ows recognized in a lacustrine sedimentary succession: sedimentology , chronostratigraphy and cause of triggering. *The Holocene* **13**: 907–920.

Smith K, Tobin GA (1979) Topics in Applied Geography: Human adjustment to the Flood Hazard (Longman, London).

Sprenke K.F., Rember W.C., Bender S.F., Hoffmann M.L., Rabbi F., Chamberlain V.E. (2000) Toxic metal contamination in the lateral lakes of the Coeur d'Alene River valley, Idaho. *Environmental Geology* **39**: 575-586.

Stanley CJ, Vaughan DJ (1982) Copper, lead, zinc and cobalt mineralization in the English Lake District: classification, conditions of formation and genesis. *Journal of the Geological Society* **139**: 569–579 doi:10.1144/gsjgs.139.5.0569.

Steffen W, Crutzen J, McNeill JR (2007) The Anthropocene: are humans now overwhelming the great forces of Nature? *Ambio* **36**: 614–621.

Sternberg RW, Larsen LH (1975) Threshold of sediment movement by open ocean waves : observations. *Deep Sea Research and Oceanographic Abstracts* **22**: 299–302.

Stewart MM, Grosjean M, Kuglitsch FG, Nussbaumer SU, von Gunten L (2011) Reconstructions of late Holocene paleofloods and glacier length changes in the Upper Engadine, Switzerland (ca. 1450 BC–AD 420). *Palaeogeography, Palaeoclimatology, Palaeoecology* **311**: 215–223 doi:10.1016/j.palaeo.2011.08.022.

Stinchcomb GE, Stewart RM, Messner TC, Nordt LC, Driese SG, Allen PM (2013) Using event stratigraphy to map the Anthropocene – An example from the historic coal mining region in eastern Pennsylvania, USA. *Anthropocene* 1–9 doi:10.1016/j.ancene.2013.06.001.

Stokes GG (1851) On the effect of the internal friction of fluids on the motion of pendulums. *Transactions of the Cambridge Philiosophical Society* **IX**: 8.

St-Onge G, Chapron E, Mulsow S, Salas M, Viel M, Debret M, Foucher A, Mulder T, Winiarski T, Desmet M, Costa PJM, Ghaleb B, Jaouen A, Locat J (2012) Comparison of earthquake-triggered turbidites from the Saguenay (Eastern Canada) and Reloncavi (Chilean margin) Fjords: Implications for paleoseismicity and sedimentology. *Sedimentary Geology* **243-244**: 89–107 doi:10.1016/j.sedgeo.2011.11.003.

St-Onge G, Mulder T, Piper DJW, Hillaire-Marcel C, Stoner JS (2004) Earthquake and flood-induced turbidites in the Saguenay Fjord (Québec): a Holocene paleoseismicity record. *Quaternary Science Reviews* **23**: 283–294 doi:10.1016/j.quascirev.2003.03.001.

Von Storch H, Costa-Cabral M, Hagner C, Feser F, Pacyna J, Pacyna E, Kolb S (2003) Four decades of gasoline lead emissions and control policies in Europe: a retrospective assessment. *The Science of the total environment* **311**: 151–176 doi:10.1016/S0048-9697(03)00051-2.

Støren EN, Dahl SO, Nesje A, Paasche Ø (2010) Identifying the sedimentary imprint of high-frequency Holocene river floods in lake sediments: development and application of a new method. *Quaternary Science Reviews* **29**: 3021–3033 doi:10.1016/j.quascirev.2010.06.038.

Sturm M, Matter A (1978) Turbidites and varves in Lake Brienz (Switzerland): deposition of clastic detritus by density currents. In Modern and Ancient Lake Sediments, A. Matter, and M. Tucker, eds. (Blackwell Scientific Publications, Oxford), pp. 145–166.

Sun D, Bloemendal J, Rea D., Vandenberghe J, Jiang F, An Z, Su R (2002) Grain-size distribution function of polymodal sediments in hydraulic and aeolian environments, and numerical partitioning of the sedimentary components. *Sedimentary Geology* **152**: 263–277 doi:10.1016/S0037-0738(02)00082-9.

Swierczynski T, Brauer a., Lauterbach S, Martin-Puertas C, Dulski P, von Grafenstein U, Rohr C (2012) A 1600 yr seasonally resolved record of decadal-scale flood variability from the Austrian Pre-Alps. *Geology* **40**: 1047–1050 doi:10.1130/G33493.1.

Swierczynski T, Lauterbach S, Dulski P, Delgado J, Merz B, Brauer A (2013) Mid- to late Holocene flood frequency changes in the northeastern Alps as recorded in varved

sediments of Lake Mondsee (Upper Austria). *Quaternary Science Reviews* **80**: 78–90 doi:10.1016/j.quascirev.2013.08.018.

Szefer P, Skwarzec B. (1988) Distribution and Possible Sources of Some Elements in the Sediment Cores of the Southern Baltic. *Marine Chemistry* **23**: 109-129.

Taboada T, Cortizas AM, García C, García-Rodeja E (2006) Particle-size fractionation of titanium and zirconium during weathering and pedogenesis of granitic rocks in NW Spain. *Geoderma* **131**: 218–236 doi:10.1016/j.geoderma.2005.03.025.

Talbot MR, Allen PA (1996) Lakes. In Sedimentary Environments: Processes, Facies and Stratigraphy, H.G. Reading, ed. (Blackwell Science, Oxford), p. 688.

Tapia J., Audry S., Townley B, Duprey J.L (2012) Geochemical background, baseline and origin of contaminants from sediments in the mining-impacted Altiplano and Eastern Cordillera of Oruro, Bolivia. *Geochemistry: Exploration, Environmental, Analysis* **12**: 3-20.

Teller JT (2004) Controls, History, Outbursts and Impacts of Large Late-Quaternary Proglacial Lakes in North America. In The Quaternary Period of the United States, A.R. Gillespie, S.C. Porter, and B.F. Atwater, eds. (Elsevier, Amsterdam), pp. 45–62.

Terasmaa J (2011) Lake basin development in the Holocene and its impact on the sedimentation dynamics in a small lake (southern Estonia). *Estonian Journal of Earth Science* **60**: 159-171.

Tertian R (1969) Quantitative chemical analysis with X-ray fluorescence spectro-metry-an accurate and general mathematical correction method for the interelement effects. *Spectrochimica Acta* **24**:

Tessier A., Carignan R., Dubreuil B, Rapin F (1989) Partitioning of Zinc between the Water Column and the Oxic Sediments in Lakes. *Geochimica Cosmochimica Acta* **53**: 1511-1522.

Thapalia A., Borrok D.M., Van Metre P.C., Musgrove M, Landa E.R.(2010) Zn and Cu Isotopes as Tracers of Anthropogenic Contamination in a Sediment Core from an Urban Lake. *Environmental Science & Technology* **44**: 1544-1550.

Thevenon F., Graham N.D., Chiaradia M., Arpagaus P., Wildi W, Poté J (2011) Local to regional scale industrial heavy metal pollution recorded in sediments of large freshwater lakes in central Europe (lakes Geneva and Lucerne) over the last centuries. *Science of the Total Environment* **412**: 239-247.

Thevenon F, Poté J (2012) Water Pollution History of Switzerland Recorded by Sediments of the Large and Deep Perialpine Lakes Lucerne and Geneva. *Water Air and Soil Pollution* **223**: 6157-6169.

Thevenon F, Wirth SB, Fujak M, Poté J, Girardclos S (2013) Human impact on the transport of terrigenous and anthropogenic elements to peri-alpine lakes (Switzerland) over the last decades. *Aquatic Sciences* **75**: 413–424 doi:10.1007/s00027-013-0287-6.

Thomas RL (1972) Distribution of Mercury in Sediments of Lake Ontario. *Canadian Journal of Earth Science* **9**: 636-651.

Thorndycraft V, Hu Y, Oldfield F, Crooks PRJ, Appleby PG (1998) Individual flood events detected in the recent sediment of the Petit Lac d'Annecy, eastern France. *The Holocene* **8**: 741–746 doi:10.1191/095968398668590504.

Thorndycraft VR, Benito G, Sanchez-Moya Y, Sopena a. (2011) Bayesian age modelling applied to palaeoflood geochronologies and the investigation of Holocene flood magnitude and frequency. *The Holocene* **22**: 13–22 doi:10.1177/0959683611409782.

Tipping R (1998) Towards an environmental history of the Bowmont Valley and the northern Cheviot Hills. *Landscape History* **20**: 41–50 doi:10.1080/01433768.1998.10594501.

Tipping R, Halliday SP (1994) The age of alluvial fan deposition at a site in the southern uplands of scotland. *Earth Surface Processes and Landforms* **19**: 333–348 doi:10.1002/esp.3290190405.

Tjallingii R, Röhl U, Kölling M, Bickert T (2007) Influence of the water content on X-ray fluorescence core-scanning measurements in soft marine sediments. *Geochemistry, Geophysics, Geosystems* **8**: n/a – n/a doi:10.1029/2006GC001393.

Todd B, Macdonald N, Chiverrell RC (2014) Revision and extension of the composite Carlisle rainfall record, northwest England: 1757-2012. *International Journal of Climatology* n/a – n/a doi:10.1002/joc.4233.

Tropea AE, Paterson AM, Keller W (Bill), Smol JP (2010) Sudbury Sediments Revisited: Evaluating Limnological Recovery in a Multiple-Stressor Environment. *Water, Air, & Soil Pollution* **210**: 317–333 doi:10.1007/s11270-009-0255-x.

Trouet V, Esper J, Graham NE, Baker A, Scourse JD, Frank DC (2009) Persistent positive North Atlantic oscillation mode dominated the Medieval Climate Anomaly. *Science (New York, NY)* **324**: 78–80 doi:10.1126/science.1166349.

Turney CSM, Lowe JJ, Davies SM, Hall V, Lowe DJ, Wastegård S, Hoek WZ, Alloway B (2004) Tephrochronology of last termination sequences in Europe: a protocol for improved analytical precision and robust correlation procedures(a joint SCOTAV–INTIMATE proposal). *Journal of Quaternary Science* **19**: 111–120 doi:10.1002/jqs.822.

Tyler I (1992) Greenside: A Tale of Lakeland Miners (Red Earth Publications, Cumbria).

Tyler I (2001) Greenside and the mines of the Ullswater Valley (Blue Rock Publications, Cumbria).

Tyler I (2006) The Lakes and Cumbria Mines Guide (Blue Rock Publications, Cumbria).

Tylmann W (2005) Lithological and geochemical record of anthropogenic changes in recent sediments of a small and shallow lake (Lake Pusty Staw, northern Poland). *Journal of Paleolimnology* **33**: 313-325.

Urban NR, Lu X, Chai Y, Apul DS (2004) Sediment Trap Studies in Lake Superior: Insights into Resuspension, Cross-margin Transport, and Carbon Cycling. *Journal of Great Lakes Research* **30**: 147–161 doi:10.1016/S0380-1330(04)70383-4.

Vasskog K, Nesje a., Storen EN, Waldmann N, Chapron E, Ariztegui D (2011) A Holocene record of snow-avalanche and flood activity reconstructed from a lacustrine sedimentary sequence in Oldevatnet, western Norway. *The Holocene* **21**: 597–614 doi:10.1177/0959683610391316.

Vermillion B., Brugam R., Retzlaff W, Bala I. (2005) The sedimentary record of environmental lead contamination at St. Louis, Missouri (USA) area smelters. *Journal of Paleolimnology* **33**: 189-203.

Waheed S., Siddique N, Hamid Q. (2010) Analysis of municipal waste dump soil using a low power reactor: a study by instrumental neutron activation analysis. *Radiochimica Acta* **98**: 533-538.

Walling DE, Moorehead PW (1989) The particle size characteristics of fluvial suspended sediment: an overview. *Hydrobiologia* **176/177**: 125–149.

Wang R, Dearing J a, Langdon PG, Zhang E, Yang X, Dakos V, Scheffer M (2012) Flickering gives early warning signals of a critical transition to a eutrophic lake state. *Nature* **492**: 419–422 doi:10.1038/nature11655.

Wedepohl K.H. 1995. The Composition of the Continental-Crust. *Geochimica Cosmochimica Acta* **59**: 1217-1232.

Wei C.Y, Wen H.L. (2012) Geochemical baselines of heavy metals in the sediments of two large freshwater lakes in China: implications for contamination character and history. *Environmental Geochemistry and Health* **34**: 737-748.

Weltje GJ, Prins MA (2003) Muddled or mixed? Inferring palaeoclimate from size distributions of deep-sea clastics. *Sedimentary Geology* **162**: 39–62 doi:10.1016/S0037-0738(03)00235-5.

Weltje GJ, Tjallingii R (2008) Calibration of XRF core scanners for quantitative geochemical logging of sediment cores: Theory and application. *Earth and Planetary Science Letters* **274**: 423–438 doi:10.1016/j.epsl.2008.07.054.

Werritty A, Paine JL, Macdonald N, Rowan JS, McEwen LJ (2006) Use of multi-proxy flood records to improve estimates of flood risk: Lower River Tay, Scotland. *Catena* **66**: 107–119 doi:10.1016/j.catena.2005.07.012.

Wetter O, Pfister C, Weingartner R, Luterbacher J, Reist T, Trösch J (2011) The largest floods in the High Rhine basin since 1268 assessed from documentary and

instrumental evidence. *Hydrological Sciences Journal* **56**: 733–758 doi:10.1080/02626667.2011.583613.

White DS, Miller MF (2008) Benthic invertebrate activity in lakes: linking present and historical bioturbation patterns. *Aquatic Biology* **2**: 269–277.

Wilby RL, Beven KJ, Reynard NS (2008) Climate change and fluvial flood risk in the UK: more of the same? *Hydrological Processes* **22**: 2511–2523 doi:10.1002/hyp.

Wilby RL, Dalgleish H, Foster IDL (1997) The impact of weather patterns on historic and contemporary catchment sediment yields. *Earth Surface Processes and Landforms1* **22**: 353–363.

Wilhelm B, Arnaud F, Enters D, Allignol F, Legaz A, Magand O, Revillon S, Giguet-Covex C, Malet E (2012) Does global warming favour the occurrence of extreme floods in European Alps? First evidences from a NW Alps proglacial lake sediment record. *Climatic Change* **113**: 563–581 doi:10.1007/s10584-011-0376-2.

Wilhelm B, Arnaud F, Sabatier P, Magand O, Chapron E, Courp T, Tachikawa K, Fanget B, Malet E, Pignol C, Bard E, Delannoy JJ (2013) Palaeoflood activity and climate change over the last 1400 years recorded by lake sediments in the north-west European Alps. *Journal of Quaternary Science* **28**: 189–199 doi:10.1002/jqs.2609.

Wilson R, Miles D, Loader NJ, Melvin T, Cunningham L, Cooper R, Briffa K (2013) A millennial long March–July precipitation reconstruction for southern-central England. *Climate Dynamics* **40**: 997–1017 doi:10.1007/s00382-012-1318-z.

Winchester A (1987) Landscape and society in medieval Cumbria (John Donald, Edinburgh).

Wirth SB, Gilli A, Simonneau A, Ariztegui D, Vannière B, Glur L, Chapron E, Magny M, Anselmetti FS (2013a) A 2000 year long seasonal record of floods in the southern European Alps. *Geophysical Research Letters* **40**: 4025–4029 doi:10.1002/grl.50741.

Wirth SB, Girardclos S, Rellstab C, Anselmetti FS (2011) The sedimentary response to a pioneer geo-engineering project: Tracking the Kander River deviation in the sediments

of Lake Thun (Switzerland). *Sedimentology* **58**: 1737–1761 doi:10.1111/j.1365-3091.2011.01237.x.

Wirth SB, Glur L, Gilli A, Anselmetti FS (2013b) Holocene flood frequency across the Central Alps – solar forcing and evidence for variations in North Atlantic atmospheric circulation. *Quaternary Science Reviews* **80**: 112–128 doi:10.1016/j.quascirev.2013.09.002.

Wolfe A.P, Hartling J.W. (1997) Early holocene trace metal enrichment in organic lake sediments, Baffin Island, Arctic Canada. *Arctic and Alpine Research* **29**: 24-31.

Wolfe BB, Hall RI, Last WM, Edwards TWD, English MC, Karst-riddoch TL, Paterson A, Palmini R (2006) Reconstruction of multi-century flood histories from oxbow lake sediments, Peace-Athabasca Delta, Canada. *Hydrological Processes* **20**: 4131–4153 doi:10.1002/hyp.

Wong HK., Gauthier A, Nriagu J. (1999) Dispersion and toxicity of metals from abandoned gold mine tailings at Goldenville, Nova Scotia, Canada. *Science of The Total Environment* **228**: 35–47 doi:10.1016/S0048-9697(99)00021-2.

Wulf S, Kraml M, Brauer A, Keller J, Negendank JFW (2004) Tephrochronology of the 100ka lacustrine sediment record of Lago Grande di Monticchio (southern Italy). *Quaternary International* **122**: 7–30 doi:10.1016/j.quaint.2004.01.028.

Yang H.D. (2010) Historical mercury contamination in sediments and catchment soils of Diss Mere, UK. *Environmental Pollution* **158**: 2504-2510.

Yang H, Rose N (2005) Trace element pollution records in some UK lake sediments, their history, influence factors and regional differences. *Environment International* **31**: 63–75 doi:10.1016/j.envint.2004.06.010.

Yang H.D., Rose N.L., Battarbee R.W, Boyle J.F. (2002) Mercury and lead budgets for Lochnagar, a Scottish mountain lake and its catchment. *Environmental Science and Technology* **36**: 1383-1388.

Zhang Y, Adeloju S.B. (2008) A novel sequential injection - Cold vapour atomic absorption spectrometric system for rapid and reliable determination of mercury. *Talanta* **74**: 951-957.

Young BR, Millward D, Cooper AH (1992) Regional geochemistry of the Lake District and adjacent areas (Keyworth, Nottingham).

Ziegler M, Jilbert T, de Lange GJ, Lourens LJ, Reichart G-J (2008) Bromine counts from XRF scanning as an estimate of the marine organic carbon content of sediment cores. *Geochemistry, Geophysics, Geosystems* **9**: Q05009. doi:10.1029/2007GC001932.

Zillén L, Wastegård S, Snowball I (2002) Calendar year ages of three mid-Holocene tephra layers identified in varved lake sediments in west central Sweden. *Quaternary Science Reviews* **21**: 1583–1591.